Biogeographic, ontogenetic, and evolutionary patterns of salicinoid diversity in *Populus heterophylla* and related species in the Salicaceae

By

Tyler Hampton Wintermute

A dissertation submitted in partial fulfillment of

the requirements for the degree of

Doctor of Philosophy

(Botany)

at the

UNIVERSITY OF WISCONSIN-MADISON

2025

Date of final oral examination: 05/27/2025

The dissertation is approved by the following members of the Final Oral Committee:

Ken Keefover-Ring, Associate Professor, Botany and Geography
Amy M. Trowbridge, Associate Professor, Forest and Wildlife Ecology
Hiroshi A. Maeda, Professor, Botany
Eric L. Kruger, Professor, Forest and Wildlife Ecology
Kenneth J. Sytsma, Professor, Botany

Table of contents

Acknowledgements

I have so many people to thank, enough to fill an entire dissertation, but I am afraid that a combination of my ADHD and months spent writing all of this up are going to team-up and I am going to forget some folks. If I do, I am sorry, but just know that I am incredibly grateful for all you have done for myself and others. Chronologically, in the order of people that I've met, I guess I need to start with my parents. Mom and Dad, you have been there for me since day one, and have been instrumental to my success as a person. You encouraged me to be curious, and were *extremely* patient for the first decade of my life before we found an ADHD medication that worked for me. Our annual family vacations let me see much of the country via car, and thus when I set out on a road trip by myself at the height of the COVID-19 Pandemic to collect samples for Chapters 1 and 2 I had a bit of a feeling of nostalgia. Your support of me in scouts exposed me to a world beyond the suburbs, and through which I developed a foundational appreciation of life and the natural world, even with an early paralyzing fear of arthropods. It's incredible to think that I once wouldn't fall asleep at camp because a lady beetle was inside of my mosquito net, and yet here I am nearly two decades later excited to raise some insects on plant tissue and see what happens. You raised me to see the world with kindness and respect, and even though that kindness and respect might seem fleeting in our world lately I still have an unwavering mindset that everything will turn out alright. I love both of you so much, and could not have become the person I am today without you.

To my siblings, Dylan and Ash, thank you for engaging with my humor and providing plenty of happy childhood memories, even if we didn't always get along, which I think is just a contract you unwittingly sign when you are siblings. I am incredibly proud of the paths you have taken. Dylan, you have found your niche and excel with technology, and I hope that artificial "intelligence" doesn't take your job anytime soon. Ash, you have an immense passion for

storytelling and the history of a place, and the work you do ensures that the people who came before us and the things they did are not forgotten.

For my grandparents, thank you for your unwavering support and excitement to hear what I've been up to. To Grandma and Grandpa Griffith, the short trip across DC traffic felt longer than it actually was, but the frequency with which I was able to see you two growing up always provided me with joy. Going to Southern Maryland Blue Crabs games, holidays, just hanging out, provided me with an appreciation of not needing an occasion to say hi or to be with those you love. To Grandma Griffith in particular, I enjoy our phone calls and your incredible knowledge of sports, and we always have something to chat about. To Grandpa Griffith, as I've gotten older I realize that I am probably the most like you of all of my grandparents, and your subtle (and sometimes not-so-subtle) humor is something I have developed myself over time.

To Grandma and Grandpa Wintermute, the summers spent on the gators in the woods of Missouri were an opportunity for me to truly be outside and explore. The week we would spend each year out there was a reminder that life doesn't need to be plugged in all the time, and that there is plenty of joy to be found in hobbies and craftsmanship. Your garden was always impressive, and something my dad brought with him to Virginia, and that which no doubt had an influence on my passion for plants.

To Grandma and Grandpa Jinkerson, I wish you could see me now. I remember the last time I talked to you Grandma, as I was driving through Missouri on the way to Mingo Swamp to collect some trees in 2020. You suggested I should stop on by and spend the night, but I was cautious due to the pandemic and feared that I might get you and Grandpa sick. That might be one of my biggest regrets so far in life, and I wish now more than ever I had taken the two or so hour detour to stop on by and at least say hi. You had an immense influence on my belief in

public education, history of places and of people, and a love of music that doesn't need to have lyrics. Even today, I often struggle to remember the words to a song, but the melody and harmony are things that become ingrained in my head. Mornings watching the birdfeeders with you was my first exposure to taxonomic diversity, and I'll treasure our relationship forever. Grandpa Jinkerson, you really showed me what it meant to have a good nap in a chair, and your dedication and love for Grandma was something that I don't think I fully recognized until after you both had passed. Your smile and laughter are things I will never forget.

To Aunt Susan and Uncle Chuck, thank you for becoming a sort of home away from home once I moved to Indiana for college, and then up here to Wisconsin. Spending Easters and Thanksgivings and even just weekend trips with you in St. Louis has been incredibly rewarding, and your laid-back approach to life with a healthy dose of fun and hard work is something I think has rubbed off a bit on me. I'm excited to see y'all soon, and plan to continue to make trips on down to see you from wherever I end up.

To Aunt Donine and Uncle Bernie (who has the deepest laugh I have ever heard) you have been inspirations to excellence for me. Growing up with y'all nearby in Virginia brought plenty of joy to see family other than those that I lived with in childhood, and the trip out to Steamboat to see y'all about a decade ago for the fourth of July is one of the best I've had. You both seemingly excel in everything you do (I could always tell which gifts were from Donine because of the meticulous wrapping) and to see that hard work pay off with your hobbies and the reward of retirement in Steamboat is incredible. I still remember when I lost your wedding ring during rehearsal as the ring bearer, and the ensuing Ziploc bag I had to carry in during the actual wedding, and the smarties I was rewarded with by Bernie for good behavior during the

ceremony. That might have been a prelude to the physical comedy I often find myself in, and is one of my most cherished memories.

To my cousins, Kirsten (and Daniel), Alyssa, Danielle, Jack, Michael, Justin (and Kyle), and Marcus, thanks for memories from summers and other times, and especially for being constant reminders to have fun. It always feels like a celebration or a special occasion when we get together! And it is especially comforting to know that I have extended family of my generation that I know will be there for me. Charlotte, we've met once, but it's exciting to see the next generation start strong!

To my many teachers through K-12, thank you for taking the time to provide a foundational level of knowledge. Especially to my teachers in elementary and middle school, thank you for your exceptional patience as I figured out my ADHD. Similarly, thanks to the case managers for my IEP, without you I don't think I would have made it through a system designed for people to complete a task in a short amount of time. I would like to especially thank some of my teachers in high school, Mr. Sarmento for changing my perspective on math, and for providing a blueprint for teaching and learning, and for sponsoring an incredible trip to the Galapagos; Mr. Smith and Mrs. Nichols for introducing me to the world of chemistry, Mrs. Blackwell for teaching me about environmental science and really my first introduction to ecology, and Dr. Buchanan for letting me experiment during that independent project on biofuels from grass clippings. Obviously, I know way more now about plant chemistry than I did then, but that was my first foray into experimental design. Thank you to my track coaches, Coach Colebank and Coach Treble, for pushing me to improve and keep working even when I (often) didn't PR.

To Melinda, my supervisor when I was a resident assistant at the University of Evansville, thank you for helping me learn how to foster and cultivate community, and for being a guide for me during some really formative years. You kept it real, and you helped improve my perspective of the world in a way that I really needed. Also, you were right about Wisconsin and cheese curds!

To the faculty at the University of Evansville, thank you for your focus on holistic undergraduate education. While UE certainly didn't have the resources nor the breadth of knowledge that UW-Madison has, and sometimes I feel that there are massive gaps in my botanical education, I still do not think I would have found my way as I did at UE. The commitment to undergraduate education and the immense amount of time you put into making sure students succeed is incredible, and is the approach I try to take with students I have now. You've had an incredible impact on my life. Dr. Edwards, thank you for teaching the Evolutionary Ecology course. The integration of those two disciplines, and in my mind, the inseparability of the two, continues to guide my scientific thinking today. Dr. Slade, thank you for somehow alleviating the struggle of organic chemistry. Without your approach, I certainly would not had the confidence to continue down the chemical path. Dr. Powell, thank you for your horticulture, ethnobotany, and plant diversity courses. Dr. Gordon, your environmental perspectives course certainly gave me a perspective, and being able to read A Sand County Almanac and then moving to Wisconsin is a somewhat magical experience. Importantly, it was your Tropical Ecology of Costa Rica course that truly set me on a botanical course, as I was amazed at the diversity of plant forms in that country, and that was the trip that turned me into a Botanist.

And of course, I have to give a special thanks to Dr. Arlen Kaufman and Dr. Cris Hochwender for being the dynamic duo holding the Environmental Studies department together and putting the chemistry and the ecology into chemical ecology. The combination of Arlen's particularness (as any true analytical chemist portrays) with Cris's statistical prowess for disentangling complex ecological patterns made for the best combination of advisors that I, a budding chemical ecologist, could have asked for. When I asked Arlen about a summer research project on "plant chemistry" I had no idea what it actually was that I wanted to research, and I had no idea what I truly meant by "chemistry". As I outline in the introduction to this document, that choice that Arlen made to take me on as a student was foundational to the scientist I have become. It opened my eyes to a world I never knew existed, a world that dictates the continued existence of life around us, cycling constantly in the background of everything else. Further, having access to an LCMS, HPLC-UV/vis, preperatory LC and other equipment as an undergrad really let me get my feet wet. Arlen's words to me were "I've taken the safeties off the instruments (looking back, I realize there were likely no safeties), go learn how to use them and don't break them" and that was the extent of his guidance, save an occasional check-in. I learned much about the value of figuring things out on your own and what to do when things go wrong, and developed the self-confidence and efficacy needed to work independently.

Taking that initial summer's experience in analytical chemistry, and then taking Ecology with Cris that following semester really set me up to hit a home run, as now I could utilize my emerging skills in analyzing plant chemistry and begin to apply them in an ecological context. Cris was the perfect mentor for me at this stage, as he was a chemical ecologist in his own merit. Cris had published on *Salix* and salicinoids before, looking at hybrid crosses between *S. serecia* and *S. eriocephala* and how salicinoids influenced slug feeding preferences, among other things.

Further, he had integrated his teaching into the local natural systems of “exotic” Southern Indiana, really hammering home that cool ecology is happening everywhere. There was a point in that ecology course where we were selecting papers to present from a list, and I (perhaps foolishly) chose the only two on the list that Cris had published, both dealing with willows. I didn’t have the best grasp on what was going on in those papers then, but it was a first hint to me at what was possible statistically with ecology. I would be remiss to not mention the impact that Cris had on my writing, as I turned in a rather poor research proposal in his course. Your comments on that document spurred me to take science a little more seriously, and by the end of that course I had begun to amass the initial knowledge and framework that would become Chapter 2 of my dissertation, and I was awarded a summer research grant to carry out that study, which ended up providing me some insight that would inform how I conducted my experiments in Chapter 2. Arlen and Cris, if you ever need someone to talk to students or give a guest lecture, I would be more than happy to return the favors you did for me years ago.

Finally, from UE, I need to thank my Environmental Studies cohort of Spencer Willem, Branndon Castellano, and Anna Jean Hallman. You three are some of the sharpest, logical, dedicated people I know, and it was fantastic to be able to go through four years of classes and studying with you.

Now, On Wisconsin! This is a state I didn’t think too much of before moving here, but I have truly fallen in love with it. While I did grow up in Virginia following the briefest of stints in Pennsylvania, the proximity with which I grew up to DC and homogenized feel of suburbia, and maybe to an extent the fact that I just happened to live there and didn’t really choose that (nothing wrong with that it’s just how it happens when you’re a kid) it really didn’t feel like “home”, or at least I didn’t realize what home could feel like. These past six years in Madison,

Wisconsin have been the first time in my life where I really feel like I can call a place my home. I have become enamored with the Wisconsin Idea (even if those ideals are maybe not in full swing today) and impressed with just how much I have enjoyed living here. The nature, the people, the brats, the lakes, the cheese, the weather (even if winter goes on a little long), and the history of this place really speaks to me. Since time immemorial, people have called Wisconsin home, and I feel blessed that for a short time, I too have had the opportunity to do so. I'm going to miss living here, but I hope to be back one day.

Part of this enjoyment comes from the people I have had the chance to spend time with. All of the members of the Department of Botany, you have been welcoming and even if at times I *really* felt some imposter syndrome due to a limited prior botanical education (I really came to grad school thinking I knew a ton about plants and I have never felt more wrong) you have all always been there to answer my questions and I just really value that. I think the integrative nature of this department is what makes it so great, truly spanning genes to ecosystems in our work, and that viewpoint and expertise has enabled me to develop a holistic view of my research, and pushes me to continue to learn new things. Especially to the folks that are new to the department, thank you for providing me some perspective on how far I have come as a scientist, and for providing an avenue through which I can help and provide advice in the manner that senior graduate students once provided me years ago. Thank you to the Friday Afternoon Club (FAC) for being a stable presence throughout my time in grad school (including weathering COVID!) and being a place to hang out with other members of the department and not have to think about science, though sometimes we couldn't resist. Thank you to the various members of Hiroshi Maeda's lab over the years for being wonderful neighbors in the lab space. A special thanks goes to all of the Botany Greenhouse and Gardens staff, especially Cara Streekstra and

Molly Campbell, for their guidance and help with raising research plants. Thank you Beth Reuter, Sophia Lawrence, Julie Olson, John Newton, Sarah Friedrich, Gabe Skiff, Mark Connolly, and all of the other staff that ensure the department continues to function. I thoroughly enjoyed all of my interactions with all of you, and without you none of the work would be possible. Thanks also to the folks that make the Introductory Biology sequence possible, especially Kerry Martin, from who I learned a lot about teaching.

I would like to thank the members of my committee: Ken Keefover-Ring, Amy Trowbridge, Hiroshi Maeda, Eric Kruger, and Ken Sytsma. My preliminary exam did not turn out how I expected it to go, but the outcome of it fundamentally altered my trajectory as a scientist for the better, and solidified an ethos of a growth mindset in me. You have each provided feedback (some more, some less) on my work at multiple stages of this process, and as I wrote chapters I could hear some of your voices in my head asking questions, which was a good sign to shore up some of my knowledge. The process of preparing for this defense with the mindset of what each of you might be interested in asking me has forced me to view these chapters from multiple dimensions, and has resulted in me continuing to learn new things about these projects and results even in the past few weeks.

Additionally, I have some scientific acknowledgments to make. Thank you Steve Difazio and Sandra Simon for being interested in *Populus heterophylla*, and thank you for collaborating on Chapter 1. Steve and Sandy collected many of the samples for which we have genetic data for, and who conducted the sequencing, alignment, and quality control of the *P. heterophylla* genetic sequences, and have provided advice on rooting and dating the *P. heterophylla* tree. The results of this chapter have turned out great, and I'm excited to continue to work on it to publication with them. I would also like to thank Ariel Sorg and Steven Augustine for assisting

with sample collection during the second summer of sampling for chemistry, and for all of the sites which granted me permits for collections. For Chapter 2, I would like to thank Sarah Kapsner and Steven Augustine for assisting with data collection, the Arlington Agricultural Research Station team for assistance with garden site establishment and equipment for maintenance, and Jorge El-Azaz for assistance with qPCR techniques. Indeed, Jorge was a huge help in two of these chapters and taught me how to design primers, extract RNA, make cDNA and conduct PCR for sequencing and qPCR for relative expression of genes. I have never actually taken a course on genetics (whoops), and never imagined when I started graduate school I would have a genetic component to my chapters, but here I am having done something with genetics in all three of my chapters and Jorge had a big part in enabling this. For Chapter 3, I would like to thank Sarah Kapsner for taking on the project when it was a small idea in my head, and for completing about two-thirds of the chemical extractions and running those samples on the LCMS. You are one of the chilliest people I have met, and I had a great time working with you! I need to thank the Morton Arboretum in Lisle, Illinois, without which many of the samples (especially of *Salix*) would not have been collected, and a special thanks goes to Katrina Lewin for driving around with me for half a day to enable the bulk of those collections. I would like to thank Adam Black and Annaliese Sander from Bartlett Tree Experts for many of the *Populus* species from Mexico, Bryan Connelly for some of the *Populus* hybrids and two *P. heterophylla* from Connecticut, Jason Smith for the *Populus mexicana* samples, and to the New York Botanical Garden for the two *Idesia polycarpa* samples. I would like to thank Lauren Frankel for collaborating on that project, and for constructing and calibrating the phylogenies. I do not think either of us thought, when I proposed collaborating with you on that tiny sailboat in the relatively large waves of Lake Mendota, how much of a headache trying to reconcile the topology of

various *Salix* phylogenies was going to be, but I think that this has turned into a very cool project and I'm excited to get it to publication. Finally, I would like to thank Cécile Ané for her advice on the methodology of this project.

To those whom I have had the absolute *pleasure* of going to one of 90+ Fish Frys: THANK YOU. Words cannot explain how much each of you means to me, and I am so lucky to have been able to know you. This feels repetitive to a certain point, but I really do mean that you have had a great impact on my time here in Madison, and are friends (and collaborators!) I'll cherish for life. I could write an entire chapter's worth of thanks (it's approaching that level right now) but there are some specific folks I want to thank in the space I have here: To Tabitha Faber and Patricia Chan, thanks for the support and friendship, especially during our first couple of years here when COVID made meeting new people a bit of a challenge. To Ben Iuliano, for being an exceptional entomologist, agroecologist, and for providing wonderful perspectives on the intersection of science and society, and for being my movie buddy. To Madelyn Reinagel, for providing copious laughter from Evansville to Madison, I am so glad we stayed in touch and ended up in the same city, and you provide a perspective from outside the academic bubble that I find grounding in the best way. To Katherine Brinsko, for being one of the most organized scientists I've ever worked with in a professional context, and to Kieth Brinsko, who is a somewhat organized scientist I haven't worked with in a professional context: you two are amazing people and have been incredible friends, and Football Sundays just aren't the same without you, Rage, and Punk. To Ariel Sorg, who assisted me with collections in Chapter 1, and with who I share a certain flavor of "oh my gosh I can't believe that just happened" humor, you're an incredible human and a meticulous scientist, and I'm bummed that we'll just miss each other here in Madison. To Nathan Kiel, I wish the maximum allowed free baseball. Your calm,

cool perspectives in ecology and life are enlightening, and fieldwork with you is always a good time. To Michael Peyton, who has a mind for ordinations and prickly statistics. You're an excellent community ecologist, and you have an infectious laughter and personality and are always down for a good time. To Sam Anderson and Olivia Kovacs, I can't think of better people to go to a rodeo with. Both of you ooze Wisconsin, and Sam, your integration of historical knowledge, be it ecology or people, in modern contexts, particularly in Wisconsin, is impressive, and you always have a good story to tell. To Lauren Frankel, thanks for recommending Whitney at Curl Bound Salon, the official curly hair specialist of this here document. When I think of New Jersey, I think of Lauren, and when I think of Lauren, I think of some hot takes and honest gossip, but also of an extremely analytical scientist who has a healthy dose of skepticism of many a statistical method due in part to your quest to determine how "true" we are in our predictions. I had a blast being FAC Co-Czar with you! To Christian Villenueva, for always being ready to hold a gathering and have a good time.

I would like to think the members of the Keefover-Ring Lab, for their support over my time in Madison: Tabitha Faber, Thalia Hoenkirk, and Linden Taylor. You three have provided great insight and discussion about chemical ecology and teaching methods, and I would like to especially thank Linden for listening to me occasionally sharing some cool data and for having engaging conversations about science or life in the office. I would especially like to thank Ken Keefover-Ring for taking a chance on me from an email and a thirty-minute phone call. You have shown me that there can be a work-life balance in academia, and have reinforced the concept of science is done by people, so not only it is inherently political, but that we need to treat each other as people first, and scientists second. Your patience and understanding have been immensely influential, and provide me with methods to build my future mentorship style off of.

Finally, I would like to thank Lena Berry for being a part of my life, especially during the last semester. It has been a real capital-T Time trying to get the many dimensions of this dissertation together for this defense, including some long days and nights writing and running code. You have been a fundamental presence in my life over the past two years, but especially so in the final two months before my defense. I am so proud to see you develop into a capable, confident, competent scientist yourself, and am excited to see you continue to excel in everything you do. I love you, and I could not have done this without you.

Finally, finally, I need to thank Alice the Cat for being a great conversationalist and providing excellent feedback on all three of my chapters in the form of various “meows” and only one instance of two yowls followed by what I hope was a hairball, but I am unsure. I know that you have loved having someone to spend time with all day (even though you spend most of it asleep) and that you don’t know I am writing about you right now, but you were an integral part of my dissertation and are a perfect cat in my mind. I have had two pets before (Dixie and Kalyn) both of whom were dogs from my childhood, and I had an excellent relationship with Kalyn in part due to her personality. She really made my day every time I got home from school, when we would go on walks, or when we would run around in the backyard, and she was one of the smartest dogs I’ve known. I did not realize how much I missed having a furry friend in my life until this past year, and Alice, you have been able to make my day with your quirks and your presence, and reminded me when I get a bit tired of thinking about science, that it is alright to just zone out and be a chill cat every now and then.

"The world is not coloured green to the herbivore's eyes, but rather is painted morphine, l-DOPA, calcium oxalate, cannabinol, caffeine, mustard oil, strychnine, rotenone, etc."

- Daniel H. Janzen, 1975

"...this species, which gets least recognition of all, does at present most of the work in the family. It is said that 50 per cent of all excelsior now used in the United States comes from Swamp Cottonwood. And, indeed, as eastern Cottonwood is becoming exhausted as a commercial tree, Swamp Cottonwood is replacing it, in the utilitarian work of the lumber world, by furnishing cheap boxes and crates of all sorts. Commonplace such uses may be, but once far nobler trees were put to them; more fitting is it that a species like this, of value for nothing else and of no particular beauty, should serve in this role."

- Donald C. Peattie, 1950

Abstract

Salicinoids are a class of plant secondary chemicals that function as anti-herbivore defenses produced by *Populus* and *Salix* species and the composition of salicinoid arsenals varies by species and organ. In these chapters, I investigated salicinoid diversity across space, ontogeny, and evolutionary time. One understudied species, *Populus heterophylla* L. (swamp cottonwood), has been historically reported to not produce many salicinoids, though I have found individuals of the species to be salicinoid-rich. *P. heterophylla* is native to eastern North America and has a U-shaped distribution around the Appalachian Mountains, likely preventing gene flow through wind dispersed pollen and seeds between populations on different sides of the mountains. Restricted gene flow can lead to populations evolving different traits over time, including chemical defenses, such as salicinoids. In Chapter One, I collected and analyzed *P. heterophylla* foliage over much of its range and showed that it has four salicinoid phenotypes, and that populations west of the mountains have a lower diversity of salicinoid phenotypes than populations east of the mountains. I also showed that this distribution is correlated with the population structure of *P. heterophylla*, as there are two population lineages, both originating in the southeast part of the species' distribution, and expanding north on either side of the mountains as time progressed. In Chapter Two, using a common garden of genotypes cloned from throughout the range of *P. heterophylla*, I showed that immature carbon-sink leaves are better defended via salicinoids but less physiologically active than mature carbon-source leaves, consistent with the Optimal Defense Hypothesis and ideas about the value of a leaf. In Chapter Three, I investigated the evolution of salicinoids in 52 species of *Populus* and *Salix* using phylogenetic comparative methods. I found that the ancestral salicinoid arsenal was likely similar to many extant species such as *Populus tremuloides* and *Salix amygdaloides*, and that

novel salicinoids have evolved independently in many clades and species in both genera. I discuss reasons for the evolution of salicinoid diversity, and implore researchers to be intentional when studying salicinoids and plant chemistry in general, such that we can develop a better understanding of its existence.

Introduction

Plants produce an incredible amount of chemicals to aid them in their daily lives. They are responsible for reproduction, hormone signaling, pigmentation, stress relief, and numerous other essential functions of these green organisms. The greenness of plants itself comes from the pigment chlorophyll, which is essential for optimal photosynthesis, the process by which plants convert energy from the sun into a usable form for most of the rest of terrestrial life on our planet. This energy, now in the form of sugars and starches (as well as other carbon products contributing to the 450 gigatons of carbon in plants worldwide, or 81% of all biomass on Earth; Bar-on et al. 2018), is the envy of the animal and fungal kingdoms, and plants are under constant pressure from antagonists (herbivores and pathogens) which seek to exploit their sessile nature for an easy meal. The fact that these immobile plants are not consumed back to the soil by mobile predators has given rise to a "Why is the world green" hypothesis (Hairston et al. 1960; Wilkinson & Sherratt 2016) with some proponents arguing that it is the control of plant antagonists by another layer of predators that enable the growth of plants worldwide, but this view reduces plants to a "damsel-in-distress" that must be saved from predation by a charismatic guild of predators. Hairston et al. (1960) must not have read Gottfried Fraenkel's "raison d'Être of secondary plant substances" published the year prior in 1959; had they done so, they might have been aware that plants are not helpless against their enemies, but rather produce an amazing arsenal of chemical defenses that inhibit the growth or (in some cases) outright kill those that dare to consume them. In this regard, if plants are the organisms that harness the sun's energy, then plant chemical defenses are the small metabolites which mediate the flow of that energy to the rest of terrestrial life on earth.

When I first encountered this concept while an undergraduate at the University of Evansville in southern Indiana, I was blown away by the thought that plants investing some amount of carbon to defense could dictate whether they are consumed or not. After learning this, the summer of my sophomore year in 2017 I began working in Dr. Arlen Kaufman's lab, applying leaf spray mass spectrometry to the analysis of plant defense chemicals, a technique with which his group (along with Dr. Cris Hochwender, who became my Ecology professor) had published a couple of years prior (Snyder et al. 2015). Arlen had me read the paper "Phenolic glycosides of the Salicaceae and their role as anti-herbivore defenses" by Boeckler et al. (2011) which served as my true introduction into chemical ecology, and my fascination with plant chemical defenses was set in stone. Here was a paper detailing with so many dimensions of this one group of compounds (the salicinoids) from a genetic, biosynthetic, taxonomic, and ecological perspective. These were compounds underlying the mechanisms by which "Beaver browsing benefits beetles" (Martinson et al. 1998) and by which the Viceroy Butterfly (*Limenitis archippus*, Nymphalidae: Limenitinae) was reclassified as a Müllerian, and not a Batesian, mimic of the famous Monarch (*Danaus plexippus*, Nymphalidae: Danainae) (Prudic et al. 2007). These salicinoid phenolic glycosides are produced by aspens, cottonwoods, poplars (collectively, the genus *Populus*) and willows (the genus *Salix*) in the plant family Salicaceae, all of which are storied plants in human history in their own right, including (but not limited to) being the inspiration for aspirin, an excellent basketry material, and the canvas for the Mona Lisa. Evidence even suggests that hominid relationships with these plants and chemicals are not restricted to our species, as Neanderthals also self-medicated with poplar bark (which contains these salicinoids) over 40,000 years ago to relieve pain (Weyrich et al. 2017)! I was sold on this system of study, and eagerly got to work in the lab.

For some reason (probably naivety), after reading Boeckler et al. (2011) and some other papers on salicinoid phenolic glycosides, I thought that maybe we had a firm grasp on the understanding of their dynamics in plants. Part of this perspective likely came from the sheer amount of papers published on *Populus* alone, as a 2007 study detailed over 4000 publications, of which the University of Wisconsin had published 321 (in part due to the work of Dr. Richard Lindroth and colleagues and ranked as third most world-wide at the time) and the breadth of topics that had been explored in the genus, solidifying *Populus* as a model tree system and leading to the first tree (and third plant) genome being sequenced for *Populus trichocarpa* in 2006 (Tuskan et al. 2006). My perspective was shattered when one day, rather than continuing to look at the chemical constituents of *Populus deltoides* (eastern cottonwood), which the lab had published the 2015 leaf spray paper on, I went down to Cris' garden of over 100 species native to Indiana. In the center of the garden, just beginning to tower over the other plants, was a female *Populus heterophylla* (swamp cottonwood) strategically planted in a drainage ditch. Boeckler et al. (2011) had detailed a table of salicinoid occurrence in *Populus* and *Salix*, and in that table *P. heterophylla* conspicuously produced a single salicinoid according to Pearl and Darling (1977). I took a leaf from the tree, went back up to the lab, and within a minute had ions flowing from the leaf into the mass spectrometer. Immediately, I could tell that Pearl and Darling (1977) had missed something, as there was a diversity of compounds in the mass spectrum, and the signal appeared very different from the *P. deltoides* I was used to. I had a single, overarching question at that moment: *Why*? Why did *P. heterophylla*'s chemistry look like this? Why were the chemical profiles of these two plants different? Why had this not been reported before? Why did parts of *P. heterophylla*'s salicinoid arsenal resemble that of *Populus tremula* (European aspen, Keefover-Ring et al. 2014) or those of species in *Salix*? I immediately went to find Arlen with

these questions, and he explained that unfortunately, those answers were beyond what we could do at the time, and redirected me back to the *P. deltoides* project. I learned quite a bit more working on that project, but those questions of *why* never left my mind.

As I began to think about grad school, I knew that I wanted to continue to work on the salicinoid system, and I remembered that one of the best places for salicinoid research was the University of Wisconsin-Madison, the name of which adorned many of the papers I had read as an undergraduate. I reached out to Dr. Ken Keefover-Ring, had a short phone call about chemical ecology, and began grad school in the Department of Botany in the fall of 2019. As I was thinking about a project to work on, I thought back to my encounter with the salicinoids of *P. heterophylla* and the innate "*why?*" they elicited from me. Thus, I proposed a project to Ken, and over the next six years I began to find some of the answers to that *why*, the results of which are detailed in the following three chapters.

The first chapter is partially inspired by Ken's findings with *P. tremula* in Keefover-Ring et al. (2014), where salicinoids were sampled from *P. tremula* individuals throughout Sweden, leading to the discovery of multiple chemical phenotypes, or chemotypes, in the species. My work with *P. heterophylla* would be starting from a much smaller knowledge base, as a single research paper has been published in the past 50 years on the species, the work of Pearl and Darling (1977). Before I began to ask any more questions, I wanted to know what was chemically possible in *P. heterophylla*, and, due to its unique U-shaped range around the Appalachian Mountains in addition to its wind-dispersed pollen and seeds, if restricted gene flow or population structure might modulate the distribution of chemotypes (if any) in the species, such that there would be different chemistry on either side of the mountains. In this chapter, I utilize modern chemical methods to investigate the diversity of salicinoids in *P. heterophylla*, and

use genetic sequencing of individuals from throughout the species range to explore the relationship of gene flow and population structure to that salicinoid diversity.

The second chapter expands on my fascination with Optimal Defense that began in Cris's Ecology course (and on which I wrote an undergraduate grant to support myself and another student in the summer of 2018) but implements those ideas in a more elegant manner. Cloning trees of different chemotypes from throughout the range of *P. heterophylla*, I established a common garden thirty minutes north of Madison at the University of Wisconsin-Madison's Arlington Agricultural Research Station, and over the course of summer 2022 I conducted a suite of measurements to explore what Optimal Defense looks like in young carbon-sink and mature carbon-source leaves of *P. heterophylla*. This is notable because of the diversity of compounds produced in this species, and because of the physical and physiological differences between its young, carbon-sink and mature, carbon-source leaves. Utilizing physiological, chemical, and genetic data, I show that Optimal Defense strategies can be complex but clearly essential to the growth of these trees.

The final chapter began as an undergraduate senior research project for Sarah Kapsner (who was instrumental in collecting data for Chapter Two), but here is greatly expanded in its scope as Chapter 3 of my dissertation. In it, I pair my chemical knowledge with phylogenetic comparative methods to explore the evolution of salicinoids across *Populus* and *Salix*, and present ideas about why extant salicinoid diversity is the way it is, as well as some paths forward to enhance our understanding of this ecologically important group of compounds.

In all, I have spent eight years wrestling with that initial question of *why*, and while I now have many more questions, I believe the answers I have found set a foundation for future research on both *Populus heterophylla* and the reasons behind salicinoid diversity.

References

Bar-On, Y. M., Phillips, R., & Milo, R. (2018). The biomass distribution on Earth. *Proceedings of the National Academy of Sciences*, *115*(25), 6506–6511. https://doi.org/10.1073/pnas.1711842115

Boeckler, G. A., Gershenzon, J., & Unsicker, S. B. (2011). Phenolic glycosides of the Salicaceae and their role as anti-herbivore defenses. *Phytochemistry*, *72*(13), 1497–1509. https://doi.org/10.1016/j.phytochem.2011.01.038

Cooke, J. E. K., & Rood, S. B. (2007). Trees of the people: The growing science of poplars in Canada and worldwide. *Canadian Journal of Botany*, *85*(12), 1103–1110. https://doi.org/10.1139/B07-125

Fraenkel, G. S. (1959). The raison d'Être of secondary plant substances. *Science*, *129*(3361), 1466–1470.

Hairston, N. G., Smith, F. E., & Slobodkin, L. B. (1960). Community structure, population control, and competition. *The American Naturalist*, *94*(879), 421–425.

Martinsen, G. D., Driebe, E. M., & Whitham, T. G. (1998). Indirect interactions mediated by changing plant chemistry: Beaver browsing benefits beetles. *Ecology*, *79*(1), 192–200. https://doi.org/10.1890/0012-9658(1998)079[0192:IIMBCP]2.0.CO;2

Pearl, I. A., & Darling, S. F. (1977). Studies on the leaves of the family Salicaceae. 17. Hot-water extractives of the leaves of Populus heterophylla L. Journal of Agricultural and Food Chemistry, 25(4), 730–734. https://doi.org/10.1021/jf60212a035

Prudic, K. L., Khera, S., Sólyom, A., & Timmermann, B. N. (2007). Isolation, identification, and quantification of potential defensive compounds in the viceroy butterfly and its larval host–plant, carolina willow. *Journal of Chemical Ecology*, *33*(6), 1149–1159. https://doi.org/10.1007/s10886-007-9282-5

Snyder, D. T., Schilling, M. C., Hochwender, C. G., & Kaufman, A. D. (2015). Profiling phenolic glycosides in *Populus deltoides* and *Populus grandidentata* by leaf spray ionization tandem mass spectrometry. *Analytical Methods*, *7*(3), 870–876. https://doi.org/10.1039/C4AY02639J

Tuskan, G. A., DiFazio, S., Jansson, S., Bohlmann, J., Grigoriev, I., Hellsten, U., Putnam, N., Ralph, S., Rombauts, S., Salamov, A., Schein, J., Sterck, L., Aerts, A., Bhalerao, R. R., Bhalerao, R. P., Blaudez, D., Boerjan, W., Brun, A., Brunner, A., … Rokhsar, D. (2006). The genome of black cottonwood, *Populus trichocarpa* (Torr. & Gray). *Science*, *313*(5793), 1596–1604. https://doi.org/10.1126/science.1128691

Weyrich, L. S., Duchene, S., Soubrier, J., Arriola, L., Llamas, B., Breen, J., Morris, A. G., Alt, K. W., Caramelli, D., Dresely, V., Farrell, M., Farrer, A. G., Francken, M., Gully, N., Haak, W., Hardy, K., Harvati, K., Held, P., Holmes, E. C., … Cooper, A. (2017). Neanderthal behaviour, diet, and disease inferred from ancient DNA in dental calculus. *Nature*, *544*(7650), 357–361. https://doi.org/10.1038/nature21674

Wilkinson, D. M., & Sherratt, T. N. (2016). Why is the world green? The interactions of top–down and bottom–up processes in terrestrial vegetation ecology. *Plant Ecology & Diversity*, *9*(2), 127–140. https://doi.org/10.1080/17550874.2016.1178353

Chapter 1

Biogeography and population structure of *Populus heterophylla* defensive chemistry

Tyler H. Wintermute[1], Sandra J. Simon[2,3], Bryan A. Connolly[4], Stephen P. DiFazio[3], Ken Keefover-Ring[1,5]

[1]Department of Botany, University of Wisconsin-Madison

[2]School of Arts and Sciences, Biology & Biochemistry Department, Emory & Henry University

[3]Department of Biology, West Virginia University

[4]Department of Biology, Eastern Connecticut State University

[5]Department of Geography, University of Wisconsin-Madison

Author Contributions: THW, KK-R conceived study; THW, KK-R, and SPD developed study design; THW, BAC, and SPD collected samples; THW and SJS conducted lab work and bioinformatics; THW analyzed the data with input from SJS, SPD, and KK-R; THW wrote the manuscript with input from SJS, SPD, and KK-R.

Introduction

An integral part of plant life history is the production of chemicals to defend against antagonists, such as herbivorous animals (Fraenkel 1959). Plant defensive chemistry can result in speciation, where certain populations evolve a novel defensive compound or a suite of compounds which allow them to "escape" from predation, resulting in a large fitness advantage and relaxed selective pressures, enabling those populations to diversify and "radiate" into new species. This is the basis of the "escape-and-radiate" hypothesis first proposed by Ehrlich and Raven (1964) and has guided decades of evolutionary research related to chemical ecology, providing both an explanation for speciation and for plant chemical diversity (Farrell et al. 1991; Marquis et al. 2016; Maron et al. 2019; Cogni et al. 2022). However, at least for chemical diversity, the opposite might also be true. Lineages might first experience a radiation due to other, non-chemical-defense mechanisms, and be able to disperse into novel environments. In these environments these new populations could experience either predator release in the absence of their co-evolved antagonists, or naïve predators maladapted to the dispersed species' defenses (Maron et al. 2019). In this scenario, plant defenses might experience a de-escalation to a simplified arsenal that is "good enough" at defense in a new environment, reducing the biosynthetic cost of defense that was previously complex or produced in high quantities to deal with ancestral antagonists in favor of lower quantities or simplified defenses to deter these new and naïve antagonists (Janzen 1973; Vourc'h et al. 2001). This decrease in defense cost can allow these plants to invest resources in other areas, such as optimizing growth and physiological fitness (Monson et al. 2022), and the decreased selective pressure on the genetic region which codes for certain defenses might allow that part of the genome to mutate in ways that create new chemicals, which may be better or orthogonal in mode of action when compared to the original

compounds, in what can be termed “re-escalation” of defenses (Zangerl & Berenbaum 2005; Maron et al. 2019), resulting in novel chemical phenotypes, or chemotypes, in a species (Keefover-Ring et al. 2009). Chemotypes can be defined in different ways depending on an author’s goals, but here I define them broadly as the pattern of chemical compounds in a given organ or individual in respect to their relative abundance. The quantity of these chemicals might shift depending on ontogeny or environment, but in general their relative abundances should remain stable. The process of de/re-escalation of defense has been observed in a time scale of a few hundred years (Tewes et al. 2018) and is the basis of the Shifting Defense Hypothesis (Doorduin & Vrieling 2011) in invasion ecology, but given enough time these shifts in defense could become fixed evolutionarily in a population or species.

An important mechanism for the maintenance of de/re-escalated defense arsenals is reduced gene flow between ancestral populations and the dispersed populations, either due to vicariance or barriers to sexual reproduction. These dispersed populations are often at the edges of a species range and likely encounter novel environments and antagonists compared to the rest of the species, leading to the de/re-escalation relative to the ancestral environment (López-Goldar & Agrawal 2021). If gene flow is maintained between these edge populations and their ancestral populations, there might be a continual re-introduction of ancestral genes to these novel environments, resulting in a genetic swamping (Sexton et al. 2009) of the novel phenotypes (Futuyama 1987), homogenizing phenotypes within a species. Thus, it is more likely for this “de/re-escalation” to occur when barriers to gene flow (and thus introgression) are substantial, such as under an isolation-by-distance model when populations are extremely far from each other or when there are substantial geographic barriers to gene flow (Sexton et al. 2014). Trait polymorphisms that arise and are maintained in the presences of barriers to gene flow across a

species range have been studied in other plant traits such as floral pigmentation (Hernández et al. 2022) but this phenomenon has not been investigated for chemical defenses.

One group of plants well-suited for dispersal into new environments are species in the plant family Salicaceae tribe Saliceae, which includes the genera *Salix* (the willows) and *Populus* (the cottonwoods, aspens, and poplars), due to their wind-dispersed pollen and seeds which can cover vast distances. Indeed, these genera are widespread in the northern hemisphere, with a few species native to regions south of the equator, and exhibit great intraspecific variation in the traits enabling single species to survive in many habitats (Godbout et al. 2020). These genera also contain species adapted to diverse environments such as alpine peaks and dry deserts, with a range of growth forms from dwarf willows growing no more than a few centimeters in height, to towering trees in both genera (Dickmann & Kuzovkina 2014). While there are clearly few limitations for these species to disperse into new geographic locations, their ability to speciate is inhibited by their wind-pollination and wind-dispersal syndromes, which enables long-distance gene flow (Slavlov et al. 2009; DiFazio et al. 2012) and could be keeping species in a sort of stasis due to the aforementioned genetic swamping and introgression of traits throughout a species' range. This is evidenced by the disparity in species richness between the genera: while *Populus*, which is solely wind-pollinated, has about 35 species, *Salix* species, which are wind- and insect-pollinated, number around 500 species, likely owing to insect preferences and selection for floral traits, resulting in more intentional gene flow and enabling speciation (Wessinger 2021); although purifying selection has also been proposed for this discrepancy (Hou et al. 2019). Additionally, while many members of *Populus* freely hybridize with each other, there is evidence for selection against recombinant hybrids, which can maintain these species boundaries even with rampant gene flow (Christe et al. 2016).

All species of *Populus* produce salicinoids, anti-herbivory defensive compounds which mediate interactions between the plant and their antagonists (Boeckler et al. 2011). At their simplest, these compounds are two-component defenses where a saligenin moiety is linked to a glucose moiety to form the salicinoid salicin (Fig. 1). Following damage by antagonists, salicinoids are released from vacuolar storage and come into contact with the plant's β-glucosidases, releasing the toxic aglycone moiety which can then be oxidized to become protein-crosslinking reactive oxygen species (Pentzold et al. 2014). Notably, more complex salicinoids, such as salicortin and tremulacin, are not believed to be formed by simply decorating an existing salicin structure but rather by adding additional organic acids to the saligenin component before linkage to the glucose moiety, and then can be further decorated with additional functional groups, although the full biosynthetic pathway for any salicinoid is not currently known (Fellenberg et al. 2020; Gordon et al. 2022). Once formed, these compounds can make up to 30% of the dry mass of individual leaves (Donaldson et al. 2006) but this value can decline with leaf (Wintermute, see Chapter 2) and plant age (Cole et al. 2021).

Within *Populus*, some species have limited salicinoid diversity (*P. tremuloides*, Cope et al. 2020; *P. grandidentata*, Lindroth & Pajutee 1987) while others are more diverse (*P. deltoides*, Snyder et al. 2015; *P. tremula*, Keefover-Ring et al. 2014). How salicinoid diversity arose in these species is unknown (more about this in Chapter 3), but one clue to this diversity might lie in the chemotypes of salicinoid-rich species. In *P. tremula*, there are four chemotypes: cinnamoyl, acetyl, cinnamoyl-acetyl, and *tremuloides*-like (Keefover-Ring et al. 2014). The *tremuloides*-like chemotype is not very salicinoid-rich, resembling the chemistry of the rest of the members of *Populus* section *Populus*. However, the other chemotypes have a greater diversity of salicinoids, and there is a trade-off observed between tremulacin and salicortin, the

two most abundant salicinoids in *P. tremula*. This trade-off is clear when comparing *tremuloides*-like and cinnamoyl chemotypes, suggesting that instead of producing large amounts of tremulacin those cinnamoyl chemotypes are instead favoring the production of cinnamoyl-salicortin, which would provide some form of novel defense against antagonists adapted to *tremuloides*-like chemotypes or increase the complexity of the aglycones in a herbivore's gut, slowing down detoxification or metabolism. This defensive advantage would satisfy some of the Moving-Target hypothesis of plant defense, which states that it is adventitious for plants to evolve (or produce) many defensive compounds such that it is difficult for antagonists such as herbivores to adapt their detoxification mechanisms to handle all of the different chemical compounds (Wetzel & Whitehead 2020). Thus, if the simple *tremuloides*-like chemotype is viewed as the ancestral chemotype of *P. tremula* (Chapter 3), then *P. tremula* might be thought of as being in a transition-state of salicinoid defense in the genus. The cinnamoyl, acetyl, and cinnamoyl-acetyl individuals could have a defensive fitness advantage when compared to the *tremuloides*-like chemotype, and given enough time those chemotypes could go to fixation in the species, but given that the *tremuloides*-like chemotype still confers adequate defense (inferred by those salicinoids being the sole salicinoids in other related species, Boeckler et al. 2011; Chapter 3), in addition to the lack of population structure in *P. tremula* in Sweden (Ingvarsson & Bernhardsson 2020) and geographic structure of these chemotypes (Keefover-Ring et al. 2014), this is unlikely to happen.

One species that might also represent a transition state of salicinoid diversity in *Populus* is *Populus heterophylla* L. (swamp cottonwood, *Populus* subgenus *Eupopulus* section *Leucoides*). Native to eastern North America, *P. heterophylla* is a wind-pollinated and wind-dispersed tree which can be found in bottomland swamps and wetlands in a U-shaped

distribution around, but not in, the Appalachian Mountains (Fig. 2). The species has suffered from the drainage and conversion of these wetlands to other uses, and is now extirpated from one state, endangered in six others, and endangered in Canada, though there are large, healthy populations in the Carolinas and occasionally in the Mississippi River floodplain. Like other members of *Populus*, *P. heterophylla* is an early successional species, favoring sunny, exposed habitats, although it is not immediately clear why it is found in some wetlands and not in others throughout its range, a feature that makes it difficult to find without prior knowledge of a population's location. Additionally, like members of *Populus* section *Populus*, and some other members of *Populus* subgenus *Eupopulus*, *P. heterophylla* can reproduce asexually through suckering, a trait that has allowed some species of *Populus* to survive for millennia (Pineau et al. 2024).

In contrast to a lack of salicinoids historically reported in *P. heterophylla* (Pearl & Darling 1977), I have found the species to have more than 20 salicinoids. This discrepancy is likely due to differences in extraction methods (Pearl & Darling 1977 used hot water extracts, I use chilled methanol and sonication) and analytical instrumentation. This initial report on the chemistry of *P. heterophylla*, combined with the species penchant for "unpleasant" swampy conditions, may have deterred research on the species over the following decades, save for the occasional observance in a species inventory (Searcy & Ascher 2001). Regardless, the diversity of salicinoids in *P. heterophylla* could mean that, similar to *P. tremula*, there is a possibility of having multiple chemotypes in the species, with various combinations or relative amounts of salicinoids depending on the chemotype, as seen in *P. tremula* (Keefover-Ring et al. 2014). However, unlike *P. tremula*, which likely has very limited geographic barriers to gene flow other than isolation-by-distance (de Carvalho et al. 2010), *P. heterophylla* is restricted to wetlands

around the Appalachian Mountains, and those mountains likely inhibit gene flow via wind-pollination and wind-dispersal, as at the northern ends of its range there is a 300-km distance between populations of *P. heterophylla* in Ohio and New York. Indeed, the Appalachian Mountain Discontinuity has been well-documented in other species (Soltis et al. 2006; Lyman & Edwards 2022), although mostly in animals and rarely with plants. Limited gene flow between the two sides of the Appalachian Mountains could allow for the allopatric evolution of unique chemistry and chemotypes in the species, and provide a possible explanation for salicinoid diversity in *P. heterophylla*. In general, aspens (members of *Populus* section *Populus*) tend to have a lower diversity of salicinoids (but see Keefover-Ring et al. 2014) than members of *Populus* subgenus *Eupopulus* (Chapter 3) and the two groups are generally sexually incompatible due to pre- and post-zygotic barriers (Vanden Broeck et al. 2005) limiting introgression between sections (Wang et al. 2020) and thus of salicinoids via hybridization (Rehill et al. 2005; Caseys et al. 2015; Woolbright et al. 2018). Phylogenetic analyses show that, after the divergence of subgenus *Eupopulus* and the rest of *Populus,* the ancestor of *P. heterophylla* was the first to diverge from the rest of the subgenus, and *P. heterophylla* is now sister to the rest of extant subgen. *Eupopulus* (Wang et al. 2020; Wang et al. 2022; Sanderson et al. 2023). Patterns of chemical diversity in *P. heterophylla*, especially if they mirror *P. tremula's* chemotypes, could provide a possible mechanism for the divergence of salicinoid diversity between the two groups, whereby the ancestor of subgenus *Eupopulus* radiated into a wetter environment [members of subgenus *Eupopulus* tend to prefer and succeed in wetter environments that members of section *Populus,* with a few exceptions (Dickmann & Kuzovkina 2014)] than its upland aspen relatives, encountering novel antagonists, and experiencing some format of a de/re-escalation of its defenses, resulting in the present-day divergence in chemistry between the groups. Certainly,

living in different environments (dry vs wet) could have been the initial barrier to gene flow between the subgenus *Eupopulus* ancestor and the section *Populus* ancestor, allowing for allopatric speciation and divergence in sexual traits, leading to the incompatibility between the two groups today, and preventing the introgression of salicinoids between the groups via hybridization, allowing the subgenus *Eupopulus* ancestor to acquire mutations leading to greater chemical diversity independent of section *Populus*.

I hypothesize that if there are geographical patterns of chemotype distributions in *P. heterophylla*, those distributions will have been maintained in-part by a lack of gene flow between those populations. This is due both to the allopatry caused by lack of suitable upland habitat for this species in the Appalachian Mountains, and the improbability of pollen and wind travelling vast distances over those mountains.

To determine if salicinoid diversity in *P. heterophylla* is in-part due to biogeographic restrictions on gene-flow, two sets of data are needed. The first is an analysis of the distribution of chemotypes (if they exist) in the species. The second is an analysis of the population structure, gene-flow, and evolution of biogeography in the species. To accomplish the first, I collected samples from 52 swamps throughout the range of *P. heterophylla*, analyzed their chemistry via ultra-high pressure liquid chromatography and tandem mass spectrometry (UHPLC-MS^2), and tested for spatial autocorrelation. To accomplish the second, I extracted DNA from a subset of the individuals sampled for chemistry, sequenced portions of their genome, built a phylogeny of filtered samples, and explored population structure and the evolution of geography on that phylogeny. Finally, I combine both sets of data to demonstrate the relationship between population structure and history on the geographical distribution of chemotypes in *P. heterophylla*.

Methods

Site selection

Sites for sampling were selected based on herbarium records accessed via the SEINet Regional Network of North American Herbaria (SEINet, https://symbiota.org/seinet/) as well as iNaturalist records (https://www.inaturalist.org/taxa/167295-Populus-heterophylla). From these sources, sites were selected based on probability of having swamp cottonwood, which was determined by the recency of the record and confirmation of vegetation via satellite imagery (i.e. if the location of a herbaria record was now a parking lot) and proximity to other sites to balance geographic coverage with travel time. If required, collection permits were obtained, and private landowner permission granted. A full list of sites and the dates of collection can be found in Table S1.

Sample collection for chemistry

Samples were collected in the summers of 2020 and 2022. For the first round of collections, at least 5 fully-expanded mature, undamaged leaves from 5 individuals at each site were collected, and then stored in paper envelopes inside of plastic bags with silica at ambient temperature. These leaves were then transported back to Madison over the course of a week. For the second, at each site at least 5 mature, undamaged leaves were collected from up to 10 individuals at each site. These leaves were kept in paper envelopes inside of plastic bags with silica gel beads, and then in a cooler of dry ice for transport back to Madison. For both rounds of collection, care was taken to not collect leaves from clones, and each individual was at least 20 meters from another tree, when possible. One site, in Massachusetts, is known to be just a single clonal male with 90 stems; 5 samples were collected from this site as well, but results were averaged for analyses. GPS coordinates were recorded for each individual. Once back in

Madison, samples were immediately flash-frozen in liquid nitrogen, lyophilized, and stored at -20 °C until chemical analysis.

Salicinoid Extraction and Analysis

Dried samples were ground in a ball mills, and then ca. 10 mg of tissue was extracted with 1 mL methanol with phenyl-β-D-glucopyranoside as an internal standard. Samples were sonicated for 30 minutes at 4 °C, centrifuged, and then a 200 µL aliquot was transferred to an autosampler vial with a glass insert. Samples were stored in an autosampler chamber at 7 °C, and 1 µL was injected onto a Acquity C_{18} CSH column (2.1 x 100 mm, 1.7 µm, Waters Corporation, Milford, Massachusetts, US) inline on a Vanquish UHPLC system coupled to a QExactive Orbitrap mass spectrometer via a HESI-II electrospray probe (instruments from Thermo Fisher Scientific Inc., Waltham, Massachusetts, US). LCMS-grade Water with 0.1% formic acid was used for mobile phase A, and LCMS-grade Acetonitrile with 0.1% formic acid was used for mobile phase B. The gradient was as follows: 0 -18 minutes, 0.1% to 100% B; 18 – 21 minutes, 100% B; 21-21.05 minutes, 100%-0.1% B; 21.05-26 minutes, 0.1% B. Data was collected via negative ionization. Data-Dependent Acquisition was used to collect full-scan chromatograms and fragmentation patterns for ions of interest simultaneously, with a collision energy of 25. Salicinoids were identified via comparison with purified standards (kindly provided by Dr. Richard Lindroth) and fragmentation pattern and parent mass. Peaks were integrated using Thermo Xcalibur version 4.4.16.14, and samples were assigned chemotypes according to presence or absence of characteristic salicinoids.

Tissue Collection, Genomic DNA Extraction, and Sequencing

Leaf tissue was sampled from 60 *P. heterophylla* trees collected across the species range in 13 different states. Tissue was preserved and genomic DNA (gDNA) was extracted from a

subset of genotypes using a CTAB DNA extraction protocol (Doyle & Doyle, 1987) with the remaining genotypes extracted using a DNeasy plant mini kit (Qiagen, Hilden, Germany; Cat. No. 69104). DNA libraries were prepared from gDNA using the QuantaBio sparQ DNA Frag and Library Prep Kit (QuantaBio, Beverly, Massachusetts, USA, Cat. No. 95194-096). The finished libraries were quantified/pooled at the West Virginia University (WVU) Genomics Core via Bioanalyzer High Sensitivity (0.5-5 ng/uL) DNA Chip and sequenced at the Marshall University Genomics Core Facility using an NextSeq P3 200 cycle flow cell (Illumina, Inc., San Diego, CA, USA).

Genome Alignments and Variant Calling

Sequencing reads were trimmed and filtered for quality using BBduk in the BBtools software package (BBMap – Bushnell B. – sourceforge.net/projects/bbmap/) with the following parameters: hammingdistance=1 \ k=20 \ minlength=60 \ trimq=20. Reads were then aligned to the *Populus deltoides* WV94 v2.1 genome (https://phytozome-next.jgi.doe.gov/info/PdeltoidesWV94_v2_1) using bwa mem (bwa v0.7.17) (Li, 2013). Optical duplicates were marked in the genome alignments using MarkDuplicates in the GATK (v4.4.0.0) software package (McKenna *et al.*, 2010) via Broad Institute's best practices recommendations (DePristo *et al.*, 2011). Alignment quality was estimated using flagstat in the Samtools (v1.17) software package (Danecek *et al.,* 2021). Variants were called using HaplotypeCaller GATK (v4.4.0.0) for each chromosome interval separately for each genotype and then GVCF files were merged into a single file using CombineGVCFs GATK (v4.4.0.0).

Variant Hard Filtering and Single Nucleotide Polymorphism (SNP) Thinning

Insertion deletion polymorphisms (indels) were separated from single nucleotide polymorphisms (SNPs) variants using SelectVariants GATK (v4.4.0.0). After consideration of the

distribution of quality scores, SNPs were filtered with VariantFiltration GATK (v4.4.0.0) using the Broad Institute's best practices with the following hard filters: MQ < 40.00 | | SOR > 3.000 | | QD < 2.000 | | FS > 60.000 | | MQRankSum < −12.500 | | ReadPosRankSum < −8.000 | | ReadPosRankSum > 8.000 | | DP < 6. SNPs were further thinned using VCFtools (v0.1.13) (Danecek *et al.*, 2011) with the following parameters: --maf 0.05 \ --max-maf 0.95 \ --max-missing 0.90 \ --min-meanDP 5.00 \ --max-meanDP 25.00 \ --thin 2000 \. Given the use of a different species genome for alignments (i.e. *Populus deltoides* WV94 v2.1 genome) 28,112 SNP variants that overlapped with WV94 repeats were removed from the dataset. After quality filtering and thinning the dataset for analysis contained 47 *P. heterophylla* genotypes and 74,309 SNP variants.

Clone Assessment

The SNP variant dataset was imported to TASSEL (v5.2.93) (Trait Analysis by aSSociation, Evolution and Linkage) software (Bradbury *et al.*, 2007) to evaluate relatedness between genotypes. Distance and kinship matrices were generated to pairwise compare the genotypes. *P. heterophylla* genotypes PH73F and PH66F showed a high degree of relatedness (distance = 0.1673; kinship = 0.7512) suggesting possible clonality. PH66F was removed from the dataset leaving 46 *P. heterophylla* genotypes for final analysis.

Phylogenetic tree estimation and time calibration

SNP variants were used to estimate a phylogenetic tree in IQ-Tree. SNPs of *P. deltoides* WV94 were obtained by filtering the genome for only SNPs at the positions in the 46 *P. heterophylla* genotypes left. These 47 sequences were used with an UNREST+FO model of substitution in IQ-Tree v2.4.0 (Minh et al. 2020) to obtain a consensus rooted tree with rootstrap support. The tree was exported to R, and then the tree was calibrated using an age estimate of the

MRCA between *P. heterophylla* and *P. deltoides.* Sanderson et al. (2023) used *BEAST2 on two sets of 5 genes to generate two estimates for the divergence of the ancestors of *P. heterophylla* and *P. deltoides* to be either 7.48mya (Figure 2a in Sanderson et al. 2023) or 5.97mya (Figure 2b in Sanderson et al. 2023), with the first set of genes found to be the best set of the two according to the criteria in their methods. Liu et al. (2022) found an average divergence time of 7.29mya for these two species using 34 chloroplast fragments from 34 species in *Populus*, which is closer to the 7.48mya estimate from Sanderson et al. (2023). Thus, I chose the 7.48mya estimate to use to calibrate my tree, which was done using the chronoPL() function from the R package 'ape'.

Chemotype mapping

Spatial autocorrelation of chemotypes was assessed using the 'spdep' package in R. This was conducted on an individual and a site level to determine if 1) individuals of the same chemotype were clustered in space more often than individuals of differing chemotypes and 2) if sites containing individuals of rare chemotypes were more likely to be near sites containing rare chemotypes than sites comprised only of a common chemotype. To do so, chemotype data were converted into a binary format, where "0" represented the most abundant chemotype, and "1" represented any other chemotype. Individuals were assigned these codes according to their chemotype, and sites that had at least one individual with a "1" were assigned a "1" while sites only containing the most abundant chemotype were assigned a "0". K-nearest-neighbors was used to assign spatial weights for site-level data, and for individual-level data K-nearest-neighbors were assigned for K-neighbors not occurring at the same site as a given individual. Global spatial autocorrelation was assessed using the moran.test() function, and local spatial autocorrelation, which takes into account the lagged values, that is, the values of neighbors' neighbors, was assessed using the localmoran() function in R.

Population Structure

The fastStructure package (Raj *et al.*, 2014) was installed using the Anaconda (v2024.06-1) (*Anaconda Software Distribution* 2020) computer program. The structure.py script was used to infer admixture among ancestral populations with K clusters = 1-5 and set seed = 100. The appropriate number of model components was estimated using the choose.py script. Admixture proportions among genotypes was visualized via the distruct.py script.

Analysis of Molecular Variance (AMOVA) and F-statistic Estimation

All population genetic analyses we conducted using the R language and environment for statistical computing (R Core Team 2021). Trees were grouped based on population of origin as determined by fastStructure analysis. The population structure of these groupings was assessed with an analysis of molecular variance (AMOVA) using the '*poppr.amova*' function in the Poppr software package (Kamvar *et al.*, 2015). A 1,000-iteration permutation test was utilized to test phi statistics for significance via the '*randtest*' function. The '*basic.stat*' function in the hierfstat package (Goudet, 2005) was used to estimate observed heterozygosity (Ho), observed gene diversities (Hs), inbreeding coefficient(Fis), and fixation index (Fst) across all loci. Finally the '*genet.dist*' function in the hierfstat package was used to determine pairwise Fst among population groupings.

Estimation of Ancestral Areas

The R package BioGeoBEARS (Matzke, 2013, 2014) was used to estimate the ancestral range of *P. heterophylla* phylogeny using a dispersal, extinction, and cladogenesis (DEC) model, as well as one with a "jump" parameter of cladogenesis. Genotypes were assigned one of six regions (upper Midwest, Midwest, south, southern Atlantic, mid-Atlantic, and northeast)

according to general regions where they were collected from, and an adjacency matrix for these regions was created, with a maximum of two areas allowed for ancestral areas.

Results

Four Salicinoid Chemotypes in Populus heterophylla

A total of 24 salicinoids were found in *P. heterophylla* (Table 1) and four chemotypes identified based on combinations of those salicinoids, many of which are the most abundant in those chemotypes (Fig. 1). The HCH-tremulacin chemotypes (16/290 trees) were characterized by the presence of HCH-tremulacin and tremulacin-A. The HCH-nigracin (74/290 trees) chemotype is characterized by the presence of two HCH-nigracin isomers, as well as tremulacin-B and tremulacin-C. The nigracin-tremulacin chemotype (4/290 trees) is characterized by the presence of two isomers of HCH-nigracin along with HCH-tremulacin, and all three isomers of tremulacin. Finally, the "standard" chemotype (196/290) is characterized by the absence of HCH-tremulacin, only a single isomer of HCH-nigracin, and tremulacin-C, with all other salicinoids in this chemotype being present in the other chemotype. Additionally, the non-tremulacin-based chemotypes (HCH-nigracin and Standard) show two isomers of salicortin, and the tremulacin chemotypes (nigracin-tremulacin and HCH-tremulacin) with very high abundances of tremulacin and HCH-tremulacin have limited HCH-salicortin in their chromatograms.

Geographical structure of chemotypes – site-level

The geographic distribution of chemotypes appeared to be non-random across the landscape (Fig. 2). Regardless of the number of neighbors used, there was global spatial autocorrelation of sites according to the presence or absence of non-standard chemotypes at a given site (Fig. 3). However, the Local Indicators of Spatial Autocorrelation (LISA) calculated

using localmoran() had slightly different results depending on the number of K-neighbors used. For example, at K = 6, the smallest number of neighbors that resulted in a single network, there were low-low sites (sites containing only Standard chemotypes were neighbors with other sites containing only Standard chemotypes) west of the Appalachian Mountains, and some high-high (sites with at least one non-Standard chemotype were neighbors with other sites containing at least one non-standard chemotype) sites east of the Appalachian Mountains, with a few high-low (sites with at least one non-Standard chemotype were neighbors with sites containing only Standard chemotypes) sites west of the Appalachian Mountains (Fig. 4). This pattern was the same when K = 17, which is one-third of the total number of sites, but much more sites returned a significant statistic for local spatial autocorrelation, and there were now a few low-high sites (sites containing only Standard chemotypes were neighbors with sites containing at least one non-Standard chemotype) east of the Appalachian Mountains (Fig. 5). Finally, this pattern stayed consistent when K = 17 with inverse distance weighting (closer sites have more spatial weight than further sites), albeit fewer sites returned a significant statistic for local spatial autocorrelation (Fig. 6).

Geographical structure of chemotypes – individual-level

We see the same patterns for individual-level spatial data as we do site-level data. All levels of K return a significant positive Moran's I statistic (Fig. 7). For LISA, the patterns are similar to site-level data, and the intensity of those patterns changes as we increase K. For example, at K = 20, the smallest number of neighbors that returned a single network, and with inverse-distance weighting, there were low-low neighbors and high-low neighbors west of the Appalachian Mountains, and high-high and low-high neighbors east of the Appalachian Mountains (Fig. 8). However, with the resolution afforded with individual-level data, there is

additional clustering of low-low neighbors in the northeast, and some high-low neighbors in the south Atlantic. These patterns shift a bit when K-neighbors is increased to 96 (just under one-third of the total individuals) but largely remain the same (Fig. 9).

Population Structure

The model complexity that maximized marginal likelihood = 2 and model components used to explain the structure in the variant dataset = 2. Genotypes were assigned to a population of origin based on the degree of admixture proportion as determined by their mean q values (Table 2; Figs. 10 and 11).

Analysis of Molecular Variance (AMOVA) and F-statistic Estimation

AMOVA (Table 3; Fig. 12) results showed 74.9% of the genetic variation in the data was explained between genotypes within populations which was significantly greater than expected by chance (phi = 0.781, sigma = 3263.9, p-value < 0.001). 4.08% of the genetic variation was explained by population of origin which significantly greater than expected by chance (phi = 0.0408, sigma = 177.9, p-value < 0.001). Twenty one percent of the genetic variation was explained within genotypes which was significantly less than expected by chance (phi = 0.789, sigma = 916.8, p-value < 0.001). Average observed heterozygosity and observed gene diversity was found to be 0.3107 and 0.2933, respectively and the F-statistic coefficient values were low (Fst = 0.0386, Fstp = 0.0743; Table 4).

Estimation of ancestral areas

The DEC model had a log-likelihood of -49.62, with an estimation of 0.11 for range-dispersal and 0.017 for range-extinction (Figure 13). The DEC+J model had a log-likelihood of -37.13, but collapsed the range dispersal and extinction parameters to 0, attributing all changes in range to the "jump" parameter, which returned a non-parsimonious result where *P. heterophylla-*

like ancestors would skip back-and-forth over entire parts of its range where extant members of the species are found (Fig. 14). This follows some of the critique of the +J parameter (Ree & Sanmartín 2018) and due to this issue (and the results of the DEC being more logical biologically) I present the results of the DEC model.

Under the DEC model, roughly 2 mya, the ancestor of *P. heterophylla* existed in the present-day Carolinas and Virginia, and proceeded to disperse southward towards the Gulf of Mexico. Following this, two clades formed, one in the Midwest near the Mississippi River, and one along the East Coast. The Midwest clade dispersed north about 1.5mya, reaching the modern-day confluence of the Mississippi and Ohio Rivers, and traveled along the Ohio River valley to reach the current upper Midwest distribution in Ohio, Michigan, and Ontario. The East Coast clade similarly began in the south near Apalachicola, dispersed north to the Carolinas and Virginia, and then further north into the Delmarva Peninsula and finally into the Northeast (New York, Connecticut, Rhode Island, Massachusetts).

Discussion

In this work, I demonstrate that there is geographical structure to the distribution of salicinoid chemotypes in *P. heterophylla*, and that this distribution matches the population structure of the species, suggesting that the two are linked. Exhaustive sampling of chemistry of any species across an entire geographic range is time-consuming and difficult, and thus it is rarely done (Keefover-Ring et al. 2014, Pratt et al. 2014, Keefover-Ring 2022), however, doing so can give a clearer picture of the chemotypes in a species, and provide directions for future work to establish how those chemotypes came to be. For *Populus,* much work has focused on the salicinoids salicin, salicortin, tremuloidin, and tremulacin, as those are the main salicinoids found in many species (Chapter 3), but also some of the most-studied species in the genus (Boeckler et

al. 2011; Cole et al. 2021). Salicinoids other than those four have received much less attention (but see Keefover-Ring et al. 2014) and clearly those four salicinoids are not the only ones in the genus. The diversity of salicinoids in *P. heterophylla*, as well as the possibility of clear genetic differences between populations and regions that are more likely to have one chemotype than another, provide some targets for future study to elucidate the genetic and biosynthetic controls of specific salicinoid production and increase our understanding of plant defense in a model tree system (Douglas 2017).

Geographic distribution of chemotypes

There is clear spatial autocorrelation of chemotypes in *P. heterophylla*, that is, if we bin the chemotypes into two groups, one being the standard chemotype, and one being the non-standard chemotypes, then trees with certain chemotypes are more likely to be located near other trees which share their chemotype, than expected by chance. Trees west of the Appalachian Mountains tend to be the standard chemotype, while trees east of the Appalachian Mountains tend to be either the standard or the HCH-nigracin chemotype, with an occasional HCH-tremulacin or nigracin-tremulacin chemotype. Interestingly, trees in the northeastern region tend to be the standard chemotype. While these distributions could be due to selection by different antagonists on either side of the Appalachian Mountains, interactions of *P. heterophylla* and other organisms are not well characterized. Certainly, I did not see any large differences, as the only interactions that stood out to me were beaver damage in the Midwest, and a leaf galler that was found on both sides of the mountains. Regardless, as stated previously, it is unclear if certain chemotypes are better at defense, and likely any differences are minimal due to the shared mode of action of HCH-groups, thus the differences in the distribution of chemotypes may be due less to selective pressure from antagonists and more to genetic differences in the populations.

Population structure of Populus heterophylla

From the dated phylogeny, I estimate extant *P. heterophylla* lineages to originate about 2 million years ago at the beginning of the Pleistocene. Notably, this date is based on estimates of the most recent common ancestor between *P. deltoides* and *P. heterophylla* to be about 7.48 mya (Sanderson et al. 2023). There are some technical issues with using *P. deltoides* to root and date *P. heterophylla* which I will discuss later and how I will address those issues, however, the results I present here are not likely to change. The species likely originated in the south Atlantic or Mid-Atlantic region, near the present-day Carolinas and Virginia, where there are currently stable and sizable extant populations. Following dispersal farther south, the species split into two clades: one in the Midwest, originating near the Mobile and Mississippi Rivers, and one closer to the east coast, with ancestral populations near the Apalachicola River. As time progressed, these clades began to move northward, with the Midwest population travelling up the Mississippi River, reaching its confluence with the Ohio River and then proceeding northeasterly through the Ohio River Valley. Similarly, the clade east of the Appalachians proceeded north along the Atlantic coast, establishing populations in the Carolinas and Virginia, as well as travelling further north to Delaware and finally the Northeast. There is little gene flow between these two clades today except for in the South along the Gulf coast, although our sampling for genetics in that region is limited (Fig. 11). Future studies should thoroughly sample along the gulf to determine the full area in which there is gene flow between the clades. Regardless of the results of re-rooting and re-dating the phylogeny, these two clades will likely still largely remain the same, and the DEC model results are likely robust geographically, even if temporally they may change.

Chemotypes of Populus heterophylla

The presence of four chemotypes in *P. heterophylla* has similarities to the four *P. tremula* chemotypes (Keefover-Ring et al. 2014). In particular, both species have a chemotype characterized by high concentrations of tremulacin. This chemotype is common throughout *Populus* and *Salix* (Chapter 3) and possibly represents the ancestral chemotype for the two genera. The majority of *Populus* section *Populus* still has this *tremuloides*-like chemotype, characterized by high levels of tremulacin and salicortin, and lower levels of salicin and tremuloidin. The position of *P. tremula* within *Populus* section *Populus* suggests that the additional chemotypes in *P. tremula* are recent innovations in the species. Similarly, the ancestor to *P. heterophylla* is sister to the rest of *Populus* subgenus *Eupopulus*, estimated to diverge from the shared ancestor with section *Populus* roughly 11-14 mya (Sanderson et al. 2023), and the presence of the HCH-tremulacin chemotype in *P. heterophylla* suggests that this chemotype is a remnant from that ancestral *Populus-Eupopulus* tremuloides-like chemotype. The patterns of salicinoids among the chemotypes described in Keefover-Ring et al. (2014) demonstrate some level of enzymatic promiscuity or competition for substrates, particularly between cinnamoyl or benzoyl groups. While cinnamoyl-salicinoids are not detected in *P. heterophylla*, other salicinoids such as nigracin and HCH-nigracin are, and similar tradeoffs in salicinoid composition as those found in *P. tremula* are observed.

The presence of nigracin and HCH-nigracin in *P. heterophylla* represents a reversion from the ancestral *tremuloides*-like chemotype back to the *Idesia*-like chemotype that the ancestor of *Populus* and *Salix* likely possessed (Chapter 3), although these compounds are still present in the HCH-tremulacin chemotype of *P. heterophylla*. While the defensive efficacy of tremulacin is well-known (Boeckler et al. 2016), it is unclear how well nigracin and HCH-nigracin perform as defensive compounds, as a study that compared *P. nigra* and *I. polycarpa*

leaves in feeding trails did not report the concentrations of compounds in the leaves they used of either species even though they reported the insect herbivores performed much worse on *I. polycarpa* than *P. nigra* (Feistel et al. 2017). Another salicinoid not in the ancestral *tremuloides*-like chemotype but present in high abundance in *P. heterophylla* is HCH-salicortin, which theoretically confers twice as much defense as tremulacin does on a per-molecule basis due to the additional HCH-unit (Schnurrer & Paetz 2023), which is oxidized to a reactive oxygen species that can crosslink proteins (Pentzold et al. 2014). Investment in HCH-salicortin might thus be more economical than investment in tremulacin due to the delivery of two HCH-unites to antagonsists. Lasiandrin, an acetylated version of HCH-salicortin, likely confers a similar advantage. While present in small amounts in these chemotypes of the mature leaves I present here, lasiandrin is produced at high quantities in young leaves of *P. heterophylla* (Chapter 2) and is the main salicinoid produced in some species of *Salix* (Chapter 3). In all, there are a few different scenarios for compositions of salicinoids in the chemotypes of *P. heterophylla*.

The HCH-tremulacin chemotypes, and especially the nigracin-tremulacin chemotype, likely are as effective at defense as they are in *P. tremuloides* (Lindroth et al. 1988), if not slightly more so due to the increased complexity of their arsenal with other salicinoids such as nigracin. However, although this dataset has a limited number of HCH-tremulacin chemotypes (15 out of 290 individuals, plus four additional nigracin-tremulacin chemotypes), there appears to be a strong tradeoff between tremulacin/HCH-tremulacin and HCH-salicortin (Fig. 1). Notably, many HCH-tremulacin chemotypes have a single isomer of salicortin, salicortin-B, while non-HCH-tremulacin chemotypes have both salicortin-A and salicortin-B. There are a few implications of this pattern, but unfortunately, without knowing the full biosynthetic pathway of HCH-salicortin (Gordon et al. 2022 demonstrate the pathway up to salicortin and tremulacin)

these are purely speculative. The data presented here and in Chapter 3 show a correlation between two isomers of salicortin and the production of HCH-salicortin, and that when there are low (or no) levels of HCH-salicortin in a chemotype, there is usually no salicortin-A, suggesting that production of salicortin-A is somehow related to or involved in (either directly or indirectly) the production of HCH-salicortin at high concentrations. In *P. heterophylla*'s HCH-tremulacin chemotypes, there are high levels of tremulacin-A, which is the same isomer of tremulacin found in *P. tremuloides* and in *P. tremula,* but lower levels of HCH-salicortin. In the non-tremulacin chemotypes, where there is great investment in HCH-salicortin, levels of tremulacin plummet, but don't entirely disappear. This, in combination with the reduced levels of HCH-salicortin, suggests that there is competition between the tremulacin and HCH-salicortin pathways, as suggested by Keefover-Ring et al. (2014) in *P. tremula*. The fact that tremulacin doesn't entirely disappear, but rather remains at low levels of other isomers, is also suggestive of enzymatic promiscuity, especially when compared with levels of HCH-nigracin. When there is a single isomer of HCH-nigracin (the standard-chemotype) there is also a single isomer of tremulacin, tremulacin-C. When there are two isomers of HCH-nigracin (such as in the HCH-nigracin-chemotype) there are also two isomers of tremulacin, tremulacin-B and tremulacin-C. However, if there is more HCH-nigracin-A than HCH-nigracin-B, then there will be more tremulacin-B than tremulacin-C, and if there is instead more HCH-nigracin-B than HCH-nigracin-A, then there will be more tremulacin-C than tremulacin-B. This congruity suggests that the biosynthetic processes that are making HCH-nigracin isomers occasionally make a tremulacin isomer as well, or that there are regulatory mechanisms that are the same between certain isomers of HCH-nigracin and tremulacin.

These patterns are suggestive of a grid-like biosynthetic pathway for these salicinoids, rather than many independent and linear pathways. The work from Gordon et al. (2022) supports this notion, and there is evidence in other systems such as *Inga* (Coley et al. 2018; Forrister et al. 2023) that plants can produce a great diversity of chemicals reusing a few building blocks in different combinations. Without knowing the exact sequences and regulatory pathways for all of the salicinoids in *P. heterophylla*, it is not unreasonable that slight mutations on those genes have led to these slight differences in target substrates and enzymatic patterns that have then resulted in the four chemotypes I present here. However, more work is needed to confirm this.

Linking chemotypes with population structure

There is a clear correlation between the geography of the population structure and the geography of the chemotypes in *P. heterophylla*, suggesting that the two are linked in some manner. Likely, this is due to mutations (genetic drift) in the genes coding for salicinoid biosynthesis that have arisen in certain populations, and then are shared between populations with ample gene flow. Over time, this could eventually result in certain alleles reaching fixation due to random change in the absence of direct natural selection. The chance of alleles reaching fixation or extinction via genetic drift increases with smaller population sizes and if there is a genetic bottleneck, either due to a sharp decrease in population size due to some event, or due to a founder effect as a species expands its range. This can be thought of a "null" model of evolution, where traits reach fixation or extinction in populations purely due to chance. In the case of *P. heterophylla's* chemotypes, which are likely to provide roughly equal defense against herbivory at equal quantitative levels, this is a possibility. Should the ancestral area for *P. heterophylla* be in the South-South Atlantic region, then those populations have likely persisted throughout the Pleistocene, and could have greater genetic diversity than populations in the

Midwest and Northeast, which are more recent range expansions, and could have experienced a bottleneck due to a founder effect. This lower genetic diversity could thus be a reason why most individuals in those regions are the Standard chemotype, and why the South, South Atlantic, and Mid-Atlantic regions have greater variation in their chemotypic identities. The presence of non-Standard chemotypes in the Northeast and Midwest could be due to the relative ease with which the biosynthetic pathways of salicinoids can be altered, allowing them to occasionally arise, but ultimately be kept at low levels due to the genetic swamping via gene flow from Standard chemotypes in those regions. This is one hypothesis about how the distribution of chemotypes in *P. heterophylla* came to be, and I will call it Hypothesis 1, or the null hypothesis, purely based on genetic drift and random chance.

A second hypothesis is that these chemotypes do actually have a cost or benefit to the producing plant. More complex chemotypes could be more costly to produce, but if a grid-like biosynthetic pathway exists for salicinoids, then likely it is not much more costly to produce a diverse arsenal than a simple arsenal. Even so, there is probably a non-zero increased cost to produce complex arsenals, either through real carbon invested in the molecules themselves or the biosynthetic machinery involved. Under this scenario, the Standard chemotype is less complex than any of the non-standard chemotypes, as most investment is in the production of HCH-salicortin, with moderate levels of investment in nigracin and even less in the other salicinoids in that chemotype. The Midwest and Northeast experience colder winters on-average than the South, South Atlantic, and Mid-Atlantic populations do due to the buffer provided by proximity to large bodies of water for the latter populations. When collecting cuttings during winter for propagation for Chapter 2, there were numerous sites in the Midwest and Northeast where the trees were growing in frozen wetlands, even as far south as the confluence of the Mississippi and

Ohio Rivers. More efficient construction of salicinoids arsenals in the Standard chemotype could provide a surplus of resources that are able to be invested in other areas in a shift towards the conservative end of the Leaf Economics Spectrum (Wright et al. 2004; Agrawal 2020), allowing for other investments such as increased thickness of leaves, upregulation of other chemical pathways to protect against freezing (Oberschelp et al. 2020), or to increase growth during shorter growing seasons (Soolanayakanahally et al. 2015). Additionally, there is a possibility that the salicinoids in the standard chemotype or other unmeasured metabolites in the metabolome confer stress tolerance directly to the trees. While this has not been shown for salicinoids, other species have chemotype-specific tolerances of abiotic stress. For example, the seven chemotypes in *Thymus vulgaris* show differential responses to drought and freezing, whereby the phenolic monoterpenoid chemotypes perform better in milder climates with greater drought stress than non-phenolic monoterpenoid chemotypes, but non-phenolic chemotypes have greater low-temperature tolerances than phenolic chemotypes, which is reflected in the spatial distribution of these chemotypes across a landscape (Thompson et al. 2007). These chemotypes are genetically controlled in an epistatic cascade of dominance (Vernet et al. 1986) and yet the differential tolerances of stressors exhibited by these chemotypes maintains their spatial distribution even when there is substantial gene flow between populations (Bataillon et al. 2022). While the genetic controls of salicinoid chemotypes in *P. heterophylla* and other *Populus* species is unknown, different responses of Standard and non-Standard chemotypes to environmental stress could be a reason for the bias toward Standard chemotypes in the Midwest and Northeast. Whether those responses are directly related to the salicinoids produced, or indirectly due to reduced cost of producing certain chemotypes is unknown, but this is the basis of Hypothesis 2,

which is that the cost of chemotypic defense in different regions has resulted in the current distribution of chemotypes in *P. heterophylla*.

Finally, the extant distribution of chemotypes in *P. heterophylla* could be a combination of these hypotheses, where genetic differences due to bottlenecks or founder's effects predisposed certain regions to being dominated by one chemotype, which was then reinforced further by selection due to costs and benefits of producing those chemotypes. Under this scenario, there is still an occasional reversion back to the ancestral HCH-tremulacin chemotype due to mutations, and there is still a diversity of chemotypes in the South, South Atlantic, and MidAtlantic due to the potential genetic diversity still present in those ancestral populations.

Limitations

A limitation in this study is the rooting and dating of the phylogeny, which was done with SNPs from the *Populus deltoides* "WV94" genome, which is the same individual used as the reference genome for aligning the *P. heterophylla* sequenced reads. First, while extremely rare, *P. deltoides* and *P. heterophylla* naturally hybridize, so there is a possibility that introgression exists between the two species (Wang et al. 2020) and any *P. deltoides* alleles in *P. heterophylla* populations could affect both the position of individual genotypes and our divergence time estimates, as the two species would appear closer related than they actually are. Second, by using the same genome as the outgroup as I used for a reference for *P. heterophylla*, I am assuming that *P. deltoides* is homozygous at every position for which *P. heterophylla* is heterozygous. This could be the case, but is a big assumption to make. With these possible issues, it is surprising that only a single genotype (BAN3) is sister to the two geographical clades. While it is possible for the overall topology to change following re-rooting, I expect those clades to remain stable.

To re-root and re-date the phylogeny of *P. heterophylla*, I will use published Illumina reads of *P. tremuloides*, as it is sexually incompatible with *P. heterophylla* (Dickmann & Kuzovkina, 2014); *Populus simonii*, which is in *Populus* subgen. *Eupopulus*, but is native to another continent (Dickmann & Kuzovkina, 2014); *Populus nigra*, which is frequently planted as a male clone 'Lombardy' or as its hybrid with *P. deltoides*, *Populus* x *canadensis* (Dickmann & Kuzovkina, 2014), which could also introgress into *P. heterophylla*, and thus will serve as an additional check for certain alleles to be filtered out. These species, some sister to all of subgen. *Eupopulus* and others nested inside of it, should provide enough statistical power to properly root and date the *P. heterophylla* phylogeny, allowing me to make better inferences of the timing of range expansion in swamp cottonwood. If BAN3 does end up nesting inside one of the two clades, then I expect the DEC model will estimate the geographic origin of *P. heterophylla* to be in the South.

Future Directions

This work is foundational in providing some clear avenues of future research to understand the chemotypes, and thus a primary form of anti-herbivore defense and resource allocation, of *P. heterophylla* and other species of *Populus* and *Salix*. First, a more detailed investigation of the genes that code for the different salicinoids in these chemotypes, and the positions of those genes both in *P. heterophylla* and related species. By selecting individuals of certain chemotypes, and in certain portions of *P. heterophylla'*s range (and thus phylogeny), researchers can use transcriptomics to find certain genes that are shared between individuals which share chemistry, and doing this in young and old leaves would further narrow down the candidate genes (Chapter 2).

Second, sequencing more individuals from the southern portion of *P. heterophylla*'s range and from the MidAtlantic, near the BAN3 individual, could provide a clearer picture of how much gene flow occurs between the eastern and western clades, where the true transition between the two clades lies, and provide additional insight into where the species originated. The results I presented here, pending a re-rooting, suggest that the species originated in the South-Atlantic/Mid-Atlantic. However, it is unclear if one clade emerged before the other, or if they both began their northward range expansion at roughly the same time. Each clade has a few individuals from the southern portion of *P. heterophylla'*s range, but if additional genotypes from the south are sister to both clades, then their current geographic location could indicate from which direction the range expansion of *P. heterophylla* initiated. If new genotypes nest into the current clades, and none are sister to both clades, then that would suggest that the range expansion of the clades occurred at roughly the same time.

Conclusions

My work here emphasizes the value in exhaustive sampling of a species entire range to determine what is chemically possible in a species. Contrasting my results with those of Pearl and Darling (1977) highlights the chasm caused when a single individual is sampled for chemistry, using unoptimized methods. Had Pearl and Darling (1977) found the diversity of salicinoids that I have, rather than a dearth of compounds, then it's possible that more (re: any) research would have been conducted on *Populus heterophylla* in the nearly five decades since. The diversity of salicinoids in *P. heterophylla*, and their correlations with population structure, should provide a foundation for future research on both this rare swamp tree species and salicinoid diversity in Salicaceae.

Figures

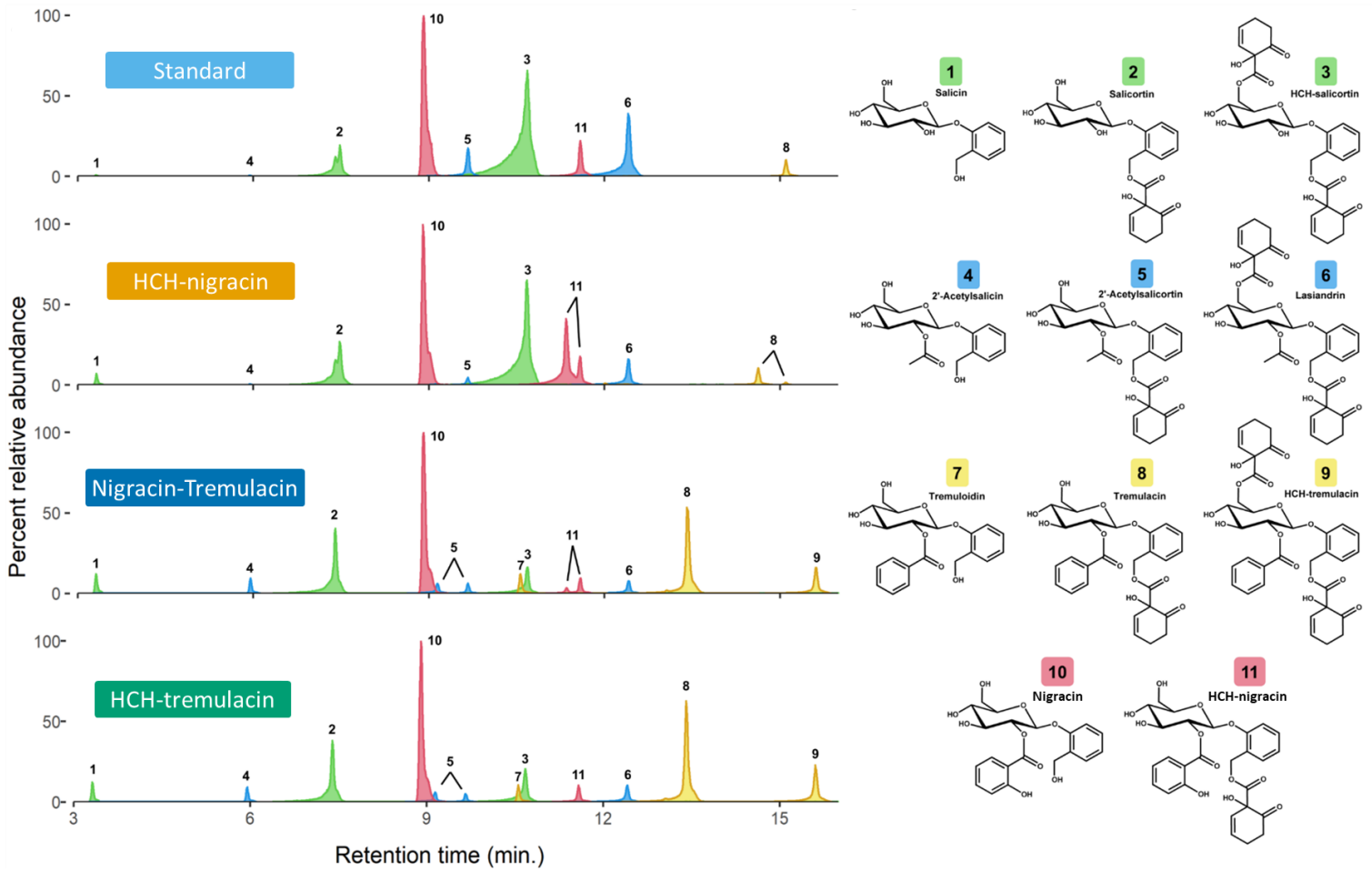

Figure 1. Representative chromatograms of the salicinoid chemotypes of *Populus heterophylla*. On the left, extracted-ion chromatograms of the most abundant salicinoids in each chemotype. Peaks are colored according to structural similarity. Numbers above peaks correspond to the numbered salicinoid structures on the right.

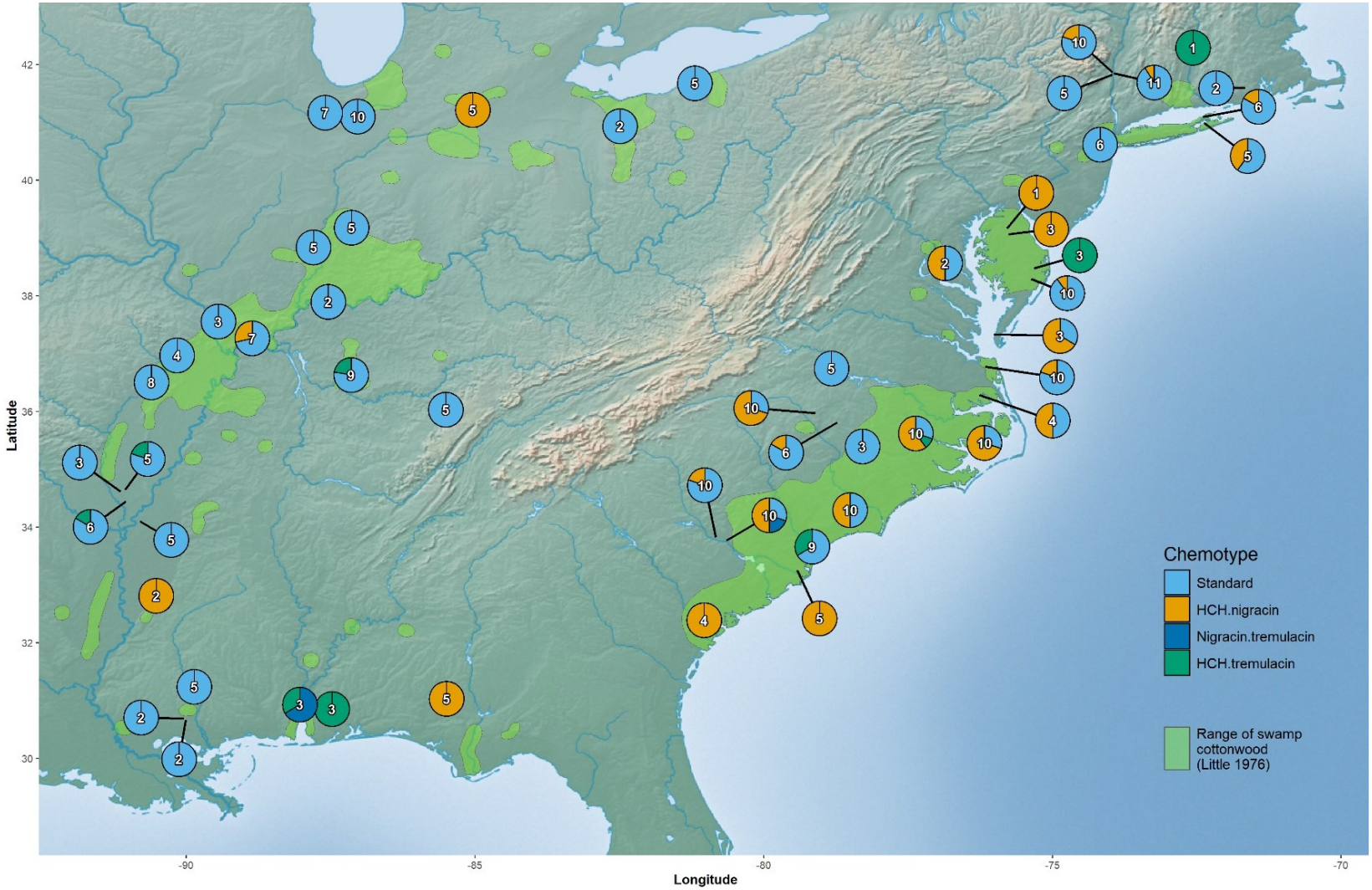

Figure 2. The geographic distribution of chemotypes in *Populus heterophylla*. Numbers on each pie-chart are the number of individuals sampled at each site, with numbers less than 10 indicating how many individuals were found at each site. Charts are colored according to the chemotypes of the individuals sampled at each site. Areas highlighted in green are the native range of *Populus heterophylla*, as reported by Little (1976).

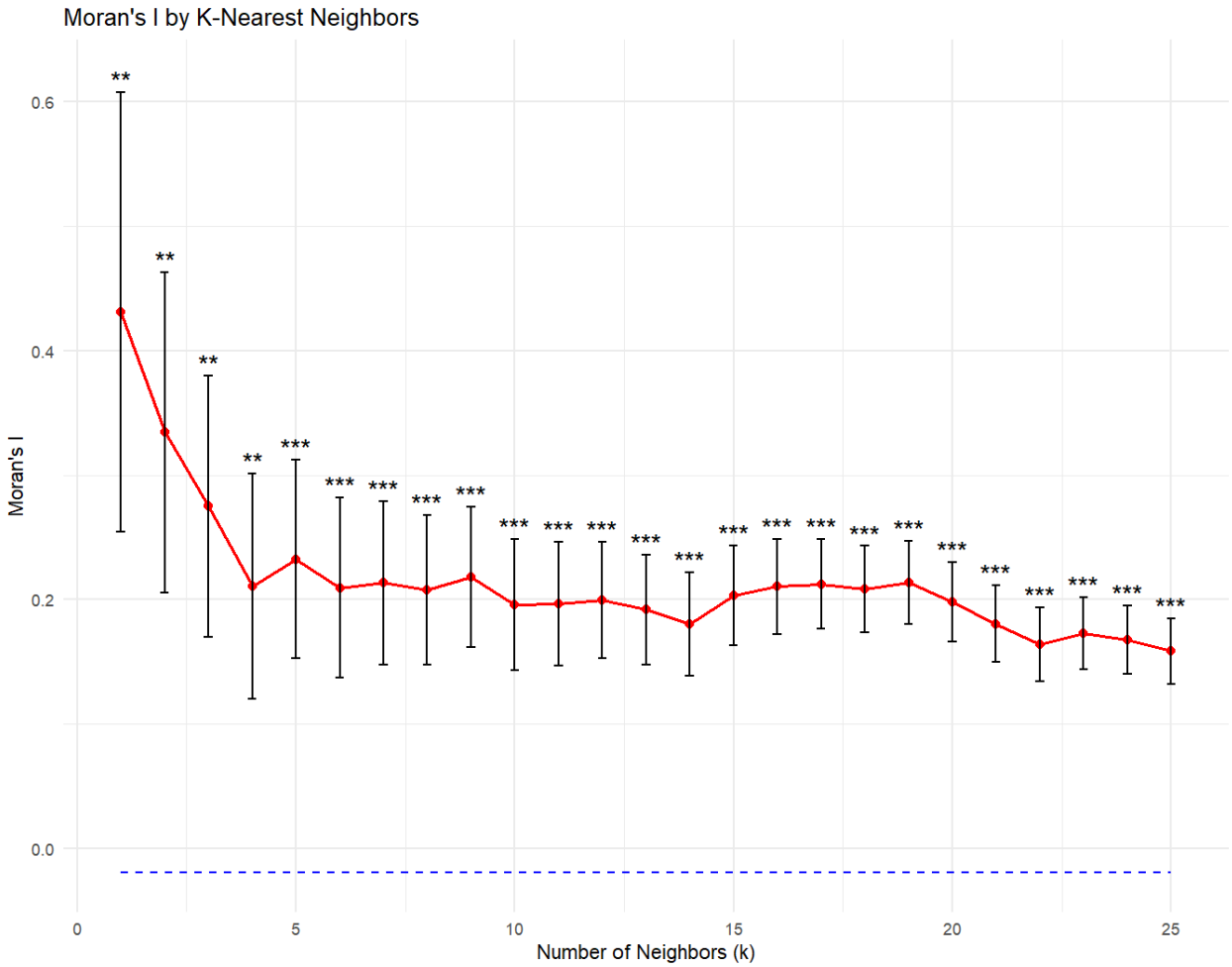

Figure 3. Global Moran's I for site clustering as the number of neighboring *Populus heterophylla* sites in the spatial weights matrix increases. Sites were coded "0" if they only contained sampled individuals with the Standard chemotype, and "1" if they had at least one individual of another chemotype. The red points are the Moran's I statistic, with values closer to 1 indicating greater positive spatial autocorrelation. The blue dashed line is the null hypothesis for this test, that sites with at least one non-Standard chemotypes are randomly dispersed throughout the range of *Populus heterophylla*. The bars represent the standard deviation of the null distribution at each K, and the p-values for each K are plotted above the Moran's I value for that K. * = $p < 0.05$; ** = $p < 0.01$; *** = $p < 0.001$.

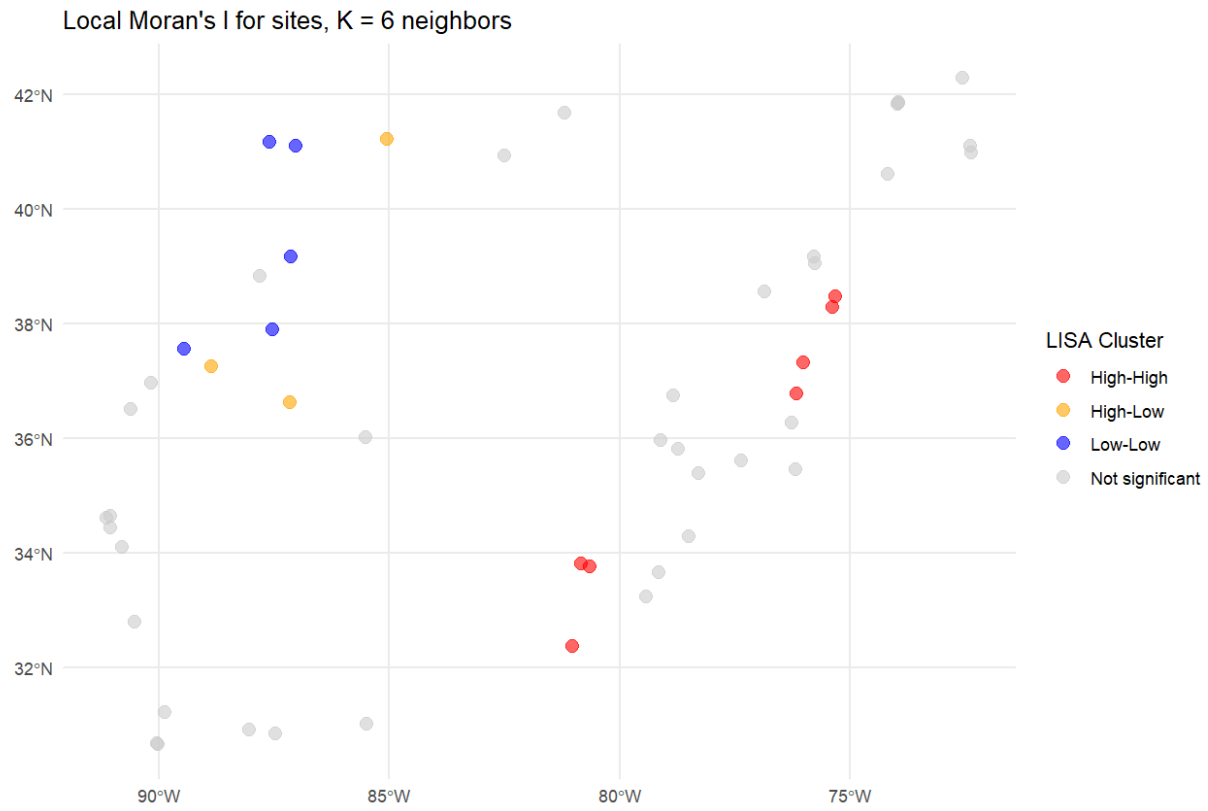

Figure 4. Local Moran's I for spatial autocorrelation for site-level *Populus heterophylla* chemotype data with K = 6 nearest neighbors. High-High are sites with at least one non-Standard chemotype neighbored by other sites with at least one non-Standard chemotypes, High-Low are sites with at least one non-Standard chemotype neighbored by other sites with only Standard chemotypes, and Low-Low are sites with only Standard chemotypes neighbored by sites with only Standard chemotypes. Not significant indicates sites that returned a $p > 0.05$ for Local Moran's I.

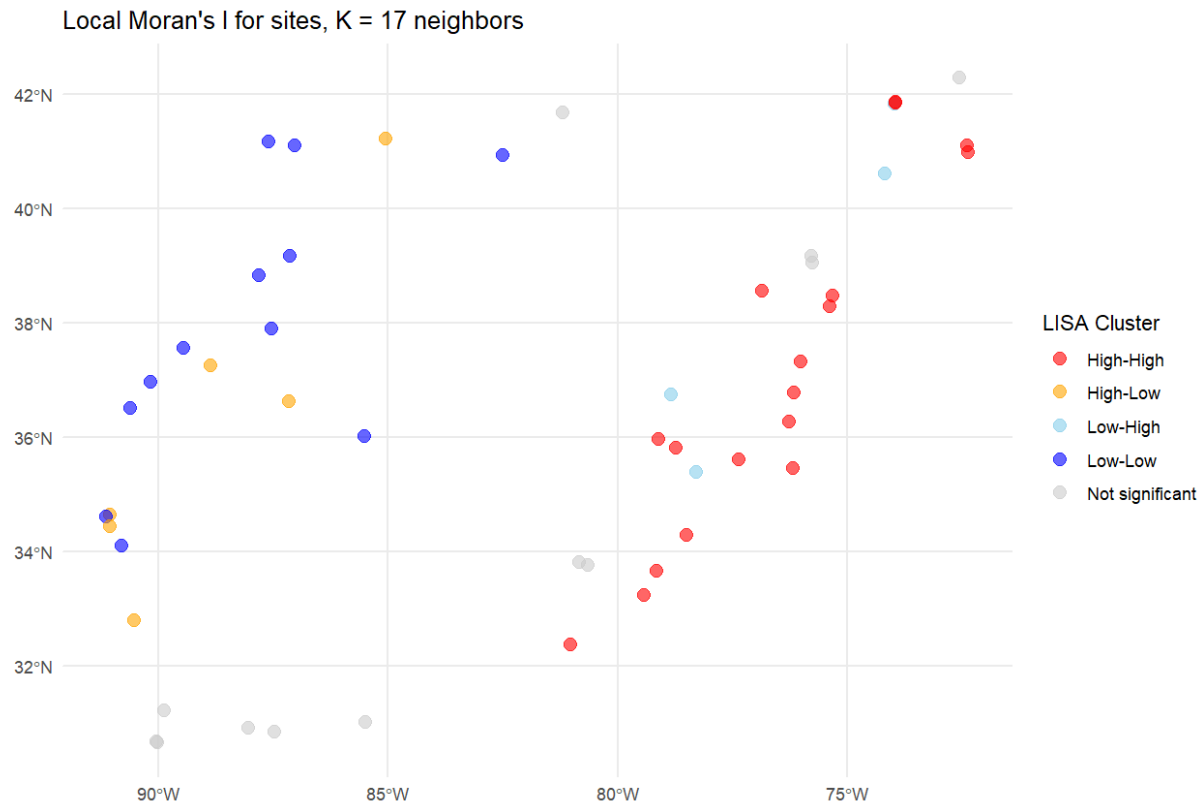

Figure 5. Local Moran's I for spatial autocorrelation for site-level *Populus heterophylla* chemotype data with K = 17 nearest neighbors. High-High are sites with at least one non-Standard chemotype neighbored by other sites with at least one non-Standard chemotypes, High-Low are sites with at least one non-Standard chemotype neighbored by other sites with only Standard chemotypes, Low-High are sites with only Standard chemotypes neighbored by sites with at least one non-Standard chemotype, and Low-Low are sites with only Standard chemotypes neighbored by sites with only Standard chemotypes. Not significant indicates sites that returned a $p > 0.05$ for Local Moran's I.

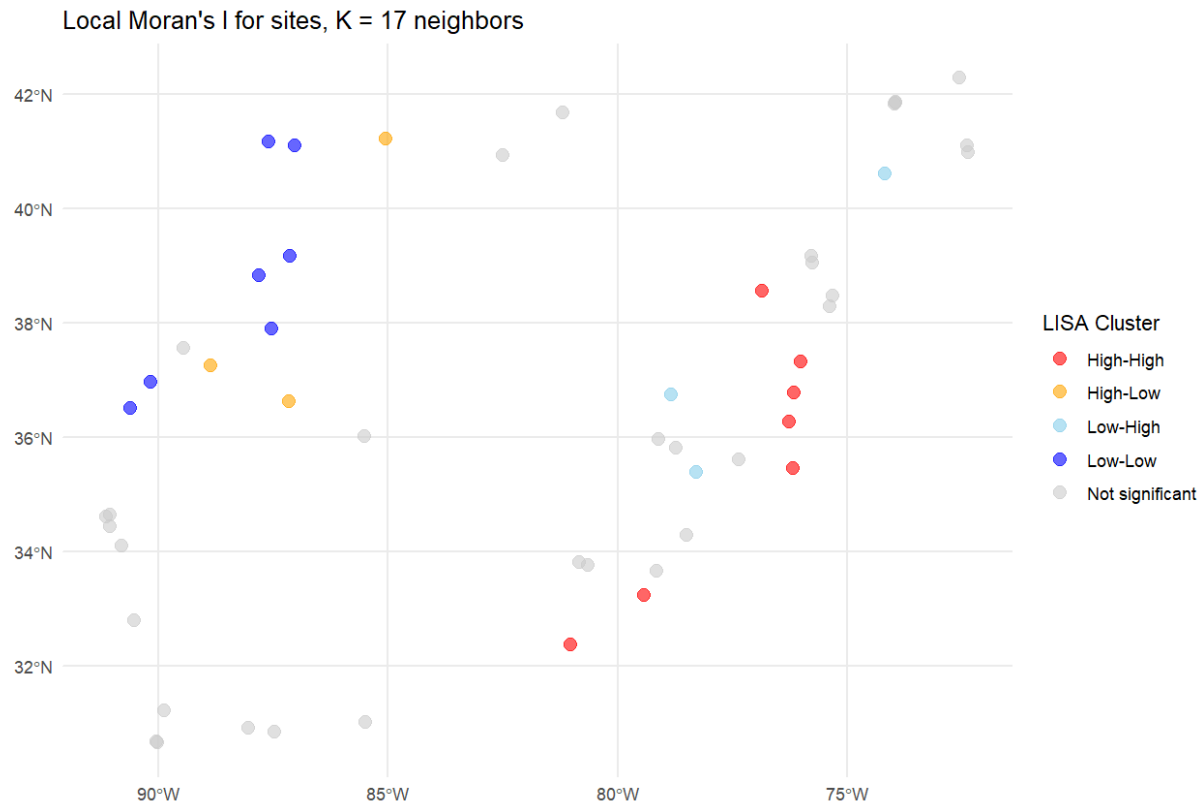

Figure 6. Local Moran's I for spatial autocorrelation for site-level *Populus heterophylla* chemotype data with K = 17 nearest neighbors and inverse distance weighting. High-High are sites with at least one non-Standard chemotype neighbored by other sites with at least one non-Standard chemotypes, High-Low are sites with at least one non-Standard chemotype neighbored by other sites with only Standard chemotypes, Low-High are sites with only Standard chemotypes neighbored by sites with at least one non-Standard chemotype, and Low-Low are sites with only Standard chemotypes neighbored by sites with only Standard chemotypes. Not significant indicates sites that returned a $p > 0.05$ for Local Moran's I.

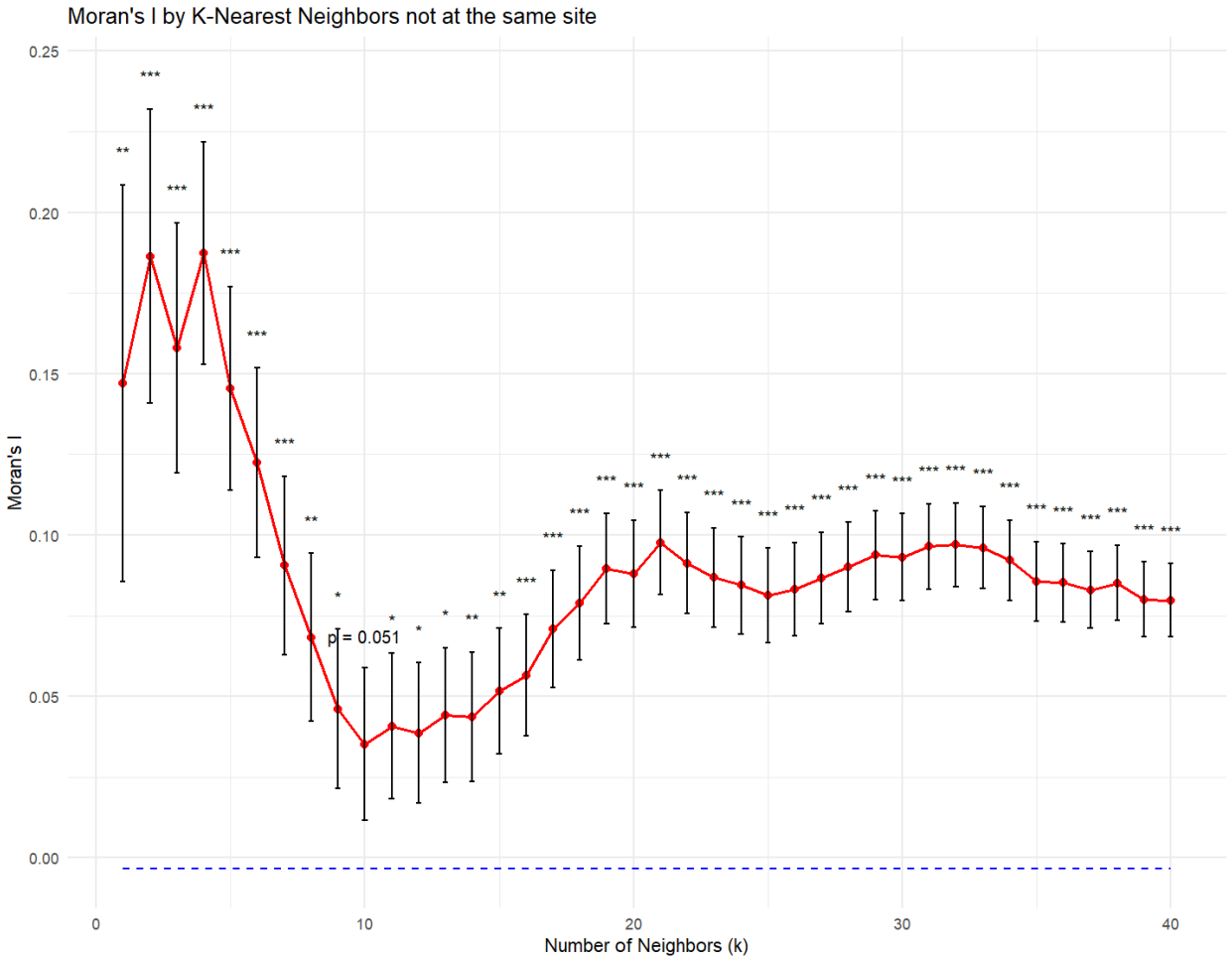

Figure 7. Global Moran's I for individual-level clustering as the number of neighboring individuals increases. Neighbors were defined as the nearest neighbors that did not occur at the same site as the target tree. Individuals were coded "0" if they had a standard chemotype, and a "1" if they had a non-standard chemotype. The red points are the Moran's I statistic, with values closer to 1 indicating greater positive spatial autocorrelation. The blue dashed line is the null hypothesis for this test, that individuals with non-standard chemotypes are randomly distributed throughout the range of *Populus heterophylla*. The bars represent the standard deviation of the null distribution at each K, and the p-values for each K are plotted about the Moran's I value for that K.

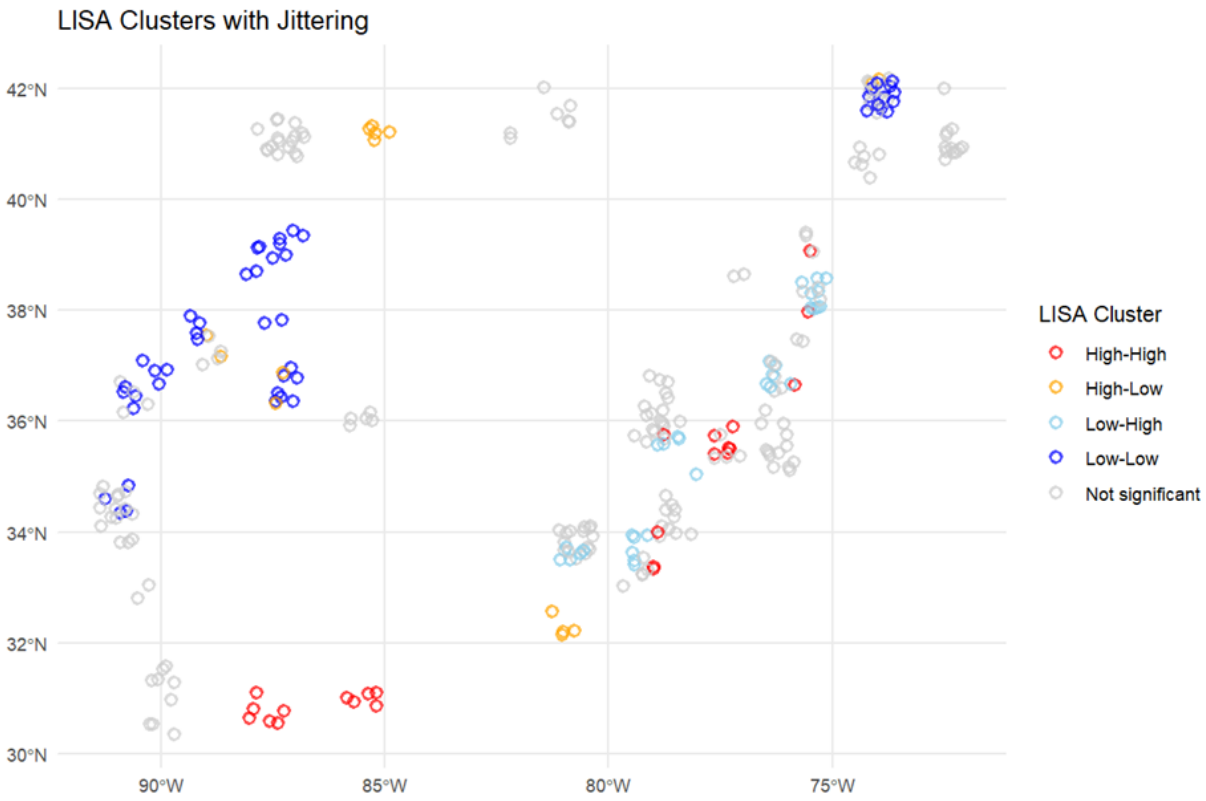

Figure 8. Local Moran's I for spatial autocorrelation for individual-level *Populus heterophylla* chemotype data with K = 20 nearest neighbors that are at a different site than an individual, with inverse distance weighting. Points are slightly jittered for clarity. High-High are individuals that are a non-standard chemotype neighbored by other individual with non-standard chemotypes, High-Low are individuals that are a non-standard chemotype neighbored by individuals that are standard chemotypes, Low-High are individuals that are standard chemotypes neighbored by individuals with non-standard chemotypes, and Low-Low are individuals that are standard chemotypes neighbored by individuals which are also non-standard chemotypes. Not significant indicates individuals that returned a $p > 0.05$ for Local Moran's I.

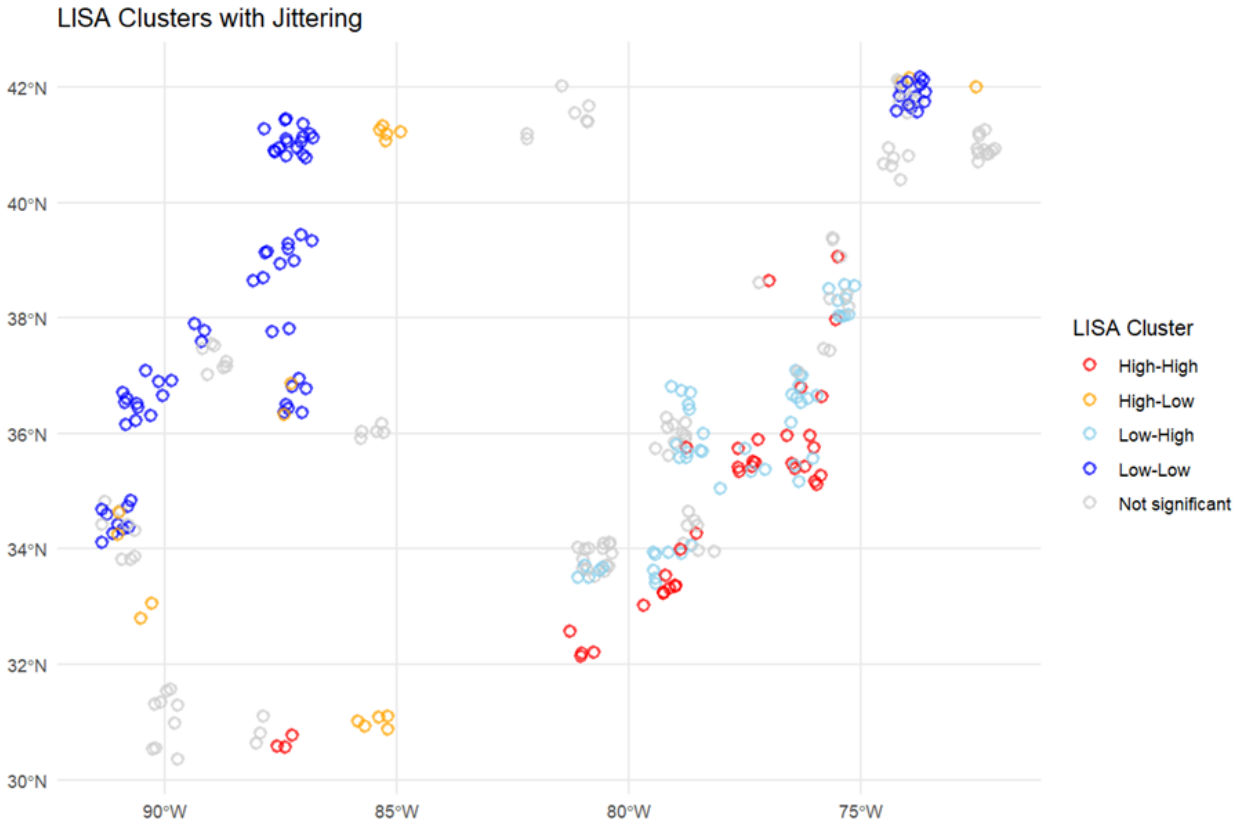

Figure 9. Local Moran's I for spatial autocorrelation for individual-level *Populus heterophylla* chemotype data with K = 96 nearest neighbors that are at a different site than an individual, with inverse distance weighting. Points are slightly jittered for clarity. High-High are individuals that are a non-standard chemotype neighbored by other individual with non-standard chemotypes, High-Low are individuals that are a non-standard chemotype neighbored by individuals that are standard chemotypes, Low-High are individuals that are standard chemotypes neighbored by individuals with non-standard chemotypes, and Low-Low are individuals that are standard chemotypes neighbored by individuals which are also non-standard chemotypes. Not significant indicates individuals that returned a $p > 0.05$ for Local Moran's I.

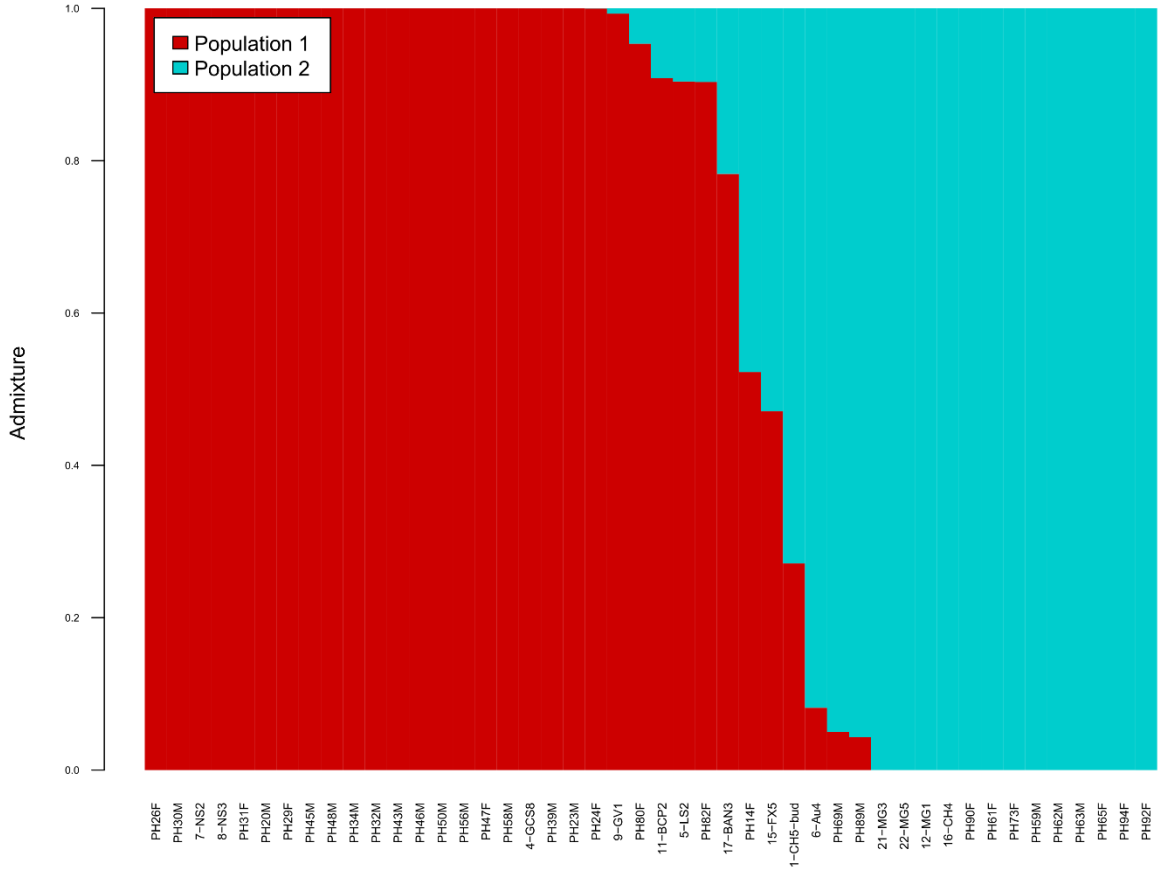

Figure 10. Structure plot depicting admixture proportions among *Populus heterophylla* genotypes with ancestral population K = 2.

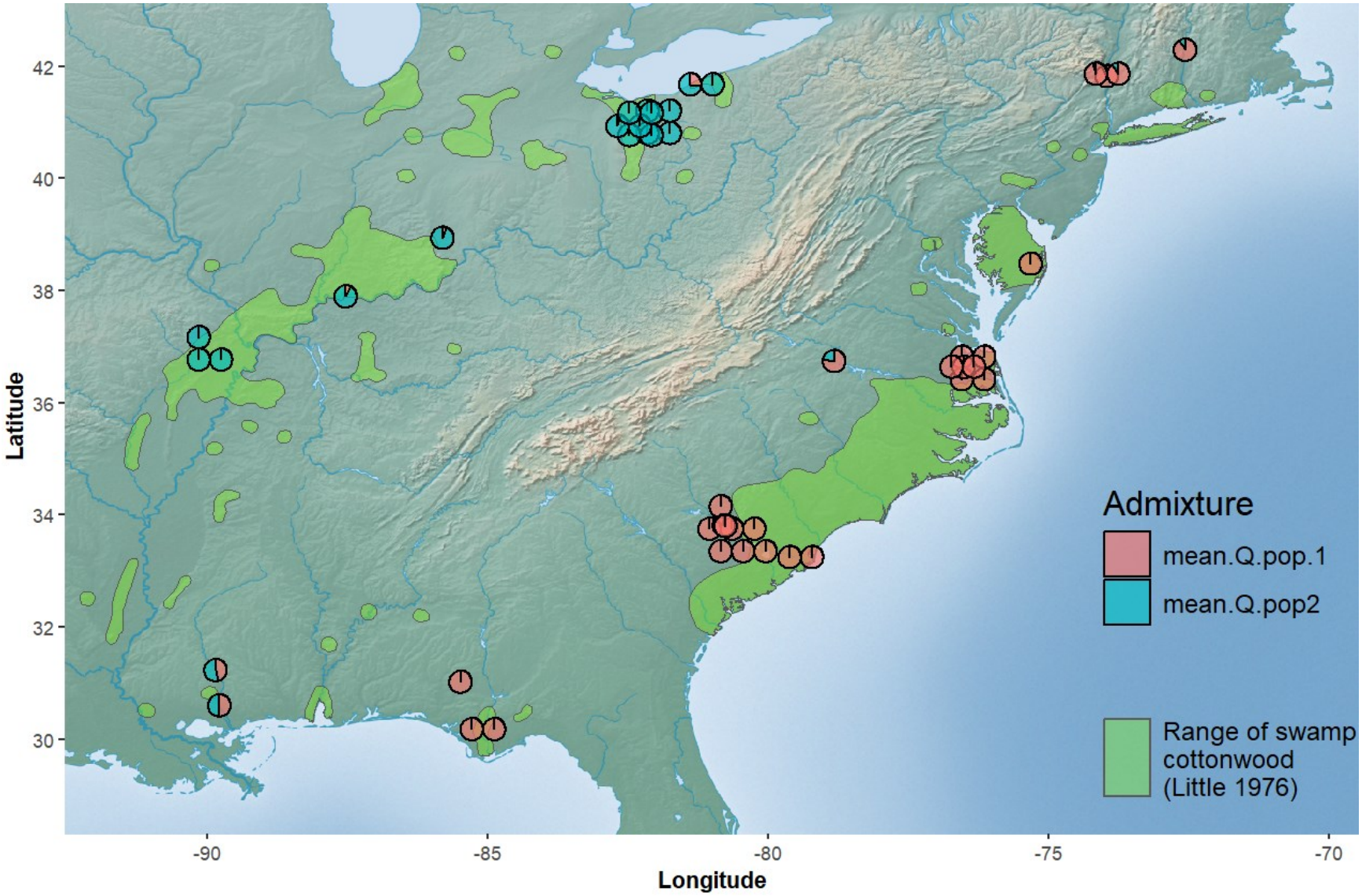

Figure 11. Map of *Populus heterophylla* genotypes in final dataset colored by admixture proportions determined by fastStructure analysis.

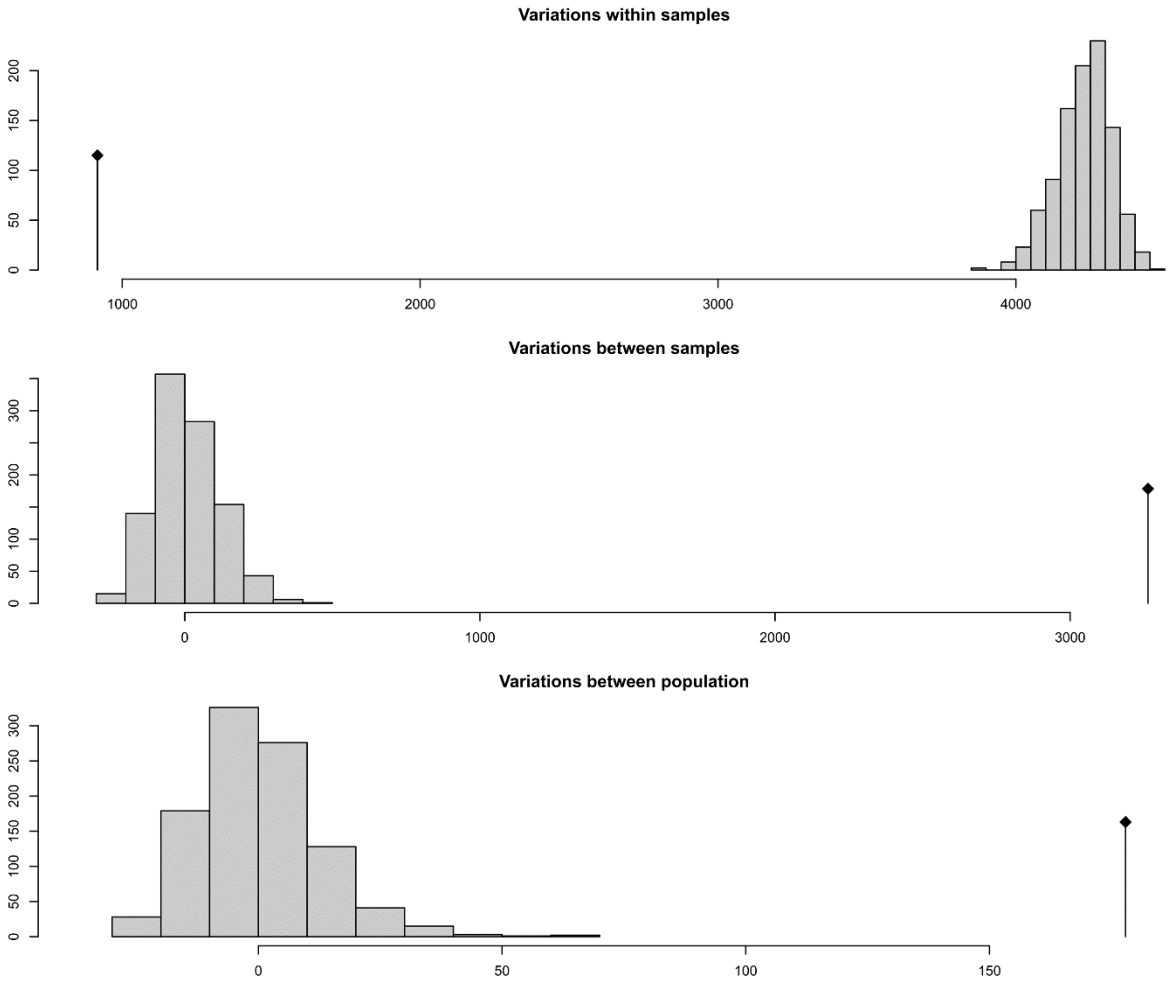

Figure 12. Histogram of permutation test utilized to test phi statistics for significance from AMOVA for samples of *Populus heterophylla*. This significance test determines how observed groupings compare to randomly permuted sample matrices, with the black line representing the observed data and the histogram bars representing the permutation results, where the x-axis represents the number of variations.

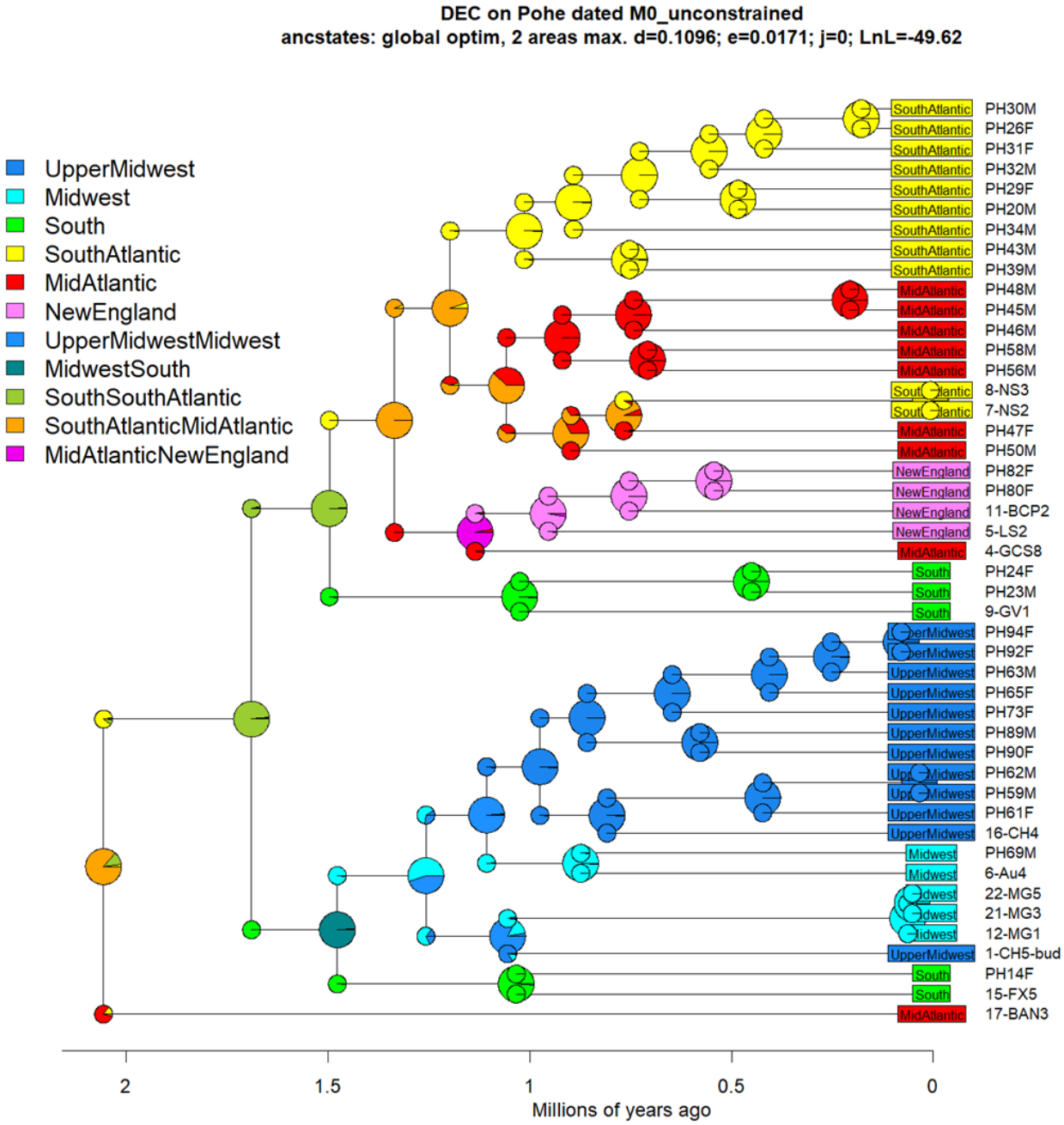

Figure 13. Estimation of ancestral geographic areas using a DEC model and the dated *Populus heterophylla* phylogeny. Areas were coded based on modern geographic regions of *P. heterophylla*, which are listed in boxes at the tips of the phylogeny. Pie charts represent probability of ancestral ranges, including paired adjacent ranges (e.g. MidwestSouth), smaller pies represent the estimated ranges before cladogenesis. Colors correspond to the areas listed in the legend in the top-left.

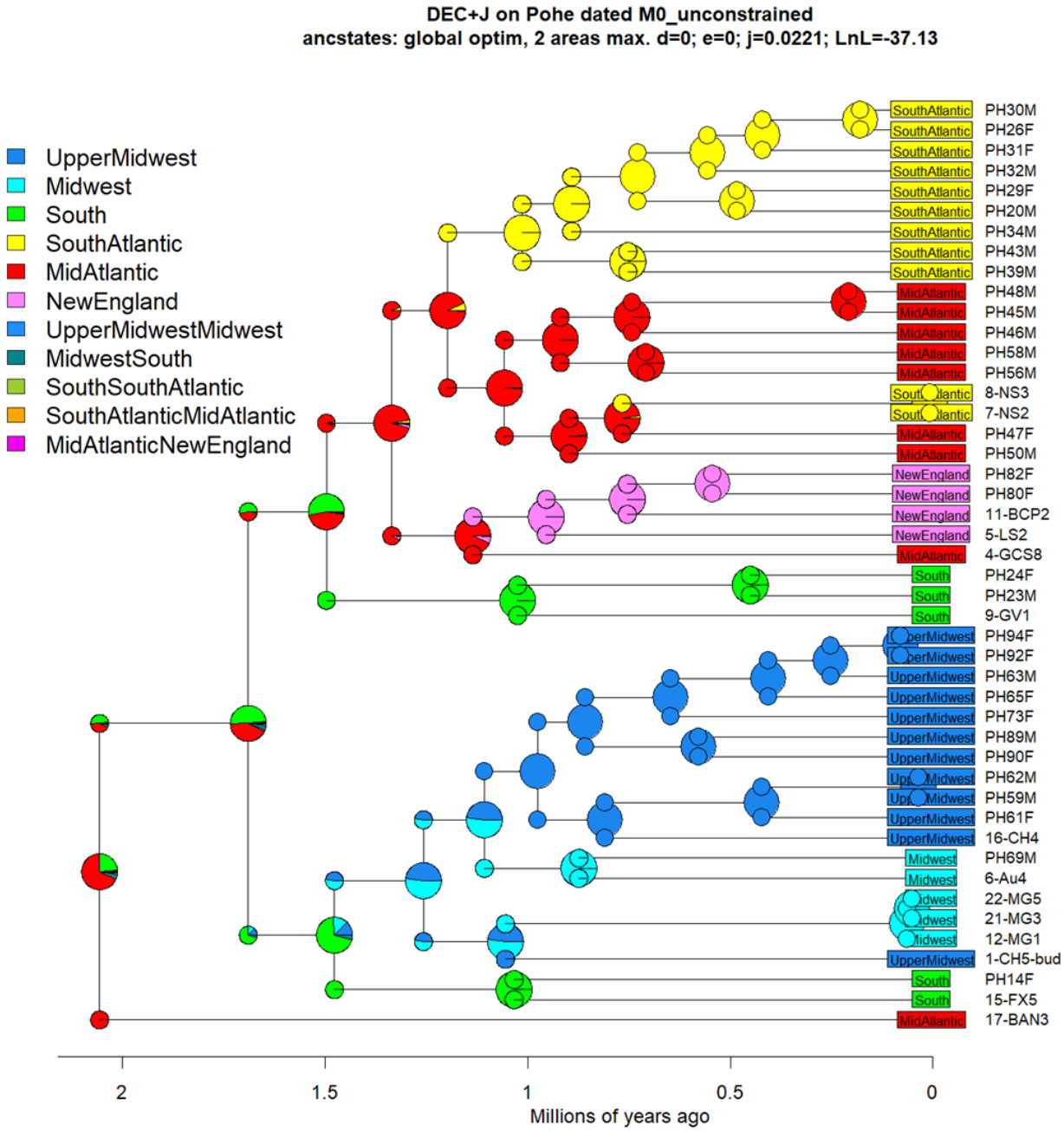

Figure 14. Estimation of ancestral geographic areas using a DEC+J model and the dated *Populus heterophylla* phylogeny. Areas were coded based on modern geographic regions of *P. heterophylla*, which are listed in boxes at the tips of the phylogeny. Pie charts represent probability of ancestral ranges, including paired adjacent ranges (e.g. MidwestSouth), smaller pies represent the estimated ranges before cladogenesis. Colors correspond to the areas listed in the legend in the top-left.

Tables

Table 1. Salicinoids found in the chemotypes of *Populus heterophylla*. A "1" means the salicinoid is present in a chemotype, a "0" means it is absent.

Salicinoid	**Standard**	**HCH-nigracin**	**Nigracin-tremulacin**	**HCH-tremulacin**
Salicin	1	1	1	1
Isosalicin	1	1	1	1
Salirepin-7-sulfate	1	1	1	1
Salicin-7-sulfate	1	1	1	1
Salicortin-7-sulfate	1	1	1	0
Salicortin-A	1	1	0	0
Salicortin-B	1	1	1	1
HCH-salicortin	1	1	1	1
Acetylsalicin	1	1	1	1
Acetylsalicortin-A	1	1	1	1
Acetylsalicortin-B	1	1	1	1
Lasiandrin	1	1	1	1
Nigracin	1	1	1	1
HCH-nigracin-A	0	1	1	0
HCH-nigracin-B	1	1	1	1
Tremuloidin	0	0	1	1
Tremulacin-A	0	0	1	1
Tremulacin-B	0	1	1	0
Tremulacin-C	1	1	0	0
HCH-tremulacin	0	0	1	1
Actyltremulacin	1	1	1	1
Salicyloyltremuloidin	1	1	1	1
Cinnamoylsalicyloylsalicin-A	1	1	1	1
Cinnamoylsalicyloylsalicin-B	1	1	1	1

Table 2. *Populus heterophylla* genotype mean q values with assigned population of origin based on admixture proportions.

Genotype	meanQ 1	meanQ 2	Assigned	Genotype	meanQ 1	meanQ 2	Assigned
PH26F	0.99	0.000009	Population 1	11-BCP2	0.91	0.091	Population 1
PH30M	0.99	0.000009	Population 1	5-LS2	0.90	0.096	Population 1
7-NS2	0.99	0.00001	Population 1	PH82F	0.90	0.096	Population 1
8-NS3	0.99	0.00001	Population 1	17-BAN3	0.78	0.22	Population 1
PH31F	0.99	0.00001	Population 1	PH14F	0.52	0.48	Population 1
PH20M	0.99	0.000011	Population 1	15-FX5	0.47	0.53	Population 2
PH29F	0.99	0.000011	Population 1	1-CH5-bud	0.27	0.73	Population 2
PH45M	0.99	0.000011	Population 1	6-Au4	0.081	0.92	Population 2
PH48M	0.99	0.000011	Population 1	PH69M	0.050	0.95	Population 2
PH34M	0.99	0.000012	Population 1	PH89M	0.043	0.96	Population 2
PH32M	0.99	0.000013	Population 1	21-MG3	0.000045	0.99	Population 2
PH43M	0.99	0.000013	Population 1	22-MG5	0.000024	0.99	Population 2
PH46M	0.99	0.000013	Population 1	12-MG1	0.000023	0.99	Population 2
PH50M	0.99	0.000013	Population 1	16-CH4	0.00002	0.99	Population 2
PH56M	0.99	0.000013	Population 1	PH90F	0.000017	0.99	Population 2
PH47F	0.99	0.000014	Population 1	PH61F	0.000014	0.99	Population 2
PH58M	0.99	0.000014	Population 1	PH73F	0.000013	0.99	Population 2
4-GCS8	0.99	0.000015	Population 1	PH59M	0.000011	0.99	Population 2
PH39M	0.99	0.000015	Population 1	PH62M	0.000011	0.99	Population 2
PH23M	0.99	0.00002	Population 1	PH63M	0.000009	0.99	Population 2
PH24F	0.99	0.00017	Population 1	PH65F	0.000009	0.99	Population 2

Table 3. Analysis of molecular variance (AMOVA) results explained within *Populus heterophylla* genotypes, among locations, among subpopulations (6 total), and populations (2 total).

Variable	Df	Sum sq	Mean sq	Sigma	% variation	Phi
Between populations	1	15242.46	15242.46	109.54	2.52	0.025
Between samples within population	44	327559.97	7444.54	3263.86	74.89	0.78
Between subpopulation within population	5	46164.47	9232.89	178.88	4.11	0.042
Between samples within subpopulation	39	281395.49	7215.27	3149.22	72.32	0.77
Within samples	46	42173.99	916.83	916.83	21.05	0.79
Total	91	384976.41	4230.51	4354.46	100.00	--

Table 4. Basic population statistics using fastStructure population groupings for genotypes.

Ho	Hs	Ht	Dst	Htp	Dstp	Fst	Fstp	Fis	Dest
0.31	0.29	0.31	0.012	0.32	0.024	0.039	0.074	-0.059	0.033

Table S1. (Pages 53-60) Location information for each *Populus heterophylla* individual sampled for this study.

Site and Tree Number	Abbreviation	Latitude	Longitude
Axis 1	AX1	30.92807	-88.0291
Axis 2	AX2	30.92793	-88.0291
Axis 3	AX3	30.92801	-88.029
Bogue Chitto 1	BC1	30.66373	-90.0087
Bogue Chitto 2	BC2	30.66374	-90.0087
Chauncey 1	CM1	38.83574	-87.7947
Chauncey 2	CM2	38.83574	-87.7947
Chauncey 3	CM3	38.83669	-87.7945
Chauncey 4	CM4	38.8386	-87.795
Chauncey 5	CM5	38.83863	-87.7949
Congaree National Park/601 1	CONG1	33.76568	-80.642
Congaree National Park/601 10	CONG10	33.76556	-80.642
Congaree National Park/601 2	CONG2	33.76568	-80.642
Congaree National Park/601 3	CONG3	33.76568	-80.642
Congaree National Park/601 4	CONG4	33.76561	-80.6421
Congaree National Park/601 5	CONG5	33.76561	-80.6421
Congaree National Park/601 6	CONG6	33.76561	-80.6421

Congaree National Park/601 7	CONG7	33.76501	-80.6422
Congaree National Park/601 8	CONG8	33.76469	-80.6423
Congaree National Park/601 9	CONG9	33.76433	-80.6424
Durham 1	DH1	35.96963	-79.1042
Durham 10	DH10	35.96957	-79.1038
Durham 2	DH2	35.96963	-79.1042
Durham 3	DH3	35.96963	-79.1042
Durham 4	DH4	35.96963	-79.1042
Durham 5	DH5	35.96963	-79.1042
Durham 6	DH6	35.96963	-79.1042
Durham 7	DH7	35.96963	-79.1042
Durham 8	DH8	35.96957	-79.1038
Durham 9	DH9	35.96957	-79.1038
Elizabeth A Morton 1	EAM1	40.98858	-72.3676
Elizabeth A Morton 2	EAM2	40.98858	-72.3676
Elizabeth A Morton 3	EAM3	40.98858	-72.3676
Elizabeth A Morton 4	EAM4	40.98858	-72.3676
Elizabeth A Morton 5	EAM5	40.98858	-72.3676
Elizabeth A Morton 6	EAM6	40.98858	-72.3676
Elizabeth City 1	EC1	36.2806	-76.2608
Elizabeth City 2	EC2	36.2806	-76.2608
Elizabeth City 3	EC3	36.2806	-76.2608
Elizabeth City 4	EC4	36.2806	-76.2608
Esopus Meadows 1	EM1	41.86244	-73.9522
Esopus Meadows 10	EM10	41.86325	-73.9517
Esopus Meadows 2	EM2	41.86244	-73.9522
Esopus Meadows 3	EM3	41.86244	-73.9522
Esopus Meadows 4	EM4	41.86316	-73.9515
Esopus Meadows 5	EM5	41.86316	-73.9515
Esopus Meadows 6	EM6	41.86316	-73.9515
Esopus Meadows 7	EM7	41.86325	-73.9517
Esopus Meadows 8	EM8	41.86325	-73.9517
Esopus Meadows 9	EM9	41.86325	-73.9517
Fort Wayne 1	FW1	41.2142	-85.0348
Fort Wayne 2	FW2	41.2142	-85.0348
Fort Wayne 3	FW3	41.2142	-85.0348
Fort Wayne 4	FW4	41.2142	-85.0348
Fort Wayne 5	FW5	41.2142	-85.0348
Guthrie 1	GU1	36.62808	-87.1395
Guthrie 2	GU2	36.62857	-87.14
Guthrie 3	GU3	36.62873	-87.1402
Guthrie 4	GU4	36.62878	-87.1403
Guthrie 5	GU5	36.62958	-87.1415

Guthrie 6	GU6	36.6296	-87.1415
Guthrie 7	GU7	36.62989	-87.1415
Guthrie 8	GU8	36.62967	-87.1417
Guthrie 9	GU9	36.6297	-87.1423
Jasper 1	JAS1	41.09946	-87.0279
Jasper 10	JAS10	41.09977	-87.0291
Jasper 2	JAS2	41.09959	-87.0279
Jasper 3	JAS3	41.0995	-87.028
Jasper 4	JAS4	41.09943	-87.0281
Jasper 5	JAS5	41.09962	-87.0283
Jasper 6	JAS6	41.09971	-87.0285
Jasper 7	JAS7	41.09961	-87.0285
Jasper 8	JAS8	41.0997	-87.0288
Jasper 9	JAS9	41.09979	-87.029
Lemon Road 1	LER1	30.85055	-87.4715
Lemon Road 2	LER2	30.85056	-87.4713
Lemon Road 3	LER3	30.85056	-87.4713
Long Island 1	LI1	41.09515	-72.3898
Long Island 2	LI2	41.09515	-72.3898
Long Island 3	LI3	41.09515	-72.3898
Long Island 4	LI4	41.09515	-72.3898
Long Island 5	LI5	41.09515	-72.3898
Long Island 6	LI6	41.09515	-72.3898
Long Island 7	LI7	41.09515	-72.3898
Louisiana Purchase 1	LP1	34.64668	-91.0545
Louisiana Purchase 2	LP2	34.64585	-91.0541
Louisiana Purchase 3	LP3	34.64588	-91.0539
Louisiana Purchase 4	LP4	34.64566	-91.0563
Louisiana Purchase 5	LP5	34.64568	-91.0565
LaRue 1	LR1	37.5549	-89.4408
LaRue 2	LR2	37.5549	-89.4408
LaRue 3	LR3	37.5549	-89.4408
Mattamuskeet 1	MATT1	35.45372	-76.1753
Mattamuskeet 10	MATT10	35.45456	-76.1757
Mattamuskeet 2	MATT2	35.45372	-76.1753
Mattamuskeet 3	MATT3	35.45372	-76.1753
Mattamuskeet 4	MATT4	35.45371	-76.1755
Mattamuskeet 5	MATT5	35.45371	-76.1755
Mattamuskeet 6	MATT6	35.45371	-76.1755
Mattamuskeet 7	MATT7	35.45371	-76.1755
Mattamuskeet 8	MATT8	35.45387	-76.1762
Mattamuskeet 9	MATT9	35.45387	-76.1762
Mermet 1	MER1	37.26954	-88.8523

Mermet 2	MER2	37.26959	-88.8522
Mermet 3	MER3	37.26959	-88.8522
Mermet 4	MER4	37.26959	-88.8522
Mermet 5	MER5	37.25623	-88.8577
Mermet 6	MER6	37.25582	-88.8592
Mermet 7	MER7	37.25582	-88.8592
Mills Norrie 1	MN1	41.85011	-73.9369
Mills Norrie 10	MN10	41.84824	-73.9371
Mills Norrie 11	MN11	41.84824	-73.9371
Mills Norrie 12	MN12	41.84824	-73.9371
Mills Norrie 2	MN2	41.85017	-73.9367
Mills Norrie 3	MN3	41.85017	-73.9367
Mills Norrie 4	MN4	41.85017	-73.9367
Mills Norrie 5	MN5	41.84888	-73.9374
Mills Norrie 6	MN6	41.84888	-73.9374
Mills Norrie 7	MN7	41.84888	-73.9374
Mills Norrie 8	MN8	41.84888	-73.9374
Mills Norrie 9	MN9	41.84824	-73.9371
Momence 1	MO1	41.16643	-87.5921
Momence 2	MO2	41.16643	-87.5921
Momence 3	MO3	41.16643	-87.5921
Momence 4	MO4	41.16643	-87.5921
Momence 5	MO5	41.16643	-87.5921
Momence 6	MO6	41.16643	-87.5921
Momence 7	MO7	41.16643	-87.5921
Northeast Maryland	NEMARY	39.16921	-75.7817
Pine City 1	PC1	34.61569	-91.1407
Pine City 2	PC2	34.61485	-91.1383
Pine City 3	PC3	34.61474	-91.1383
Pee Dee River/Waccamaw NWR 1	PD1	33.66048	-79.1551
Pee Dee River/Waccamaw NWR 10	PD10	33.65922	-79.1569
Pee Dee River/Waccamaw NWR 2	PD2	33.66048	-79.1551
Pee Dee River/Waccamaw NWR 3	PD3	33.66048	-79.1551
Pee Dee River/Waccamaw NWR 4	PD4	33.66032	-79.1553
Pee Dee River/Waccamaw NWR 5	PD5	33.66032	-79.1553
Pee Dee River/Waccamaw NWR 6	PD6	33.66032	-79.1553
Pee Dee River/Waccamaw NWR 7	PD7	33.65922	-79.1569
Pee Dee River/Waccamaw NWR 8	PD8	33.65922	-79.1569
Pee Dee River/Waccamaw NWR 9	PD9	33.65922	-79.1569
Panther Swamp 1	PS1	32.81001	-90.5193
Panther Swamp 2	PS2	32.81001	-90.5193
Raleigh 1	RAL1	35.80953	-78.7197
Raleigh 2	RAL2	35.80953	-78.7197

Raleigh 3	RAL3	35.80953	-78.7197
Raleigh 4	RAL4	35.80953	-78.7197
Raleigh 5	RAL5	35.80953	-78.7197
Raleigh 6	RAL6	35.80953	-78.7197
Salisbury 1	SAL1	38.28681	-75.3689
Salisbury 10	SAL10	38.28703	-75.3668
Salisbury 2	SAL2	38.28681	-75.3689
Salisbury 3	SAL3	38.28684	-75.3678
Salisbury 4	SAL4	38.28684	-75.3678
Salisbury 5	SAL5	38.28684	-75.3678
Salisbury 6	SAL6	38.28692	-75.3674
Salisbury 7	SAL7	38.28703	-75.3668
Salisbury 8	SAL8	38.28703	-75.3668
Salisbury 9	SAL9	38.28703	-75.3668
Stumpy Lake 1	SL1	36.77461	-76.1603
Stumpy Lake 10	SL10	36.7753	-76.1603
Stumpy Lake 2	SL2	36.77472	-76.1603
Stumpy Lake 3	SL3	36.7748	-76.1603
Stumpy Lake 4	SL4	36.77486	-76.1603
Stumpy Lake 5	SL5	36.77486	-76.1603
Stumpy Lake 6	SL6	36.77496	-76.1602
Stumpy Lake 7	SL7	36.77558	-76.1597
Stumpy Lake 8	SL8	36.77558	-76.1597
Stumpy Lake 9	SL9	36.7753	-76.1603
Side of Road 1	SOR1	34.4386	-91.0457
Side of Road 2	SOR2	34.43853	-91.0457
Side of Road 3	SOR3	34.43846	-91.0457
Side of Road 4	SOR4	34.43843	-91.0457
Side of Road 5	SOR5	34.4384	-91.0458
Side of Road 6	SOR6	34.43832	-91.0458
Sand Pond 1	SP1	36.50348	-90.6004
Sand Pond 2	SP2	36.50336	-90.5998
Sand Pond 3	SP3	36.50335	-90.6004
Sand Pond 4	SP4	36.50336	-90.6004
Sand Pond 5	SP5	36.50344	-90.6006
Sand Pond 6	SP6	36.50345	-90.6006
Sand Pond 7	SP7	36.50345	-90.6006
Sand Pond 8	SP8	36.50344	-90.6006
Staten Island 1	ST1	40.61463	-74.1713
Staten Island 2	ST2	40.61463	-74.1713
Staten Island 3	ST3	40.61463	-74.1713
Staten Island 4	ST4	40.61463	-74.1713
Staten Island 5	ST5	40.61463	-74.1713

Staten Island 6	ST6	40.61463	-74.1713
Tar River 1	TAR1	35.61646	-77.3633
Tar River 10	TAR10	35.62039	-77.3626
Tar River 2	TAR2	35.61646	-77.3633
Tar River 3	TAR3	35.61709	-77.364
Tar River 4	TAR4	35.61742	-77.3639
Tar River 5	TAR5	35.61872	-77.3632
Tar River 6	TAR6	35.61887	-77.3632
Tar River 7	TAR7	35.61885	-77.3633
Tar River 8	TAR8	35.6191	-77.3631
Tar River 9	TAR9	35.62039	-77.3626
True Light Church Road 1	TLC1	30.68569	-90.0377
True Light Church Road 2	TLC2	30.68552	-90.0374
Visitor Center (Congaree NP) 1	VC1	33.82144	-80.8345
Visitor Center (Congaree NP) 10	VC10	33.82473	-80.8213
Visitor Center (Congaree NP) 2	VC2	33.82496	-80.8257
Visitor Center (Congaree NP) 3	VC3	33.82494	-80.8256
Visitor Center (Congaree NP) 4	VC4	33.82495	-80.8256
Visitor Center (Congaree NP) 5	VC5	33.82495	-80.8256
Visitor Center (Congaree NP) 6	VC6	33.825	-80.8255
Visitor Center (Congaree NP) 7	VC7	33.81982	-80.823
Visitor Center (Congaree NP) 8	VC8	33.81982	-80.823
Visitor Center (Congaree NP) 9	VC9	33.82346	-80.8213
Lake Waccamaw 1	WSP1	34.30658	-78.4918
Lake Waccamaw 10	WSP10	34.2606	-78.5237
Lake Waccamaw 2	WSP2	34.30658	-78.4918
Lake Waccamaw 3	WSP3	34.30658	-78.4918
Lake Waccamaw 4	WSP4	34.30658	-78.4918
Lake Waccamaw 5	WSP5	34.30658	-78.4918
Lake Waccamaw 6	WSP6	34.30658	-78.4918
Lake Waccamaw 7	WSP7	34.30658	-78.4918
Lake Waccamaw 8	WSP8	34.25979	-78.5236
Lake Waccamaw 9	WSP9	34.25978	-78.5236
Howesville 1	Howes 1	39.17708	-87.1351
Howesville 2	Howes 2	39.17708	-87.1351
Howesville 3	Howes 3	39.17722	-87.1348
Howesville 4	Howes 4	39.17722	-87.1348
Howesville 5	Howes 5	39.17724	-87.1349
Mingo Swamp NWR 1	Mingo 1	36.96878	-90.157
Mingo Swamp NWR 2	Mingo 2	36.96878	-90.157
Mingo Swamp NWR 3	Mingo 3	36.96882	-90.1571
Mingo Swamp NWR 4	Mingo 4	36.96874	-90.157
Mingo Swamp NWR 5	Mingo 5	36.96874	-90.157

Hillhouse 1	Hill 1	34.10038	-90.7976
Hillhouse 2	Hill 2	34.10038	-90.7976
Hillhouse 3	Hill 3	34.10038	-90.7976
Hillhouse 4	Hill 4	34.10038	-90.7976
Hillhouse 5	Hill 5	34.10038	-90.7976
Guthrie 1	Guth 1	36.6297	-87.1414
Guthrie 2	Guth 2	36.6297	-87.1414
Guthrie 3	Guth 3	36.6297	-87.1414
Guthrie 4	Guth 4	36.6297	-87.1414
Guthrie 5	Guth 5	36.6297	-87.1414
Foxworth 1	Fox 1	31.23631	-89.8588
Foxworth 2	Fox 2	31.23631	-89.8588
Foxworth 3	Fox 3	31.23631	-89.8588
Foxworth 4	Fox 4	31.23631	-89.8588
Foxworth 5	Fox 5	31.23631	-89.8588
Caryville 1	Cary 1	30.7633	-85.812
Caryville 2	Cary 2	30.7633	-85.812
Caryville 3	Cary 3	30.7633	-85.812
Geneva 1	Gen 1	31.02825	-85.4886
Geneva 2	Gen 2	31.02823	-85.4883
Geneva 3	Gen 3	31.02823	-85.4883
Geneva 4	Gen 4	31.02817	-85.4888
Geneva 5	Gen 5	31.02817	-85.4888
Macedonia 1	Mace 1	36.02881	-85.5019
Macedonia 2	Mace 2	36.02881	-85.5019
Macedonia 3	Mace 3	36.02881	-85.5019
Macedonia 4	Mace 4	36.02881	-85.5019
Macedonia 5	Mace 5	36.02881	-85.5019
Adario 1	Adario 1	40.93217	-82.4855
Adario 2	Adario 2	40.93217	-82.4855
Cottonwood Hollow 1	CH 1	41.67609	-81.1895
Cottonwood Hollow 2	CH 2	41.67609	-81.1895
Cottonwood Hollow 3	CH 3	41.67609	-81.1895
Cottonwood Hollow 4	CH 4	41.67609	-81.1895
Cottonwood Hollow 5	CH 5	41.67609	-81.1895
Black Creek Preserve 1	Hud 1	41.82071	-73.959
Black Creek Preserve 2	Hud 2	41.82071	-73.959
Black Creek Preserve 3	Hud 3	41.82071	-73.959
Black Creek Preserve 4	Hud 4	41.82071	-73.959
Black Creek Preserve 5	Hud 5	41.82071	-73.959
Lithia Springs 1	Mass 1	42.29043	-72.5625
Lithia Springs 2	Mass 2	42.29043	-72.5625
Lithia Springs 3	Mass 3	42.29043	-72.5625

Lithia Springs 4	Mass 4	42.29043	-72.5625
Lithia Springs 5	Mass 5	42.29043	-72.5625
Jackson Lane Preserve 1	Jack 1	39.0599	-75.7577
Jackson Lane Preserve 2	Jack 2	39.0599	-75.7577
Jackson Lane Preserve 3	Jack 3	39.0599	-75.7577
Jackson Lane Preserve 4	Jack 4	39.0599	-75.7577
Jackson Lane Preserve 5	Jack 5	39.0599	-75.7577
Great Cypress Swamp 1	GCS 1	38.47393	-75.3133
Great Cypress Swamp 2	GCS 2	38.47393	-75.3133
Great Cypress Swamp 3	GCS 3	38.47393	-75.3133
Great Cypress Swamp 4	GCS 4	38.47393	-75.3133
Great Cypress Swamp 5	GCS 5	38.47393	-75.3133
Savage Neck Dunes 1	SND 1	37.33105	-76.0113
Savage Neck Dunes 2	SND 2	37.33105	-76.0113
Savage Neck Dunes 3	SND 3	37.33105	-76.0113
Savage Neck Dunes 4	SND 4	37.33105	-76.0113
Savage Neck Dunes 5	SND 5	37.33105	-76.0113
Zekiah Swamp 1	Zk 1	38.56271	-76.8562
Zekiah Swamp 2	Zk 2	38.56271	-76.8562
Banister River WMA 1	Ban 1	36.74318	-78.8226
Banister River WMA 2	Ban 2	36.74318	-78.8226
Banister River WMA 3	Ban 3	36.74318	-78.8226
Banister River WMA 4	Ban 4	36.74318	-78.8226
Banister River WMA 5	Ban 5	36.74318	-78.8226
Neuse River 1	Neu 1	35.39309	-78.2858
Neuse River 2	Neu 2	35.39309	-78.2858
Neuse River 3	Neu 3	35.39309	-78.2858
Neuse River 4	Neu 4	35.39309	-78.2858
North Santee 1	NS 1	33.2497	-79.4152
North Santee 2	NS 2	33.2497	-79.4152
North Santee 3	NS 3	33.2497	-79.4152
North Santee 4	NS 4	33.2497	-79.4152
North Santee 5	NS 5	33.2497	-79.4152
Swamps North of Savannah 1	Sav 1	32.38738	-81.028
Swamps North of Savannah 2	Sav 2	32.38738	-81.028
Swamps North of Savannah 3	Sav 3	32.38738	-81.028
Swamps North of Savannah 4	Sav 4	32.38738	-81.028
Swamps North of Savannah 5	Sav 5	32.38738	-81.028

References:

Agrawal, A. A. (2020). A scale-dependent framework for trade-offs, syndromes, and specialization in organismal biology. *Ecology*, *101*(2), 1–24.

Agrawal, A. A., Fishbein, M., Halitschke, R., Hastings, A. P., Rabosky, D. L., & Rasmann, S. (2009). Evidence for adaptive radiation from a phylogenetic study of plant defenses. *Proceedings of the National Academy of Sciences*, *106*(43), 18067–18072. https://doi.org/10.1073/pnas.0904862106

Bagley, J. C., Heming, N. M., Gutiérrez, E. E., Devisetty, U. K., Mock, K. E., Eckert, A. J., & Strauss, S. H. (2020). Genotyping-by-sequencing and ecological niche modeling illuminate phylogeography, admixture, and Pleistocene range dynamics in quaking aspen (Populus tremuloides). *Ecology and Evolution*, *10*(11), 4609–4629. https://doi.org/10.1002/ece3.6214

Bataillon, T., Gauthier, P., Villesen, P., Santoni, S., Thompson, J. D., & Ehlers, B. K. (2022). From genotype to phenotype: Genetic redundancy and the maintenance of an adaptive polymorphism in the context of high gene flow. *Evolution Letters*, *6*(2), 189–202. https://doi.org/10.1002/evl3.277

Berenbaum, M. R., & Zangerl, A. R. (1996). Phytochemical Diversity. In J. T. Romeo, J. A. Saunders, & P. Barbosa (Eds.), *Phytochemical Diversity and Redundancy in Ecological Interactions* (pp. 1–24). Springer US. https://doi.org/10.1007/978-1-4899-1754-6_1

Boeckler, G. A., Gershenzon, J., & Unsicker, S. B. (2011). Phenolic glycosides of the Salicaceae and their role as anti-herbivore defenses. *Phytochemistry*, *72*(13), 1497–1509. https://doi.org/10.1016/j.phytochem.2011.01.038

Boeckler, G. A., Gershenzon, J., & Unsicker, S. B. (2013). Gypsy moth caterpillar feeding has only a marginal impact on phenolic compounds in old-growth black poplar. *Journal of Chemical Ecology*, *39*(10), 1301–1312. https://doi.org/10.1007/s10886-013-0350-8

Bradburd, G. S., Coop, G. M., & Ralph, P. L. (2018). Inferring continuous and discrete population genetic structure across space. *Genetics*, *210*(1), 33–52.

Caseys, C., Stritt, C., Glauser, G., Blanchard, T., & Lexer, C. (2015). Effects of hybridization and evolutionary constraints on secondary metabolites: the genetic architecture of phenylpropanoids in european populus species. *PLOS ONE*, *10*(5), e0128200. https://doi.org/10.1371/journal.pone.0128200

Chou, C.-J., Lin, L.-C., Tsai, W.-J., Hsu, S.-Y., & Ho, L.-K. (1997). Phenyl β-d-glucopyranoside derivatives from the fruits of *Idesia polycarpa*. *Journal of Natural Products*, *60*(4), 375–377. https://doi.org/10.1021/np960335n

Christe, C., Stölting, K. N., Bresadola, L., Fussi, B., Heinze, B., Wegmann, D., & Lexer, C. (2016). Selection against recombinant hybrids maintains reproductive isolation in hybridizing Populus species despite F1 fertility and recurrent gene flow. *Molecular Ecology*, *25*(11), 2482–2498. https://doi.org/10.1111/mec.13587

Cogni, R., Quental, T. B., & Guimarães, P. R. (2022). Ehrlich and Raven escape and radiate coevolution hypothesis at different levels of organization: Past and future perspectives. *Evolution*, *76*(6), 1108–1123. https://doi.org/10.1111/evo.14456

Cole, C. T., Morrow, C. J., Barker, H. L., Rubert-Nason, K. F., Riehl, J. F. L., Köllner, T. G., Lackus, N. D., & Lindroth, R. L. (2021). Growing up aspen: Ontogeny and trade-offs shape growth, defence and reproduction in a foundation species. *Annals of Botany*, *127*(4), 505–517. https://doi.org/10.1093/aob/mcaa070

Coley, P. D., Endara, M.-J., & Kursar, T. A. (2018). Consequences of interspecific variation in defenses and herbivore host choice for the ecology and evolution of Inga, a speciose rainforest tree. *Oecologia*, *187*(2), 361–376. https://doi.org/10.1007/s00442-018-4080-z

De Carvalho, D., Ingvarsson, P. K., Joseph, J., Suter, L., Sedivy, C., Macaya-Sanz, D., Cottrell, J., Heinze, B., Schanzer, I., & Lexer, C. (2010). Admixture facilitates adaptation from standing variation in the European aspen (*Populus tremula* L.), a widespread forest tree. *Molecular Ecology*, *19*(8), 1638–1650. https://doi.org/10.1111/j.1365-94X.2010.04595.x

Dickmann, D. I., & Kuzovkina, J. (2014). Poplars and willows of the world, with emphasis on silviculturally important species. In *Poplars and willows: Trees for society and the environment* (pp. 8–91). CABI.

DiFazio, S. P., Leonardi, S., Slavov, G. T., Garman, S. L., Adams, W. T., & Strauss, S. H. (2012). Gene flow and simulation of transgene dispersal from hybrid poplar plantations. *New Phytologist*, *193*(4), 903–915. https://doi.org/10.1111/j.1469-8137.2011.04012.x

Donaldson, J. R., Stevens, M. T., Barnhill, H. R., & Lindroth, R. L. (2006). Age-related shifts in leaf chemistry of clonal aspen (*Populus tremuloides*). *Journal of Chemical Ecology*, *32*(7), 1415–1429. https://doi.org/10.1007/s10886-006-9059-2

Doorduin, L. J., & Vrieling, K. (2011). A review of the phytochemical support for the shifting defence hypothesis. *Phytochemistry Reviews*, *10*(1), 99–106. https://doi.org/10.1007/s11101-010-9195-8

Douglas, C. J. (2017). Populus as a Model Tree. In A. Groover & Q. Cronk (Eds.), *Comparative and Evolutionary Genomics of Angiosperm Trees* (pp. 61–84). Springer International Publishing. https://doi.org/10.1007/7397_2016_12

Ehrlich, P. R., & Raven, P. H. (1964). Butterflies and plants: A study in coevolution. *Evolution*, *18*(4), 586–608. https://doi.org/10.2307/2406212

Farrell, B. D., Dussourd, D. E., & Mitter, C. (1991). Escalation of plant defense: do latex and resin canals spur plant diversification? *The American Naturalist*, *138*(4), 881–900.

Feistel, F., Paetz, C., Lorenz, S., Beran, F., Kunert, G., & Schneider, B. (2017). *Idesia polycarpa* (Salicaceae) leaf constituents and their toxic effect on *Cerura vinula* and *Lymantria dispar* (Lepidoptera) larvae. *Phytochemistry*, *143*, 170–179. https://doi.org/10.1016/j.phytochem.2017.08.008

Fellenberg, C., Corea, O., Yan, L.-H., Archinuk, F., Piirtola, E.-M., Gordon, H., Reichelt, M., Brandt, W., Wulff, J., Ehlting, J., & Peter Constabel, C. (2020). Discovery of salicyl benzoate UDP-glycosyltransferase, a central enzyme in poplar salicinoid phenolic glycoside biosynthesis. *The Plant Journal*, *102*(1), 99–115. https://doi.org/10.1111/tpj.14615

Forrister, D. L., Endara, M.-J., Soule, A. J., Younkin, G. C., Mills, A. G., Lokvam, J., Dexter, K. G., Pennington, R. T., Kidner, C. A., Nicholls, J. A., Loiseau, O., Kursar, T. A., & Coley,

P. D. (2023). Diversity and divergence: Evolution of secondary metabolism in the tropical tree genus Inga. *New Phytologist*, *237*(2), 631–642. https://doi.org/10.1111/nph.18554

Fraenkel, G. S. (1959). The Raison d'Être of Secondary Plant Substances. *Science*, *129*(3361), 1466–1470.

Futuyma, D. J. (1987). On the role of species in anagenesis. *The American Naturalist*, *130*(3), 465–473. https://doi.org/10.1086/284724

Godbout, J., Gros-Louis, M.-C., Lamothe, M., & Isabel, N. (2020). Going with the flow: Intraspecific variation may act as a natural ally to counterbalance the impacts of global change for the riparian species Populus deltoides. *Evolutionary Applications*, *13*(1), 176–194. https://doi.org/10.1111/eva.12854

Goessen, R., Isabel, N., Wehenkel, C., Pavy, N., Tischenko, L., Touchette, L., Giguère, I., Gros-Louis, M.-C., Laroche, J., Boyle, B., Soolanayakanahally, R., Mock, K., Hernández-Velasco, J., Simental-Rodriguez, S. L., Bousquet, J., & Porth, I. M. (2022). Coping with environmental constraints: Geographically divergent adaptive evolution and germination plasticity in the transcontinental. *PLANTS, PEOPLE, PLANET*, *4*(6), 638–654. https://doi.org/10.1002/ppp3.10297

Gordon, H., Fellenberg, C., Lackus, N. D., Archinuk, F., Sproule, A., Nakamura, Y., Köllner, T. G., Gershenzon, J., Overy, D. P., & Constabel, C. P. (2022). CRISPR/Cas9 disruption of UGT71L1 in poplar connects salicinoid and salicylic acid metabolism and alters growth and morphology. *The Plant Cell*, *34*(8), 2925–2947. https://doi.org/10.1093/plcell/koac135

Hernández, A. I., Landis, J. B., & Specht, C. D. (2022). Phylogeography and population genetics reveal ring species patterns in a highly polymorphic California lily. *Journal of Biogeography*, *49*(2), 416–430. https://doi.org/10.1111/jbi.14313

Hou, J., Wei, S., Pan, H., Zhuge, Q., & Yin, T. (2019). Uneven selection pressure accelerating divergence of *Populus* and *Salix*. *Horticulture Research*, *6*(1), 37. https://doi.org/10.1038/s41438-019-0121-y

Ingvarsson, P. K., & Bernhardsson, C. (2020). Genome-wide signatures of environmental adaptation in European aspen (*Populus tremula*) under current and future climate conditions. *Evolutionary Applications*, *13*(1), 132–142. https://doi.org/10.1111/eva.12792

Isebrands, J. G., & Richardson, J. (2014). *Poplars and willows: Trees for society and the environment*. CABI.

Janzen, D. H. (1973). Dissolution of mutualism between cecropia and its azteca ants. *Biotropica*, *5*(1), 15–28. https://doi.org/10.2307/2989677

Keefover-Ring, K., Ahnlund, M., Abreu, I. N., Jansson, S., Moritz, T., & Albrectsen, B. R. (2014). No Evidence of Geographical Structure of Salicinoid Chemotypes within *Populus tremula*. *PLOS ONE*, *9*(10), e107189. https://doi.org/10.1371/journal.pone.0107189

Keefover-Ring, K., Thompson, J. D., & Linhart, Y. B. (2009). Beyond six scents: Defining a seventh *Thymus vulgaris* chemotype new to southern France by ethanol extraction. *Flavour and Fragrance Journal*, *24*(3), 117–122. https://doi.org/10.1002/ffj.1921

Kessler, A., & Kalske, A. (2018). Plant secondary metabolite diversity and species interactions. *Annual Review of Ecology, Evolution, and Systematics*, *49*(1), 115–138. https://doi.org/10.1146/annurev-ecolsys-110617-062406

Kosiński, P., Sękiewicz, K., Walas, Ł., Boratyński, A., & Dering, M. (2019). Spatial genetic structure of the endemic alpine plant *Salix serpillifolia*: Genetic swamping on nunataks due to secondary colonization? *Alpine Botany*, *129*(2), 107–121. https://doi.org/10.1007/s00035-019-00224-4

Lencioni, S. J., Massatti, R., Keefover-Ring, K., & Holeski, L. M. (2024). The cost of self-defense: browsing effects in the rare plant species *Salix arizonica*. *Ecology and Evolution*, *14*(11), e70582. https://doi.org/10.1002/ece3.70582

Lexer, C., Fay, M. F., Joseph, J. A., Nica, M.-S., & Heinze, B. (2005). Barrier to gene flow between two ecologically divergent *Populus* species, *P.* alba (white poplar) and *P. tremula* (European aspen): The role of ecology and life history in gene introgression. *Molecular Ecology*, *14*(4), 1045–1057. https://doi.org/10.1111/j.1365-294X.2005.02469.x

Lindroth, R. L., Scriber, J. M., & Hsia, M. T. S. (1988). Chemical ecology of the tiger swallowtail: mediation of host use by phenolic glycosides. *Ecology*, *69*(3), 814–822. https://doi.org/10.2307/1941031

López-Goldar, X., & Agrawal, A. A. (2021). Ecological interactions, environmental gradients, and gene flow in local adaptation. *Trends in Plant Science*, *26*(8), 796–809. https://doi.org/10.1016/j.tplants.2021.03.006

Lyman, R. A., & Edwards, C. E. (2022). Revisiting the comparative phylogeography of unglaciated eastern North America: 15 years of patterns and progress. *Ecology and Evolution*, *12*(4), e8827. https://doi.org/10.1002/ece3.8827

Maron, J. L., Agrawal, A. A., & Schemske, D. W. (2019). Plant–herbivore coevolution and plant speciation. *Ecology*, *100*(7), e02704. https://doi.org/10.1002/ecy.2704

Marquis, R. J., Salazar, D., Baer, C., Reinhardt, J., Priest, G., & Barnett, K. (2016). Ode to Ehrlich and Raven or how herbivorous insects might drive plant speciation. *Ecology*, *97*(11), 2939–2951. https://doi.org/10.1002/ecy.1534

Monson, R. K., Trowbridge, A. M., Lindroth, R. L., & Lerdau, M. T. (2022). Coordinated resource allocation to plant growth–defense tradeoffs. *New Phytologist*, *233*(3), 1051–1066. https://doi.org/10.1111/nph.17773

Oberschelp, G. P. J., Guarnaschelli, A. B., Teson, N., Harrand, L., Podestá, F. E., & Margarit, E. (2020). Cold acclimation and freezing tolerance in three *Eucalyptus* species: A metabolomic and proteomic approach. *Plant Physiology and Biochemistry*, *154*, 316–327. https://doi.org/10.1016/j.plaphy.2020.05.026

Pearl, I. A., & Darling, S. F. (1977). Studies on the leaves of the family Salicaceae. 17. Hot-water extractives of the leaves of Populus heterophylla L. Journal of Agricultural and Food Chemistry, 25(4), 730–734. https://doi.org/10.1021/jf60212a035

Pentzold, S., Zagrobelny, M., Rook, F., & Bak, S. (2014). How insects overcome two-component plant chemical defence: Plant β-glucosidases as the main target for herbivore adaptation. *Biological Reviews*, *89*(3), 531–551. https://doi.org/10.1111/brv.12066

Pineau, R. M., Mock, K. E., Morris, J., Kraklow, V., Brunelle, A., Pageot, A., Ratcliff, W. C., & Gompert, Z. (2024). Mosaic of somatic mutations in earth's oldest living organism, Pando. *bioRxiv*, 2024.10.19.619233. https://doi.org/10.1101/2024.10.19.619233

Pratt, J. D., Keefover-Ring, K., Liu L. Y. and Mooney, K. A. Genetically based latitudinal variation in *Artemisia californica* secondary chemistry. Oikos, 123(8), 953-963

Ree, R. H., & Sanmartín, I. (2018). Conceptual and statistical problems with the DEC+J model of founder-event speciation and its comparison with DEC via model selection. *Journal of Biogeography*, *45*(4), 741–749. https://doi.org/10.1111/jbi.13173

Rehill, B., Clauss, A., Wieczorek, L., Whitham, T., & Lindroth, R. (2005). Foliar phenolic glycosides from *Populus fremontii*, *Populus angustifolia*, and their hybrids. *Biochemical Systematics and Ecology*, *33*(2), 125–131. https://doi.org/10.1016/j.bse.2004.06.004

Sanderson, B. J., Gambhir, D., Feng, G., Hu, N., Cronk, Q. C., Percy, D. M., Freaner, F. M., Johnson, M. G., Smart, L. B., Keefover-Ring, K., Yin, T., Ma, T., DiFazio, S. P., Liu, J., & Olson, M. S. (2023). Phylogenomics reveals patterns of ancient hybridization and differential diversification that contribute to phylogenetic conflict in willows, poplars, and close relatives. *Systematic Biology*, *72*(6), 1220–1232. https://doi.org/10.1093/sysbio/syad042

Schnurrer, F., & Paetz, C. (2023). Reductive conversion leads to detoxification of salicortin-like chemical defenses (salicortinoids) in Lepidopteran specialist herbivores (Notodontidae). *Journal of Chemical Ecology*, *49*(5), 251–261. https://doi.org/10.1007/s10886-023-01423-4

Searcy, K. B., & Ascher, R. (2001). The first record of *Populus Heterophylla* (swamp cottonwood, Salicaceae) in Massachusetts. *Rhodora*, *103*(914), 224–226.

Sexton, J. P., Hangartner, S. B., & Hoffmann, A. A. (2014). Genetic isolation by environment or distance: which pattern of gene flow is most common? *Evolution*, *68*(1), 1–15. https://doi.org/10.1111/evo.12258

Sexton, J. P., McIntyre, P. J., Angert, A. L., & Rice, K. J. (2009). Evolution and ecology of species range limits. *Annual Review of Ecology, Evolution, and Systematics*, *40*(1), 415–436. https://doi.org/10.1146/annurev.ecolsys.110308.120317

Slavov, G. T., Leonardi, S., Burczyk, J., Adams, W. T., Strauss, S. H., & Difazio, S. P. (2009). Extensive pollen flow in two ecologically contrasting populations of *Populus trichocarpa*. *Molecular Ecology*, *18*(2), 357–373. https://doi.org/10.1111/j.1365-294X.2008.04016.x

Soolanayakanahally, R. Y., Guy, R. D., Street, N. R., Robinson, K. M., Silim, S. N., Albrectsen, B. R., & Jansson, S. (2015). Comparative physiology of allopatric *Populus* species: Geographic clines in photosynthesis, height growth, and carbon isotope discrimination in common gardens. *Frontiers in Plant Science*, *6*. https://doi.org/10.3389/fpls.2015.00528

Stamp, N. (2003). Out of the quagmire of plant defense hypotheses. *The Quarterly Review of Biology*, *78*(1), 23–55. https://doi.org/10.1086/367580

Tewes, L. J., Michling, F., Koch, M. A., & Müller, C. (2018). Intracontinental plant invader shows matching genetic and chemical profiles and might benefit from high defence variation within populations. *Journal of Ecology*, *106*(2), 714–726. https://doi.org/10.1111/1365-2745.12869

Thompson, J. D., Gauthier, P., Amiot, J., Ehlers, B. K., Collin, C., Fossat, J., Barrios, V., Arnaud-Miramont, F., Keefover-Ring, K., & Linhart, Y. B. (2007). Ongoing adaptation to mediterranean climate extremes in a chemically polymorphic plant. *Ecological Monographs*, *77*(3), 421–439. https://doi.org/10.1890/06-1973.1

Vanden Broeck, A., Villar, M., Van Bockstaele, E., & VanSlycken, J. (2005). Natural hybridization between cultivated poplars and their wild relatives: Evidence and consequences for native poplar populations. *Annals of Forest Science*, *62*(7), 601–613. https://doi.org/10.1051/forest:2005072

Vermeij, G. J. (1994). The evolutionary interaction among species: selection, escalation, and coevolution. *Annual Review of Ecology and Systematics*, *25*, 219–236.

Vernet, P., Gouyon, P. H., & Valdeyron, G. (1986). Genetic control of the oil content in *Thymus vulgaris* L.: A case of polymorphism in a biosynthetic chain. *Genetica*, *69*(3), 227–231.

Vourc'h, G., Martin, J.-L., Duncan, P., Escarré, J., & Clausen, T. P. (2001). Defensive adaptations of *Thuja plicata* to ungulate browsing: A comparative study between mainland and island populations. *Oecologia*, *126*(1), 84–93. https://doi.org/10.1007/s004420000491

Wang, M., Zhang, L., Zhang, Z., Li, M., Wang, D., Zhang, X., Xi, Z., Keefover-Ring, K., Smart, L. B., DiFazio, S. P., Olson, M. S., Yin, T., Liu, J., & Ma, T. (2020). Phylogenomics of the genus *Populus* reveals extensive interspecific gene flow and balancing selection. *New Phytologist*, *225*(3), 1370–1382. https://doi.org/10.1111/nph.16215

Wang, Y., Huang, J., Li, E., Xu, S., Zhan, Z., Zhang, X., Yang, Z., Guo, F., Liu, K., Liu, D., Shen, X., Shang, C., & Zhang, Z. (2022). Phylogenomics and biogeography of *Populus* based on comprehensive sampling reveal deep-level relationships and multiple intercontinental dispersals. *Frontiers in Plant Science*, *13*. https://doi.org/10.3389/fpls.2022.813177

Wessinger, C. A. (2021). From pollen dispersal to plant diversification: Genetic consequences of pollination mode. *New Phytologist*, *229*(6), 3125–3132. https://doi.org/10.1111/nph.17073

Wetzel, W. C., & Whitehead, S. R. (2020). The many dimensions of phytochemical diversity: Linking theory to practice. *Ecology Letters*, *23*(1), 16–32. https://doi.org/10.1111/ele.13422

Wittmann, M. J., & Bräutigam, A. (2025). How does plant chemodiversity evolve? Testing five hypotheses in one population genetic model. *New Phytologist*, *245*(3), 1302–1314. https://doi.org/10.1111/nph.20096

Woolbright, S. A., Rehill, B. J., Lindroth, R. L., DiFazio, S. P., Martinsen, G. D., Zinkgraf, M. S., Allan, G. J., Keim, P., & Whitham, T. G. (2018). Large effect quantitative trait loci for

salicinoid phenolic glycosides in *Populus*: Implications for gene discovery. *Ecology and Evolution*, *8*(7), 3726–3737. https://doi.org/10.1002/ece3.3932

Wright, I. J., Reich, P. B., Westoby, M., Ackerly, D. D., Baruch, Z., Bongers, F., Cavender-Bares, J., Chapin, T., Cornelissen, J. H. C., Diemer, M., Flexas, J., Garnier, E., Groom, P. K., Gulias, J., Hikosaka, K., Lamont, B. B., Lee, T., Lee, W., Lusk, C., … Villar, R. (2004). The worldwide leaf economics spectrum. *Nature*, *428*(6985), 821–827. https://doi.org/10.1038/nature02403

Zangerl, A. R., & Berenbaum, M. R. (2005). Increase in toxicity of an invasive weed after reassociation with its coevolved herbivore. *Proceedings of the National Academy of Sciences*, *102*(43), 15529–15532. https://doi.org/10.1073/pnas.0507805102

Chapter 2

Quantitative and qualitative shifts in salicinoid optimal defense between carbon-source and carbon-sink leaves of *Populus heterophylla*

Tyler H. Wintermute[1], Sarah Kapsner[2], Jorge El-Azaz[1], Ken Keefover-Ring[1,3]

[1]Department of Botany, University of Wisconsin-Madison

[2]Department of Chemistry, University of Wisconsin-Madison

[3]Department of Geography, University of Wisconsin-Madison

Author Contributions: THW and KK-R conceived and developed study design; THW and SK collected field data; THW, SK, and JEA conducted lab work; THW analyzed the data; THW wrote the manuscript with input from JEA and KK-R.

Introduction

A great diversity of secondary metabololites – chemical compounds not involved in primary metabolism (but see Erb & Kliebenstein 2020) – have evolved in plants due to various bottom-up (genetic, biosynthetic) and top-down (climate, species interactions) selection pressures (Wink 2003; Maeda & Fernie 2021). These compounds, often produced in patterns called chemical phenotypes, or "chemotypes," assist plants in a myriad of ways (Erb & Kliebenstein 2020; Dötterl & Gershenzon 2023). However, a plant's ability to make these chemicals is not unrestricted. There are costs to producing metabolites, not only in the maintenance of both the genes that code for and the biosynthetic machinery that produces them, but also in the chemical elements needed for their structures which divert resources away from growth or reproduction (Cole et al. 2021). Over evolutionary time, selective pressures on resource-limited growth-defense tradeoffs have resulted in genetically-controlled coordinated resource allocation strategies in plants (Monson et al. 2022) and understanding the principles behind how plants allocate their resources has thus been a major research focus of biologists for half a century, and numerous hypotheses have emerged from this empirical work (Stamp et al. 2003; Agrawal 2020).

One well-supported hypothesis, the Optimal Defense Hypothesis, states that plants should optimally defend their tissues according to their fitness value, that is, the decrease in plant fitness following removal or damage to that organ (Stamp, 2003). Optimal Defense (OD) has been demonstrated across the plant kingdom with different defense types, both physical (Farji-Brener et al. 2023) and chemical (McCall & Fordyce, 2010; Barton & Koricheva, 2010), and across tissue types, including fruits (Keith & Mitchell-Olds, 2017), shoots and roots (Tsunoda et al. 2017), and leaves (Godschalx et al. 2016; Hunziker et al. 2021). Understanding OD strategies

and their mechanisms can give us a clearer picture of how plants invest their resources, which has implications for growth-defense tradeoffs (Cope et al. 2021), agriculture (Mitchell et al. 2016), and carbon-sequestration and cycling in the face of climate change (Ayres, 1993; Simon & Adamczyk et al. 2019). The relationship of OD to carbon assimilation and allocation can also vary within a plant with leaf phenology. For instance, young leaves, while not photosynthetically mature, are often quantitatively better chemically defended than older, photosynthetically active leaves (Coleman 1986; Barton et al. 2019). These young leaves function as carbon sinks, but a plants' investment in their defense can be considered an investment in future carbon gains – which should increase plant fitness – when those sinks develop into carbon sources, consistent with ideas about the value of a leaf as it ages (Harper 1989; Iwasa et al. 1996; van Dam et al. 1996). Additionally, a given area of damage to an immature leaf can have an outsized effect on the photosynthetic area available to that leaf once mature due to not only the loss of cells that have yet to expand, but also the loss of xylem and phloem used to transport material necessary for leaf maturation (Coleman & Leonard, 1995). Such a reduction in final leaf area – up to 40% in some cases – due to past damage highlights the importance of defending immature leaves (Coleman & Leonard, 1995). The young-old leaf model of OD has been explored in many species (Barton et al. 2019); however, the biosynthetic mechanisms that result in OD appear to be lineage-specific. For example, *Arabadopsis thaliana* glucosinolate transporter knockout mutants demonstrated that quantitative increases in young leaf defense are a function of anti-herbivore glucosinolates being produced in mature leaves and then transported to young leaves (Hunziker et al. 2021). Other species produce defensive compounds locally, which has been suggested for salicinoids (aka, phenolic glycosides) in *Populus* through ^{13}C-labeling (Massad et al. 2014) and measuring gene expression (Fellenberg et al. 2020).

When testing for OD, many studies aggregate defense into a single metric, such as phenolics (Moreira et al. 2012) or cyanogenic potential (Godschalx et al. 2016), but few studies have explored how the quality or composition of defense might alter the quantity of defense plants need for optimality (Barton et al. 2019). Using a single defensive metric has biological value, as herbivores or pathogens encounter the defensive suite as a whole (Kursar & Coley 2003). Yet, even within a chemical class there are compounds of differing bioactivity toward herbivores and other natural enemies. Thus, measuring concentrations of individual compounds in different tissues, such as source and sink leaves, especially in species which deploy a diverse suite of chemical defenses, can provide insight into the ecological function of those specific compounds, as there may be selection pressures (both bottom-up and top-down) influencing the composition of optimal defenses or expression of specific defense compounds in space and time (Agrawal & Hastings 2023).

Populus heterophylla (swamp cottonwood) is a locally-rare – endangered in six US states and in Canada – but widely-dispersed tree species in *Populus* sect. *Leucoides* found in bottomland wetlands in eastern North America, which has received very little attention from researchers (McMaster, 2003). Like other members of Salicaceae, *P. heterophylla* produces salicinoids a class of at least 119 (Chapter 3) chemical compounds that can constitute up to 30% of a leaf's dry mass. These compounds can be present in distinctive patterns according to the plant's chemical phenotype, or chemotype (Keefover-Ring et al. 2014) and confer broad anti-herbivore properties to the plant through oxidation of various moieties into reactive oxygen species which can crosslink proteins when tissue is consumed (Boeckler et al. 2011; Pentzold et al. 2014). However, unlike many *Populus* species, which only have a few salicinoids (Boeckler et al. 2011), *P. heterophylla* produces at least 25 (Chapter 1). Each of these compounds has a

biosynthetic cost, both in actual carbon and the machinery needed to produce them (Babst et al. 2010; Fellenberg et al. 2020; Gordon et al. 2022), and that cost has implications for the genetic compositions of forest trees, shown with a related species, *P. tremuloides* (Cope et al. 2021). The cost of the production of a single salicinoid can be contrasted against the defense efficacy of that compound, with more complex and costlier salicinoids shown to be more deterrent to herbivores (Lindroth et al. 1988), due to a synergistic interaction of the various chemical groups attached to the base structure (Boeckler et al. 2016). Salicinoids have also been shown to metabolically turnover through time, although there are discrepancies on how quick this process is (Kliener et al. 1999; Ruuhola & Julkunen-Tiitto 2000; Massad et al. 2014)

According to OD, when a plant produces multiple salicinoids, there should be selection pressures over evolutionary time that have resulted in "optimal" levels of expression of those compounds depending on this cost-by-effect tradeoff, and those expression levels could vary from organ to organ. However, because most *Populus* species only have a few salicinoids (Boeckler et al. 2011; but see Keefover-Ring et al. 2014), most studies of leaf chemistry, including OD, in the genus have either grouped salicinoids as a single quantitative metric (Kleiner et al. 1999; Arnold et al. 2004) or have only examined a couple compounds (Boeckler et al. 2011; Massad et al. 2014), so it is unknown what patterns of expression are "optimal" when plants have a suite of salicinoids at their disposal. Determining the production levels of each compound, and where and when in the plant that compound is expressed or produced, could provide insight into why so many salicinoids exist in *P. heterophylla*.

Here, I explore chemical defense patterns in leaves of *P. heterophylla* using the sink-source model of leaf Optimal Defense. While I expect a greater quantity of defense in young, carbon-sink leaves when compared to mature, carbon-source leaves, there is no prediction on

how the composition or quality of defense might differ between these organs. Older leaves, because they are more numerous on a single tree, might have greater proportions of less expensive defenses, resulting in less overall biosynthetic strain on the plant. Younger leaves, because they constitute a lower proportion of the total number of leaves on a tree, might have higher proportions of costlier compounds, because trees might be able to afford expensive but highly effective defenses for this limited number of organs with future value. To answer these questions, I used ultra-high-performance liquid chromatography-mass spectrometry (UHPLC-MS) to measure the amounts of multiple salicinoids in source and sink leaves of *P. heterophylla*, as well as monitor the expression of various genes involved in their biosynthesis in both leaf types to determine the production location of these compounds in this species. I conducted these tests over a three-month period during the growing season in a common garden of *P. heterophylla* to disentangle and control for any seasonal effects, such as bud-flush or bud-set, which might otherwise cloud the understanding of OD in this species, if I were to examine leaves at a single timepoint. I also collected gas exchange data on young and old leaves to confirm their carbon-sink or -source status, which highlights their value to the plant in the context of optimal defense.

Methods

Plant material and common garden

In January 2021, dormant vegetative cuttings were collected from *P. heterophylla* trees throughout its native range. Cuttings were submerged in ice water, transported back to Madison, Wisconsin, and propagated in the Walnut Street Greenhouse on the University of Wisconsin-Madison campus. Rooted cuttings were planted in a common garden consisting of a 10 x 10 grid with 6-foot spacing at 43.2904°N, 89.3655°W at Arlington Agricultural Research Station in

Arlington, Wisconsin in June 2021. Trees were well-watered for the rest of the growing season to promote establishment. Notably, this site experienced a rotation of wheat and alfalfa for years prior and is not a wetland, but the water table is about 20 ft deep. Vole guards were placed at the base of the trees and a perimeter deer fence erected to discourage mammalian herbivory.

Leaf collection

Leaves were collected in June, July, and August in the summer of 2022. During each collection event, for each tree, a random branch was selected and an undamaged immature young leaf and a mature old leaf were identified using the leaf plastochron index (LPI; Larson and Isebrands, 1971). In *Populus*, the sink-to-source transition has been reported to occur at LPI 5, and leaves are arranged such that orthostichous leaves are connected by a central trace, independent of phyllotaxy (Larson 1977). Thus, leaves of LPI 2 were selected as our young sink leaf, and they were paired with an orthostichous leaf of LPI 7 from the same branch as our mature source leaf. For the July and August sampling, leaves were collected from a previously unsampled branch to reduce any induction effects. All sampled leaves were exposed to full sun while on the tree.

Gas Exchange Measurements

To verify sink or source status for each leaf, gas exchange was measured using a LICOR-6400 from 7:00 am to noon each day that data was collected, with clear weather. Instrument settings were as follows: 2000 µmol m^{-2} s^{-1} PAR; 400 ppm CO_2 with a 300 µmol m^{-2} s^{-1} flow rate; chamber temperature at 25 °C.

Leaf areas and masses

Following gas exchange measurements, individual leaves were immediately excised at the petiole, flattened between two glass panes on white cardstock and imaged next to a ruler with

a camera for area calculations, and then placed in coolers on ice for transport back to the lab, where they were flash-frozen in liquid nitrogen and lyophilized. Once dry, leaf mass was recorded on a scale with 0.1 mg accuracy and then they were powdered using a ball mill and stored at -20 °C until chemical analyses. Leaf areas were calculated using ImageJ (Schneider et al. 2012) and then leaf mass per area (LMA) was calculated.

Herbivory scores

Herbivory was assessed for each genotype during the July collection timepoint on a scale from 0 to 5, as follows: 0, no herbivory; 1, some small damage due to herbivores (a few holes) on one leaf; 2, small damage on a few leaves; 3, moderate damage on a few leaves, including partial skeletonization (all tissue except 1°, 2°, and 3° veins consumed) of less than half a leaf; 4, one entire leaf skeletonized; 5, multiple leaves skeletonized. Most herbivore damage was attributed to *Popillia japonica* (Japanese beetle), a generalist which avoids leaf veins when feeding, of which there was an outbreak at the garden site in 2022.

Chemical analyses

Chemicals were extracted from 10 mg of dry tissue with 1 mL of HPLC-grade methanol solution with ca. 0.2 mg/mL phenyl-β-D-glucopyranoside (MilliporeSigma, Burlington, MA) as an internal standard. Samples were sonicated for 30 minutes at 4 °C, centrifuged at 20,627 x *g*, and then a 200 µL aliquot was transferred to an autosampler vial with a glass insert. Samples were in an autosampler chamber at 7 °C and 1 µL was injected onto a Acquity C_{18} CSH column (2.1 x 100 mm, 1.7 µm, Waters Corporation, Milford, Massachusetts, US) inline on a Vanquish UHPLC system coupled to a QExactive Orbitrap mass spectrometer via a HESI-II electrospray probe (Thermo Fisher Scientific Inc., Waltham, Massachusetts, US). LCMS-grade water with 0.1% formic acid was used for mobile phase A, and LCMS-grade acetonitrile with 0.1% formic

acid was used for mobile phase B. The gradient was as follows: 0 -18 minutes, 0.1% to 100% B; 18 – 21 minutes, 100% B; 21-21.05 minutes, 100%-0.1% B; 21.05-26 minutes, 0.1% B. Data was collected in the negative ionization mode. Data-Dependent Acquisition was used to collect full-scan chromatograms and fragmentation patterns for ions of interest simultaneously, with a collision energy set to 25 (arbitrary units). Salicinoids were identified via purified standards (generously provided by Rick Lindroth), fragmentation patterns, and parent mass. Peaks were integrated using Thermo Xcalibur version 4.4.16.14, and salicinoids were quantified using calibration curves of purified standards of salicin, salicortin, HCH-salicortin, tremuloidin, and tremulacin. Leaf salicinoids that are not one of those five standards were quantified using the calibration curve of the most structurally-similar salicinoid. A sucrose peak was detected in the chromatograms and used to quantify sucrose concentrations in old and young leaves using the integration methods described for salicinoids and a calibration curve built with an analytical sucrose standards.

Quantitative PCR for salicinoid gene expression

While prior work has suggested or confirmed that salicinoids are locally synthesized in young and old leaves (Massad et al. 2014, Fellenberg et al. 2020), I wanted to confirm this for *P. heterophylla*, which is in a different taxonomic subgenus than previously investigated *Populus* species. I chose to quantify relative expression of the *UGT71L1* (UDP-dependent glycosyltransferase; Potri.016G014500) gene central to salicinoid production (Fellenberg et al. 2020; Kulasekaran et al. 2021; Gordon et al. 2022), the *SABT* (salicyl benzoate UDP-glycosyltransferase; Potri.013G074500) and *BEBT* (benzoyl-CoA:benzyl alcohol O-benzoyltransferase; Potri.019G043600) genes involved in biosynthesis of salicinoid precursor molecules (Chedgy et al. 2015), as well as *PtSOT1* (Potri.012G032700), a gene found to produce

sulfonated salicinoids (Lackus et al. 2020), which I also find in *P. heterophylla,* including salicortin-7-sulfate, which is reported here for the first time in *Populus*.

Primers were designed using sequences for each gene from *P. trichocarpa* from Phytozome (Goodstein et al. 2012), as well as their orthologues in *P. deltoides* and *P. nigra* x *maximowizcii,* and cross-checked against homologues in each of those species using MultAlin (Corpet 1988). The qPCR reference gene *PT1* (POPTR_0014s03160) was selected for its demonstrated stability between immature and mature leaves of *Populus* (Pettengill et al. 2012). Primer sequences for each gene were ordered from MilliporeSigma (MilliporeSigma, Burlington, MA, Table 1). Four genotypes of *P. heterophylla* with ample tissue available for all three collection dates were selected to measure gene expression. Total RNA was extracted from around 10 mg of dry mass ground plant tissue by using the CTAB/LiCl method (Liao et al. 2004) with modifications (Canales et al. 2012). RNA quantification and quality assessment were conducted using a plate reader (Tecan Infinite M Plex, Tecan). Complementary DNA (cDNA) synthesis was performed with 500 ng of total RNA using random hexamer primers and M-MLV Reverse Transcriptase (Promega) following manufacturer's instructions. Quantitative PCR analysis was conducted using a QuantStudio3 (Thermo) instrument and GoTaq qPCR Master Mix (Promega) using the purchased primers with 10 ng of cDNA per reaction. The PCR program consisted of: hot-start 95ºC for 5 min, denaturing 95ºC for 30 sec, annealing 57 ºC for 30 sec, extension 72 ºC for 30 sec, x40 cycles; after amplification, melting curve was made between 55 ºC to 93.78 ºC in 0.305 ºC steps for all wells to assess amplification specificity. All biological samples were run in duplicate. Primer amplification efficiency was checked on two plant samples by plotting Ct (threshold cycle) values against various concentrations of cDNA in

between 0 (water control) and 10 ng per reaction using three technical replicates for each. qPCR results were normalized to the reference genes.

Statistical analysis

All statistical analyses were conducted in R (R Core Team, 2024). Because of genotypic differences in the onset of budset in August that can result in a leaf at LPI 2 to be fully mature, particularly for genotypes of a northern origin, data were first cleaned to remove young leaves which had become mature source leaves, in the context of physiological data from June and July. Any "sink" leaves that had photosynthetic and LMA values within 10% of those of their paired "source" leaf were identified, and then those pairs were removed from further analyses.

A repeated-measures ANOVA with an interaction between leaf age and month was conducted using the package 'afex' (Singmann et al. 2024) to explore changes in photosynthesis, stomatal conductance, LMA, sucrose, and total salicinoids. When there was no significant interaction effect, that term was removed and the test was conducted again. Estimated-marginal means was used for post-hoc analyses using the 'emmeans()' function from the 'emmeans' package, with a Bonferroni correction applied within the test for each trait. To assess the relationship of traits to each other, Pearson's correlation coefficient was calculated for old and young leaves.

Herbivory scores were compared to the total concentration of salicinoids for the mature source leaves of each genotype in July, as those would be the concentrations encountered by herbivores when the scores were assessed. Linear, exponential, and log models were fit to the data, and AIC scores were used to select the best model. Throughout the entire experiment herbivore damage was almost exclusively seen on mature source leaves and only a single young sink leaf was damaged, resulting in a small hole about 5mm in diameter.

For concentration of salicinoids, I conducted a repeated-measures MANOVA using the 'multRM()' function from the 'RM.MANOVA' package (Friedrich et al. 2016) on a subset of genotypes such that each genotype had at least one sink-source leaf pair from among their replicate individuals for each time point, leaving 21 genotypes (11 standard chemotypes, 10 nigracin chemotypes). I used salicinoids as response variables, chemotype, leaf age, and month as independent within-subject variables with an interaction, and genotype as the subject. This test returned a modified ANOVA-type statistic (MATS; Friedrich & Pauly 2018) and a p-value following parametric bootstrapping with 999 iterations. I followed up a significant global result by conducting a repeated-measures ANOVA for each individual salicinoid using the same model structure as the repeated-measures MANOVA, with estimated-marginal means as a post-hoc test and a Bonferroni correction within each estimated-marginal means test. The p-values for individual repeated-measures ANOVAs were corrected globally using the Benjamini-Hochberg (BH) procedure (Benjamini & Hochberg, 1995). If there were no significant effect for a term, including in interactions, that term was removed from the model. This procedure was repeated for the composition of salicinoids, that is, how much each individual salicinoid contributed to the total salicinoids (individual salicinoid % of total).

A repeated-measures ANOVA with an interaction between leaf age and month was conducted using the package 'afex' (Singmann et al. 2024) to test for differences in gene expression in each age class and month. Estimated-marginal means was used for post-hoc analyses using the 'emmeans()' function from the 'emmeans' package (Lenth, 2025) for each gene. Pearsons correlation coefficient was used to model the relationship between expression of each gene and the total concentration of salicinoids for an individual leaf. For the gene PtSOT1

the total concentration of the sulfonated salicinoids was used, instead of the total concentration of all salicinoids.

Results

For photosynthesis, repeated-measures ANOVA results for age showed mature leaves had twice the assimilation rate than young leaves ($F_{1, 20} = 182.5$, $p < 0.001$). Assimilation rates in July were slightly lower than in August, but June assimilation rates did not differ from the latter months ($F_{2, 40} = 10.9$, $p < 0.001$), but there was no two-way interaction between age and month ($F_{2, 40} = 0.48$, $p = 0.62$; Fig. 1a). For stomatal conductance, mature leaves had moderately greater rates of gas exchange than young leaves ($F_{1, 20} = 74.1$, $p < 0.001$). Gas exchange differed slightly between months ($F_{1.5, 30.05} = 17.7$, $p < 0.001$), but there was a two-way interaction between age and month, where mature leaves in August had nearly double the rate of gas exchange than mature leaves in the prior two months and double the rate of gas exchange as young leaves during that August ($F_{2, 40} = 18.9$, $p < 0.001$; Fig. 1b). For sucrose content, mature leaves had over double the sucrose concentration of young leaves ($F_{1, 20} = 564.8$. $p < 0.001$). Sucrose content decreased slightly in August when compared to July ($F_{1.43, 28.57} = 7.3$, $p = 0.006$). Th two-way interaction between age and month resulted in mature leaves having slightly less sucrose in August than in June and July ($F_{1.54, 30.86} = 8.9$, $p = 0.002$; Fig. 1c). For LMA, mature leaves had 1.5x to 2x greater LMA than young leaves ($F_{1, 20} = 133.4$, $p < 0.001$) but those values changed slightly depending on the month ($F_{2, 40} = 4.7$, $p = 0.014$). There were evident two-way interactions between age and month, whereby young leaves in June had greater LMA than young leaves in July and August, and mature leaves in August had greater LMA than mature leaves in June and July ($F_{2, 40} = 18.9$, $p < 0.001$; Fig. 1d).

Total salicinoid concentration results contrasted the rest of the trait data, whereby young leaves had double the salicinoid concentrations than mature leaves ($F_{1, 20} = 121.3$, $p < 0.001$). Salicinoid concentrations were lowest in June, but greater in July and August ($F_{2, 40} = 57.9$, $p < 0.001$). There was a two-way interaction between age and month, whereby mature leaves in June had the lowest salicinoid concentrations of any age:month category and young leaves in June had the same salicinoid concentrations as mature leaves in July and August ($F_{1.41, 28.22} = 25.6$, $p < 0.001$; Fig. 1e). Post-hoc estimated-marginal means showed that there was a difference between young and old leaves in each month for each trait measured (Fig. 1). Across all three months, mature leaves had greater photosynthesis, stomatal conductance, sucrose content, and LMA than young leaves, but young leaves had greater (often double) salicinoid concentrations than mature leaves across the same time period (Fig. 1). Interestingly, many genotypes had low salicinoid concentrations in young leaves in June, but those leaves still had higher salicinoid concentrations than their mature counterparts (Fig. 1e).

For trait correlations, as LMA increases in mature source leaves there is no change in photosynthesis (Fig. 2a), but there was an increase in stomatal conductance (Fig. 2b) and decreases in sucrose content (Fig. 2c) and salicinoid concentrations (Fig. 2d). In young leaves, as LMA increased there was no change in sucrose content (Fig. 2c), but photosynthesis (Fig. 2a), stomatal conductance (Fig. 2b), and salicinoid concentration (Fig. 2d) all decreased. The mature source leaves with nearly no salicinoid concentration in Fig. 2d were collected in June, and reflect the age-by-month interaction for salicinoid concentration in this species.

For herbivory scores for each genotype, I fit a model using the formula herbivory ~ ln(salicinoid concentration) using the herbivory scores of each genotype in July and the total salicinoid concentration mean of each genotype for mature leaves in July. This model had the

lowest AIC when compared to a linear model (herbivory ~ salicinoid concentration) and an exponential model [herbivory ~ exp(salicinoid concentration)], the latter of which is used in Van Dam et al. (1996). The logistic model returned a strong negative non-linear regression (R^2 = 0.807, $p < 0.001$) between herbivory and salicinoid concertation with the equation *herbivory*(salicinoid concentration) = -0.985 × ln(salicinoid concentration) + 2.543 (Fig. 3).

The repeated-measures MANOVA for concentration of individual salicinoids (Table 2, Fig. 4) showed an effect of chemotype (MATS = 232.20, $p < 0.001$), age (MATS = 491.1. $p < 0.001$), month (MATS = 1033.1, $p < 0.001$), an age:month interaction (MATS = 272.3, $p < 0.001$), a chemotype:age interaction (MATS = 63.56, $p = 0.006$), a chemotype:month interaction (MATS = 180.23, $p < 0.001$), and a chemotype:age:month interaction (MATS = 53.87, $p = 0.021$). The repeated-measures MANOVA for individual salicinoid percent compositions (Table 3, Fig. 5) showed an effect of chemotype (MATS = 1199.14, $p < 0.001$), age (MATS = 373.5, $p < 0.001$), month (MATS = 525.9, $p < 0.001$), a chemotype:age interaction (MATS = 73.4, $p < 0.001$), an age:month interaction (MATS = 146.6, $p < 0.001$), a chemotype:month interaction (MATS = 232.4, $p < 0.001$), but no chemotype:age:month interaction (MATS = 25.6, $p = 0.13$). The repeated-measures ANOVAs for the concentration of individual salicinoids shows that some salicinoids had some effect of chemotype (lasiandrin, HCH-nigracin-A, HCH-nigracin-B, and tremulacin; Table 4) though the nature of that effect depended on the salicinoid (Fig. 4f, h, i, j). All salicinoids were affected by age, month, and an age:month interaction, with exceptions for no effect of an age:month interaction for HCH-nigracin-B, and no effect of age or the age:month interaction for salicortin-7-sulfate (Table 4). All salicinoids with a significant effect of age had greater concentrations in young sink leaves than mature source leaves, ranging from 1.5x to 12x greater concentrations depending on the salicinoid, with the exception of some salicinoids having

no difference in concentration between young sink and mature source leaves in June (acetylsalicin, lasiandrin, HCH-nigracin-A, and salicortin-7-sulfate; Fig. 4d, f, h, l). When there was an effect of month, salicinoids tended to be at greater concentrations in July and August than they were in June, but that amount varied by age class of the leaf and by salicinoid (Fig. 4)

For the repeated-measures ANOVAs for the percent of total salicinoids attributed to a given salicinoid, results were mixed and their direction and magnitude depended on the salicinoid, chemotype, age, and month that the measurement was taken (Table 5, Fig. 5). There was an effect of chemotype for salicortin, acetylsalicortin, lasiandrin, HCH-nigracin-A, HCH-nigracin-B, and tremulacin, a chemotype:age interaction for HCH-nigracin-A and tremulacin, a chemotype:month interaction for salicortin, lasiandrin, HCH-nigracin-A, and tremulacin, and a chemotype:age:month interaction for HCH-nigracin-B (Table 5; Fig. 5b, e, f, h, i, j). For non-chemotype effects, there was an effect of age on salicinoid percentages for all salicinoids except for nigracin and salicin-7-sulfate, an effect of month on salicinoid percentages for all salicinoids except for salicin and salicortin-7-sulfate, and an age:month interaction for all salicinoids except salicin, salicortin, HCH-nigracin-A, salicin-7-sulfate, and salicortin-7-sulfate (Table 5). Some salicinoids, such as HCH-salicortin (Fig. 5c), nigracin (Fig. 5g), and HCH-nigracin-B (Fig. 5i) constituted a greater fraction of total salicinoids in mature source leaves than young sink leaves for July and August, but other salicinoids, such as salicin (Fig. 5a), acetylsalicin (Fig. 5d), and acetylsalicortin (Fig. 5e) constituted a greater fraction of total salicinoids in young sink leaves than in mature source leaves in July and August. Salicortin (Fig. 5b) and tremulacin (Fig. 5j) always constituted a greater fraction of total salicinoids in young sink leaves than mature source leaves in all months with the exception of tremulacin in the standard chemotype in June. Lasiandrin constituted a greater fraction of total salicinoids in young sink leaves compared to

mature source leaves in June for the standard chemotype (twice as much), July for both chemotypes (four times as much for the standard chemotype, six times as much for the nigracin chemotype), and August for the nigracin chemotype (one-and-a-half times as much; Fig. 5f).

Gene expression

For the repeated-measures ANOVA for SABT expression (Fig. 6a, Table 6), there was no effect of age ($F_{1, 2} = 2.94$, $p = 0.23$), month ($F_{1.44, 2.89} = 8.65$, $p = 0.083$), or the age:month interaction ($F_{1.24, 2.49} = 2.34$, $p = 0.29$). For BEBT expression (Fig. 6b, Table 6), there was no effect of age ($F_{1,2} = 21.35$, $p = 0.088$), month ($F_{1.26, 2.52} = 0.67$, $p = 0.52$), or the age:month interaction ($F_{1.11, 2.21} = 1.94$, $p = 0.29$). For SOT1 expression (Fig. 6c, Table 6) there was a decrease in expression as the months progressed ($F_{1.76, 5.28} = 18.45$, $p = 0.017$), but no effect of age ($F_{1, 3} = 7.74$, $p = 0.092$) or the age:month interaction ($F_{1.53, 4.58} = 2.55$, $p = 0.29$). For UGT71L1 expression (Fig. 6d, Table 6) there was no effect of age ($F_{1, 3} = 17.26$, $p = 0.088$), but there was an effect of month ($F_{1.82, 5.45} = 13.42$, $p = 0.017$) and a marginal effect of the age:month interaction ($F_{1.68, 5.04} = 12.25$, $p = 0.051$), with a 23-fold increase in expression in young sink leaves compared to mature source leaves in July. Notably, while there are many insignificant differences between young sink and mature source leaves across months for many of these genes, these genes were still expressed in both age classes of leaves in all months (Fig. 6).

Expression of the genes SABT, BEBT, and UGT71L1 were positively correlated with total salicinoid concentrations in young sink leaves, but there was no correlation in the mature source leaves (Fig. 7). The sulfonated salicinoid gene SOT1 had no correlation with salicinoid concentration in young sink or mature source leaves (Fig. 7) nor was there any correlation with sulfonated salicinoid concentrations (Fig. 8).

Discussion

While traditionally there is strong support for quantitative Optimal Defense in young leaves for the total quantity of a few or a class of chemical compounds in an individual plant, it is not clear how plants should invest in OD when they produce a complex suite of defensive compounds. For plants in the genus *Populus,* the total concentration of salicinoids in a single leaf can be up to 30% of the dry mass of that tissue, representing a substantial carbon investment, and thus there should be strong selection pressure to invest that carbon in an optimal manner. One member of the genus, *Populus heterophylla*, produces many salicinoids, and determining if there is differential allocation to certain salicinoids between leaf age classes could provide insight into both why this species produces a diversity of salicinoids and if there might be different optimal strategies for each salicinoid due to cost or fitness benefit.

To test this, I established a garden of *P. heterophylla* genotypes and used physiological, chemical, and molecular analyses on paired immature and mature leaves collected across the growing season. Immature leaves were shown to be carbon-sinks, photosynthesizing at very low rates, while mature leaves were photosynthetically-active and thus more valuable to the tree from a resource-acquisition standpoint. However, immature sink leaves were defended via salicinoids at greater levels than mature source leaves, reflecting their value to the plant in the sense of Optimal Defense. Loss of young, pre-expanded leaf tissue to herbivory would result in a disproportionate loss of photosynthetic area once that tissue expands and matures (Coleman & Leonard 1995). Over time, this decreased area for carbon assimilation can result in reduced plant growth (Zvereva et al. 2012) which can lead to tree death due to decreased competitive ability (Cope et al. 2021). Thus, genotypes which do not optimally defend their leaves die have

inherently lower fitness than those which do, and over evolutionary time optimal defense of leaves should be under positive directional selection.

In addition to the quantitative differences in salicinoids between immature and mature leaves, there was a change in the composition (qualitative difference) of salicinoids between young sink and mature source leaves, particularly in July and August, in which salicinoids that are produced in low concentrations in mature source leaves are produced at higher concentrations in immature sink leaves. Additionally, I show that depending on the chemotype there was different concentrations (Figs. 4f, h, i, j) or compositions (Figs. 5b, e, f, h, i, j) of some salicinoids, while other salicinoids that are shared between the chemotypes did not differ in their patterns of concentration or composition between those chemotypes (Figs. 4, 5). While differences in defensive efficacy of these chemotypes are undetermined, the clear differences in production of certain salicinoids between these chemotypes could differentially affect their herbivores and have different costs for the producing plant, both of which affect the fitness of individuals of this species. Finally, consistent with the notion that salicinoids are locally synthesized in tissues of related species (Fellenberg et al. 2020), I demonstrate this to be the case as well in immature sink and mature source leaves of *P. heterophylla*. While there were few statistical differences in gene expression between those age classes and across months, the salicinoid biosynthetic genes BEBT, SABT, SOT1, and UGT71L1 were expressed in both age classes in all months suggesting that local organ-specific production of salicinoids is conserved in the genus (Fig. 6). Further, when compared with the model plant *Arabidopsis thaliana*, which relies on transporters to translocate glucosinolates from their biosynthetic site in mature source leaves to young sink leaves (Hunziker et al. 2021), my results provide evidence for an alternative

path to Optimal Defense in plants via local synthesis of defensive compounds in developing leaves, which contrasts with some of the discussion in Hunziker et al. (2021).

The very low levels of sucrose in young leaves, when compared to mature leaves, suggests that any carbohydrate transported to young leaves from mature leaves is rapidly used in leaf tissue construction and local biosynthesis of salicinoids, which I confirmed via gene expression. Conversely, mature leaves have a buildup of sucrose due to their photosynthetic capabilities. Rapid expansion of leaves is proposed as one form of defense, in which quickly transitioning from flimsy, weak, and young leaves to sturdy mature leaves can decrease the temporal window in which those young leaves are vulnerable to herbivory (Coleman 1986; Kursar & Coley 2003). Decreases in the transition time of a leaf from carbon-sink to carbon-source allows a faster pay-back on its construction cost (Lawrence et al. 2022), a strategy which is very important in resource-acquisitive species such as those in the genus *Populus* (Kruger et al. 2020; Cope et al. 2021). However, by diverting up to 30% of the dry mass – in the form of carbon and other elements – in a young leaf to production of salicinoids (Fig. 1e), these trees theoretically delay the time to leaf maturation by 30%. Investment in production of salicinoids, and importantly this composition of salicinoids has, at a minimum negligible fitness cost and at a maximum high fitness benefits via defense to the plant than an up to 30% faster expansion of leaves, as there will inherently always be a window in which immature leaves are susceptable to herbivory (Kursar & Coley 2003). Hunziker et al. (2021) propose that metabolic constraints of producing specialized metabolites and their tradeoffs with growth might select for production of defensive compounds in mature source leaves rather than young sink leaves. While there are certainly some costs to local synthesis of defensive compounds, it is clear that adaptive pressures have selected for local production of defensive compounds in *Populus heterophylla*, a trait which

might exist in other trees, due to the cost of long-distance transport of these arsenals in trees and the speed at which these shoots elongate, especially when compared to smaller plants which transport defenses, such as *Nicotiana* (Ohnmeiss & Baldwin 2000) and *Arabidopsis* (Hunziker et al. 2021).

The temporal differences I found in total salicinoid concentration, primarily the lower concentrations in young and old leaves in June when compared to July and August (Fig. 1e) could be explained by the windows of opportunity for plant growth in relation to those opportunities for herbivory (Falk et al. 2018). The mature leaves collected in June originate as preformed leaves built at the end of the previous growing season and the young leaves collected during June are some of the first *de novo* constructed leaves during the current growing season. These young leaves occur very early during the year, when there are still occasional periods of colder weather which might decrease herbivore presence (Schwartzberg et al. 2014; Ward et al. 2019), including for specialists (Seifert et al. 2021) and before many migratory or overwintering insects which feed on trees have had a chance to lay their eggs and/or for their larvae to hatch (Uelmen Jr. et al. 2016).

On an evolutionary time scale, temporal windows of reduced herbivory might have selected for lower defenses in leaves during the early parts of the growing season in favor of increased investment in leaf construction and expansion, allowing trees to expand their canopies earlier than individuals which invest more resources in defense (Cope et al. 2021) and thus begin to assimilate carbon at a greater rate earlier in the growing season. Once their initial canopies are established and herbivore pressure begins to increase, trees might switch to a greater investment in defense, and thus optimal defense, during the peak of the growing season as they now have enough carbon sources to both afford higher levels of defense investment as well as moderate-to-

high levels of growth. However, in *Populus tremuloides* salicinoid concentration is highest immediately after budbreak, falls off quickly after a few days (Falk et al. 2018), and continues to decrease throughout the growing season (Lindroth et al. 1987). The June data I present were collected roughly one month after budbreak in these trees, so immediately after budbreak salicinoids levels could have been very high in all young sink leaves, and the lower levels I then observed in June (when compared to levels in July and August) in both age classes could have been a result of leaf expansion effectively "diluting" the salicinoids stored in the pre-formed leaves in the buds (Read et al. 2003). To test my hypothesis in light of these contrasting results, one could measure the expansion rate of leaves and shoots immediately after budbreak and throughout the growing season, as well as the levels of salicinoids in those leaves, and see how the two vary for fast-growing or slow-growing trees, as has been demonstrated in two *Populus fremontii* x *angustifolia* clones, although salicinoid concentrations did not vary between the fast-growing clone and the slow-growing clone in that study (Harding et al. 2009).

There are a few possible reasons for the differences in salicinoid composition in young sink (greater relative levels of salicin, salicortin, acetylated salicinoids, and tremulacin) and mature source (greater relative levels of HCH-salicortin, nigracin, and HCH-nigracin-B) leaves (Fig. 5). First, maintaining a diverse arsenal of defensive compounds, even when they are the same class of compounds, can be more costly than a simple arsenal, though true cost comparisons of diverse verse simple arsenals are unknown outside of simulations (Wittman & Bräutigam 2025). Simplifying the arsenal in old leaves, which are often the majority of leaves on a plant, might be more cost-effective than producing many compounds in hundreds of organs. However, this complex arsenal might be more effective either due to interaction diversity (Whitehead et al. 2021) or synergy (López-Goldar et al. 2024) and thus worth the extra resource

investment. A diverse but costly arsenal might be more feasible in young leaves, which are critical in terms of fitness (Coleman & Leonard 1995; Godshalx et al. 2016) and which make up a low proportion of the total leaves on a plant at a given time, and thus have an overall lower cost of defense than all of the mature leaves combined. However, I demonstrate that higher levels of the simplified mature leaf salicinoid arsenal are adequate at deterring herbivory (Fig. 3). Therefore, it is unclear why a complex arsenal would be required for optimal defense if the total quantity of salicinoids is already greater in immature than mature leaves (Fig. 1e).

Alternatively, the diversity of salicinoids in young leaves might be related to the rapid production of salicinoids in those leaves, as these compounds are locally synthesized (Figs. 6d, 7 (need to add letters); Massad et al. 2014; Fellenberg et al. 2020). While salicin is not a direct precursor to salicortin or tremulacin, but rather a concurrent product (Babst et al. 2010), we do not know the complete pathway for any salicinoid other than salicortin (Gordon et al. 2022). In the absence of that information, I propose that the upregulation of minor salicinoids in immature leaves of *P. heterophylla* is due to the need to rapidly create a stable arsenal of the major salicinoids (HCH-salicortin, nigracin, and HCH-nigracin) prior to the completion of leaf expansion and maturation, at which point the carbon flux through biosynthetic pathways for salicinoids is kept at low levels to maintain a certain concentration of salicinoids in mature leaves. For example, lasiandrin could be involved in these upregulated pathways in young leaves, but not in old leaves, by some unknown mechanism. When UGT71L1 (or another, yet unknown UGT) conjugates salicyl salicylate with a glucose molecule to begin to form salicortin, this enzyme might be promiscuously attaching an acetylated glucose molecule instead, leading to the buildup of these acetylated compounds prior to maturation. Acetylated salicinoids are common in certain species of *Salix* and *Populus* (Chapter 3; Keefover-Ring et al. 2014) but their

biosynthesis has received limited attention (Ruuhola & Julkunen-Tiitto 2003). Interestingly, in the species of *Salix* that produce acetylated salicinoids, those compounds are the most abundant salicinoids, but in the species of *Populus* that produce acetylated salicinoids they are found at low levels (Chapter 3), except in the high-quantities demonstrated here in immature leaves (Figs. 4e, f). The high concentration of acetylated salicinoids relative to non-acetylated salicinoids in some species of *Salix* suggests that they might confer greater defense, although if that were the case then I would expect to see lasiandrin and acetylsalicortin maintained at high levels relative to other salicinoids in mature leaves of *P. heterophylla* rather than just in young leaves (Figs. 5e, f). The higher levels of salicortin in young leaves suggests that the salicortin-to-HCH-salicortin pathway is being upregulated, and the elevated levels of tremulacin in addition to HCH-nigracin (the two compounds differ by a single OH group) suggest that there is either some enzymatic promiscuity or the presence of yet another unknown enzyme involved in their synthesis, especially in light of correlations from Chapter 1. To make sense of this shift in composition of salicinoids between young and old leaves, researchers should use transcriptomics to find other genes and enzymes responsible for salicinoid production in *P. heterophylla*. I demonstrate that young leaves are allocating resources to expansion, maturation, and salicinoid production, while old leaves are allocating resources to carbon assimilation and salicinoid production, thus a common trait between the two is production of salicinoids, even if those quantities vary. Selecting genotypes across a gradient of salicinoid concentrations should aid in isolating those genes responsible for salicinoid biosynthesis, and searching for these genes in each chemotype of *P. heterophylla* should provide candidates for certain salicinoids. While the majority of salicinoids are shared between chemotypes, there are some differences, such as the isomers of

tremulacin (Chapter 1) and HCH-nigracin A and B, as well as differences in quantity of shared salicinoids depending on chemotype (Figs. 4, 5).

In conclusion, I show the complexity of salicinoid-based Optimal Defense in young carbon sink and old carbon source leaves of *Populus heterophylla* in light of resource-acquisitive traits in those organs, and highlight a few paths forward for understanding both the temporal dynamics of salicinoid defense in this species, as well as expanding our understanding of the biosynthesis of this diverse suite of compounds and Optimal Defense in the plant kingdom.

Figures

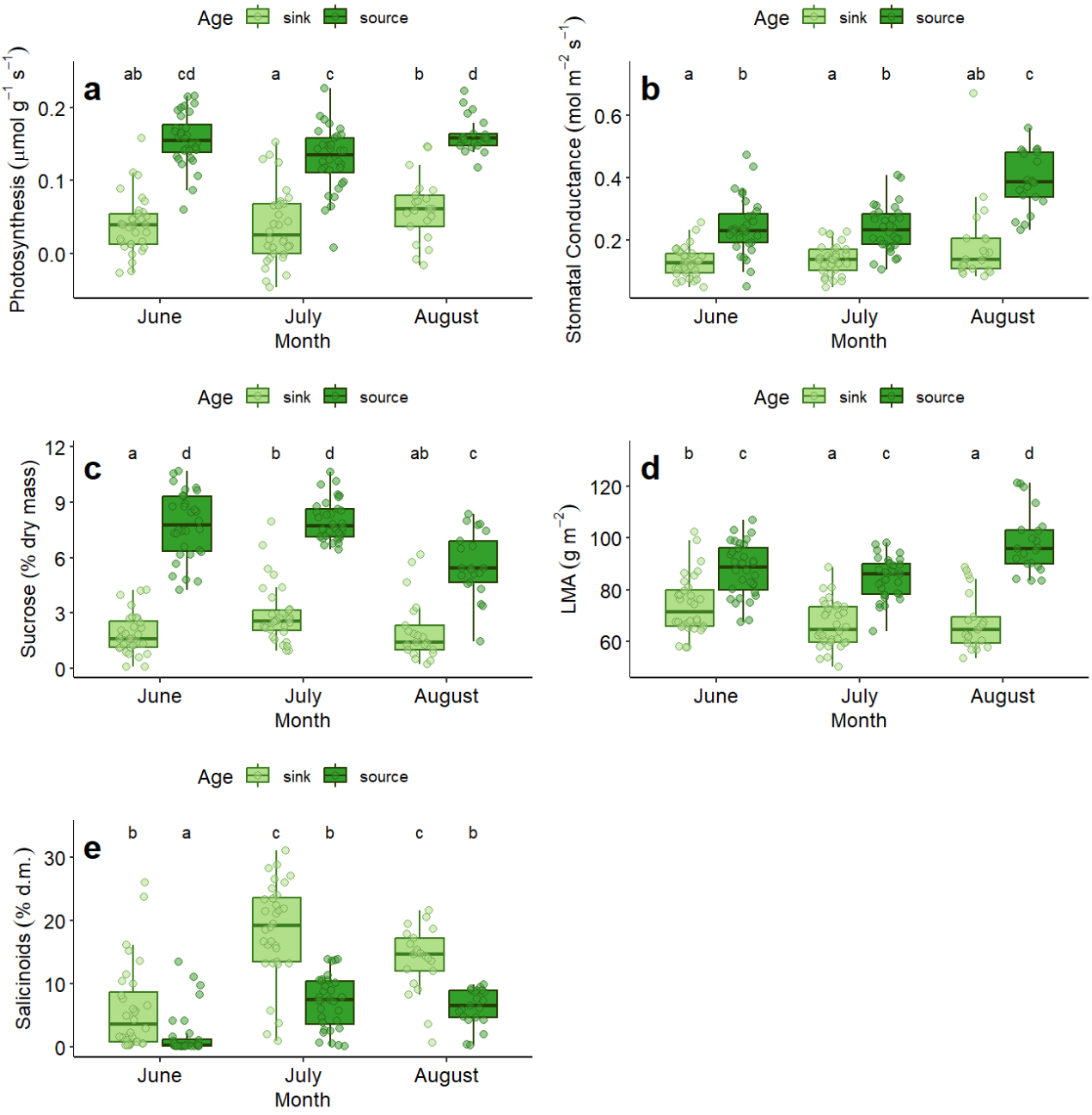

Figure 1. Repeated-measures ANOVA results for traits for young (light green bars) and mature (dark green bars) leaves of *Populus heterophylla* across three months. Within each graph, letters indicate the results of the estimated-marginal means post-hoc test with corrections for multiple testing done with the BH procedure, with letters that are different from each other indicating significant differences between groups and letters that are the same indicating that groups are not significantly different from each other.

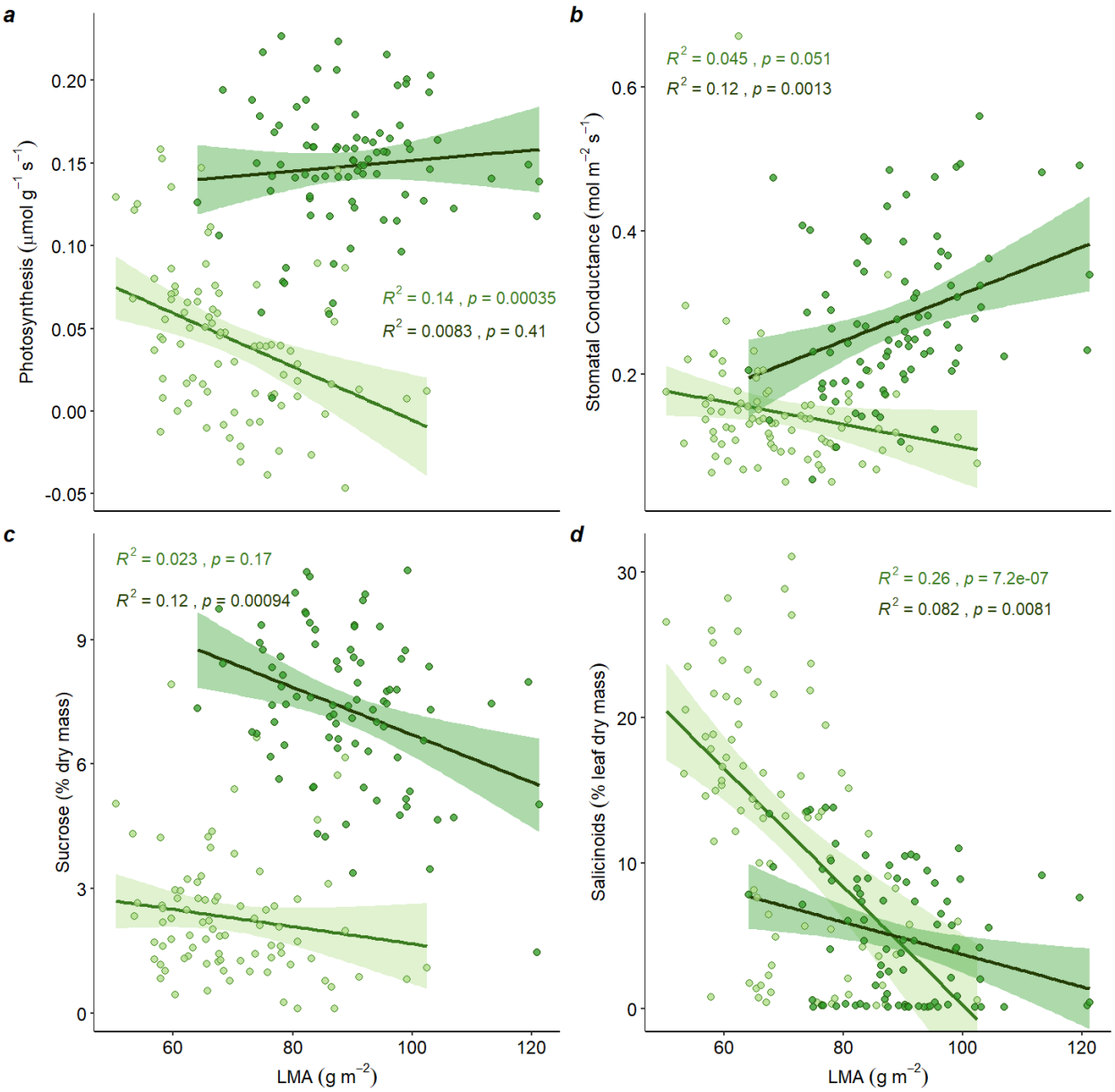

Figure 2. Correlations with LMA by (a) photosynthesis, (b) stomatal conductance, (c) sucrose content, and (d) salicinoids in young (light green shades) and mature (dark green shades) leaves of *Populus heterophylla*. All data from all months is grouped together.

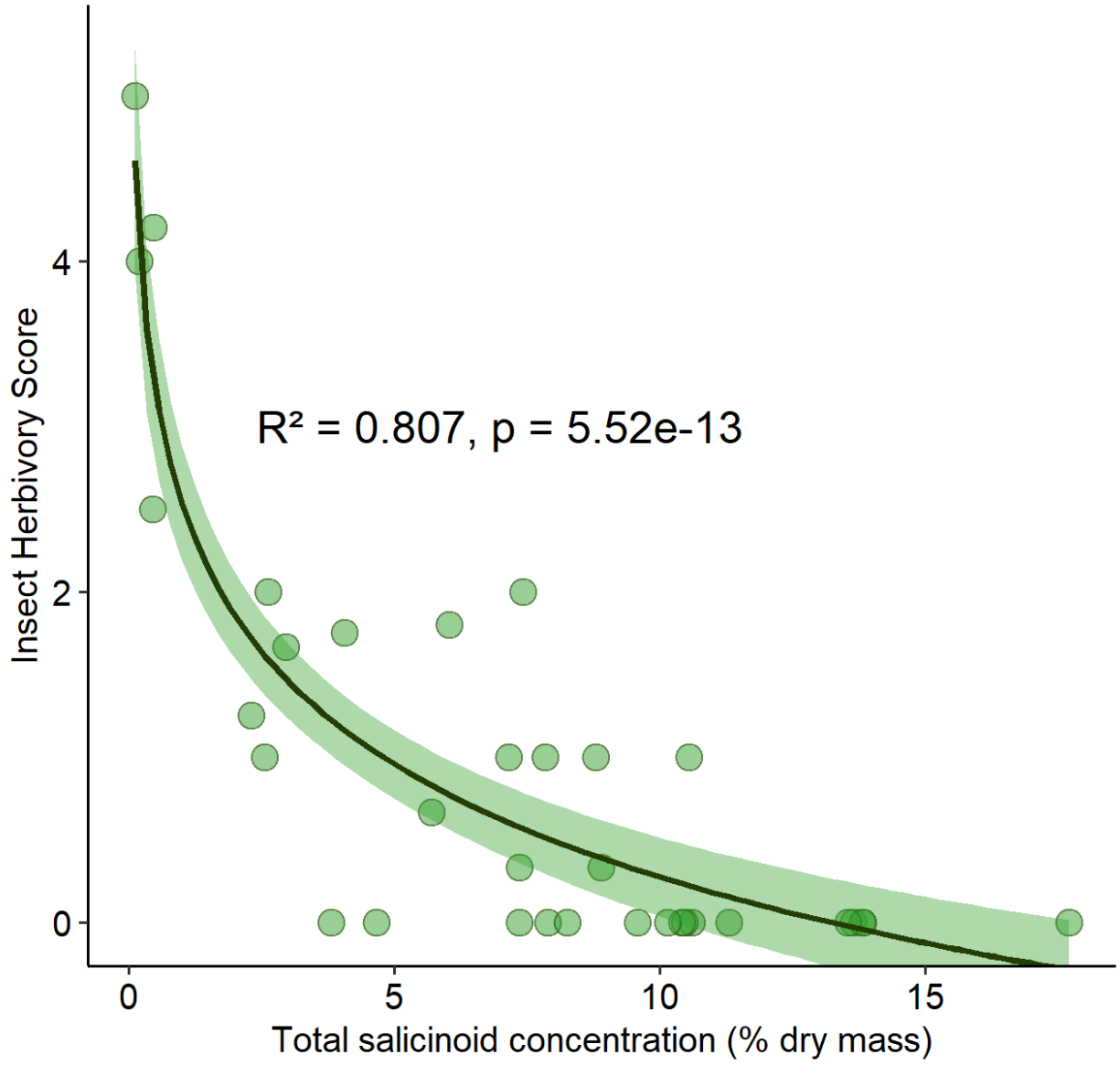

Figure 3. Insect herbivory score as a function of total salicinoid concentration in mature leaves of genotypes of *Populus heterophylla* in July. Solid line is the insect herbivory score of a genotype as a function of the natural log of total salicinoid concentration in mature leaves of that genotype, with the equation: $y(x) = 2.543 – 0.985(\ln(x))$. Herbivory was assessed visually on a 0 to 5 scale as follows: 0, no herbivory; 1, some small damage due to herbivores (a few holes) on one leaf; 2, small damage on a few leaves; 3, moderate damage on a few leaves, including partial skeletonization of less than half a leaf; 4, one entire leaf skeletonized; 5, multiple leaves skeletonized.

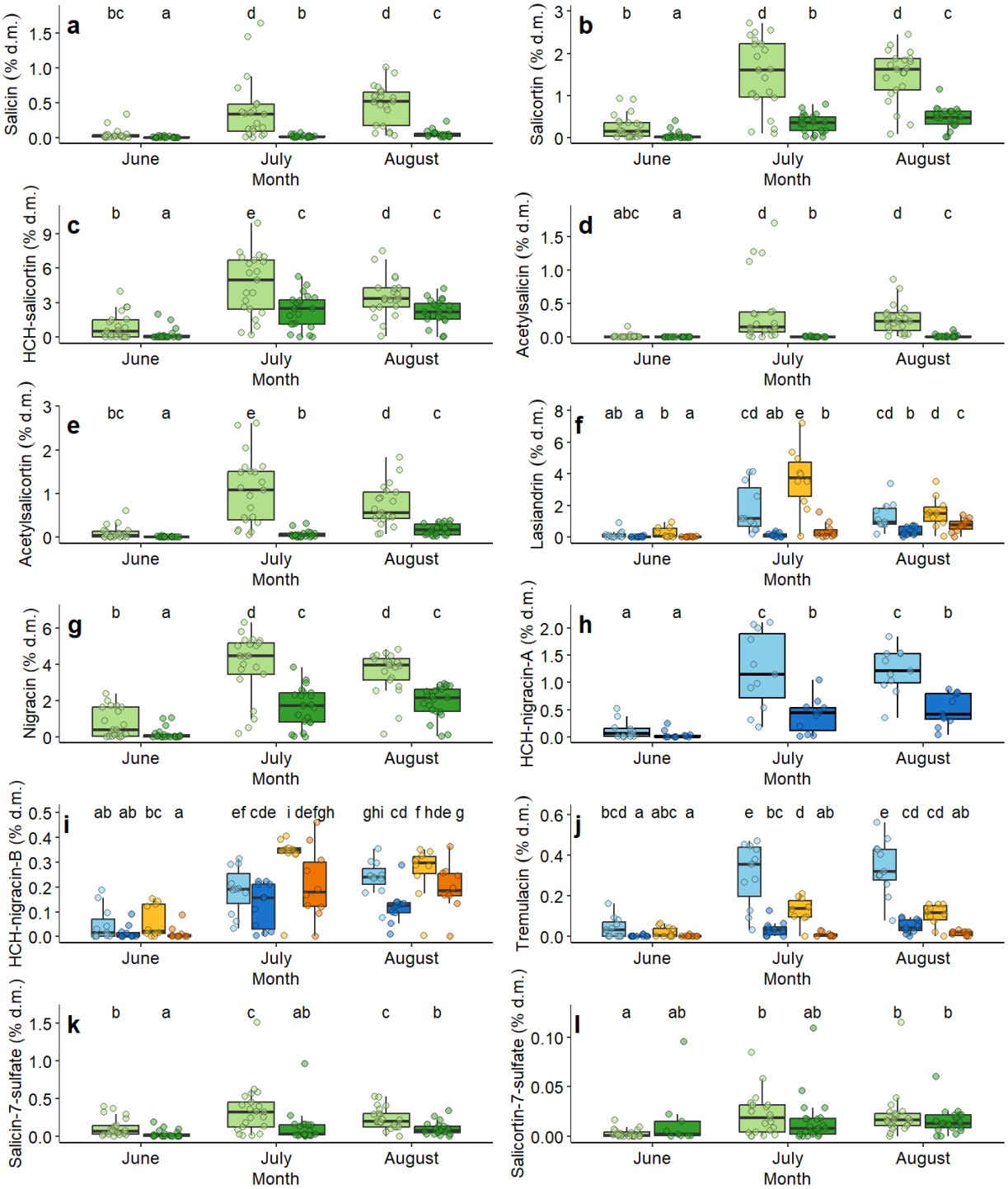

Figure 4. Results of repeated-measures ANOVAs for the concentration of each individual salicinoid in young (lighter shaded bars) and mature (darker shaded bars) leaves of *Populus heterophylla* across three months, with estimated marginal means as a post-hoc test. Letters that are the same indicate that the salicinoid concentrations for those age-month combinations are not different from each other. Salicinoids with green bars (a, b, c, d, e, g, k, l) had no effects of chemotype, while salicinoids that did have effects of chemotype are in blue shades for the nigracin chemotype, and orange shades for the standard chemotype (f, h, i, j).

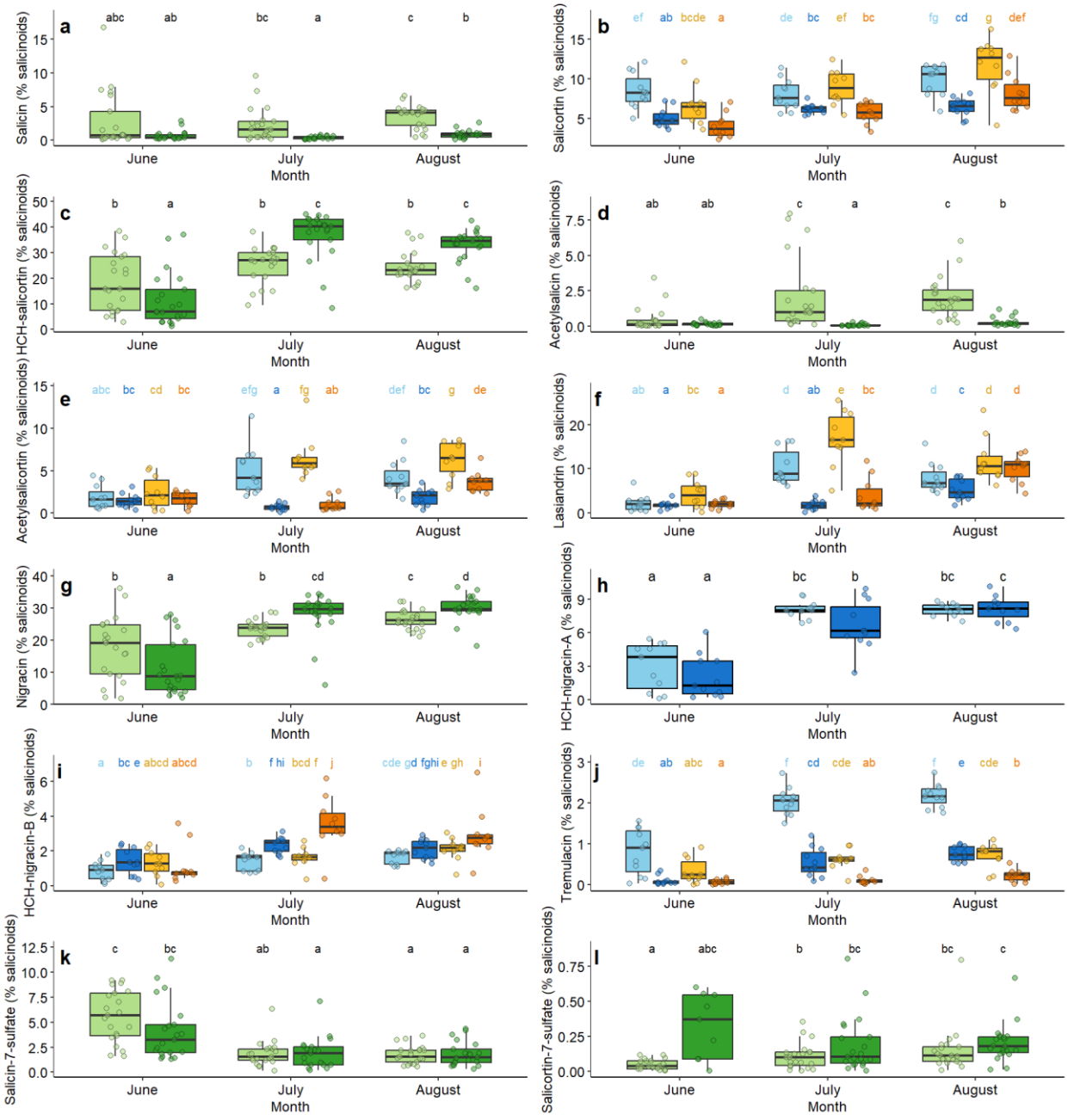

Figure 5. Results of repeated-measures ANOVAs for the composition of salicinoids (% of total salicinoids) for each salicinoid in young sink (lighter shades) and mature source (darker shades) leaves of *Populus heterophylla* across three months, with estimated marginal means as a post-hoc test. Letters that are the same indicate that the salicinoid percentages for those age-month combinations are not significantly different from each other. Salicinoids with green bars (a, c, d, g, k, l) had no effects of chemotype on composition, while salicinoids that did have effects of chemotype are in blue shades for the nigracin chemotype, and orange shades for the standard chemotype (b, e, f, h, i, j).

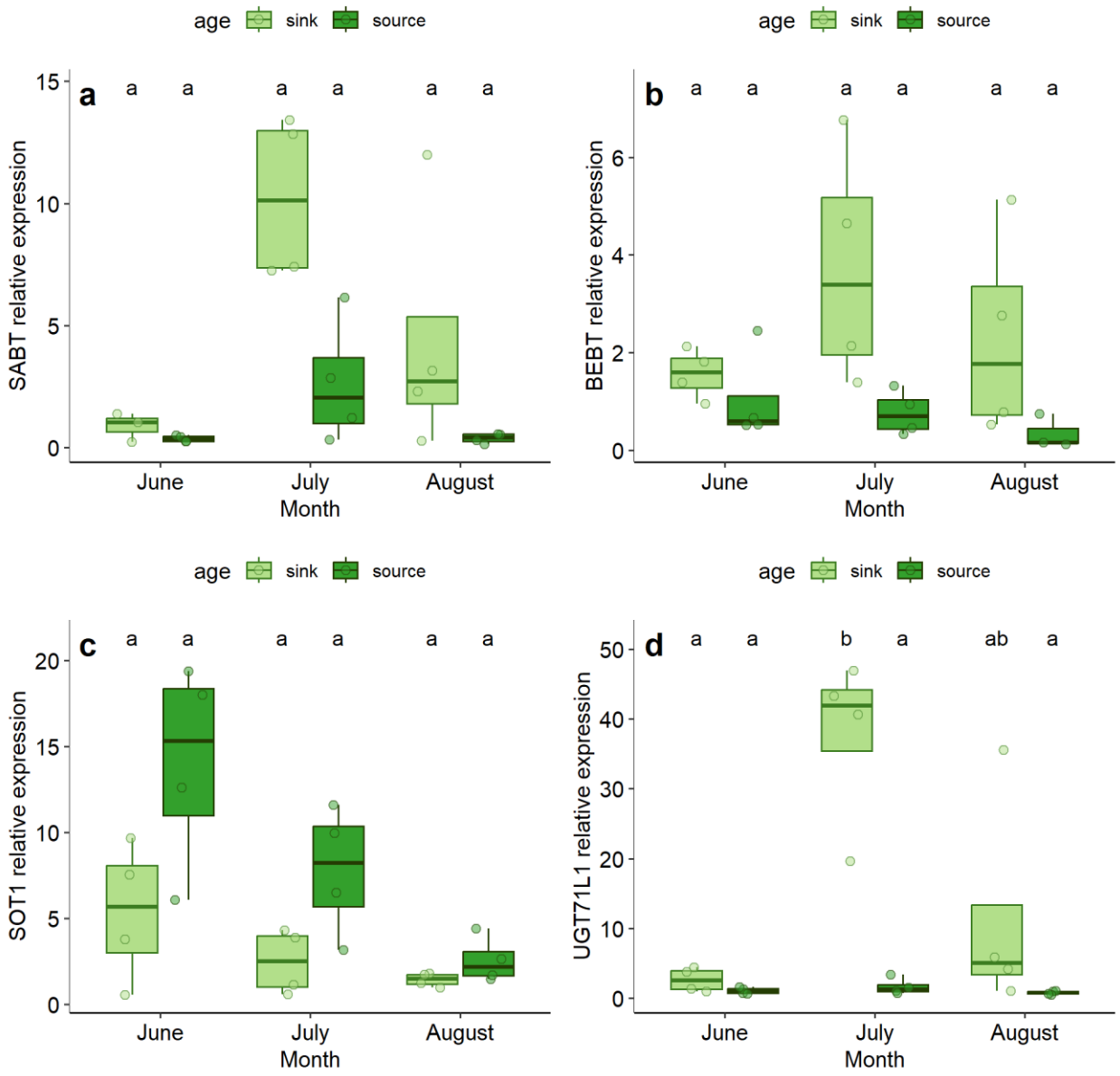

Figure 6. Results of repeated-measures ANOVAs for expression of salicinoid biosynthetic genes in young sink leaves (light shades) and mature source leaves (dark shades) across three months in four genotypes of the 'standard' chemotype of *Populus heterophylla*. Letters that are the same within a plot indicate that gene expression for those age-month combinations are not different from each other.

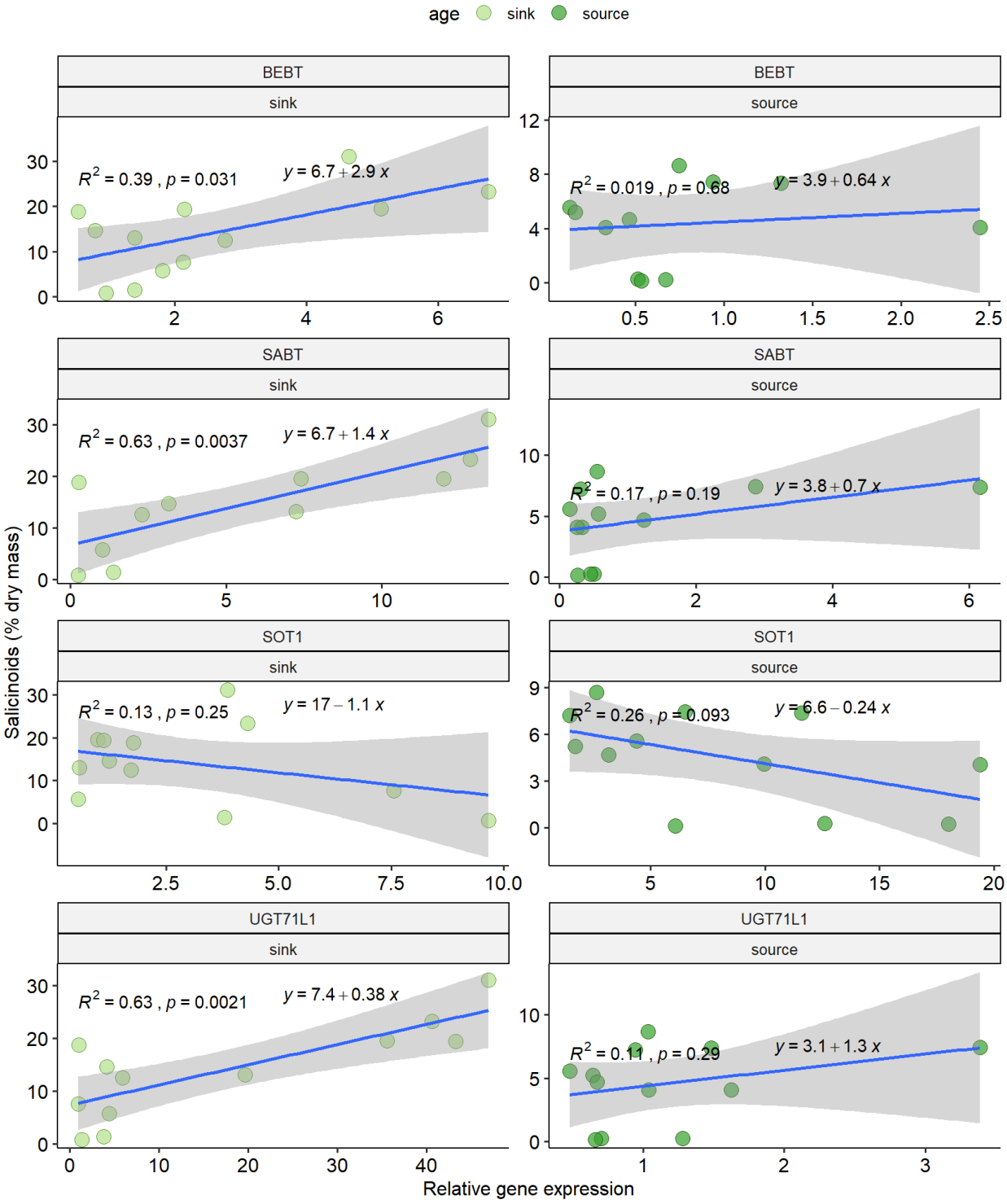

Figure 7. Correlations between expression of salicinoid biosynthesis genes and the total concentration of salicinoids in young sink (light shades) leaves and mature source (dark shades) leaves in *Populus heterophylla.*

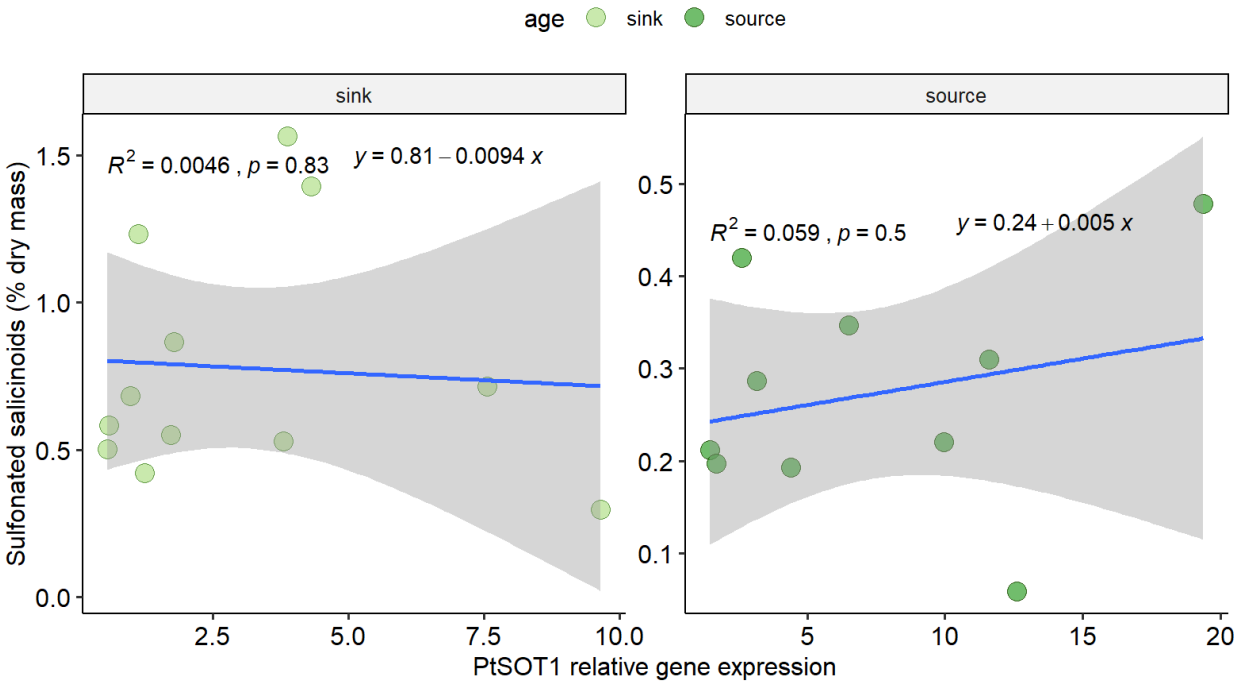

Figure 8. Correlation plots between expression of the sulfonated salicinoid gene PtSOT1 and the concentrations of sulfonated salicinoids in *Populus heterophylla* young sink leaves and mature source leaves.

Tables

Table 1. Primer sequences used for quantitative PCR of salicinoid biosynthetic gene expression in *Populus heterophylla*.

Gene Name	**Forward sequence (5' – 3')**	**Reverse sequence (5' – 3')**
BEBT	CAAAGGTGGGGTTGGCGCC	GACCAGCCAGTTAGCGCGCA
SABT	ATCTTTGGCCTTCGCCTCAAT	GCATGTTCTGAATGCAAGAA
SOT1	CCCTGCCAAGATCCATAATAG	GGCATCGGCTCTGAATCCTTC
UGT71L1	TAGCCCATAAAGCCACAGGTGC	GGCGGTGAGGTTGTGAAGGC
PT1 (*reference*)	ACCAAAAGAGGTTACGGGCAGG	TCCATGGAACAGGGGGGCTGAA

Table 2. Results of a repeated-measures MANOVA of the concentration of main salicinoids in *P. heterophylla* in young sink and mature source leaves in June, July, and August. The modified ANOVA-type statistic is used with parametric bootstrapping with 1000 iterations to calculate a p-value for each effect. * = $p < 0.05$; ** = $p < 0.01$; *** = $p < 0.001$.

Effect	MATS	p-value
chemotype	234.20	**
Age	577.35	***
chemotype:Age	63.56	**
Month	1165.20	***
chemotype:Month	180.23	***
Age:Month	315.18	***
chemotype:Age:Month	53.87	*

Table 3. Results of a repeated-measures MANOVA of the composition (% total salicinoids) of main salicinoids in *P. heterophylla* in young sink and mature source leaves in June, July, and August. The modified ANOVA-type statistic is used with parametric bootstrapping with 1000 iterations to calculate a p-value for each effect. * = $p < 0.05$; ** = $p < 0.01$; *** = $p < 0.001$.

Effect	MATS	p-value
chemotype	1199.14	***
Age	591.99	***
chemotype:Age	73.40	***
Month	740.88	***
chemotype:Month	232.40	***
Age:Month	171.25	***
chemotype:Age:Month	25.55	0.129

Table 4. (Pages 103-104) Repeated-measures ANOVA results for the concentration of salicinoids across three months in old and young leaves of two chemotypes of *Populus heterophylla* with p-values adjusted for multiple testing with the BH procedure. If there was no effect of chemotype (including in interactions) the term was removed from the model. $p<0.05$ = *, $p<0.01$ = **, $p<0.001$ = ***.

Compound	Effect	Num DF	Den DF	F	p_adj
Salicin	Age	1.00	20.00	38.57	***
	Month	1.74	34.86	15.04	***
	Age:Month	1.71	34.21	12.61	***
Salicortin	Age	1.00	20.00	95.45	***
	Month	1.62	32.49	47.94	***
	Age:Month	1.55	31.01	24.06	***
HCH-salicortin	Age	1.00	20.00	44.85	***
	Month	1.78	35.59	44.53	***
	Age:Month	1.43	28.63	5.22	*
Acetylsalicin	Age	1.00	20.00	23.90	***
	Month	1.35	26.98	8.51	**
	Age:Month	1.33	26.61	8.10	**
Acetylsalicortin	Age	1.00	20.00	45.25	***
	Month	1.56	31.15	27.57	***
	Age:Month	1.40	28.02	24.77	***
Lasiandrin	chemotype	1.00	19.00	5.06	0.057
	Age	1.00	19.00	49.41	***
	chemotype:Age	1.00	19.00	2.35	0.189
	Month	1.53	29.16	35.35	***
	chemotype:Month	1.53	29.16	5.05	*
	Age:Month	1.25	23.71	33.45	***
	chemotype:Age:Month	1.25	23.71	5.63	*
Nigracin	Age	1.00	20.00	144.04	***
	Month	1.59	31.87	73.20	***
	Age:Month	1.45	28.91	18.41	***

Compound	Effect	Num DF	Den DF	F	p_adj
HCH-nigracin-A	chemotype	1.00	19.00	43.07	***
	Age	1.00	19.00	65.59	***
	chemotype:Age	1.00	19.00	65.59	***
	Month	1.15	21.76	28.27	***
	chemotype:Month	1.15	21.76	28.27	***
	Age:Month	1.25	23.80	17.36	***
	chemotype:Age:Month	1.25	23.80	17.36	***
HCH-nigracin-B	chemotype	1.00	19.00	3.63	0.101
	Age	1.00	19.00	62.07	***
	chemotype:Age	1.00	19.00	0.07	0.794
	Month	1.66	31.60	81.39	***
	chemotype:Month	1.66	31.60	5.79	*
	Age:Month	1.18	22.46	3.53	0.11
	chemotype:Age:Month	1.18	22.46	2.69	0.129
Tremulacin	chemotype	1.00	19.00	17.53	**
	Age	1.00	19.00	90.68	***
	chemotype:Age	1.00	19.00	17.89	**
	Month	1.26	23.93	49.63	***
	chemotype:Month	1.26	23.93	13.36	**
	Age:Month	1.54	29.30	43.85	***
	chemotype:Age:Month	1.54	29.30	10.93	**
Salicin-7-sulfate	Age	1.00	20.00	64.33	***
	Month	1.26	25.13	6.46	*
	Age:Month	1.59	31.80	5.14	*
Salicortin-7-sulfate	Age	1.00	20.00	1.63	0.217
	Month	1.21	24.20	7.65	*
	Age:Month	1.76	35.26	1.79	0.217

Table 5. (Pages 105-107) Repeated-measures ANOVA results for the percent of total salicinoid concentration attributed to a given salicinoid across three months in young sink and mature source leaves of *Populus heterophylla* with p-values adjusted for multiple testing with the BH procedure. $p<0.05$ = *, $p<0.01$ = **, $p<0.001$ = ***.

Compound	Effect	Num DF	Den DF	F	p_adj
Salicin	Age	1.00	20.00	31.61	***
	Month	1.39	27.70	1.54	0.346
	Age:Month	1.41	28.21	0.38	0.616
Salicortin	chemotype	1.00	19.00	0.18	0.755
	Age	1.00	19.00	70.03	***
	chemotype:Age	1.00	19.00	0.10	0.755
	Month	1.87	35.52	22.32	***
	chemotype:Month	1.87	35.52	6.25	*
	Age:Month	1.57	29.92	1.17	0.528
	chemotype:Age:Month	1.57	29.92	1.24	0.528
HCH-salicortin	Age	1.00	20.00	17.33	***
	Month	1.36	27.18	51.68	***
	Age:Month	1.70	34.03	23.70	***
Acetylsalicin	Age	1.00	20.00	29.95	***
	Month	1.73	34.55	6.64	**
	Age:Month	1.62	32.44	6.81	**
Acetylsalicortin	chemotype	1.00	19.00	7.66	*
	Age	1.00	19.00	60.08	***
	chemotype:Age	1.00	19.00	0.79	0.539
	Month	1.91	36.33	20.45	***
	chemotype:Month	1.91	36.33	2.62	0.124
	Age:Month	1.60	30.43	34.96	***
	chemotype:Age:Month	1.60	30.43	0.49	0.575
Lasiandrin	chemotype	1.00	19.00	13.36	**

Compound	Effect	Num DF	Den DF	F	p_adj
Lasiandrin	Age	1.00	19.00	63.32	***
	chemotype:Age	1.00	19.00	2.25	0.3
	Month	1.95	36.97	59.11	***
	chemotype:Month	1.95	36.97	4.40	*
	Age:Month	1.65	31.30	48.14	***
	chemotype:Age:Month	1.65	31.30	2.80	0.199
Nigracin	Age	1.00	20.00	1.07	0.313
	Month	1.12	22.48	50.56	***
	Age:Month	1.11	22.26	17.86	***
HCH-nigracin-A	chemotype	1.00	19.00	430.11	***
	Age	1.00	19.00	13.21	**
	chemotype:Age	1.00	19.00	13.21	**
	Month	1.33	25.25	66.77	***
	chemotype:Month	1.33	25.25	66.77	***
	Age:Month	1.16	22.13	1.56	0.304
	chemotype:Age:Month	1.16	22.13	1.56	0.342
HCH-nigracin-B	chemotype	1.00	19.00	2.74	0.161
	Age	1.00	19.00	35.91	***
	chemotype:Age	1.00	19.00	0.95	0.512
	Month	1.42	27.02	37.10	***
	chemotype:Month	1.42	27.02	2.93	0.124
	Age:Month	1.55	29.52	31.55	***
	chemotype:Age:Month	1.55	29.52	15.15	***
Tremulacin	chemotype	1.00	19.00	105.95	***
	Age	1.00	19.00	321.22	***
	chemotype:Age	1.00	19.00	74.77	***
	Month	1.38	26.29	86.91	***

Compound	Effect	Num DF	Den DF	F	p_adj
Tremulacin	chemotype:Month	1.38	26.29	33.55	***
	Age:Month	1.75	33.27	10.00	**
	chemotype:Age:Month	1.75	33.27	2.83	0.199
Salicin-7-sulfate	Age	1.00	20.00	1.93	0.196
	Month	1.30	26.08	38.48	***
	Age:Month	1.14	22.77	3.52	0.154
Salicortin-7-sulfate	Age	1.00	20.00	9.60	*
	Month	1.27	25.32	3.95	0.08
	Age:Month	1.95	39.09	0.51	0.616

Table 6. Repeated-measures ANOVA results for expression of salicinoid biosynthetic genes in young sink and mature source leaves across three months for four genotypes of the 'standard' chemotype of *Populus heterophylla*. P-values were adjusted globally for multiple testing across all tests using the BH procedure. $p<0.05$ = *

Gene	Effect	Num DF	Den DF	F	p_adj
BEBT	age	1.00	2.00	21.35	0.088
	month	1.26	2.52	0.67	0.518
	age:month	1.11	2.21	1.94	0.294
SABT	age	1.00	2.00	2.94	0.228
	month	1.44	2.89	8.65	0.083
	age:month	1.24	2.49	2.34	0.294
SOT1	age	1.00	3.00	7.74	0.092
	month	1.76	5.28	18.45	*
	age:month	1.53	4.58	2.55	0.294
UGT71L1	age	1.00	3.00	17.26	0.088
	month	1.82	5.45	13.42	*
	age:month	1.68	5.04	12.25	0.051

References

Agrawal, A. A. (2020). A scale-dependent framework for trade-offs, syndromes, and specialization in organismal biology. *Ecology*, *101*(2), 1–24.

Agrawal, A. A., & Hastings, A. P. (2023). Tissue-specific plant toxins and adaptation in a specialist root herbivore. *Proceedings of the National Academy of Sciences*, *120*(22), e2302251120. https://doi.org/10.1073/pnas.2302251120

Arnold, T., Appel, H., Patel, V., Stocum, E., Kavalier, A., & Schultz, J. (2004). Carbohydrate translocation determines the phenolic content of *Populus* foliage: A test of the sink–source model of plant defense. *New Phytologist*, *164*(1), 157–164. https://doi.org/10.1111/j.1469-8137.2004.01157.x

Ayres, M. P. (1993). Plant defense, herbivory, and climate change. *Biotic Interactions and Global Change.*, 75–94.

Babst, B. A., Harding, S. A., & Tsai, C.-J. (2010). Biosynthesis of phenolic glycosides from phenylpropanoid and benzenoid precursors in *Populus*. *Journal of Chemical Ecology*, *36*(3), 286–297. https://doi.org/10.1007/s10886-010-9757-7

Barton, K. E., Edwards, K. F., & Koricheva, J. (2019). Shifts in woody plant defence syndromes during leaf development. *Functional Ecology*, *33*(11), 2095–2104. https://doi.org/10.1111/1365-2435.13435

Barton, K. E., & Koricheva, J. (2010). The ontogeny of plant defense and herbivory: Characterizing general patterns using meta-analysis. *The American Naturalist*, *175*(4), 481–493. https://doi.org/10.1086/650722

Benjamini, Y., & Hochberg, Y. (1995). Controlling the false discovery rate: a practical and powerful approach to multiple testing. *Journal of the Royal Statistical Society: Series B (Methodological)*, *57*(1), 289–300. https://doi.org/10.1111/j.2517-6161.1995.tb02031.x

Boeckler, G. A., Gershenzon, J., & Unsicker, S. B. (2011). Phenolic glycosides of the Salicaceae and their role as anti-herbivore defenses. *Phytochemistry*, *72*(13), 1497–1509. https://doi.org/10.1016/j.phytochem.2011.01.038

Boeckler, G. A., Paetz, C., Feibicke, P., Gershenzon, J., & Unsicker, S. B. (2016). Metabolism of poplar salicinoids by the generalist herbivore *Lymantria dispar* (Lepidoptera). *Insect Biochemistry and Molecular Biology*, *78*, 39–49. https://doi.org/10.1016/j.ibmb.2016.08.001

Canales, J., Rueda-López, M., Craven-Bartle, B., Avila, C., & Cánovas, F. M. (2012). Novel insights into regulation of asparagine synthetase in conifers. *Frontiers in Plant Science*, *3*. https://doi.org/10.3389/fpls.2012.00100

Chedgy, R. J., Köllner, T. G., & Constabel, C. P. (2015). Functional characterization of two acyltransferases from *Populus trichocarpa* capable of synthesizing benzyl benzoate and salicyl benzoate, potential intermediates in salicinoid phenolic glycoside biosynthesis. *Phytochemistry*, *113*, 149–159. https://doi.org/10.1016/j.phytochem.2014.10.018

Cole, C. T., Morrow, C. J., Barker, H. L., Rubert-Nason, K. F., Riehl, J. F. L., Köllner, T. G., Lackus, N. D., & Lindroth, R. L. (2021). Growing up aspen: Ontogeny and trade-offs

shape growth, defence and reproduction in a foundation species. *Annals of Botany*, *127*(4), 505–517. https://doi.org/10.1093/aob/mcaa070

Coleman, J. S. (1986). Leaf development and leaf stress: Increased susceptibility associated with sink-source transition. *Tree Physiology*, *2*(1-2–3), 289–299. https://doi.org/10.1093/treephys/2.1-2-3.289

Coleman, J. S., & Leonard, A. S. (1995). Why it matters where on a leaf a folivore feeds. *Oecologia*, *101*(3), 324–328. https://doi.org/10.1007/BF00328818

Cope, O. L., Keefover-Ring, K., Kruger, E. L., & Lindroth, R. L. (2021). Growth–defense trade-offs shape population genetic composition in an iconic forest tree species. *Proceedings of the National Academy of Sciences*, *118*(37), e2103162118. https://doi.org/10.1073/pnas.2103162118

Dötterl, S., & Gershenzon, J. (2023). Chemistry, biosynthesis and biology of floral volatiles: Roles in pollination and other functions. *Natural Product Reports*, *40*(12), 1901–1937. https://doi.org/10.1039/D3NP00024A

Erb, M., & Kliebenstein, D. J. (2020). Plant secondary metabolites as defenses, regulators, and primary metabolites: the blurred functional trichotomy. *Plant Physiology*, *184*(1), 39–52. https://doi.org/10.1104/pp.20.00433

Falk, M. A., Lindroth, R. L., Keefover-Ring, K., & Raffa, K. F. (2018). Genetic variation in aspen phytochemical patterns structures windows of opportunity for gypsy moth larvae. *Oecologia*, *187*(2), 471–482. https://doi.org/10.1007/s00442-018-4160-0

Farji-Brener, A., Díaz, D. E., Holanda, I., Ricaurte, A. S., Barrantes, K., & Gutiérrez-Campos, P. J. (2023). Changes in spinescence across leaf ontogeny support the optimal defence hypothesis in blackberries (Rubus adenotrichos). *Journal of Tropical Ecology*, *39*, e30. https://doi.org/10.1017/S0266467423000202

Fellenberg, C., Corea, O., Yan, L.-H., Archinuk, F., Piirtola, E.-M., Gordon, H., Reichelt, M., Brandt, W., Wulff, J., Ehlting, J., & Peter Constabel, C. (2020). Discovery of salicyl benzoate UDP-glycosyltransferase, a central enzyme in poplar salicinoid phenolic glycoside biosynthesis. *The Plant Journal*, *102*(1), 99–115. https://doi.org/10.1111/tpj.14615

Friedrich, S., Konietschke, F., & Pauly, M. (2019). Resampling-Based Analysis of Multivariate Data and Repeated Measures Designs with the R Package MANOVA.RM. *The R Journal*, *11*(2), 380. https://doi.org/10.32614/RJ-2019-051

Friedrich, S., & Pauly, M. (2018). MATS: Inference for potentially singular and heteroscedastic MANOVA. *Journal of Multivariate Analysis*, *165*, 166–179. https://doi.org/10.1016/j.jmva.2017.12.008

Godschalx, A. L., Stady, L., Watzig, B., & Ballhorn, D. J. (2016). Is protection against florivory consistent with the optimal defense hypothesis? *BMC Plant Biology*, *16*(1), 32. https://doi.org/10.1186/s12870-016-0719-2

Goodstein, D. M., Shu, S., Howson, R., Neupane, R., Hayes, R. D., Fazo, J., Mitros, T., Dirks, W., Hellsten, U., Putnam, N., & Rokhsar, D. S. (2012). Phytozome: A comparative

platform for green plant genomics. *Nucleic Acids Research*, *40*(D1), D1178–D1186. https://doi.org/10.1093/nar/gkr944

Gordon, H., Fellenberg, C., Lackus, N. D., Archinuk, F., Sproule, A., Nakamura, Y., Köllner, T. G., Gershenzon, J., Overy, D. P., & Constabel, C. P. (2022). CRISPR/Cas9 disruption of UGT71L1 in poplar connects salicinoid and salicylic acid metabolism and alters growth and morphology. *The Plant Cell*, *34*(8), 2925–2947. https://doi.org/10.1093/plcell/koac135

Harding, S. A., Jarvie, M. M., Lindroth, R. L., & Tsai, C.-J. (2009). A comparative analysis of phenylpropanoid metabolism, N utilization, and carbon partitioning in fast- and slow-growing *Populus* hybrid clones. *Journal of Experimental Botany*, *60*(12), 3443–3452. https://doi.org/10.1093/jxb/erp180

Harper, J. L. (1989). The value of a leaf. *Oecologia*, *80*(1), 53–58. https://doi.org/10.1007/BF00789931

Hillabrand, R. M., Gordon, H., Hynes, B., Constabel, C. P., & Landhäusser, S. M. (2024). Populus root salicinoid phenolic glycosides are not mobilized to support metabolism and regrowth under carbon-limited conditions. *Tree Physiology*, *44*(13), 58–69. https://doi.org/10.1093/treephys/tpad020

Hunziker, P., Lambertz, S. K., Weber, K., Crocoll, C., Halkier, B. A., & Schulz, A. (2021). Herbivore feeding preference corroborates optimal defense theory for specialized metabolites within plants. *Proceedings of the National Academy of Sciences*, *118*(47), e2111977118. https://doi.org/10.1073/pnas.2111977118

Iwasa, Y., Kubo, T., van Dam, N., & de Jong, T. J. (1996). Optimal level of chemical defense decreasing with leaf age. *Theoretical Population Biology*, *50*(2), 124–148. https://doi.org/10.1006/tpbi.1996.0026

Jeong, M. L., Jiang, H., Chen, H.-S., Tsai, C.-J., & Harding, S. A. (2004). Metabolic profiling of the sink-to-source transition in developing leaves of quaking aspen. *Plant Physiology*, *136*(2), 3364–3375. https://doi.org/10.1104/pp.104.044776

Jørgensen, M. E., Nour-Eldin, H. H., & Halkier, B. A. (2015). Transport of defense compounds from source to sink: Lessons learned from glucosinolates. *Trends in Plant Science*, *20*(8), 508–514. https://doi.org/10.1016/j.tplants.2015.04.006

Keefover-Ring, K., Ahnlund, M., Abreu, I. N., Jansson, S., Moritz, T., & Albrectsen, B. R. (2014). No evidence of geographical structure of salicinoid chemotypes within *Populus tremula*. *PLOS ONE*, *9*(10), e107189. https://doi.org/10.1371/journal.pone.0107189

Keith, R. A., & Mitchell-Olds, T. (2017). Testing the optimal defense hypothesis in nature: Variation for glucosinolate profiles within plants. *PLOS ONE*, *12*(7), e0180971. https://doi.org/10.1371/journal.pone.0180971

Kleiner, K. W., Raffa, K. F., & Dickson, R. E. (1999). Partitioning of 14C-labeled photosynthate to allelochemicals and primary metabolites in source and sink leaves of aspen: Evidence for secondary metabolite turnover. *Oecologia*, *119*(3), 408–418. https://doi.org/10.1007/s004420050802

Kruger, E. L., Keefover-Ring, K., Holeski, L. M., & Lindroth, R. L. (2020). To compete or defend: Linking functional trait variation with life-history tradeoffs in a foundation tree species. *Oecologia*, *192*(4), 893–907. https://doi.org/10.1007/s00442-020-04622-y

Kulasekaran, S., Cerezo-Medina, S., Harflett, C., Lomax, C., de Jong, F., Rendour, A., Ruvo, G., Hanley, S. J., Beale, M. H., & Ward, J. L. (2021). A willow UDP-glycosyltransferase involved in salicinoid biosynthesis. *Journal of Experimental Botany*, *72*(5), 1634–1648. https://doi.org/10.1093/jxb/eraa562

Kursar, T. A., & Coley, P. D. (2003). Convergence in defense syndromes of young leaves in tropical rainforests. *Biochemical Systematics and Ecology*, *31*(8), 929–949. https://doi.org/10.1016/S0305-1978(03)00087-5

Lackus, N. D., Müller, A., Kröber, T. D. U., Reichelt, M., Schmidt, A., Nakamura, Y., Paetz, C., Luck, K., Lindroth, R. L., Constabel, C. P., Unsicker, S. B., Gershenzon, J., & Köllner, T. G. (2020). The occurrence of sulfated salicinoids in poplar and their formation by sulfotransferase11 [OPEN]. *Plant Physiology*, *183*(1), 137–151. https://doi.org/10.1104/pp.19.01447

Landhäusser, S. M., Chow, P. S., Dickman, L. T., Furze, M. E., Kuhlman, I., Schmid, S., Wiesenbauer, J., Wild, B., Gleixner, G., Hartmann, H., Hoch, G., McDowell, N. G., Richardson, A. D., Richter, A., & Adams, H. D. (2018). Standardized protocols and procedures can precisely and accurately quantify non-structural carbohydrates. *Tree Physiology*, *38*(12), 1764–1778. https://doi.org/10.1093/treephys/tpy118

Larson, P. R. (1977). Phyllotactic transitions in the vascular system of Populus deltoides bartr. As determined by 14C labeling. *Planta*, *134*(3), 241–249. https://doi.org/10.1007/BF00384188

Larson, P. R., & Isebrands, J. G. (1971). The plastochron index as applied to developmental studies of cottonwood. *Canadian Journal of Forest Research*, *1*(1), 1–11. https://doi.org/10.1139/x71-001

Lawrence, E. H., Springer, C. J., Helliker, B. R., & Poethig, R. S. (2022). The carbon economics of vegetative phase change. *Plant, Cell & Environment*, *45*(4), 1286–1297. https://doi.org/10.1111/pce.14281

Lenth, R. V., Banfai, B., Bolker, B., Buerkner, P., Giné-Vázquez, I., Herve, M., Jung, M., Love, J., Miguez, F., Piaskowski, J., Riebl, H., & Singmann, H. (2025). *emmeans: Estimated Marginal Means, aka Least-Squares Means* (Version 1.11.1) [Computer software]. https://cran.r-project.org/web/packages/emmeans/index.html

Liao, Z., Chen ,Min, Guo ,Liang, Gong ,Yifu, Tang ,Feng, Sun ,Xiaofen, & and Tang, K. (2004). Rapid isolation of high-quality total RNA from *Taxus* and *Ginkgo*. *Preparative Biochemistry & Biotechnology*, *34*(3), 209–214. https://doi.org/10.1081/PB-200026790

Lindroth, R. L., Hsia, M. T. S., & Scriber, J. M. (1987). Seasonal patterns in the phytochemistry of three *Populus* species. *Biochemical Systematics and Ecology*, *15*(6), 681–686. https://doi.org/10.1016/0305-1978(87)90046-9

Lindroth, R. L., Scriber, J. M., & Hsia, M. T. S. (1988). Chemical ecology of the tiger swallowtail: mediation of host use by phenolic glycosides. *Ecology*, *69*(3), 814–822. https://doi.org/10.2307/1941031

López-Goldar, X., Zhang, X., Hastings, A. P., Duplais, C., & Agrawal, A. A. (2024). Plant chemical diversity enhances defense against herbivory. *Proceedings of the National Academy of Sciences*, *121*(51), e2417524121. https://doi.org/10.1073/pnas.2417524121

Maeda, H. A., & Fernie, A. R. (2021). Evolutionary History of Plant Metabolism. *Annual Review of Plant Biology*, *72*(1), 185–216. https://doi.org/10.1146/annurev-arplant-080620-031054

Massad, T. J., Trumbore, S. E., Ganbat, G., Reichelt, M., Unsicker, S., Boeckler, A., Gleixner, G., Gershenzon, J., & Ruehlow, S. (2014). An optimal defense strategy for phenolic glycoside production in *Populus trichocarpa* – isotope labeling demonstrates secondary metabolite production in growing leaves. *New Phytologist*, *203*(2), 607–619. https://doi.org/10.1111/nph.12811

McCall, A. C., & Fordyce, J. A. (2010). Can optimal defence theory be used to predict the distribution of plant chemical defences? *Journal of Ecology*, *98*(5), 985–992. https://doi.org/10.1111/j.1365-2745.2010.01693.x

McMaster, R. T. (2003). *Populus heterophylla L. Swamp cottonwood*. Nativeplanttrust.Org. https://newfs-society.s3.amazonaws.com/documents/Populusheterophylla.PDF

Mitchell, C., Brennan, R. M., Graham, J., & Karley, A. J. (2016). Plant defense against herbivorous pests: exploiting resistance and tolerance traits for sustainable crop protection. *Frontiers in Plant Science*, *7*. https://www.frontiersin.org/articles/10.3389/fpls.2016.01132

Monson, R. K., Trowbridge, A. M., Lindroth, R. L., & Lerdau, M. T. (2022). Coordinated resource allocation to plant growth–defense tradeoffs. *New Phytologist*, *233*(3), 1051–1066. https://doi.org/10.1111/nph.17773

Moreira, X., Zas, R., & Sampedro, L. (2012). Differential allocation of constitutive and induced chemical defenses in pine tree juveniles: a test of the optimal defense theory. *PLOS ONE*, *7*(3), e34006. https://doi.org/10.1371/journal.pone.0034006

Ohnmeiss, T. E., & Baldwin, I. T. (2000). Optimal Defense Theory Predicts the Ontogeny of an Induced Nicotine Defense. Ecology, 81(7), 1765–1783. https://doi.org/10.1890/0012-9658(2000)081[1765:ODTPTO]2.0.CO;2

Pentzold, S., Zagrobelny, M., Rook, F., & Bak, S. (2014). How insects overcome two-component plant chemical defence: Plant β-glucosidases as the main target for herbivore adaptation. *Biological Reviews*, *89*(3), 531–551. https://doi.org/10.1111/brv.12066

Pettengill, E. A., Parmentier-Line, C., & Coleman, G. D. (2012). Evaluation of qPCR reference genes in two genotypes of *Populus* for use in photoperiod and low-temperature studies. *BMC Research Notes*, *5*(1), 366. https://doi.org/10.1186/1756-0500-5-366

R Core Team. (2025). *R: The R Project for Statistical Computing*. https://www.r-project.org/

Read, J., Gras, E., Sanson, G. D., Clissold, F., & Brunt, C. (2003). Does chemical defence decline more in developing leaves that become strong and tough at maturity? *Australian Journal of Botany*, *51*(5), 489. https://doi.org/10.1071/BT03044

Rhoades, D. F., & Cates, R. G. (1976). Toward a general theory of plant antiherbivore chemistry. In J. W. Wallace & R. L. Mansell (Eds.), *Biochemical Interaction Between Plants and Insects* (pp. 168–213). Springer US. https://doi.org/10.1007/978-1-4684-2646-5_4

Ruuhola, T. M., & Julkunen-Tiitto, M.-R. K. (2000). Salicylates of Intact Salix myrsinifolia Plantlets Do Not Undergo Rapid Metabolic Turnover1. Plant Physiology, 122(3), 895–906. https://doi.org/10.1104/pp.122.3.895

Ruuhola, T., & Julkunen-Tiitto, R. (2003). TRADE-OFF BETWEEN SYNTHESIS OF SALICYLATES AND. *Journal of Chemical Ecology*.

Sarah Friedrich, Frank Konietschke, Markus Pauly. (2016). *MANOVA.RM: Resampling-Based Analysis of Multivariate Data and Repeated Measures Designs* (p. 0.5.4) [Dataset]. https://doi.org/10.32614/CRAN.package.MANOVA.RM

Schneider, C. A., Rasband, W. S., & Eliceiri, K. W. (2012). NIH Image to ImageJ: 25 years of image analysis. *Nature Methods*, *9*(7), 671–675. https://doi.org/10.1038/nmeth.2089

Schwartzberg, E. G., Jamieson, M. A., Raffa, K. F., Reich, P. B., Montgomery, R. A., & Lindroth, R. L. (2014). Simulated climate warming alters phenological synchrony between an outbreak insect herbivore and host trees. *Oecologia*, *175*(3), 1041–1049. https://doi.org/10.1007/s00442-014-2960-4

Seifert, C. L., Jorge, L. R., Volf, M., Wagner, D. L., Lamarre, G. P. A., Miller, S. E., Gonzalez-Akre, E., Anderson-Teixeira, K. J., & Novotný, V. (2021). Seasonality affects specialisation of a temperate forest herbivore community. *Oikos*, *130*(9), 1450–1461. https://doi.org/10.1111/oik.08265

Simon, J., & Adamczyk, B. (2019). Editorial: Plant secondary compounds in forest ecosystems under global change: from defense to carbon sequestration. *Frontiers in Plant Science*, *10*. https://www.frontiersin.org/articles/10.3389/fpls.2019.00831

Singmann, H., Bolker, B., Westfall, J., Aust, F., Ben-Shachar, M. S., Højsgaard, S., Fox, J., Lawrence, M. A., Mertens, U., Love, J., Lenth, R., & Christensen, R. H. B. (2024). *afex: Analysis of Factorial Experiments* (Version 1.4-1) [Computer software]. https://cran.r-project.org/web/packages/afex/index.html

Stamp, N. (2003). Out of the quagmire of plant defense hypotheses. *The Quarterly Review of Biology*, *78*(1), 23–55. https://doi.org/10.1086/367580

Tsunoda, T., Krosse, S., & van Dam, N. M. (2017). Root and shoot glucosinolate allocation patterns follow optimal defence allocation theory. *Journal of Ecology*, *105*(5), 1256–1266. https://doi.org/10.1111/1365-2745.12793

Uelmen, J. A., Lindroth, R. L., Tobin, P. C., Reich, P. B., Schwartzberg, E. G., & Raffa, K. F. (2016). Effects of winter temperatures, spring degree-day accumulation, and insect population source on phenological synchrony between forest tent caterpillar and host trees. *Forest Ecology and Management*, *362*, 241–250. https://doi.org/10.1016/j.foreco.2015.11.045

Van Dam, N. M., De Jong, T. J., Iwasa, Y., & Kubo, T. (1996). Optimal distribution of defences: Are plants smart investors? *Functional Ecology*, *10*(1), 128–136. https://doi.org/10.2307/2390271

Ward, S. F., Moon, R. D., Herms, D. A., & Aukema, B. H. (2019). Determinants and consequences of plant–insect phenological synchrony for a non-native herbivore on a deciduous conifer: Implications for invasion success. *Oecologia*, *190*(4), 867–878. https://doi.org/10.1007/s00442-019-04465-2

Whitehead, S. R., Bass, E., Corrigan, A., Kessler, A., & Poveda, K. (2021). Interaction diversity explains the maintenance of phytochemical diversity. *Ecology Letters*, *24*(6), 1205–1214. https://doi.org/10.1111/ele.13736

Wink, M. (2003). Evolution of secondary metabolites from an ecological and molecular phylogenetic perspective. *Phytochemistry*, *64*(1), 3–19. https://doi.org/10.1016/S0031-9422(03)00300-5

Wittmann, M. J., & Bräutigam, A. (2025). How does plant chemodiversity evolve? Testing five hypotheses in one population genetic model. *New Phytologist*, *245*(3), 1302–1314. https://doi.org/10.1111/nph.20096

Zvereva, E. L., Zverev, V., & Kozlov, M. V. (2012). Little strokes fell great oaks: Minor but chronic herbivory substantially reduces birch growth. *Oikos*, *121*(12), 2036–2043. https://doi.org/10.1111/j.1600-0706.2012.20688.x

Chapter 3

Salicinoid salad: Evolution of salicinoids in *Populus* and *Salix*

Tyler Wintermute[1], Lauren E. Frankel[1], Sarah Kapsner[2], Bryan A. Connolly[3], Ken Keefover-Ring[1,4]

[1]Department of Botany, University of Wisconsin-Madison

[2]Department of Chemistry, University of Wisconsin-Madison

[3]Department of Biology, Eastern Connecticut State University

[4]Department of Geography, University of Wisconsin-Madison

Author Contributions: THW and KK-R conceived and developed study design; THW, SK, and BAC collected field samples; THW and SK conducted lab work; THW and LEF analyzed the data; THW wrote the manuscript with input from LEF and KK-R.

Introduction

Plants make a myriad of compounds, resulting in incredible phytochemical diversity (Kessler & Kalske, 2018). Many hypotheses have been proposed for this diversity (Wetzel & Whitehead 2021) and studies have explored this diversity in various experiments (for a review, see Petrén et al. 2024). One major component of plant metabolomes (the sum of all chemical metabolites in a plant) are defensive compounds (Frankael 1959), which confer great fitness advantages to the producing plants when herbivores or pathogens are present but can reduce fitness when herbivores or pathogens are absent (Cope et al. 2021), due to the cost of maintaining these compounds (Kruger et al. 2020). Thus, it might be expected that plants invest in optimal defense strategies, allocating resources to defense in tissues based on apparency to herbivores (Feeny 1976; Smilanich et al. 2016) and fitness-benefit to the plant (Rhoades & Cates 1976; Stamp 2003; Godschalx et al. 2016; Hunziker et al. 2021). At the same time, due to the cost of maintaining defenses, plants have strategies related to trade-offs between allocating resources to defense quantity or growth (Stamp 2003; Monson et al. 2022). Furthermore, plants might be expected to either reduce the number of unique biosynthetic pathways producing unique compounds (Neilson et al. 2013) or reduce the number of unique defensive compounds to minimize the biosynthetic machinery and genetic resources needed to maintain a diversity of defense compounds (de-escalation; Cacho et al. 2015; Núñez-Farfán & Kariñho-Betancourt, 2015) reducing their cost of defense in favor of growth or tolerance (Agrawal & Fishbein, 2008). Such a reduction in defense diversity might only be feasible under scenarios with constant low herbivory or predation (Lencioni et al. 2024; Wittmann & Brautigam, 2024). This is at odds with the reality that plants often have diverse interactions with antagonists, including generalist predators against which quantitative defenses are effective, and specialist predators which seek

out those quantitative defenses and must be combated by other mechanisms, such as qualitative defenses or a paradoxical reduction in quantitative defenses (Smilanich et al. 2016). These interactions form the basis of the Interaction Diversity Hypothesis, whereby plants produce diverse chemicals to mediate diverse interactions (Berenbaum & Zangerl, 1996; Kessler & Kalske, 2018). Unsurprisingly, not all plants have the same interactions, and thus plant metabolomes and defenses vary greatly across the lineages of the plant kingdom. While this provides a possible answer as to *why* different extant species (even closely related ones) have different defense profiles, deciphering *how* different species acquired different chemical defenses across evolutionary time can be challenging (Maeda & Fernie 2021).

One possible reason for how some lineages gained interspecific variation in defense is the classical "escape and radiate" hypothesis, whereby novel and effective defensive compounds evolve in plants faster than their predators can adapt to those defenses, conferring a large fitness advantage to the producing plant species via predator release and thus spurring speciation (Ehrlich & Raven, 1964; Marquis et al. 2016; Maron et al. 2019). There are a few ways this could occur. The most straightforward would be a mutation that creates a single, novel defense metabolite that confers a fitness advantage to the producing plant. A second scenario would be akin to the Synergy Hypothesis (Richards et al. 2016) where two or more compounds (at least one being a novel compound, although all interplaying metabolites could be novel) interact in a synergistic manner to increase the fitness of the producing plant. Finally, plants could escape via the Screening Hypothesis, whereby plants evolve grid-like biosynthetic pathways which, in conjunction with promiscuous enzymes, enables them to make iterations on the same core compound(s) resulting in a large diversity of metabolites, one or more of which might be the "golden" novel defense compound(s) in the escape and radiate scenario (Jones & Firn, 1991;

Carmona et al. 2011). However, this grid scenario might be more favorable for compound diversity *within* a class of chemicals, and not diversity *between* multiple classes of chemicals, such as terpenes and flavonoids, due to different biosynthetic pathways and the limitations of the promiscuous enzymes required under such a scenario (Wang et al. 2019; Fernie & Tohge 2017; Maeda & Fernie 2021).

In simulations (Wittmann & Brautigam, 2024) and bioassay experiments (Whitehead et al. 2021) there has been limited support for the screening hypothesis, although these either did not indicate the types/classes of defense compounds (Wittmann & Brautigam, 2024 only had nameless, shapeless metabolites that had defense values) or all of the compounds tested had some level of bioactivity (Whitehead et al. 2021) counter to the predictions of the screening hypothesis (Jones & Firn 1991). The latter case may be the result of selection against compounds with little to no bioactivity but still have biosynthetic cost; indeed, Whitehead et al. (2021) selected compounds for bioassays that tended to be in high abundance in apples, suggesting they had already been "screened" by herbivores and pathogens. Compounds with no activity, but some cost (e.g. biosynthetic, atomic) should therefore not be under any selection pressure to continue to exist, and (through mutations or other means) might be lost through evolutionary time (Moore et al. 2014). Further, there are a few studies that have explored diversity and quantity of defense in certain lineages, and have found cases of low defense richness but high quantitative defense investment, (Alder et al. 1995; Moore et al. 2004) supporting this idea of optimizing biosynthetic pathways post-screening of metabolites. However, it is unclear why closely related species can have very different strategies with some showing richness or redundancy in a suite of defensive chemicals, while others have seemingly optimized their defense production to a few compounds within that same class.

One chemical system to explore how defensive suites of compounds evolve are the salicinoids, quantitative defenses found in the Salicaceae, and specifically within the tribe Saliceae (or Salicaceae *sensu stricto*) consisting of *Populus* (poplars, cottonwoods, aspens) and *Salix* (willows) (reviewed in Boeckler et al. 2011). Also called phenolic glycosides or salicylates, these compounds can constitute up to 30% of the dry mass of the leaves of these species (Donaldson et al. 2006), representing a considerable resource investment for the plant, and are important mediators of many ecological interactions (Martinsen et al. 1998; Prudic et al. 2007; Diner et al. 2009; Vorel et al. 2015; Cope et al. 2021). Salicinoid richness can vary greatly between species, ranging from four to dozens of compounds (Boeckler et al. 2011), and yet individuals of a salicinoid-rich species can produce the same high quantities of total salicinoids that an individual of a salicinoid-poor species can (Keefover-Ring et al. 2014; Cole et al. 2021). The combinatorial synthesis of salicinoids across a grid-like biosynthetic pathway (Ruuhola & Julkunen-Tiito 2003; Babst et al. 2010; Fellenberg et al. 2020) could allow species with disparate salicinoid richness to achieve similar total concentrations of salicinoids via up or downregulating certain parts of the grid, allowing equal levels of flux through large or small biosynthetic grids (Sweetlove et al. 2025). Different iterations of this grid might be possible due to the structural simplicity of most salicinoids, which consist of a core of a β-D-glucopyranose moiety ether linked to a salicyl alcohol, and on its own this core is called salicin. This core can be further decorated with various moieties (often simple acids or alcohols from the phenylpropanoid pathway) to form more complex salicinoids such as salicortin or tremulacin (Fig. 1), although salicin itself is not a precursor of salicortin or tremulacin (Babst et al. 2010; Gordon et al. 2022). Including glucopyranose, there are 13 known moieties that can be combined in this “Lego-chemistry” fashion (Sherman 2005; Forrister et al. 2023) to form dozens of salicinoid isomers

and conformers, although it is rare to have more than three or four unique moeities on a single salicinoid (Boeckler et al. 2011).

The full pathway or genes involved in salicinoid biosynthesis are unknown and information about the differences in the defensive efficacy of specific salicinoids are limited to a few compounds (Lindroth et al. 1988; Lindroth et al. 1990; Boeckler et al. 2016). Thus, our ability to infer genetic or ecological mechanisms of salicinoid evolution are limited. Furthermore, knowledge of salicinoid diversity across genera is incomplete (Boeckler et al. 2011), due to different methods used on different species (Pearl & Darling 1977; Lindroth et al. 1987; Rubert-Nason et al. 2014; Rubert-Nason et al. 2018) and different definitions or terminology of salicinoids (Ruuhola & Julkunen-Tiito 2003; Boeckler et al. 2011; Volf et al. 2023), which can make comparing salicinoids across studies challenging. This has hindered researchers' ability to make informed decisions when selecting species to use in experiments testing for the function of certain salicinoids and their biosynthesis. In Chapter 1, I demonstrate the utility of using modern methods in salicinoid analyses to revisit an understudied species formerly thought to produce low levels of a single salicinoid (Pearl & Darling 1977; Boeckler et al. 2011) and uncovered patterns of diversity shaped by genetics and ecology where there were thought to be none before. Here, I use similar methods to study salicinoid diversity across members of *Populus* and *Salix* to determine salicinoid diversity and occurrence across genera and use phylogenetic comparative methods to infer patterns of salicinoid evolution, both of which can provide an atlas of salicinoids and inform future research on the ecological and genetic mechanisms behind the existence of this diverse and ecologically-important group of compounds in model plant genera.

Methods

Sample collection

A total of 53 species were included in this project. Twenty-two of these species are in the genus *Populus* (estimated to be between 35 and 100 total species; Dickmann & Kuzovkina 2014), representing five of the six traditional taxonomic sections in that genus and 29 are in the genus *Salix* (estimated to be between 300 and 500 species; Dickmann & Kuzovkina 2014). While the 29 species of *Salix* are a fraction of the total diversity of that genus, they are from across the *Salix* phylogeny and represent the three main subgeneric groups and many of the sections of this genus, which has been challenging to phylogenetically resolve (Sanderson et al. 2023; Marinček et al. 2024; Ogutcen et al. 2024). One species, *Idesia polycarpa* (Salicaceae), is the monotypic species of the genus *Idesia*, which is frequently used as a sister taxon to *Populus* and *Salix* in phylogenetic studies and produces salicinoid and salicinoid-like phenolic glycosides (Feistel et al. 2017).

For local collections (Wisconsin and Morton Arboretum, Illinois; Table 1) individuals were identified to species or confirmed via identification tags and at least five mature, undamaged leaves were collected and stored on ice for transport back to the lab, where they were flash-frozen in liquid nitrogen, lyophilized, and then stored at -20 °C until analyses. For non-local collections (Table 1) mature, undamaged leaves were shipped overnight on dry ice, and upon arrival they were flash-frozen in liquid nitrogen, lyophilized, and stored at -20 °C until analyses.

Phylogeny construction

In lieu of completing genome-scale sequencing for all species sampled in this study, I made use of recent phylogenomic studies which have had some success in untangling the

topologies of *Populus* and *Salix*, which are notoriously challenging in large part due to rampant extant and ancient hybridization (Sanderson et al. 2023). However, because no single phylogeny contained all of the species I collected, the phylogenies of Sanderson et al. (2023), Marinček et al. (2024), and Ogutcen et al. (2024) were used to build one, as those phylogenies contained most of the species I collected, these phylogenies were some of the most recent published at the time of analysis, they used hundreds of genes or tens of thousands of SNPs in lieu of just a handful of genes, and portions of those phylogenies overlapped and agreed with each other. For species that did not have topological conflicts between the phylogenies, I grafted on taxa relative to sister species in common between phylogenies. A few species did not appear in those three published phylogenies; for those species, the literature was searched for a phylogeny containing them and a sister taxon which did appear in the main phylogenies I used (but did not sample for salicinoids) and then the species I sampled for salicinoids was placed in that position.

Gene sequencing

Of the 53 species in this study, five had no NCBI data or were not part of published phylogenies. To establish a phylogenetic position, I designed nested primers for the barcode genes *matK*, *rbcL*, and *ITS* (Lauron-Moreau et al. 2015) using published *Populus* and *Salix* sequences for those genes on NCBI (Sayers et al. 2025) and MultAlin (Corpet 1988). Primers were ordered from MilliporeSigma (MilliporeSigma, Burlington, MA; Table 2). Total RNA was extracted from around 10 mg of dry mass ground plant tissue from using the CTAB/LiCl method (Liao et al. 2004) with modifications (Canales et al. 2012). RNA quantification and quality assessment were conducted using a plate reader (Tecan Infinite M Plex, Tecan). Complementary DNA (cDNA) synthesis was performed with 500 ng of total RNA using random hexamer primers and M-MLV Reverse Transcriptase (Promega) following manufacturer's instructions.

Sequences were amplified using PCR and the nested primers with the following cycle: initial denaturing, 98 °C, 1 min; denaturing at 98 °C, 15 secs, annealing at 56 °C, 15 secs, extension at 72 °C, 15 secs, repeat 27 times. Amplicons were confirmed via gel electrophoresis after each PCR run. Amplicons were shipped to Eurofins Genomics (Eurofins Genomics, Louisville, KY) for Sanger sequencing.

For all other taxa, I downloaded these sequences from NCBI. Most taxa had all three genes available, but some were missing one gene (Table 3). All together, these sequences were aligned in Geneious Prime v.2025.0.2, using the MUSCLE algorithm (Edgar 2004). Sequences were then visually inspected, and ends were trimmed so as to have as much overlap between species. Alignment lengths for *matK, rbcL,* and *ITS* were 336 b.p., 400 b.p., and 477 b.p., respectively. With these alignments, I inferred gene trees using RAxML v.8.2.12 (Stamatakis 2014) using the GTRCAT model (-m GTRCAT) and the automatic bootstrapping criteria (-N autoMRE). Finally, a species tree including the newly sequenced taxa was estimated from these gene trees using ASTRAL-IV v.1.19.4.6 (Zhang et al. 2018), specifying *Idesia polycarpa* as the outgroup, but otherwise using default arguments. One species for which I sequenced barcodes for, *P. simaroa*, was nested in *Populus* subgenus *Eupopulus*, directly contradicting the original description of this species which placed it in section *Populus* (Rzedowski 1975). Due to this biological discrepancy combined with the knowledge of the limitations of three-gene phylogenies in these genera, *P. simaroa* was removed from phylogenetic analyses, but its chemistry is still reported for clarity. All other taxa were biologically plausible in their placement in the phylogeny. I only used this species tree to help guide the placement of the newly sequenced taxa, and I did not use this estimated species tree otherwise, as I recognize the hundreds of genes or thousands of SNPs from Sanderson et al. (2023), Ogutcen et al. (2024), and

Marinček et al. (2024) were large advances in resolving topological questions over this few gene approach. This resulted in the final topologies used for estimating trait evolution of salicinoids.

I calibrated using average pairwise genetic distances as calculated from the gene trees. This was done in Julia v.1.11.4 (Bezanson et al. 2017) using the PhyloNetworks v.1.0.0 and PhyloTraits v.1.1.0 packages (Solís-Lemus et al. 2017; Bastide et al. 2018) available as part of the JuliaPhylo package ecosystem. Code was repurposed from the "Comparative methods on networks" workshop tutorials (https://cecileane.github.io/networkPCM-workshop/topic1-netcalibration.html).

Chemical analysis

Leaves were pooled by individual, and dried samples were ground in a ball mill with stainless steel ball bearings. Ten mg of dry tissue was extracted with 1 mL methanol, sonicated at 4 °C for 30 minutes, centrifuged at 20,627 x *g* for 10 minutes, and a 200 µL aliquot was transferred to autosampler vials with a glass insert. Extracts were stored in an autosampler chamber kept at 7 °C prior to injection on the ultra-high-performance-liquid-chromatography (UHPLC) mass spectrometry (MS) system. UHPLC-MS-MS was conducted using an Acquity C18 HSS column (2.1 mm x 100 mm, 1.8 µm, Waters Corporation Milford, Massachusetts, US) inline on a Vanquish UHPLC system coupled to a QExactive Orbitrap mass spectrometer via a HESI-II electrospray probe (Thermo Fisher Scientific Inc., Waltham, Massachusetts, US). A flow rate of 0.5 ml/minute was used with LCMS-grade water with 0.1% formic acid as mobile phase A and LCMS-grade acetonitrile with 0.1% formic acid used as mobile phase B. The elution gradient was as follows: 0 – 18 minutes, 0.1% B to 100% B; 18.01 – 21 minutes, hold at 100% B; 21.01-21.5 minutes, 100% to 0.1% B; 21.51 – 27 minutes, hold at 0.1% B. Mass spectrometry fragmentation data was collected in the negative ionization mode using data-dependent

acquisition was used to collect full-scan chromatograms and fragmentation patterns for ions of interest simultaneously, with normalized stepped collision energy set to 15, 25, and 40 (arbitrary units).

Salicinoid identification

Chromatograms were exhaustively searched for salicinoids using the list of real and theoretical salicinoids (Keefover-Ring et al. 2014) as well as salicinoid-like compounds reported in *Idesia polycarpa* (Feistel et al. 2017). Extracted ion chromatograms were generated for each putative salicinoid deprotonated $[M-H]^-$ ion and formate adduct $[M+FA-H]^-$ ion to search for compounds. Additionally, the MS2 chromatograms were filtered by common fragments of salicinoids, including sulfate from sulfonated salicinoids, to identify candidate retention times for lower-abundance isomers. Retention times of potential salicinoids were recorded and used with *m/z* values of both the $[M-H]^-$ ion and the $[M+FA-H]^-$ adduct ion of each salicinoids to build a targeted feature detection list, which was then used for the targeted feature detection module in Mzmine version 4.5.37 (Schmid et al. 2023). This module allows all fragmentation spectra for each salicinoid in each sample to be viewed consecutively and compared against a consensus spectra, allowing for high-throughput filtering of false-positive salicinoids. Each fragmentation spectra was examined for ions which would correspond to moieties of the candidate salicinoid, and possible rearrangements of those ions following fragmentation. Following filtering, a processing method was built in Xcalibur version 4.4.16.14 (Thermo Scientific) for integration of salicinoid peak areas. Xcalibur allows for the tuning of parameters for each individual feature of interest, and is thus a powerful software for targeted peak integration, although some salicinoids (such as the two isomers of salicortin) required manual integration due to differences in elution time of a few seconds which were unable to be consistently resolved.

Statistical analyses

All statistical analyses were done in the R environment (R Core Team 2025), unless otherwise stated. In *Populus* and *Salix*, intraspecific variation in total salicinoid content is large, and can range between one percent and 20 percent of a leaf's dry mass for an individual species, with some cases of 30%, regardless of the diversity of salicinoids produced (Donaldson et al. 2006; Lencioni et al. 2024; Chapter 2). To account for possible quantitative variation that might obscure patterns of salicinoid diversity, salicinoid areas were normalized within each sample to their relative abundance to the area of the most-abundant salicinoid in that sample, with the assumption that even though total quantity of salicinoids can vary between individuals of a given species, the relative abundances or ratios of those salicinoids to each other do not vary within a chemotype (Keefover-Ring et al. 2014; Chapter 2).

Using the relative abundance data, sample dissimilarity matrices were calculated in two ways using the R package *chemodiv* (Petrén et al. 2023). The first, Generalized Unique Fraction dissimilarity, is calculated by first transforming a dissimilarity matrix into a dendrogram using the UPGMA method, and then for each pair of samples, the fraction of the total branch length of the dendrogram that leads to compounds present in either sample, but not both samples, is quantified, and then that value is combined with information about the relative abundances of compounds in each sample (Chen et al. 2012, Petrén et al. 2023). For this procedure, a moiety dissimilarity matrix was constructed using the same GenUniFrac technique. First, the SMILES code for each moiety found on detected salicinoids was used with the 'compDis' function in *chemodiv*. Additionally, a "moiety abundance" table was built, whereby the number of specific moieties for a specific salicinoid was recorded. For example, HCH-salicortin, which consists of a glucose, salirepol, and HCH moiety had a '1' recorded in the columns for glucose and salirepol, a

‘2’ for HCH, and a ‘0’ for all other moieties. This moiety dissimilarity matrix was used in conjunction with the moiety abundance table and the ‘sampDis()’ function from the *chemodiv* package to generate a salicinoid dissimilarity matrix, in which isomers of one salicinoid have equal dissimilarities with all other salicinoids, while acknowledging that the true conformation of many of these salicinoid isomers is unknown. This approach differs from chemical structural similarity (CSS; Sedio et al. 2017) or spec2vec (Huber et al. 2021) dissimilarity matrices built from fragmentation patterns, which have been used in other studies of chemical diversity in plants (Sedio et al. 2017; Holmes et al. 2025), but was chosen over those two methods because of the specificity of this analysis and somewhat inconsistent fragmentation patterns of structurally-similar salicinoids. Thus, the CSS or spec2vec method would record those compounds as more dissimilar than they actually are.

The salicinoid dissimilarity matrix was then used in conjunction with the table of salicinoid relative abundances for each sample to generate a sample GenUniFrac dissimilarity matrix using the ‘sampDis’ function from the R package *chemodiv* with the α set to 0.5 to give equal weight to rare and abundant branches. This dissimilarity matrix accounts for structural dissimilarity (or similarity) between samples, that is, how dissimilar are the overall salicinoid arsenals between two samples. A Bray-Curtis dissimilarity matrix (Bray & Curtis 1957) was also constructed using the ‘sampDis’ function from the R package *chemodiv* with the salicinoid relative abundance table. Bray-Curtis dissimilarities are calculated using the presence/absence and relative abundance of variables in samples, commonly species in communities, or in this case, chemicals in a leaf. Structural dissimilarity is not accounted for in Bray-Curtis dissimilarities, thus, in this context the Bray-Curtis dissimilarity matrix can be thought of as measuring the biosynthetic differences between salicinoid arsenals, in that isomer A and isomer

B are unique chemical compounds and could arise from slightly different biosynthetic pathways, while GenUniFrac dissimilarities would treat those isomers as structurally, and thus tentatively functionally, the same, given their mode of action (Pentzold et al. 2014).

Both regular Hill Diversity and Functional Hill Diversity were calculated for the salicinoids in each sample using the relative abundance of each salicinoid as well as the salicinoid compound dissimilarity matrix for the latter calculation. A diversity order of q = 1 was used for both indices, which weighs the salicinoids in proportion of their abundances in the sample. The Hill Diversity number can be interpreted as the effective number of typical salicinoids in a sample, while Functional Hill Diversity, which incorporates pairwise distances between salicinoids, can be interpreted as the number of functional entities in a sample (Chao et al. 2014; Petrén et al. 2024). These calculations were performed using the 'calcDiv' function *chemodiv*, and were repeated for the moieties in each sample using the moiety compound dissimilarity matrix as well as an abundance table for moieties in each sample generated by multiplying the salicinoid abundances in each sample by the moiety components of those salicinoids. These diversity metrics were visualized by broad taxonomic groupings of the samples, such that there are six groups: *Idesia polycarpa*, *Populus* sect. *Abaso* (*P. mexicana*), *Populus* sect. *Populus* (the aspens and some poplars), *Populus* subgen. *Eupopulus* (the cottonwoods and some poplars), *Salix* subgen. *Salix sensu lato* (broadly, the tree willows), and *Salix* subgen. *Chamaetia*/*Vetrix* (broadly, the shrub willows). The two *Salix* groupings are outlined in Ogutcen et al. (2024), and represent traditional classifications that have moderate molecular support, though both are polyphyletic groupings and remain to be resolved (Sanderson et al. 2023; Marinček et al. 2024). I used an ANOVA to determine if there were differences in diversity metrics between these groups, and followed up a significant result using Tukey's HSD.

Both GenUniFrac and Bray-Curtis dissimilarity matrices were used to generate non-metric dimensional scaling (NMDS) ordinations using the function 'metaMDS' from the package *vegan*. The elbow method was used to determine the number of dimensions to use to minimize stress. The function 'hclust' from the package *stats* was used to convert the dissimilarity matrices into dendrograms using the "ward.D2" method (Ward 1963; Murtagh & Legendre 2014), and then the elbow method was once again used to determine the number of clusters, and then clusters were visualized using the *ggplot2* package, with *I. polycarpa* assigned its own cluster for visualization.

To elucidate the degree to which certain salicinoids contributed to dissimilarity between samples, I used a SIMPER analysis (Clarke 1993) which sequentially removes a trait from the calculation of a Bray-Curtis dissimilarity index between samples *i* and *j* to determine the contribution of that individual trait to the overall dissimilarity between samples. This analysis was conducted on only the *Populus* and *Salix* samples, as inclusion of *I. polycarpa* would inflate the contribution to dissimilarity of any salicinoid not found in *I. polycarpa*. The top 20 salicinoids ranked by contribution to dissimilarity between samples were then passively overlayed on both NMDS ordinations using the 'env.fit' function from the package *vegan*.

Trait optima shift estimation using 'l1ou'

To detect evolutionary shifts in salicinoids along the branches of the phylogenies, I use the R package *ℓ1ou*, which applies the lasso method (Tibshirani 1996) to phylogenetic data to estimate shifts in trait optima under an Ornstein-Uhlenbeck (OU) process, where traits are under selection in an adaptive environment and thus their optima should be centered around an adaptive peak (Khabbazian et al. 2016). Under an OU model, there should be a certain composition of salicinoids (a chemotype) that are the optimal arsenal for a species in its

environment due to the costs or benefits of producing that salicinoid chemotype. If a shift in salicinoid optima is detected along the branch of the phylogenetic tree, then that suggests that a new salicinoid chemotype is favored over the ancestral salicinoid chemotype in that branches' environment, either due to the cost or benefit of producing that chemotype, or due to Brownian Motion (BM) in the event that the rate of adaptation is approximately zero, which would reduce the OU process to BM, or the null model (Khabbazian et al. 2016). I use a few different but complementary approaches with this method, as salicinoids are subject to various selection pressures, and using multiple approaches thus should make the detection of shifts in optima more robust. For each of the models I generate here, I use the 'estimate_shift_configuration' function from *ℓ1ou* with the information criterion parameter set to "AICc" (Akaike information criterion, with a correction factor for small sample sizes) or "pBIC" (phylogenetic Bayesian information criterion). AICc is, in general, a more liberal information criterion for model selection (detecting more false-positive shifts) in *l1ou*, while pBIC, which expands traditional BIC to be phylogenetically-aware, tends to be more conservative (more likely to detect the true shifts), though there are instances when one might be preferred over the other (Khabbazian et al. 2016). I conduct partially-parametric bootstrapping on each model using the 'l1ou_bootstrap_support' function from *ℓ1ou* with 100 iterations and the pBIC criterion. This bootstrapping method is conservative, as only the shifts that are detected in the original model are able to receive high bootstrap support, and undetected shifts will thus have very low support and contribute to a large residual during the bootstrapping procedure (Khabbazian et al. 2016). Thus, there are instances when AICc or pBIC might be favored in the initial model selection procedure, as one might estimate a greater number or more reasonable shifts in trait optima given the data used than the other would, and then those shifts would be subject to bootstrapping to provide a level of

confidence in those shifts. I only use pBIC as the criterion in the bootstrapping procedure due to its conservative nature, but detail my choices in using AICc or pBIC for initial model selection in the results section.

The first model generated uses species' mean positions on the NMDS axes of the GenUniFrac ordination as the input trait data. This ordination captures the structural, and thus theoretically functional, similarity between samples based on all salicinoid in each sample, providing insight into ecological selection pressures on salicinoid diversity through evolutionary time when used in a *ℓ1ou* model. The second model generated uses species' mean positions on the NMDS axes of the Bray-Curtis ordination as the input trait data. This ordination captures the similarity in salicinoid arsenals of each species according to the true identity of each salicinoid, and ignores structural similarity between salicinoids, thus accounting for possible biosynthetic differences or similarities between samples, providing insight into the biosynthetic mechanisms influencing changes in salicinoid diversity through evolutionary time when used in a *ℓ1ou* model. The third model generated uses the relative abundance of the twenty salicinoids that contribute the most to dissimilarity between samples calculated from the SIMPER analysis, in addition to salirepin, idescarpin A, and homaloside D, which are the salicinoids found in *Idesia polycarpa*. These salicinoids all contributed at least 0.5% to the dissimilarity between samples, and are often the most abundant salicinoids in the individuals that produce them, suggesting that these salicinoids are the most biologically-relevant salicinoids in the species they are found in, as their high concentrations are likely the result of selection pressures. The fourth model generated uses the relative abundance of salicinoids which are present at at least five percent relative abundance in any one species, increasing the visibility of some taxonomically-rarer salicinoids for the model-selection step that otherwise might be undetected, and which might not contribute

much to overall dissimilarity between samples in the SIMPER analysis because of their taxonomic rarity. This model can be considered a relaxed, more liberal version of the third model, incorporating relative abundance data of many more salicinoids to provide a fuller picture of the arsenal of biologically-relevant salicinoids in each species.

Results

Phylogeny construction

Four possible phylogenies were constructed (Fig. 2). Most of the topology between phylogenies was stable, with two exceptions in *Salix*, resulting in the four possible combinations of topology. First, *Salix amygdaloides* could either be sister to *Salix nigra* (Fig. 2a, b) as it is in Sanderson et al. (2023), or *S. amygdaloides* could be sister to the clade of *S. alba*, and *S. serissima* (Fig. 2c, d), as it is in Ogutcen et al. (2024). The second involves a few species and represents a discrepancy between Ogutcen et al. (2024) and Marinček et al. (2024), although because Marinček et al. (2024) has better subsampling of *Salix* subgen. *Vetrix*, their topology might be favored over that of Ogutcen et al. (2024) (Martin Volf, personal communication). In Marinček et al. (2024), there is a clade formed by *S. discolor, S. humilis, S. candida, S. myricoides,* and *S. eriocephala*, of which I have added *S. irrorata* sister to *S. eriocephala* and *S. myricoides* due to *S. irrorata* having identical sequences (except for one SNP) to *S. lasiolepis* on NCBI, and *S. lasiolepis* being distantly sister to *S. eriocephala* and *S. myricoides* in Ogutcen et al. (2024) (Fig 2a, c). This clade is broken up in Ogutcen et al. (2024) and a clade of *S. irrorata, S. eriocephala, and S. myricoides* is placed sister to *S. hastata*, while a new clade is formed by placing *S. discolor* sister to a clade of *S. humilis* and *S. candida,* which is then placed sister to the clade of *S. bebbiana, S. cinerea, S. caprea,* and *S. appendiculata* (Fig. 2b, d). Based on information from the discussions of Sanderson et al. (2023), Marinček et al. (2024), and Ogutcen

et al. (2024), I used the phylogeny which included the topology of *S. amygdaloides* sister to *S. nigra* as well as the placement of *Salix* species in Marinček et al. (2024) for my primary analyses, which I present here (Fig. 2a, 3). I refer to traditional sections and subgenera within *Populus* and *Salix* (Fig. 3) when discussing chemical results of specific groups in the phylogeny, though these groupings do not always reflect true clades. While most of the results I discuss are based on the analyses of that topology, I also present some results from the topology that has *S. amygdaloides* sister to *S. nigra*, and the placement of *Salix* species in Ogutcen et al. (2024), which I refer to as "Ogutcen A" (Fig. 2b), though many are consistent between the topologies.

Salicinoid detection

A total of 119 salicinoids were detected in 140 samples across 53 species (Tables 4, 5; Figs. 1, 4). When multiple putative isomers of a salicinoid were found, they were assigned a letter in alphabetic order corresponding to the order of their retention time. Richness of detected salicinoids ranged from 42 to 107 compounds in a sample, but decreased to a range from six to 43 when only considering salicinoids of at least 1% relative abundance in a sample. Salicinoid Hill Diversity, the effective number of salicinoids in a sample, ranged from 2.94 to 20.69 with a mean of 7.95 and a median of 6.8, while Functional Hill Diversity, the effective number of functionally distinct (Chao et al. 2014) salicinoids, ranged from 2.59 to 159.37, with a mean of 29 and a median of 17.74. ANOVA results demonstrate there is a difference in Hill Diversity ($F_{5,135} = 17.41$, $p < 0.001$, Fig. 5a) and Functional Hill Diversity ($F_{5, 135} = 14.47$, $p < 0.001$, Fig. 5b) between taxonomic groups, as while *Idesia polycarpa* did not differ in diversity from any *Populus* or *Salix* group, *Populus* subgen. *Eupopulus* and *Salix* subgen. *Salix s.l.* had twice the salicinoid diversity of *Populus* sect. *Populus* and *Salix* subgen. *Chamaetia*/*Vetrix,* while *Populus*

sect. *Abaso* had comparable salicinoid diversity with the latter two groups as well as with *Salix* subgen. *Salix s.l.* (Fig. 5a, b).

Moiety Hill Diversity, the effective number of moieties in a sample, ranged from 2.61 to 6.34, with a mean of 4.61 and a median of 4.53, while Functional Hill Diversity, the effective number of functionally distinct moieties in a sample, ranged from 3.89 to 25.60, with a mean of 11.96 and a median of 11.1. ANOVA results demonstrate differences in moiety Hill Diversity ($F_{5, 135} = 47.48$, $p < 0.001$, Fig. 5c) and Functional Hill Diversity ($F_{5, 135} = 35.79$, $p < 0.001$, Fig. 5d) between taxonomic groups, as *Idesia polycarpa* had the greatest moiety diversity metrics while *Populus* subgen. *Eupopulus* had three-quarters the moiety diversity of *I. polycarpa* but greater moiety diversity than the rest of *Populus* and *Salix* (Fig. 5c, d). *Salix* subgen. *Chamaetia*/*Vetrix* had lower moiety Hill Diversity than all taxonomic groups (Fig. 5c), but comparable Functional Hill Diversity to *Populus* sect. *Abaso* and *Populus* sect. *Populus* (Fig. 5d). *Salix* subgen. *Salix s.l.* had comparable moiety Hill Diversity with *Populus* sect. *Abaso* and *Populus* sect. *Populus* (Fig. 5c), but greater Functional Hill Diversity than *Populus* sect. *Populus* and *Salix* subgen. *Chamaetia*/*Vetrix*, although Functional Hill Diversity did not differ from that of *Populus* sect. *Abaso* (Fig. 5d).

Non-metric dimensional scaling ordinations of salicinoids

For both the GenUniFrac (functional dissimilarity between samples, Fig. 6) and Bray-Curtis (biosynthetic dissimilarity between samples, Fig. 7) NMDS ordinations, four dimensions were used as they were the minimum set of dimensions which resulted in stress lower than 0.10. For both ordinations, three clusters were identified, the first of which consisted mostly of samples which produce tremuloidin-B, salicortin-B and tremulacin-A; the second of which consisted mostly of samples which produce salicortin-A and HCH-salicortin-A, with some

acetylsalicortin-A and lasiandrin-A; the final cluster consisted of samples which have reduced or no levels of tremulacin-A or salicortin-B, and instead have elevated levels of salicin, acetylsalicin-A, and/or diglucoside-salicin-C. Notably, cluster one in both ordinations consisted of a relatively even mix of both *Populus* and *Salix*, while cluster two was mostly *Populus* and cluster three was mostly *Salix*, with clusters two and three being closer to monogeneric in the Bray-Curtis ordination (Fig. 7) than in the GenUniFrac ordination (Fig. 6). The SIMPER analysis (Fig. 8) showed the salicinoids which contribute the most to Bray-Curtis dissimilarity are tremulacin-A (8%), salicortin-B (7%), HCH-salicortin-A (5%), salicin (5%), salicin-7-sulfate (4%), diglucoside-salicin-C (3.5%), salicortin-A (3%), deltoidin-A (nigracin) (2.2%), tremuloidin-B (2%), acetylsalicortin-A (1.9%), deltoidin-B (1%), and lasiandrin-A (1%). All other salicinoids contributed less than one percent to Bray-Curtis dissimilarity between samples (Fig. 8).

Shifts in salicinoid optima

The *ℓ1ou* + pBIC model using the "Marinček A" topology (Fig. 2a) conducted on the four axes of the GenUniFrac NMDS detected 12 shifts in salicinoid structural optima, with two of those shifts receiving no bootstrap support, three receiving moderate support, and the rest receiving high support (Fig. 9). Shifts for entire clades were detected at the root of *Populus* subgenus. *Eupopulus* with 64% bootstrap support (characterized by shifts in NMDS axes 1, 2, and 3) and at the root of the *S. pentandra, S. alba,* and *S. serissima* clade with 62% support (characterized by shifts in NMDS axes 2 and 3). The other shifts are scattered throughout the *Salix* phylogeny on edges leading to single taxa (Fig. 9). When this model was run on the "Ogutcen A" topology (Fig. 2b) similar results were found (Fig. 10).

The initial *ℓ1ou* + pBIC model using the "Marinček A" topology (Fig. 2a) conducted on the four axes of the Bray-Curtis NMDS did not detect any shifts in *Populus*, which is contrary to my expectations given the clustering of the NMDS and the differences in individual salicinoid relative abundances within the genus. Following the suggestions from Khabbazian et al. (2016) I re-ran the model with the more liberal AICc criterion, which did detect a shift, and then used the conservative pBIC criterion during the bootstrapping procedure. The *ℓ1ou* + AICc model detected nine shifts in salicinoid optima, with three shifts receiving moderate pBIC bootstrap support, and the rest receiving relatively high support (Fig. 11). Shifts for entire clades were detected at the root of the *Salix* and *Populus* clade (100% support, characterized by shifts in NMDS axes 1 and 3), at the root of *Populus* subgenus *Eupopulus* (40% support, characterized by shifts in NMDS axes 2 and 4), and at the root of the *S. pentandra*, *S. alba*, and *S. serissima* clade (68% support, characterized by shifts in NMDS axis 4). All other detected shifts were scattered throughout the *Salix* phylogeny on edges leading to single taxa (Fig. 11). When this model was run on the "Ogutcen A" topology using the AICc criterion, there were no shifts detected in *Populus* and only 6 shifts overall, so it was run using pBIC and detected 16 shifts, many of which were similar to the *ℓ1ou* + AICc model on "Marinček A", such as the shift at the root of *Populus* and *Salix* (100% support, characterized by shifts in NMDS 1, 2, and 3) and the shift at the root of the of the *S. pentandra*, *S. alba*, and *S. serissima* clade (81% support, characterized by shifts in NMDS 1 and 4) but there were also a few differences (Fig. 12). First, there was no longer a shift detected at the root of *Populus* subgenus *Eupopulus*, and instead shifts at the root of the *P. deltoides* and *P. fremontii* clade (94% support) and on the branch leading to *P. maximowizcii* (97% support) were found, both characterized by shifts in NMDS1 and NMDS 2 (Fig. 12). Additionally, a shift at the root leading to the clade of *S. bebbiana*, *S. cinerea*, *S.*

appendiculata, and *S. caprea* was detected (70% bootstrap support, characterized by shifts in NMDS 1 and 2) which had not been detected in any of the other models. The rest of the shifts were scattered throughout the *Salix* phylogeny, though there were more shifts detected for the Bray-Curtis NMDS under "Ogutcen A" than "Marinček A" (Fig. 12).

The *ℓ1ou* + pBIC model using the "Marinček A" topology (Fig. 2a) for the top 20 salicinoids which contribute to dissimilarity between samples calculated by SIMPER (Fig. 8), plus salirepin, idescarpin-A, and homaloside-D-1, detected 16 shifts in salicinoid optima, with all shifts receiving high bootstrap support (Fig. 13). Shifts for entire clades were detected at the root of the *Salix* and *Populus* clade (100% support, characterized by a shift from salirepin, idescarpin-A, and homaloside-D-1 to salicin, salicortin-B, tremuloidin-B, and tremulacin-A, among other salicinoids), at the root of the *P. deltoides* and *P. fremontii* clade (87% support, characterized by HCH-salicortin, salicortin-B, salicin-7-sulfate, salicortin-7-sulfate, grandidentoside-A, populoside-A-F, and a lack of tremuloidin-B and tremulacin-A), and at the root of the *S. pentandra*, *S. alba*, and *S. serissima* clade (85% support, a shift to the acetylated salicinoids and a lack of tremuloidin-B and tremulacin-A). The rest of the detected shifts were on edges leading to single taxa, with all seven of the shifts in *Populus* occurring in subgenus *Eupopulus*, and all six of the shifts in *Salix* scattered throughout that genus (Fig. 13). When this model was run using the "Ogutcen A" topology there were very similar results, with 18 shifts detected, including one at the root of *Populus* and *Salix*, one at the root of the *P. deltoides* and *P. fremontii* clade, and one at the root of the *S. pentandra, S. alba*, and *S. serissima* clade (Fig. 14).

The *ℓ1ou* + pBIC model using the "Marinček A" topology (Fig. 2a) for salicinoids which were at least 5% relative abundance in any sample detected 23 shifts in salicinoid optima, with a mix of high and low bootstrap support (Fig. 15). Shifts for entire clades were detected at the root

of the *Populus* and *Salix* clade (100% support, characterized by a shift from salirepin, idescarpin, and homaloside-D-1 to salicin, salicortin-B, tremuloidin-B, and tremulacin-A), at the root of *Populus* subgenus *Eupopulus* (11% support, characterized by a shift from tremuloidin-B and tremulacin-A to salicortin-A and HCH-salicortin-A), at the parent node of all of subgenus *Eupopulus* excluding *P. heterophylla* (8% support) at the root of the *P. deltoides* and *P. fremontii* clade (78% support, characterized by many grandidentosides and populosides), at the root of the *P. balsamifera* and *P. trichocarpa* clade (30% support, characterized by deltoidin-B and greater amounts of tremuloidin-B and tremulacin-A), and at the root of the *S. pentandra*, *S. alba*, and *S. serissima* clade (19% support, characterized by acetylated salicinoids and a lack of tremuloidin-B and tremulacin-A). The rest of the detected shifts were on edges leading to single taxa, with five of those shifts occurring in *Populus*, and 12 of those shifts occurring in *Salix* (Fig. 15). This model was run again using the "Ogutcen A" topology (Fig. 2b) and returned mostly similar results, detecting 21 shifts, however it did not detect the shift in salicinoid optima which were detected by the "Marinček A" topology at the parent branch of *Populus* subgenus *Eupopulus* and at the parent branch of all of *Populus* subgenus *Eupopulus* without *P. heterophylla*, as well as the shift at the parent branch of the *P. balsamifera* and *P. trichocarpa* clade (Fig. 16).

Discussion

Plant defensive chemistry is a key mediator of plant-organism interactions, which dictate the flow of energy from the sun to a substantial amount of life on earth. Thus, the nature of plant defensive chemistry has intrigued researchers for decades, leading to many hypotheses about how it has evolved, and the identification of study systems in which to test those hypotheses. One such system are the salicinoids, which are a diverse ecologically-important class of anti-herbivore chemical defenses in the Salicaceae genera *Populus* and *Salix*, and can represent

considerable carbon investment for individual plants (Donaldson et al. 2006; Chapter 2). Yet, even with the intense amount of work on this class of compounds (Boeckler et al. 2011 and references therein), it is unknown how salicinoids evolved and why their composition can vary so much between species. Here, I investigated the diversity of salicinoids in 52 species of *Populus*, *Salix*, and in *Idesia polycarpa*, and for the first time in both *Populus* and *Salix*, examine their patterns in a phylogenetic context (but see Volf et al. 2015; Volf et al. 2023 for a subset of *Salix*). From my findings, I estimate that the ancestral salicinoid chemotype is *tremuloides*-like (i.e. salicinoid chemistry similar to *P. tremuloides*, Lindroth et al. 1987), and consists of high relative abundances of salicortin-B and tremulacin-A, with lower levels of salicin, tremuloidin-B, and salicin-7-sulfate. The evolution of this chemotype from the arsenal of the shared *Idesia*-*Populus*-*Salix* ancestor (which I refer to here as the "salirepinoids," a subclass of salicinoids with a salirepin core, to distinguish them from the salicinoids of *Populus* and *Salix*) likely did not result in a large ecologically-functional difference between the ancestor of *Idesia* and that of *Populus/Salix*, as the salicinoids of the *tremuloides*-like chemotype (salicin, tremuloidin-B, salicortin-B, and tremulacin-A) differ structurally from the salirepinoids of *Idesia* by only a single hydroxyl group on the "phenolic" moiety of the phenolic glycoside. This small structural difference might be why the *ℓ1ou* + pBIC model of functional structural dissimilarity (Fig. 9) did not detect a shift at the root of the *Populus/Salix* clade, while all three other models, which depend on the structural identity of individual salicinoids, did (Figs. 11, 13, 15). The nature of this shift is likely characteristic of the rest of the shifts in salicinoids in these genera, where mutations occur to alter the end products of a biosynthetic grid, rather than mutations occurring and creating novel compounds that are then selected for by antagonists.

Across all four *ℓ1ou* models run using the "Marinček A" topology (Fig. 2a), only five clades had detected shifts in salicinoid optima: a shift at the root of *Populus* and *Salix* (detected in three of four models, Figs. 11, 13, 15; characterized by a switch from the salirepinoid-based defenses to a salicinoid-based defense, particularly salicin, salicortin-B, tremuloidin-B, and tremulacin-A), a shift at the root of *Populus* subgenus *Eupopulus* (detected in three of four models, Figs. 9, 11, 15; a switch from the *tremuloides*-like chemotype to a defense arsenal characterized by salicortin-A, HCH-salicortin, as well as additional iterations on salicinoid structures such as populosides), a shift at the root of the *Salix pentandra, S. alba,* and *S. serissima* clade (hereafter referred to as the acetyl-clade, detected in all models, Figs. 9, 11, 13, 15; a switch to an acetylated-salicinoid chemotype characterized by acetylsalicin-B, acetylsalicortin-A, and lasiandrin-A), a shift at the root of the *P. deltoides* and *P. fremontii* clade (only when relative abundances of individual salicinoids were used, detected in two of four models, Figs. 13, 15; A diversity of salicinoids are in this clade, including many grandidentosides and populosides), and a shift at the root of the *P. balsamifera* and *P. trichocarpa* clade (detected in one of four models, Fig. 15; characterized by a lower diversity of salicinoids compared to the rest of the subgenus). One more shift was detected in one of the four models run on "Ogutcen A" at the parent branch of the clade including *S. bebbiana, S. cinerea*, *S. appendiculata*, and *S. caprea*, driven by a reduction in salicinoid diversity and production of simple salicinoids such as salicin, acetylsalicin-A, and diglucoside-salicin-C, although *S. caprea* produces a *tremuloides*-like salicinoid chemotype with diglucoside-salicin C (Figs. 4, 12). The rest of the shifts detected were on edges leading to single taxa, highlighting what appears to be independent evolution of salicinoids across the phylogeny. Many of these single shifts were accompanied by the presence of the same salicinoids, suggesting that there might be a predisposition to certain mutations or

combinations of mutations in biosynthetic pathways leading to the evolution of the same compound independently throughout the phylogeny. For example, the salicinoid diglucoside-salicin-C is not restricted to a single species of *Salix*, but is produced intermittently across the genus, each time accompanied by a loss or reduction of tremulacin-A and occasionally salicortin-B. Similarly, HCH-salicortin is produced by many species in both *Populus* and *Salix*, though its relative abundance tends to be greater when accompanied by salicortin-A (Figs. 4, 15). The lack of a clear pattern for many salicinoids points to the complexity of salicinoid biosynthesis, and why determining these mechanisms have eluded researchers for so long (Ruuhola & Julkunen-Tiito 2003; Babst et al. 2010; Chedgy et al. 2015; Fellenberg et al. 2020; Gordon et al. 2022).

The detection of a few shifts in salicinoid optima in the ancestors of certain clades of *Populus* and *Salix*, in combination with the salicinoids those clades produce, does suggest that there are instances where mutations modifying the salicinoid grid at the root of clades that enable further diversification of salicinoids or maintain certain innovations in the descendants of those ancestors. For example, the shift in salicinoid optima detected at the root of *Populus* subgenus *Eupopulus* (Figs. 9, 11, 15) is followed by numerous shifts on daughter edges of that root when individual salicinoids are used as traits in models (Figs. 13, 15) and trait data show there is a departure from the ancestral tremulacin-based chemotypes in many of the taxa in subgen. *Eupopulus*, which instead produce a great diversity of salicinoids (Fig. 5). This shift could indicate that the regulatory mechanisms for tremulacin were altered and began to make other salicinoids, such as salicortin-A and HCH-salicortin-A, and then those mechanisms might have been altered further, resulting in the diversity of salicinoids in the rest of the subgenus. In the only model where a shift wasn't detected at the root of *Eupopulus* (the model conducted on the top 20 SIMPER salicinoids, Fig. 13) all eight detected shifts in salicinoid optima in *Populus* all

occur within the subgenus, suggesting that even if the shift at the root of *Eupopulus* is a false-positive in the models it is detected in, there are still shifts in the salicinoid arsenals in the majority of the species in the subgenus, pointing to some underlying mechanism of salicinoid diversity in the subgenus.

The other major shift in optima at a parent edge is for the clade consisting of *S. pentandra*, *S. alba*, and *S. serissima*, which is detected in all four models. These species, in addition to *S. interior,* which received strong support for a shift on its edge, produce higher levels of the acetylated salicinoids acetylsalicin-B, acetylsalicortin-A, and lasiandrin-A (HCH-acetylsalicortin) than most other salicinoids. Notably, the high levels of acetylsalicortin-A in *S. pentandra*, *S. serissima*, and *S. interior* are accompanied by higher levels of acetylsalicin-B than acetylsalicin-A, while other species producing acetylated salicinoids tend to produce more acetylsalicin-A than acetylsalicin-B. The elevated levels of acetylsalicin-B could be attributed to degradation of acetylsalicortin-A or lasiandrin, but then I would expect more acetylsalicin-B in other lasiandrin and acetylsalicortin-A producing species, such as *S. acutifolia, S. hastata, P. heterophylla*, and *P. tremula* (Figs. 4, 13, 15), but this does not appear to be the case, and thus it is unlikely to be solely degradation-related. Regardless, there appears to be some mechanism which has enabled high levels of acetylated salicinoids in this group (the clade of *S. pentandra*, *S. alba*, *S. serissima*, plus *S. interior*).

My data also suggest that differences in salicinoid arsenals between species are likely to be mostly the result of mutations altering the biosynthetic grid, rather than convergent shifts towards certain optimal combinations of salicinoids as would be expected if there were a truly an adaptive peak for salicinoid combinations due to selective pressures. This could explain why linking levels of herbivory to diversity of salicinoids might be difficult (Volf et al. 2023) as the

two may not be directly related. This points towards an instance where the null model of plant chemical diversity, the Screening Hypothesis (Jones & Firn, 1991; Wetzel & Whitehead, 2020), might be the reason for diversity in a single class of compounds. Especially when considered in the context of salicinoid chemotypes within a single species, which can be divergent in salicinoid composition but still co-occur at the same location (Keefover-Ring et al. 2014; Chapter 1), the idea that salicinoid diversity is the result of mutations and differences in regulatory genes, thus controlled in a bottom-up rather than top-down manner, is not too implausible, but does require further experimentation to be tested.

These results can inform future studies in a few ways. First, the full biosynthetic pathway for salicinoids is unknown, limiting researcher's ability to dissect the evolution of salicinoids in a manner analogous to what the *Arabidopsis* research community has done with glucosinolates (Barco & Clay 2019). Some genes and enzymes have been identified related to the synthesis of the salicinoid precursors benzyl-benzoate and salicyl-benzoate (Chedgy et al. 2015), the addition of the glucose moiety to those precursors (Fellenberg et al. 2020; Kulasekaran et al. 2021), and a sulfotransferase involved in biosynthesis of sulfonated salicinoids (Lackus et al. 2020). These genes, however, affect the production of all salicinoids, and do not appear to be specific to any one compound (Gordon et al. 2022). Without knowledge of more of these genes, we are unable to determine their presence/absence in specific species and locate their position on genomes. Such a capability would allow for inferring patterns and combinations of genes that produce a specific salicinoid arsenal via identifying which species they have evolved or been lost in (de/re-escalation, Lopez-Nieves et al. 2018) and determining the diversity of salicinoids that can be produced from a given combination of genes, therefore directly testing for the putative grid-like biosynthesis of salicinoids, by inserting them into a biochassis (Lackus et al. 2020; Gordon et al.

2022). In particular, searching for genes in the taxa sister to and on branches where shifts in salicinoid optima are detected, or in species with some similar but also contrasting salicinoid arsenals, could be promising directions to start this process.

Second, the Synergy and Interaction Diversity Hypotheses, two alternative hypotheses to the "null" screening hypothesis require knowledge about the efficacy (in this case defensive) of individual or combinations of metabolites against certain antagonists (Wetzel & Whitehead 2020). For salicinoids, known mechanisms of defense are the conversion of the HCH group to a quinone that crosslinks amino acids as well as some synergistic interactions between moieties that reduce growth of predators (Boeckler et al. 2016). However, there have not been bioassays or feeding trials with individual salicinoids outside of salicin, salicortin, tremuloidin, tremulacin, and HCH-salicortin (Lindroth et al. 1988; Boeckler et al. 2016; Schnurrer & Paetz 2023; Schnurrer et al. 2024) and feeding trials were conducted on whole leaves (Feistel et al. 2017) or with crude extracts of all salicinoids in a plant (Mason et al. 2021), so compound-specific information is limited. There are a few instances where producing one salicinoid instead of another can have an inferred fitness advantage, such as the production of HCH-salicortin compared to salicortin or tremulacin, as the former delivers two HCH-moeities per glucose molecule rather than the singular HCH-moeity per glucose molecule delivered by the latter two (Schnurrer & Paetz 2023). Tremulacin modulates this example by also delivering a benzoyl-moiety, which has been demonstrated to improve defense by slowing herbivore growth through synergistic interactions with the other moieties of tremulacin (Boeckler et al. 2016), although explicit comparisons between two units of HCH versus one unit of HCH and one unit of benzoic acid have yet to be performed.

Additionally, there are no known specialists of specific salicinoids, and most Salicaceae specialists appear to be diffuse specialists that depend on the presence of salicinoids in-general, and not specific salicinoids (Volf et al. 2015). However, recent work has shown detailed salicinoid detoxification mechanisms of a few Salicaceae specialist feeding species in the Notodontidae (Lepidoptera) when fed *P. nigra* and the hybrids *P. tremula x tremuloides* and *P. deltoides x trichocarpa* (Schnurrer & Paetz, 2023; Schnurrer et al. 2024). These specialists utilize caffeoylquinic acids produced by *Populus* to conjugate moieties of salicinoids following hydrolysis, effectively pitting two dimensions of their hosts' metabolomes against each other. Caffeoylquinic acids and other hydroxycinnamic acids, in addition to flavonoids (including proanthocyanidins) and salicinoids, are a large component of non-structural phytochemicals in *Populus* (Tsai et al. 2006). The availability of these caffeoylquinic acids in host species of Notodontidae specialists provide an ample supply of detoxification components, and the mechanisms of conjugating them with moieties of hydrolyzed salicinoids could be considered a "generalist" detoxification strategy able to deal with any sort of salicinoid their host might produce, and thus would be applying equal selection pressure on all salicinoids in a chemotype. Further, Schnurrer et al. (2024) reported that the salicylate trichocarpin, structurally related to salicinoids, did not appear to be a suitable substrate for the detoxification enzymes of *Cerura vinula* caterpillars (Notodontidae), suggesting that there is some substrate specificity of these salicinoid detoxification mechanisms, and that there might be a degree of diffuse specialization by salicinoid specialists. If a specialist adapted to a species with low salicinoid richness, such as *P. tremuloides*, performed poorly on salicinoid rich species, such as *P. heterophylla* or *P. tremula,* and analysis of frass and detoxification mechanisms show that salicinoids in the salicinoid-rich species were responsible for the poor performance, there would be evidence that novel

salicinoids could provide some mechanism of escape from herbivory, one half of the "escape-and-radiate" hypothesis. If it is also demonstrated that salicinoid diversity has evolved due to mutations on the biosynthetic grid that result in a non-linear increase in the richness of salicinoids, and some of those new salicinoids confer defense against specialists adapted to a salicinoid-poor species, then there would be evidence for the screening hypothesis (Jones & Firn 1991). Salicinoids shared between the salicinoid-rich and salicinoid-poor species would still be detoxified, and thus could be considered "inactive" against that specialist in the original sense of the screening hypothesis (Jones & Firn 1991), but it would be the individual salicinoids which present an unsuitable substrate for the detoxification mechanisms that would impair the specialist, and should be selected for. At the same time, salicinoids have been shown to be effective against generalists lacking detoxification mechanisms (Boeckler et al. 2016; Feistel et al. 2017). Thus, the mere presence of salicinoids is likely adaptive against the majority of herbivore species, which would maintain biologically-relevant levels of salicinoids which are "inactive" against specialists.

However, some of these recent studies of specialist and generalist adaptations to salicinoids (Feistel et al. 2017; Schnurrer & Paetz 2023; Schnurrer et al. 2024) do not give a detailed report of salicinoid compositions or concentrations in the actual leaves of the species and hybrids the reared specialists on. Furthermore, Schnurrer & Paetz (2023) and Schnurrer et al. (2024) do not present detailed performance data for those insects in the context of varying composition or concentrations of salicinoids, as they were focused on characterizing the salicinoid detoxification mechanisms present in those organisms. While they were successful in their goals, little can be concluded from these studies about possible differences in the host plant chemistry in the context of evolutionary hypotheses. Revisiting their experiments by using

genotypes of Salicaceae species or chemotypes of differing salicinoid composition but equal salicinoid concentrations and measuring performance of specialists of salicinoid-poor and salicinoid-rich species would be a way forward to test the ecological component of the screening hypothesis for the diversification of salicinoids. Yánez-Segovia et al. (2023) do this through their report of both the total quantity of salicinoids and specific salicinoids (salicin, salicortinA/B, tremuloidin-B, HCH-salicortin-A, tremulacin-A) in some hybrid clones in *Populus* subgenus *Eupopulus* that display varying level of resistance to the leaf miner *Leucoptera sinuella* (Lepidoptera: Lyonetiidae), though they found no correlation between levels of any individual salicinoids or total defense and resistance to the miner, suggesting something else is at play in that system and *Leucoptera sinuella* is a diffuse salicinoid specialist, at least on those salicinoids.

Finally, while the present work is the most complete analysis of specific salicinoids in the genera *Populus* and *Salix* to-date, it was conducted on a limited number of species with a limited number of replicates per species. Of course, sampling more species, such as the rest of *Populus* (especially section *Turanga*) and species of *Salix* which are sister to the species which belong to branches where non-clade shifts in optima were detected would increase the resolution of salicinoids and shifts in salicinoids in these genera, and provide more or less support for detected shifts on edges leading to single taxa. Of equal importance, I show in Chapter One, similar to Keefover-Ring et al. (2014) and Keefover-Ring (2022), that sampling species throughout a large geographic area can lead to discovery of new chemotypes in those species. In Chapter 1, of the 290 *P. heterophylla* individuals I assigned chemotypes, 15 of them were *tremuloides*-like while just four of them had a nigracin-tremulacin chemotype, indicative of how rare some chemotypes might be. However, in light of the results I present here in Chapter 3, those 19 individuals represent the presence of the ancestral salicinoid chemotype (or a chemotype very similar to it)

of *Populus* and *Salix* in a species that predominantly produces HCH-salicortin today. Those chemotypes might be undergoing directional selection in that species, or could be the result of mutations in the standard chemotype of that species. Similarly, Keefover-Ring et al. (2014) found *tremuloides*-like chemotypes in *P. tremula* in Sweden in addition to a cinnamoyl, an acetyl, and a cinnamoyl-acetyl chemotype. Of the 102 genotypes sampled, 37% were the *tremuloides*-like chemotype, with a strong trade-off found between tremulacin and salicortin (tremulacin-A and salicortin-B in this study) depending on if individuals were *tremuloides*-like or cinnamoyl chemotypes (Fig. 4 in Keefover-Ring et al. 2014). While still a minority of the genotypes samples, the high proportion of *tremuloides*-like chemotypes in *P. tremula* relative to the proportion of *tremuloides*-like chemotypes in *P. heterophylla* could be a result of *P. tremula* being less phylogenetically-removed from the ancestral chemotype due to its ancestor diverging recently (estimated to be less than 5 mya, Sanderson et al. 2023) from the rest of the *tremuloides*-like producing members of *Populus* section *Populus*, while the ancestor of *P. heterophylla*, which is sister to the rest of *Populus* subgenus *Eupopulus*, is estimated to have diverged from the ancestor of *Populus* section *Populus* between 9mya and 14mya (Sanderson et al. 2023), allowing for more time for mutations to accumulate without hybridization and thus introgression of traits from the ancestors of extant *tremuloides*-like chemotype species in *Populus* section *Populus*. This could aided by the likely wetland habitat of the ancestor of *P. heterophylla* (although ancestral range estimation with climatic variables has yet to be conducted on all members of the genus) which could have prevented hybridization and introgression entirely, or restricted it in one direction, as has been demonstrated in an extant *P. tremula* and *P. alba* system today (Lexer et al. 2005; Fussi et al. 2010). While this is a plausible explanation for the proportions of *tremuloides*-like chemotypes in these two species, until the genetic mechanisms controlling what chemotype

a genotype is this hypothesis will be unable to be truly tested. Regardless, it provides an example of what can be learned from extensive sampling of the chemistry of a species throughout its range. Doing so for the rest of the species I present here would be a daunting task, but could provide further insight into the patterns and mechanisms which resulted in the salicinoid diversity present in extant *Populus* and *Salix*.

Figures

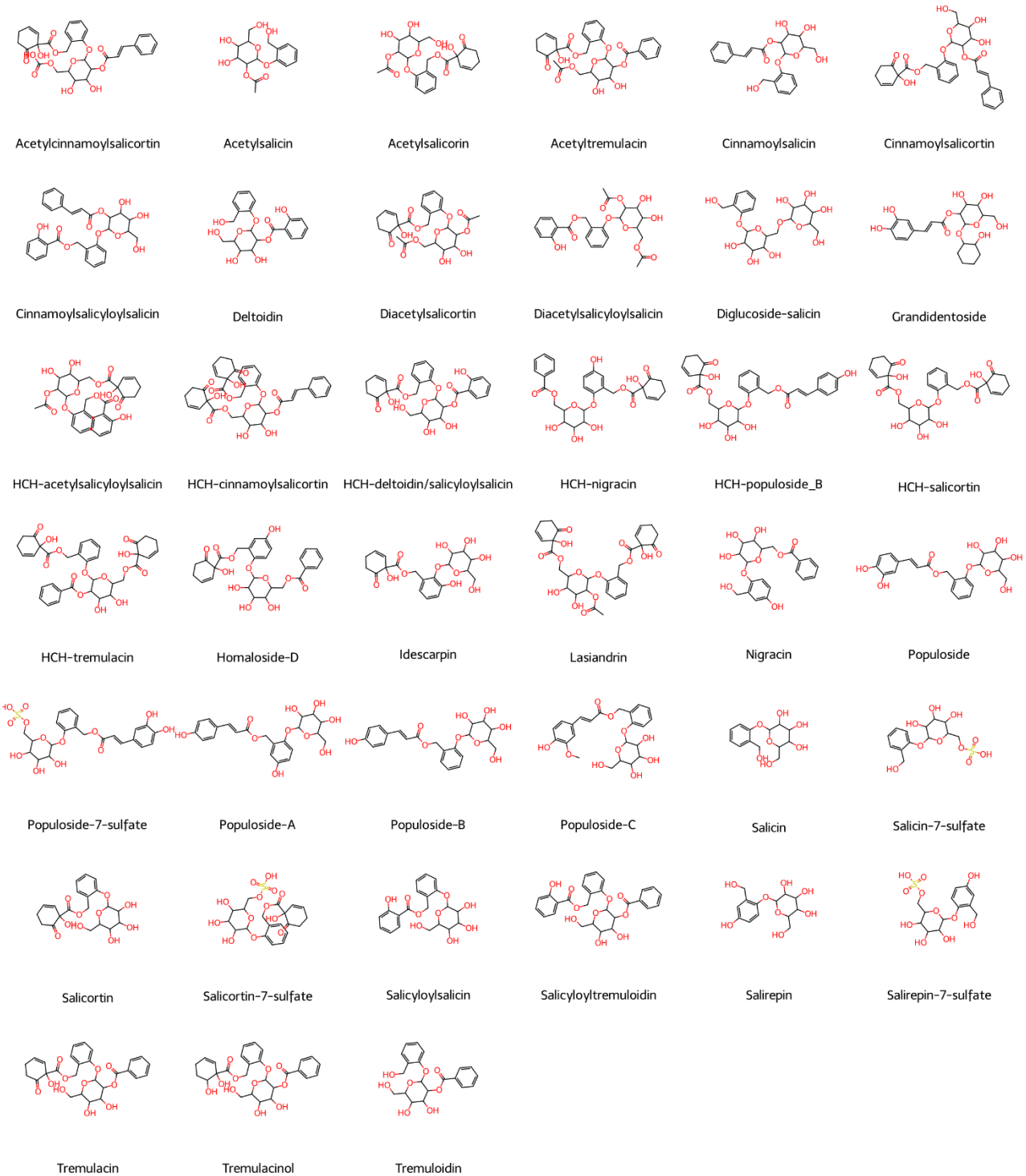

Figure 1. A figure of salicinoid structures found in *Populus*, *Salix*, and *Idesia* samples. Isomers of these structures (i.e. salicortin-A vs salicortin-B) have the same moieties but in different arrangements on the salicin core.

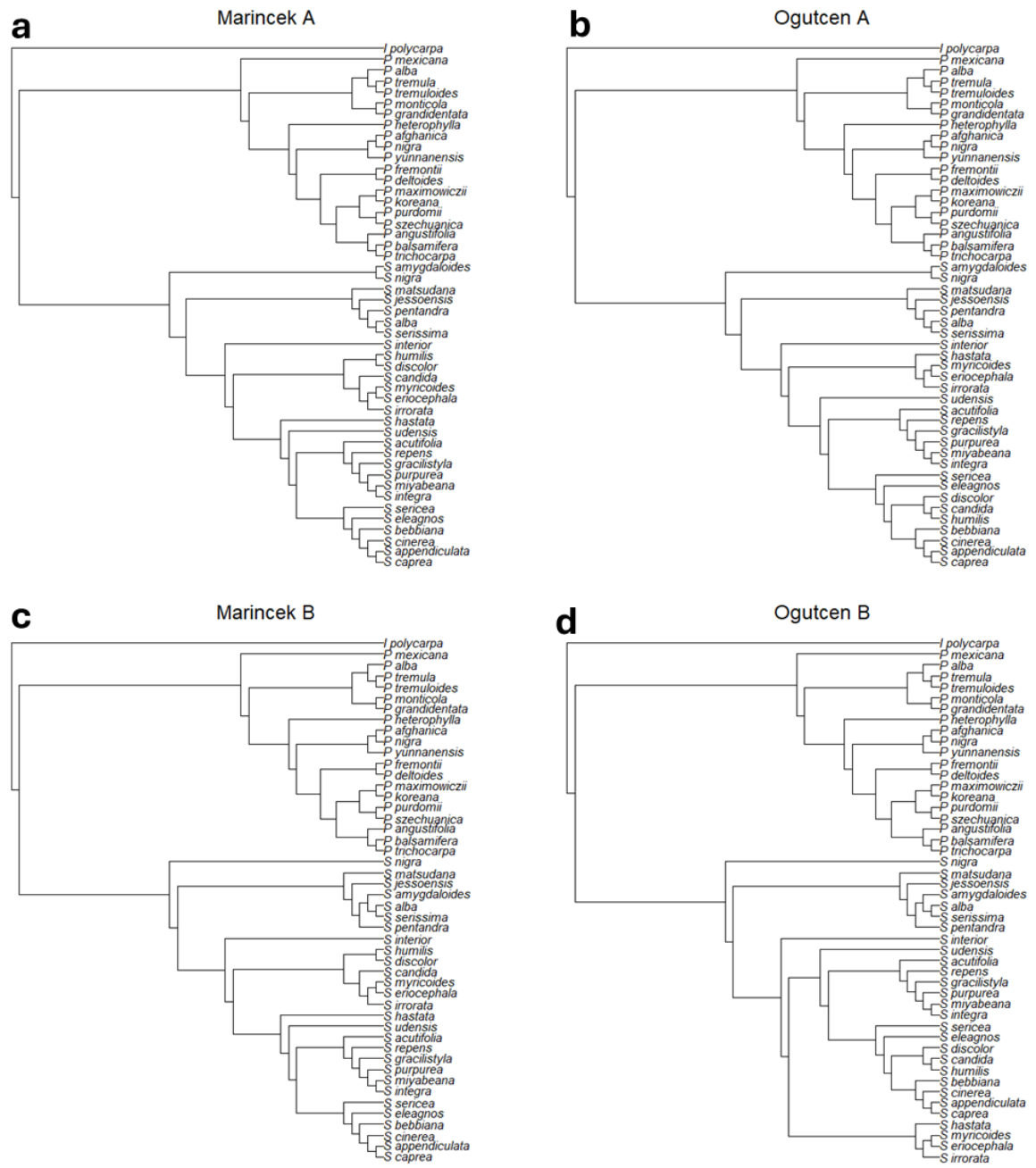

Figure 2. The four topologies of *Populus, Salix,* and *Idesia* in this study, with (a) being the main topology discussed in the text.

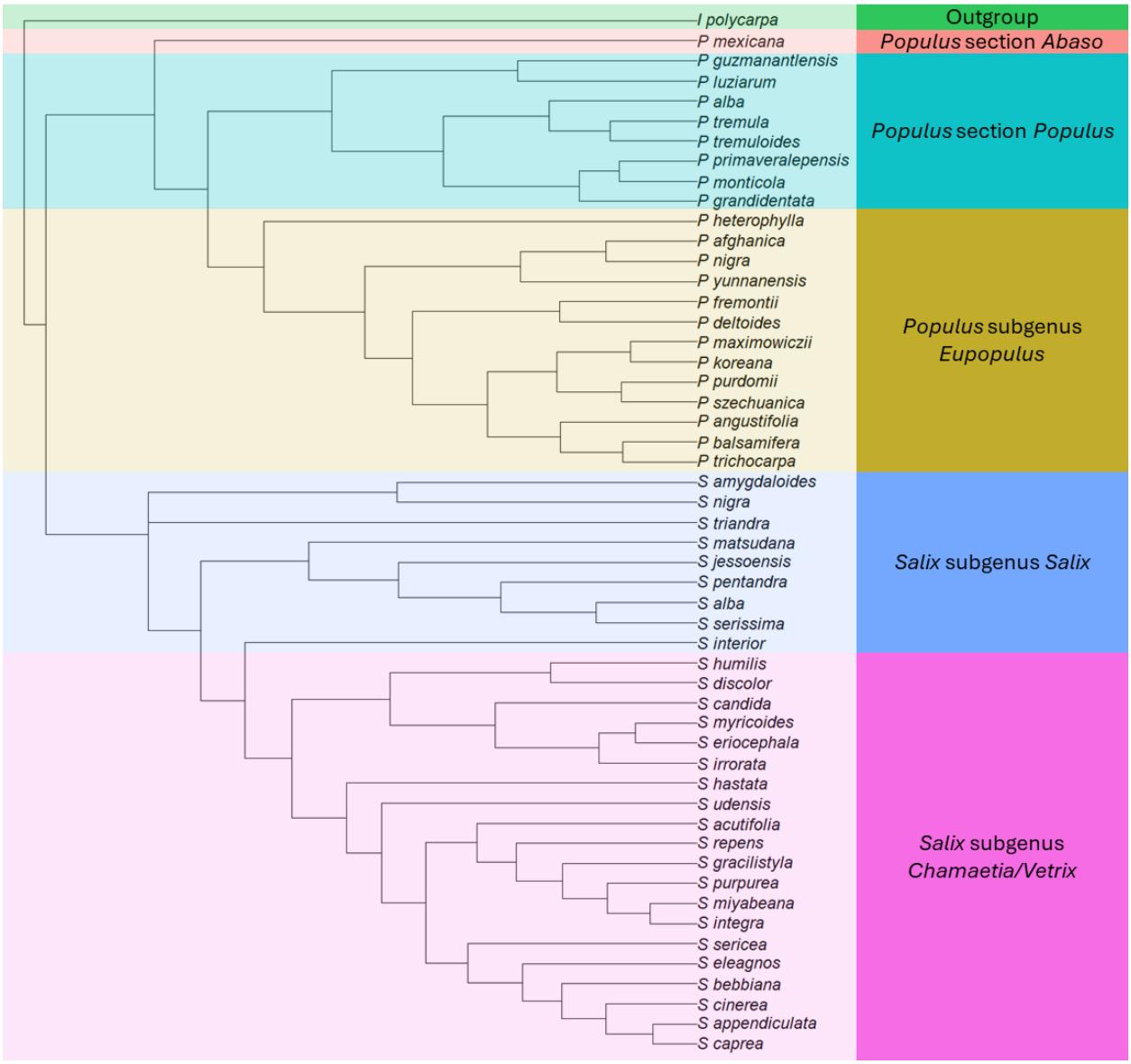

Figure 3. The main topology (Marinček A) discussed in the text, with taxa color-coded according to traditional groupings.

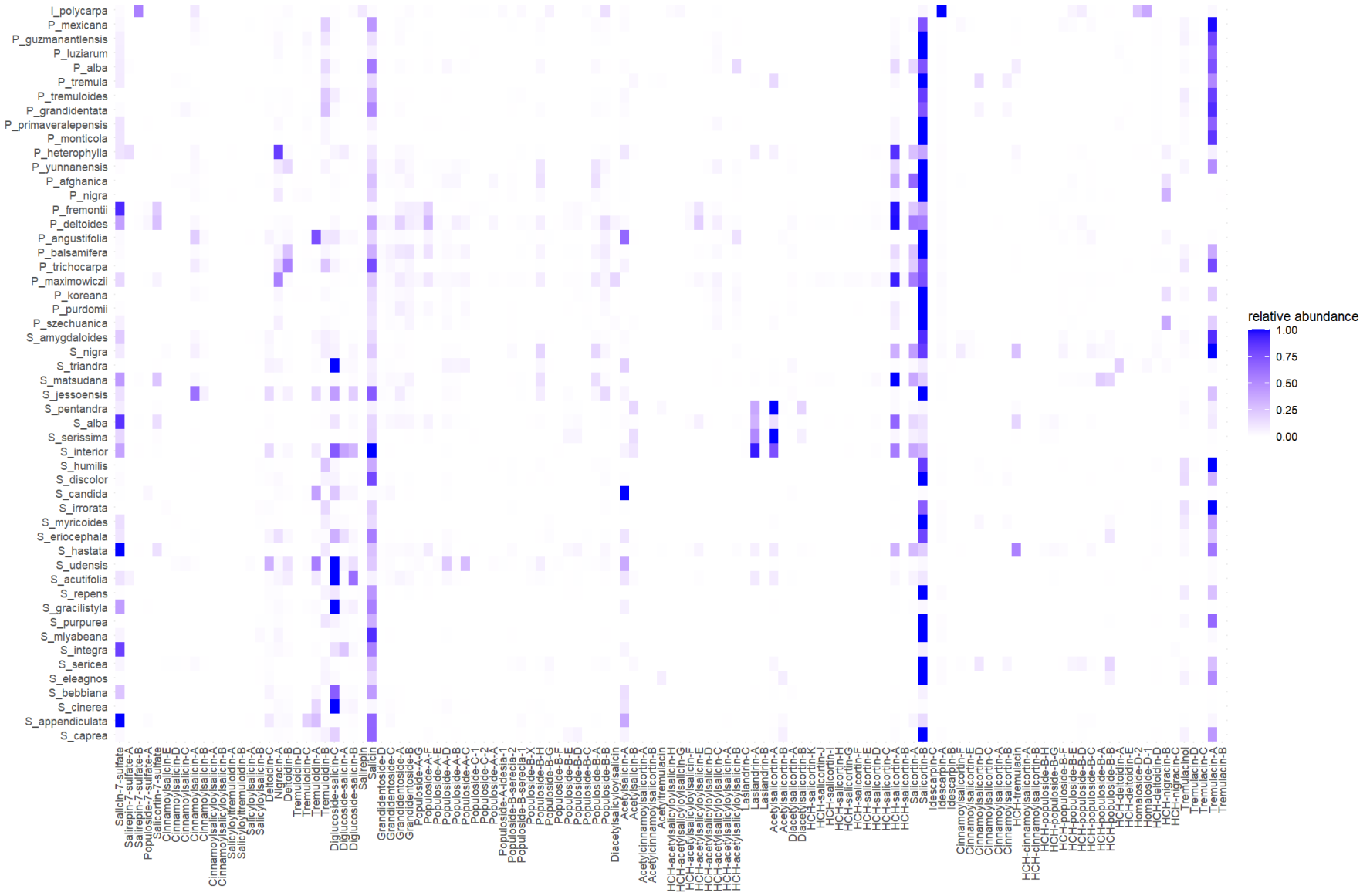

Figure 4. Heatmap of the mean relative abundance of each salicinoid detected in *Populus* and *Salix* species and *Idesia polycarpa* in this study. Salicinoids are grouped by structural similarity, and species are ordered by phylogeny.

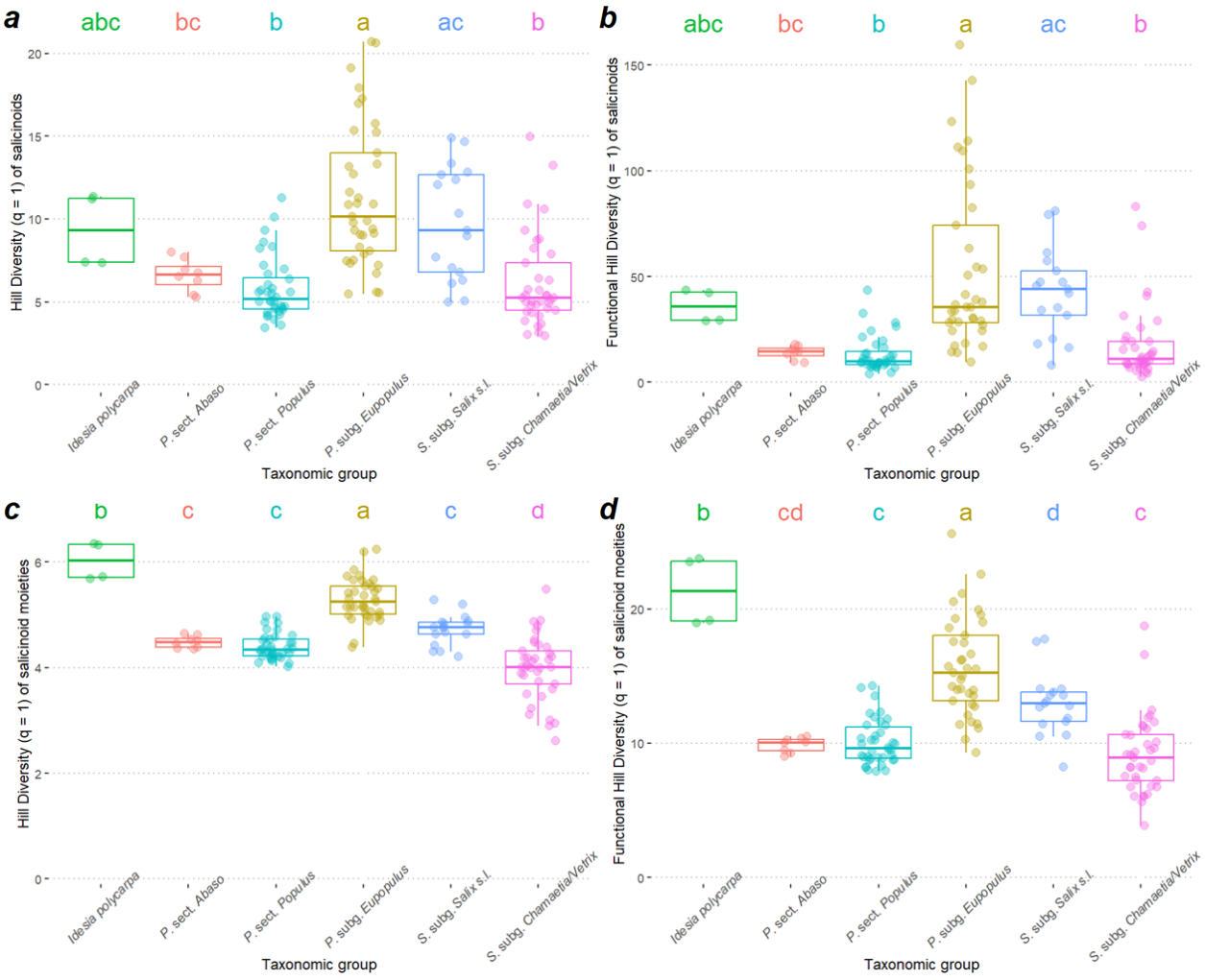

Figure 5. Results of ANOVAs for salicinoid (a) Hill Diversity and (b) Functional Hill Diversity as well as moiety (c) Hill Diversity and (d) Functional Hill Diversity across taxonomic groupings of *Populus*, *Salix*, and *Idesia* samples. All indices were calculated with q = 1, and letters represent results of Tukey's HSD post-hoc test, with letters that are the same indicating that groups are not different from each other.

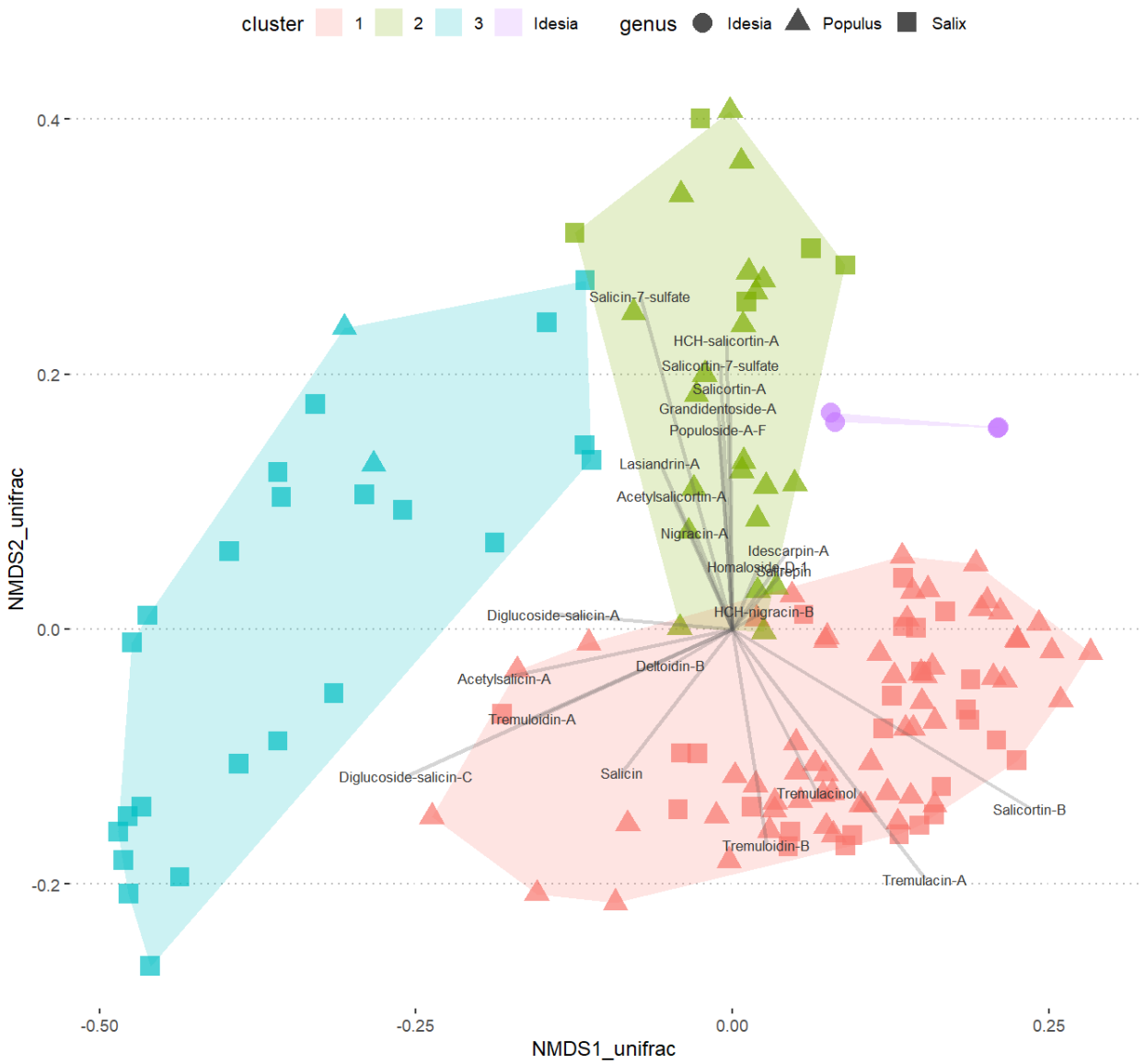

Figure 6. NMDS (k = 4, stress = 0.077) of salicinoid structural dissimilarity of samples of *Populus, Salix,* and *Idesia polycarpa* calculated using generalized unique fraction distances of the relative abundances of salicinoids in those samples. The top 20 salicinoids that contribute to dissimilarity between samples (from SIMPER), as well as characteristic *Idesia polycarpa* compounds salirepin, idescarpin, and homaloside D are passively overlayed on the ordination.

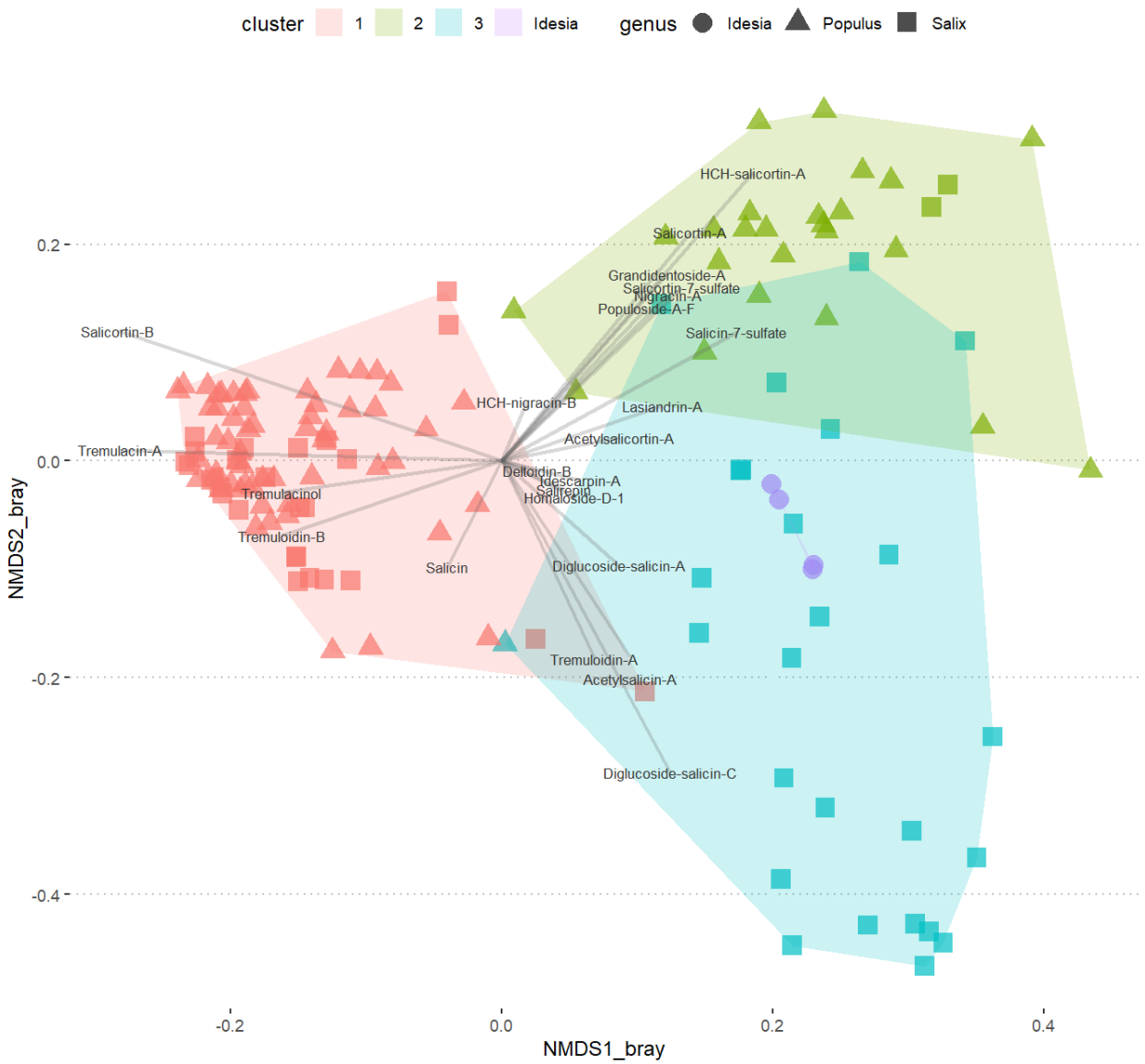

Figure 7. NMDS (k = 4, stress = 0.078) of Bray-Curtis dissimilarity of samples of *Populus, Salix,* and *Idesia polycarpa* calculated from the relative abundance of salicinoids in those samples. The top 20 salicinoids that contribute to dissimilarity between samples (from SIMPER), as well as characteristic *Idesia polycarpa* compounds salirepin, idescarpin, and homaloside D are passively overlayed on the ordination.

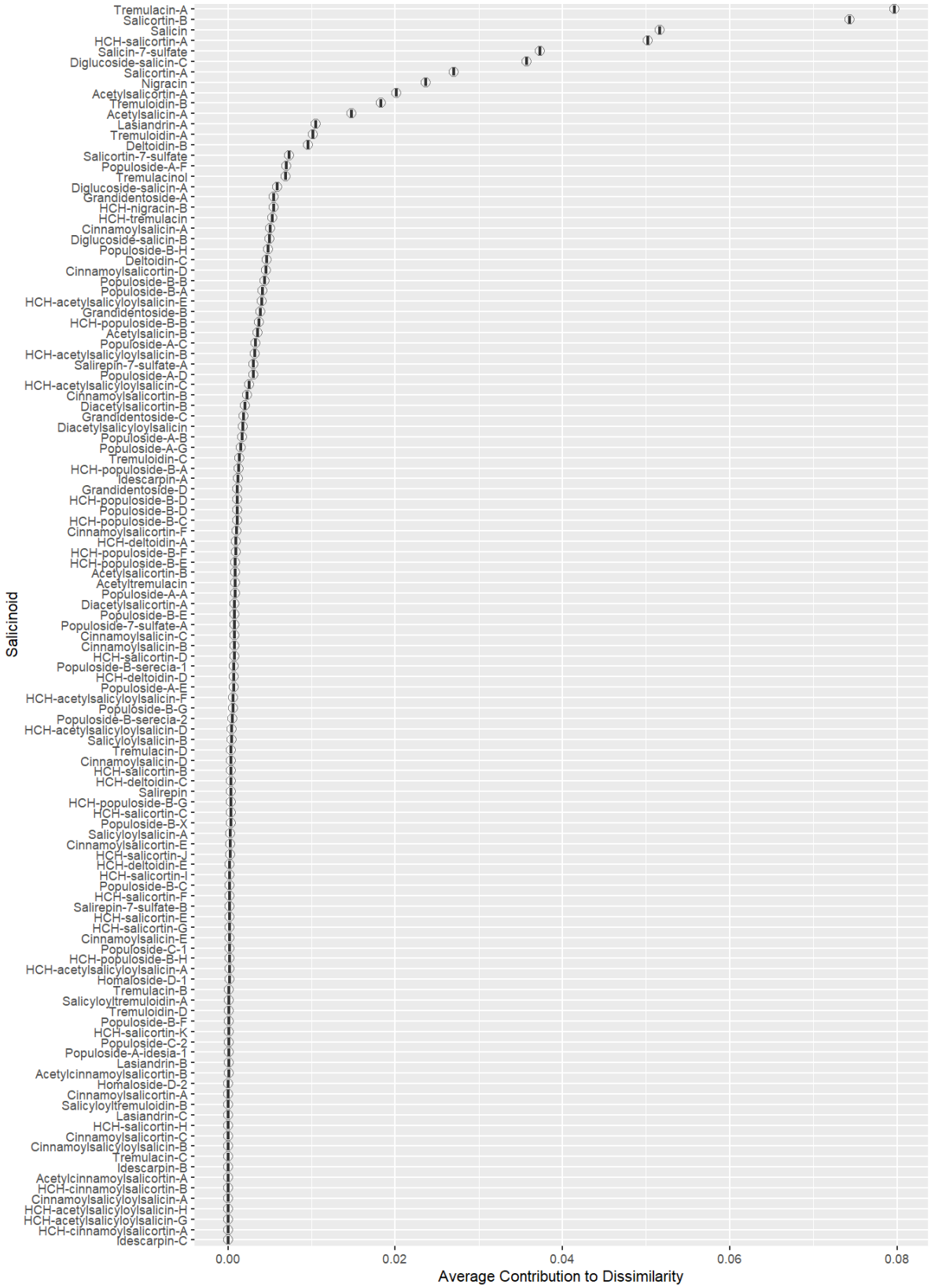

Figure 8. Similarity-Percentage (SIMPER) results of the average contribution of salicinoids found in both *Populus* and *Salix* samples to Bray-Curtis dissimilarity between samples.

Figure 9. Results of a *ℓ1ou* + pBIC model using the "Marinček A" topology (Fig. 4a) run on the species-averages of four NMDS axes of the generalized unique fraction (GenUniFrac) dissimilarity index calculated from salicinoid presence-absence, abundance, and structural dissimilarity in *Populus* and *Salix* species. Stars on edges indicate shifts in trait optima, numbers represent the support of shifts on those edges from 100 bootstraps using pBIC.

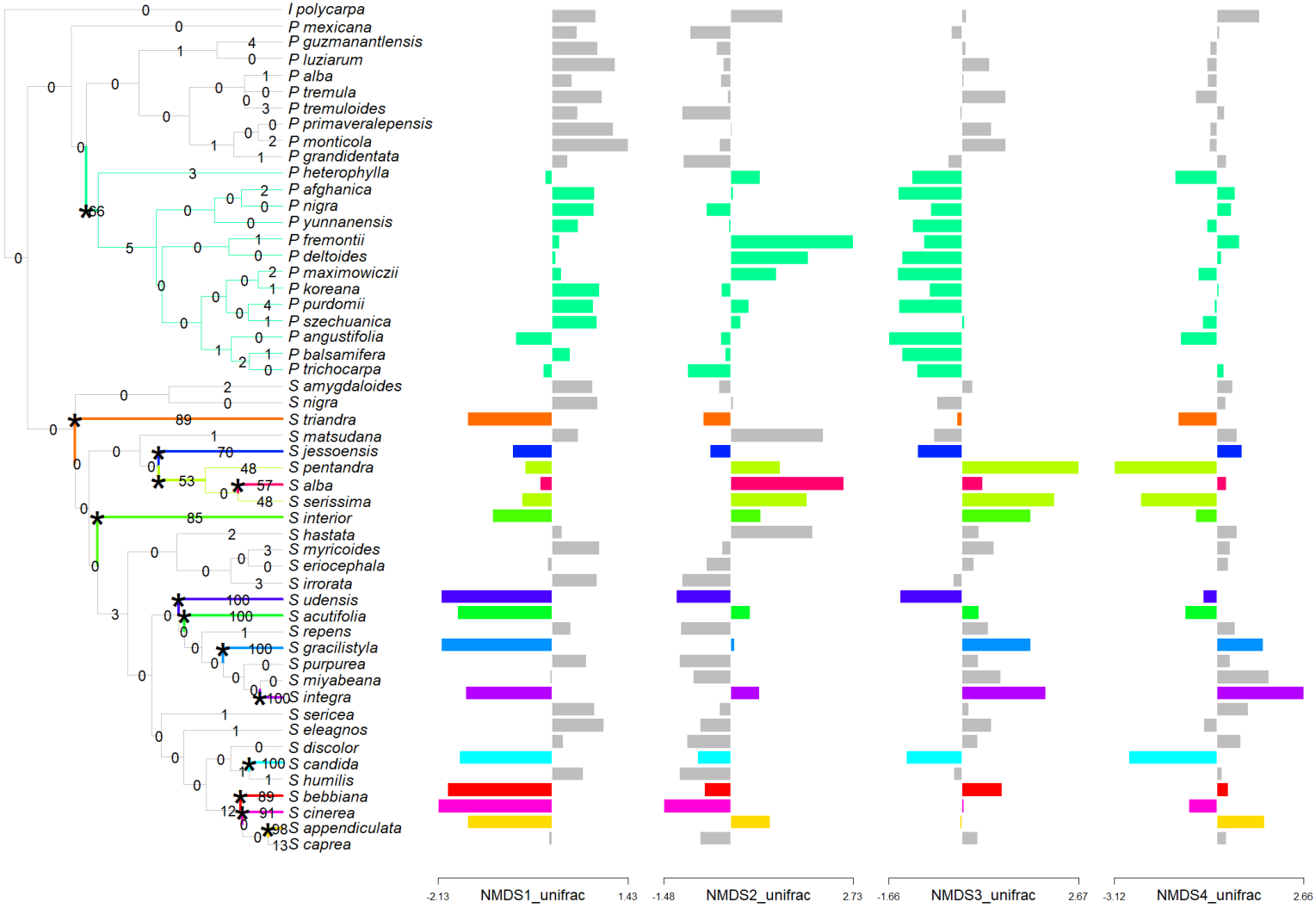

Figure 10. Results of a *ℓ1ou* + pBIC model run using the "Ogutcen A" topology (Fig. 4b) on the species-averages of four NMDS axes of the generalized unique fraction (GenUniFrac) dissimilarity index calculated from salicinoid presence-absence, abundance, and structural dissimilarity in *Populus* and *Salix* species. Stars on edges indicate shifts in trait optima, numbers represent the support of shifts on those edges from 100 bootstraps using pBIC

Figure 11. Results of a *ℓ1ou* + AICc model using the "Marinček A" topology (Fig. 4a) run on the species-averages of four NMDS axes of the Bray-Curtis dissimilarity index calculated from salicinoid presence-absence and abundance in *Populus* and *Salix* species. Stars on edges indicate shifts in trait optima, numbers represent the support of shifts on those edges from 100 bootstraps using pBIC.

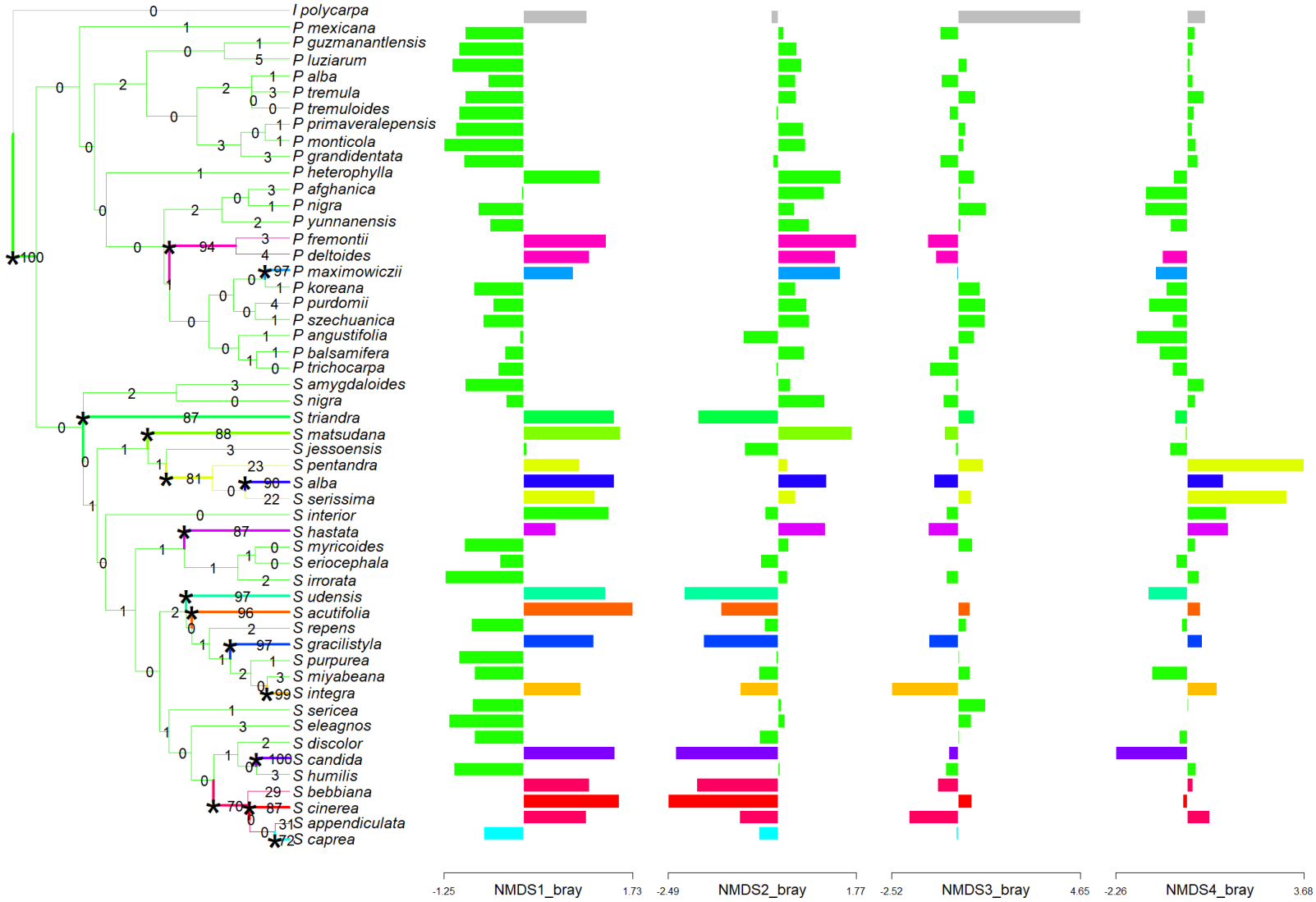

Figure 12. Results of a *ℓ1ou* + pBIC model run using the "Ogutcen A" topology (Fig. 4b) on the species-averages of four NMDS axes of the Bray-Curtis dissimilarity index calculated from salicinoid presence-absence and abundance in *Populus* and *Salix* species. Stars on edges indicate shifts in trait optima, numbers represent the support of shifts on those edges from 100 bootstraps using pBIC.

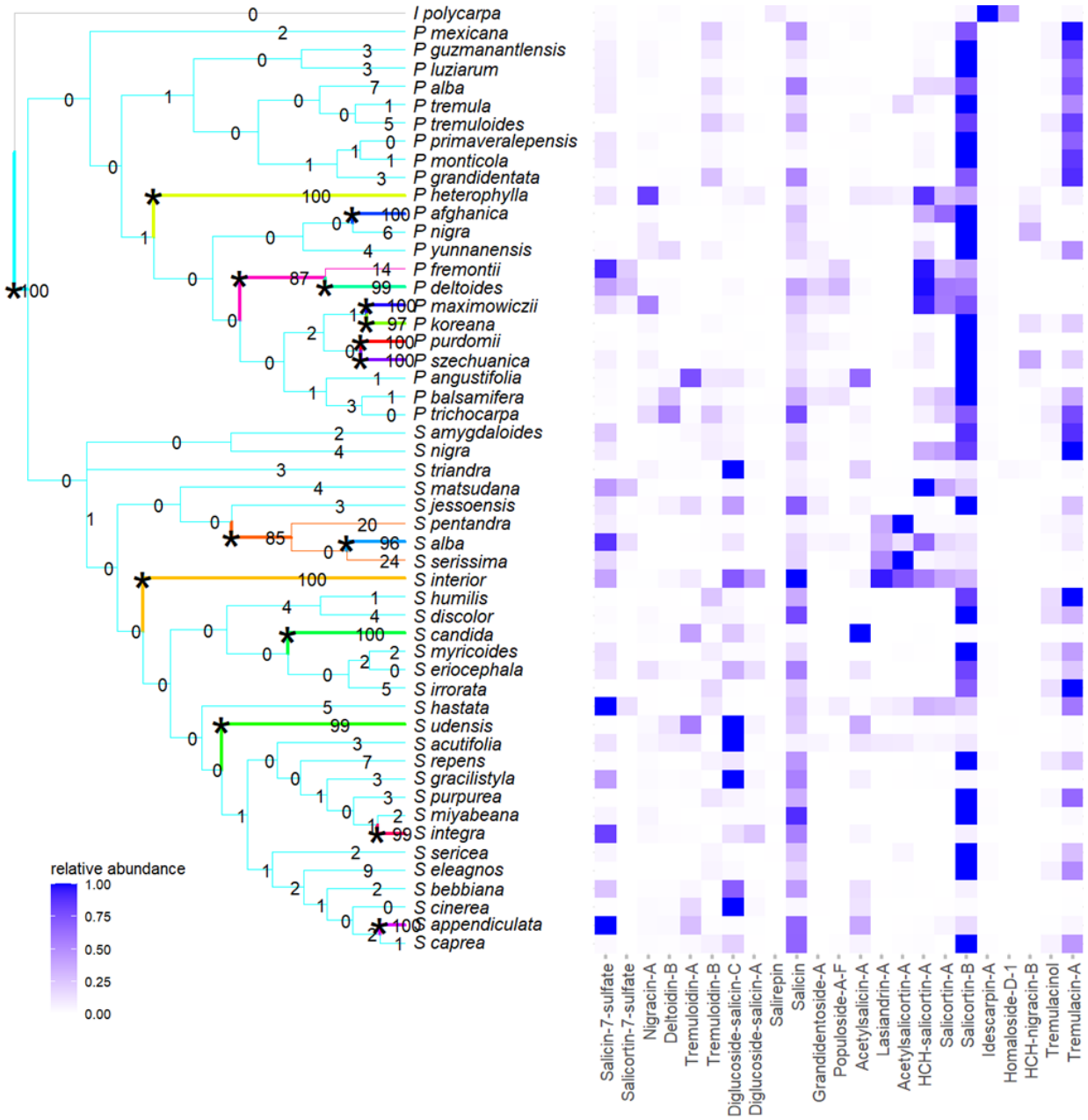

Figure 13. Results of a *ℓ1ou* + pBIC model using the "Marinček A" topology (Fig. 4a) run on the species-averages of the 20 salicinoids in *Populus* and *Salix* species which contributed most to dissimilarity between species as calculated by SIMPER, in addition to salirepin, idescarpin-A, and homaloside-D-1 from *Idesia polycarpa*. Stars on edges indicate shifts in trait optima, numbers represent the support of shifts on those edges from 100 bootstraps using pBIC.

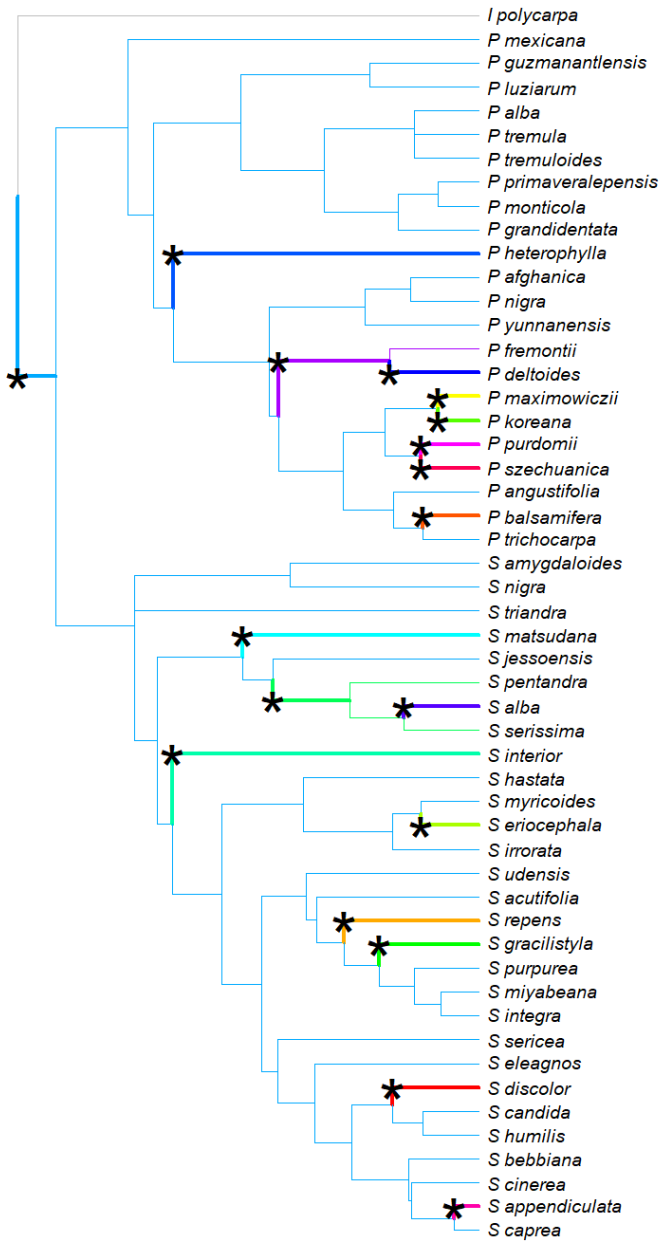

Figure 14. Results of a *ℓ1ou* + pBIC model using the "Ogutcen A" topology (Fig. 4b) run on the species-averages of the 20 salicinoids in *Populus* and *Salix* species which contributed most to dissimilarity between species as calculated by SIMPER, in addition to salirepin, idescarpin-A, and homaloside-D-1 from *Idesia polycarpa*. Stars on edges indicate shifts in trait optima.

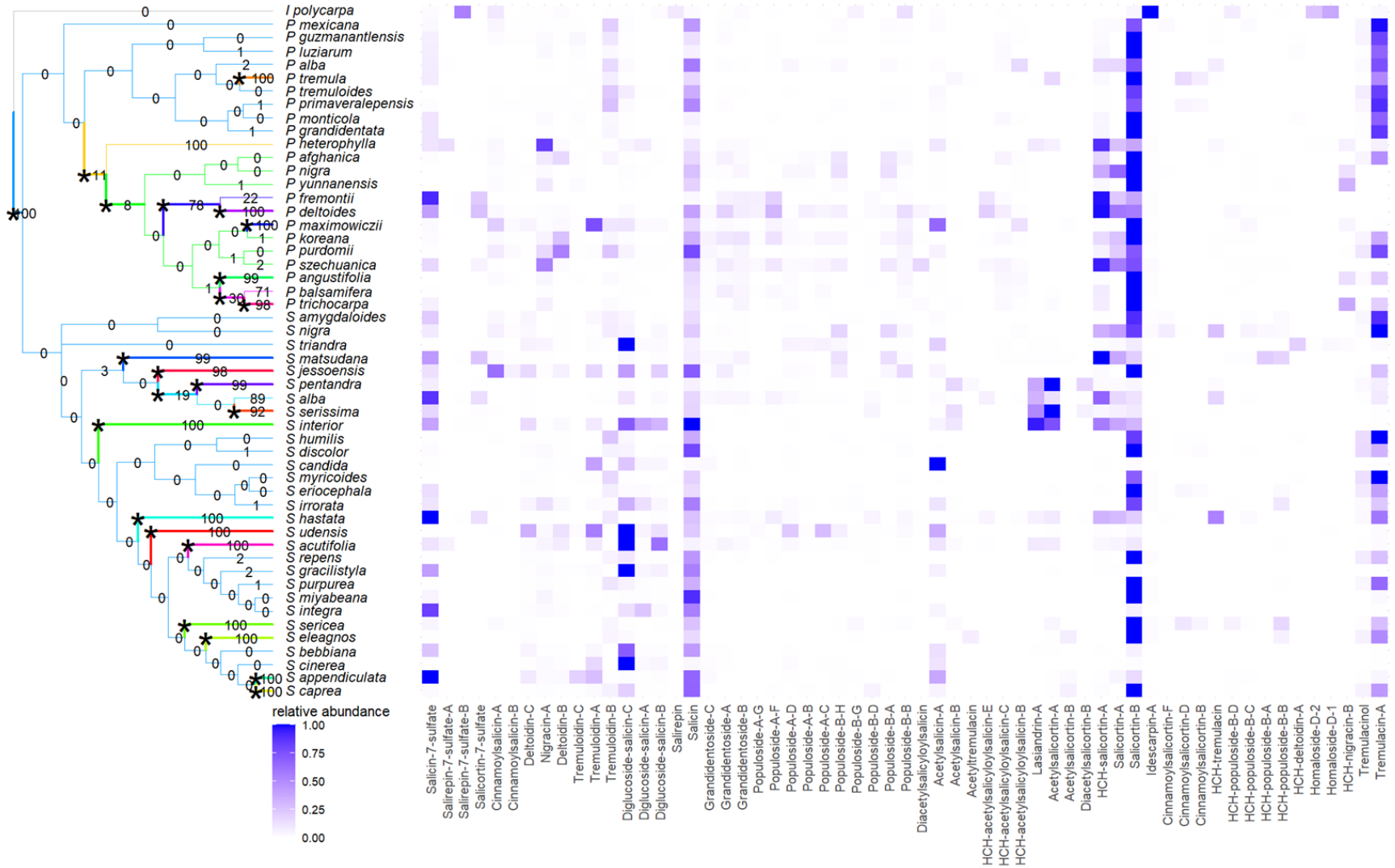

Figure 15. Results of a *ℓ1ou* + pBIC model using the "Marinček A" topology (Fig. 4a) run on the species-averages of the salicinoids in *Populus* and *Salix* species which are at least 5% relative abundance in any one sample. Stars on edges indicate shifts in trait optima, numbers represent the support of shifts on those edges from 100 bootstraps using pBIC.

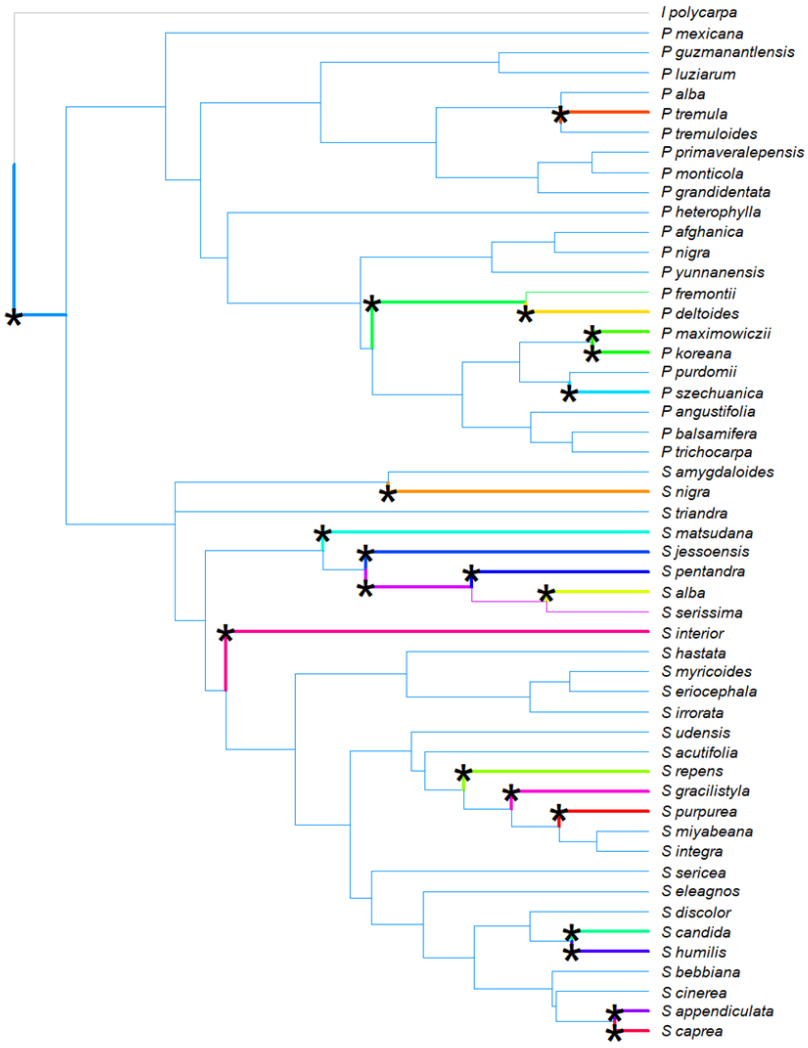

Figure 16. Results of a ℓ1ou + pBIC model using the "Ogutcen A" topology (Fig. 4b) run on the species-averages of the salicinoids in *Populus* and *Salix* species which are at least 5% relative abundance in any one sample. Stars on edges indicate shifts in trait optima.

Tables

Table 1. (Pages 167-170) Sources of samples used in this study

Genus	Species	Location	Identification code (if any)
Idesia	*polycarpa*	New York Botanical Garden	611/86B
Idesia	*polycarpa*	New York Botanical Garden	611/86L
Populus	*afghanica*	Morton Arboretum, Lisle, IL	50-2008*6
Populus	*alba*	Lake Kegonsa, Dane County, WI	
Populus	*alba*	Lake Kegonsa, Dane County, WI	
Populus	*alba*	Williams Dr., Lake Kegonsa, Dane County, WI	
Populus	*alba*	Williams Dr., Lake Kegonsa, Dane County, WI	
Populus	*alba*	Olin Park, Madison, WI	
Populus	*alba*	Morton Arboretum, Lisle, IL	swarm in eastern NA forest
Populus	*angustifolia*	Morton Arboretum, Lisle, IL	96-2020*4
Populus	*balsamifera*	UW Botany Greenhouse, from a fallen tree in Lodi Marsh, Lodi, WI	
Populus	*balsamifera*	Morton Arboretum, Lisle, IL	570-81*12
Populus	*deltoides*	South Kenosha Dr. Madison, WI	
Populus	*deltoides*	Quarry Ridge Recreation Area, Dane County, WI	
Populus	*deltoides*	Lake Kegonsa, Dane County, WI	
Populus	*deltoides*	Morton Arboretum, Lisle, IL	851-56*3
Populus	*deltoides*	Morton Arboretum, Lisle, IL	346-2019*1
Populus	*deltoides*	UW Botany Greenhouse, from a crack in the steps of Birge Hall on Bascom Hill, Madison, WI	
Populus	*deltoides*	Morton Arboretum, Lisle, IL	377-83*4
Populus	*deltoides*	Morton Arboretum, Lisle, IL	377-83*6
Populus	*fremontii*	Adam Black, Annaliese Sander, Bartlett Tree Experts	2023_1009B
Populus	*fremontii*	Adam Black, Annaliese Sander, Bartlett Tree Experts	1009A
Populus	*grandidentata*	Olin Park, Madison, WI	
Populus	*grandidentata*	Morton Arboretum, Lisle, IL	126-U*9
Populus	*grandidentata*	Olin Park, Madison, WI	
Populus	*grandidentata*	Olin Park, Madison, WI	
Populus	*grandidentata*	University of Wisconsin-Madison Veterinary Hospital Parking Lot, Madison, WI	
Populus	*grandidentata*	Lakeshore Preserve, University of Wisconsin-Madison, Madison, WI	
Populus	*guzmanantlensis*	Adam Black, Annaliese Sander, Bartlett Tree Experts	no number
Populus	*guzmanantlensis*	Adam Black, Annaliese Sander, Bartlett Tree Experts	LSE3
Populus	*heterophylla*	Morton Arboretum, Lisle, IL	144-91*1
Populus	*heterophylla*	UW Botany Greenhouse, from Connecticut, from Bryan Connelly	
Populus	*heterophylla*	UW Botany Greenhouse, from Connecticut, from Bryan Connelly	
Populus	*heterophylla*	UW Botany Greenhouse, from *P. heterophylla* seed from Illinois	
Populus	*heterophylla*	UW Botany Greenhouse, from side of road, Seneca, MD	

Populus	*heterophylla*	Tyler Wintermute, *P. heterophylla* common garden, WI	NS3-3
Populus	*heterophylla*	Tyler Wintermute, *P. heterophylla* common garden, WI	Gen4-5
Populus	*heterophylla*	Tyler Wintermute, *P. heterophylla* common garden, WI	LS2-1
Populus	*heterophylla*	Tyler Wintermute, *P. heterophylla* common garden, WI	GCS8
Populus	*koreana*	Morton Arboretum, Lisle, IL	311-2009*2
Populus	*luziarum*	Adam Black, Annaliese Sander, Bartlett Tree Experts	1032_A
Populus	*luziarum*	Adam Black, Annaliese Sander, Bartlett Tree Experts	1031A
Populus	*maximowiczii*	Morton Arboretum, Lisle, IL	347-2019*1
Populus	*maximowiczii*	Morton Arboretum, Lisle, IL	35-88*2
Populus	*maximowiczii*	Morton Arboretum, Lisle, IL	156-92*2
Populus	*mexicana*	Jason Smith, University of Mount Union	1
Populus	*mexicana*	Jason Smith, University of Mount Union	2
Populus	*mexicana*	Jason Smith, University of Mount Union	3
Populus	*mexicana*	Jason Smith, University of Mount Union	13
Populus	*mexicana*	Jason Smith, University of Mount Union	5
Populus	*mexicana*	Jason Smith, University of Mount Union	4
Populus	*mexicana*	Jason Smith, University of Mount Union	dimorpha B
Populus	*mexicana*	Jason Smith, University of Mount Union	dimorpha A
Populus	*monticola*	Adam Black, Annaliese Sander, Bartlett Tree Experts	1033A
Populus	*monticola*	Adam Black, Annaliese Sander, Bartlett Tree Experts	0851A
Populus	*nigra*	Morton Arboretum, Lisle, IL	353-2013*3
Populus	*primaveralepensis*	Adam Black, Annaliese Sander, Bartlett Tree Experts	1037A
Populus	*primaveralepensis*	Adam Black, Annaliese Sander, Bartlett Tree Experts	1034A
Populus	*primaveralepensis*	Adam Black, Annaliese Sander, Bartlett Tree Experts	1041A
Populus	*primaveralepensis*	Adam Black, Annaliese Sander, Bartlett Tree Experts	1040A
Populus	*primaveralepensis*	Adam Black, Annaliese Sander, Bartlett Tree Experts	1039A
Populus	*purdomii*	Morton Arboretum, Lisle, IL	349-2019*1
Populus	*simaroa*	Adam Black, Annaliese Sander, Bartlett Tree Experts	1025_A
Populus	*simaroa*	Adam Black, Annaliese Sander, Bartlett Tree Experts	2023_1026A
Populus	*szechuanica*	Morton Arboretum, Lisle, IL	352-2019*1
Populus	*szechuanica*	Morton Arboretum, Lisle, IL	350-2019*1
Populus	*tremula*	Ken Keefover-Ring, from the Swedish Aspen Garden	45778
Populus	*tremula*	Ken Keefover-Ring, from the Swedish Aspen Garden	65-27
Populus	*tremula*	Ken Keefover-Ring, from the Swedish Aspen Garden	50-15
Populus	*tremula*	Ken Keefover-Ring, from the Swedish Aspen Garden	26-11
Populus	*tremula*	Ken Keefover-Ring, from the Swedish Aspen Garden	51-21
Populus	*tremula*	Ken Keefover-Ring, from the Swedish Aspen Garden	60-22
Populus	*tremuloides*	Morton Arboretum, Lisle, IL	668-2004*3
Populus	*tremuloides*	Olin Park, Madison, WI	
Populus	*tremuloides*	Olin Park, Madison, WI	
Populus	*tremuloides*	University of Wisconsin-Madison Veterinary Hospital Parking Lot, Madison, WI	
Populus	*tremuloides*	Bascom Hill Planting, University of Wisconsin-Madison, Madison, WI	

Populus	*tremuloides*	Bascom Hill Planting, University of Wisconsin-Madison, Madison, WI	
Populus	*tremuloides*	Morton Arboretum, Lisle, IL	374-83*3
Populus	*trichocarpa*	From Steven Strauss, Oregon State University, Corvallis, OR	
Populus	*trichocarpa*	From Steven Strauss, Oregon State University, Corvallis, OR	
Populus	*trichocarpa*	From Steven Strauss, Oregon State University, Corvallis, OR	
Populus	*trichocarpa*	From Steven Strauss, Oregon State University, Corvallis, OR	
Populus	*trichocarpa*	From Steven Strauss, Oregon State University, Corvallis, OR	
Populus	*yunnanensis*	Morton Arboretum, Lisle, IL	354-2019*1
Salix	*acutifolia*	Morton Arboretum, Lisle, IL	192-2011*1
Salix	*alba*	Morton Arboretum, Lisle, IL	162-82*6
Salix	*alba*	Morton Arboretum, Lisle, IL	5522005*1
Salix	*amygdaloides*	Morton Arboretum, Lisle, IL	328-2014*3
Salix	*amygdaloides*	Morton Arboretum, Lisle, IL	255-89*6
Salix	*appendiculata*	Morton Arboretum, Lisle, IL	62-93*1
Salix	*aurantha*	Morton Arboretum, Lisle, IL	278-2000*1
Salix	*bebbiana*	Morton Arboretum, Lisle, IL	781-2015*1
Salix	*bebbiana*	Morton Arboretum, Lisle, IL	311-99*1
Salix	*bebbiana*	Morton Arboretum, Lisle, IL	310-2000*1
Salix	*candida*	Morton Arboretum, Lisle, IL	158-2019*5
Salix	*caprea*	Morton Arboretum, Lisle, IL	525-84*2
Salix	*cinerea*	Morton Arboretum, Lisle, IL	453-96*1
Salix	*cinerea*	Morton Arboretum, Lisle, IL	526-84*4
Salix	*discolor*	Morton Arboretum, Lisle, IL	381-83*1
Salix	*eleagnos*	Morton Arboretum, Lisle, IL	34-78*1
Salix	*eleagnos*	Morton Arboretum, Lisle, IL	527-84*4
Salix	*eriocephala*	Morton Arboretum, Lisle, IL	550-2015*4
Salix	*eriocephala*	Morton Arboretum, Lisle, IL	136-2019*1
Salix	*gracilistyla*	Morton Arboretum, Lisle, IL	819-2005*1
Salix	*hastata*	Morton Arboretum, Lisle, IL	Hatch's Meadow
Salix	*humilis*	Morton Arboretum, Lisle, IL	472-78*3
Salix	*integra*	Morton Arboretum, Lisle, IL	276-2016*1 Plt
Salix	*integra*	Morton Arboretum, Lisle, IL	276-2016*1
Salix	*integra*	Morton Arboretum, Lisle, IL	460-2012*1
Salix	*interior*	Morton Arboretum, Lisle, IL	Main Drive
Salix	*irrorata*	Morton Arboretum, Lisle, IL	530-84*2
Salix	*jessoensis*	Morton Arboretum, Lisle, IL	387-2017*1
Salix	*matsudana*	Morton Arboretum, Lisle, IL	243-89*3
Salix	*matsudana*	Morton Arboretum, Lisle, IL	366-79*11
Salix	*miyabeana*	Morton Arboretum, Lisle, IL	102-2015*2
Salix	*miyabeana*	Morton Arboretum, Lisle, IL	161-93*4
Salix	*myricoides*	Morton Arboretum, Lisle, IL	330-2014*2
Salix	*myricoides*	Morton Arboretum, Lisle, IL	197-91*1
Salix	*myricoides*	Morton Arboretum, Lisle, IL	329-2014*8

Salix	*myricoides*	Morton Arboretum, Lisle, IL	528-84*2
Salix	*nigra*	Morton Arboretum, Lisle, IL	180-88*4
Salix	*nigra*	Morton Arboretum, Lisle, IL	162-93*3
Salix	*pentandra*	Morton Arboretum, Lisle, IL	39-98*4
Salix	*pentandra*	Morton Arboretum, Lisle, IL	367-79*1
Salix	*pentandra*	Morton Arboretum, Lisle, IL	121-2006*1
Salix	*pentandra*	Morton Arboretum, Lisle, IL	415-80*2
Salix	*purpurea*	Morton Arboretum, Lisle, IL	18-75*2
Salix	*purpurea*	Morton Arboretum, Lisle, IL	536-84*3
Salix	*purpurea*	Morton Arboretum, Lisle, IL	287-2017*1
Salix	*purpurea*	Morton Arboretum, Lisle, IL	587-2001*1
Salix	*repens*	Morton Arboretum, Lisle, IL	393-82*1
Salix	*sericea*	Morton Arboretum, Lisle, IL	70-93*1
Salix	*sericea*	Morton Arboretum, Lisle, IL	372-79*3
Salix	*sericea*	Morton Arboretum, Lisle, IL	477-2000*1
Salix	*serissima*	Morton Arboretum, Lisle, IL	154-2019*2
Salix	*triandra*	Morton Arboretum, Lisle, IL	194-2011*3
Salix	*udensis*	Morton Arboretum, Lisle, IL	168-82*1
Salix	*udensis*	Morton Arboretum, Lisle, IL	416-2017*2
Salix	*udensis*	Morton Arboretum, Lisle, IL	416-2017*5

Table 2. Primers used for the sequencing of *matK*, *rbcL*, and *ITS1* sequences.

Gene	**Outer primers** 5’ – 3’	**Inner primers** 5’ – 3’
rbcL	**F:** CATGAGTTGTAGGGAGGGGC **R:** CAAAGATGATGAGAACGTGAACTC	**F:** ATGTCACCACAAACAGAGACTAAA **R:** GTAAAATCAAGTCCACCGCG
matK	**F:** CCATTTTCCTTACGATTAGTATCC **R:** GTACTTTTGTGTTTACGAGC	**F:** TACGATCAATTCATTCAATATTTCC **R:** GCAGAAATCTTTCTCATTAT
ITS1	**F:** CCTTATCATTTAGAGGAAGG **R:** GCGGAGGAAAAGAAACTTAC	**F:** CGTAACAAGGTTTCCGTAGG **R:** TGCTTAAACTCAGCGGGTAG

Table 3. (Pages 171-172) Information for the barcode genes *rbcL*, *matK*, and *ITS* for each species in this study. Identifiers for each sequence are in the right three columns, with an "n/a" meaning there was no data on NCBI for that barcode for that species. Italicized identifiers represent an entire plastome sequence, with the base pair ranges used in brackets next to them. Species at the bottom of the table with "sequenced" were the species I sequenced. *Salix medewedewii* is a synonym for *S. triandra*, so I used those sequences for that species.

genus	species	rbcL	matK	ITS
Idesia	*polycarpa*	KX016330.1	KX016117.1	KX008756.1
Populus	*afghanica*	KC485203.1	KC485111.1	KC485082.1
Populus	*alba*	MG248466.1	MG220929.1	JQ898650.1
Populus	*angustifolia*	*NC_037413.1*[55326..57181]	*NC_037413.1*[1740..3724]	MG234937.1
Populus	*balsamifera*	KC483597.1	KC475432.1	MT796554.1
Populus	*deltoides*	MH574053.1	MH574134.1	MH580346.1
Populus	*fremontii*	*NC_024734.1*[55647..57502]	*NC_024734.1*[1748..3740]	n/a
Populus	*grandidentata*	KJ593628.1	KJ593066.1	KY584371.1
Populus	*heterophylla*	MG248285.1	*MW376781.1*[1787..3771]	MG236491.1
Populus	*koreana*	MG773032.1	OP357101.1	MG772955.1
Populus	*maximowiczii*	MH574045.1	MH574126.1	MH580312.1
Populus	*mexicana*	KY196707.1	KY196688.1	n/a
Populus	*nigra*	KJ204391.1	KJ204525.1	n/a
Populus	*purdomii*	KC485223.1	KC485134.1	n/a
Populus	*szechuanica*	MH574020.1	MH574101.1	MH580307.1
Populus	*tremula*	MN192718.1	MN317539.1	MH808702.1
Populus	*tremuloides*	MG246755.1	KJ840971.1	MG235256.1
Populus	*trichocarpa*	KX679125.1	KX677658.1	JQ898636.1
Populus	*yunnanensis*	MH574068.1	MH574149.1	MH580329.1
Salix	*acutifolia*	*MW435413.1*[55028..56895]	*MW435413.1*[1709..3700]	n/a
Salix	*alba*	KX016333.1	KX016120.1	KX008759.1
Salix	*amygdaloides*	KC415324.1	KC415380.1	KC415493.1
Salix	*appendiculata*	*MW435416.1*[54978..56845]	*MW435416.1*[1710..3701]	n/a
Salix	*bebbiana*	KX016352.1	KX016139.1	KX008778.1
Salix	*candida*	KX016366.1	KX016153.1	KX008792.1
Salix	*caprea*	KX016368.1	KX016155.1	KX008794.1
Salix	*cinerea*	KX016377.1	KX016164.1	KX008803.1
Salix	*discolor*	KX016388.1	KX016175.1	KX008814.1
Salix	*eleagnos*	KX016394.1	KX016181.1	KX008820.1
Salix	*eriocephala*	KX016395.1	KX016182.1	KX008821.1
Salix	*gracilistyla*	HE612040.1	HE612074.1	HE800866.1
Salix	*hastata*	KX016416.1	KX016203.1	KX008842.1
Salix	*humilis*	KX016424.1	KX016211.1	KX008850.1

Salix	*integra*	HE856322.1	HE856320.1	HE856318.1
Salix	*interior*	KX016426.1	KX016213.1	KX008852.1
Salix	*irrorata*	KX016427.1	KX016214.1	KX008853.1
Salix	*jessoensis*	KC415348.1	KC415404.1	KC415518.1
Salix	*matsudana*	MG773038.1	MG772998.1	MG772960.1
Salix	*miyabeana*	HE612051.1	HE612082.1	HE800882.1
Salix	*myricoides*	KX016454.1	KX016241.1	KX008879.1
Salix	*nigra*	KX016453.1	KX016240.1	KX008878.1
Salix	*pentandra*	KX016472.1	KX016259.1	KX008897.1
Salix	*purpurea*	KX016459.1	KX016246.1	KX008884.1
Salix	*repens*	JN891724.1	JN895896.1	KX166369.1
Salix	*sericea*	KX016486.1	KX016273.1	KX008910.1
Salix	*serissima*	KX016503.1	KX016290.1	KX008927.1
Salix	*siuzevii*	KC415367.1	KC415423.1	KC415537.1
Salix	*udensis*	LC693968.1	LC680162.1	FR693645.1
Populus	*guzmanantlensis*	sequenced	sequenced	sequenced
Populus	*luziarum*	sequenced	sequenced	sequenced
Populus	*monticola*	sequenced	sequenced	sequenced
Populus	*primaveralepensis*	sequenced	sequenced	sequenced
Populus	*simaroa*	sequenced	sequenced	sequenced
Salix	*medwedewii (triandra)*	sequenced	sequenced	sequenced

Table 4. (Pages 173-175) Mass-to-charge ratios ($[M-H]^-$ and $[M-H+FA]^-$) and retention times (RT in minutes) of the salicinoids identified in this study. An N/A is used when an adduct ion peak was not found.

Salicinoid	**$[M-H]^-$**	**$[M-H+FA]^-$**	**RT (min)**
Salicin	285.0978	331.1031	2.87
Salirepin	301.0934	N/A	3.10
Acetylsalicin-A	327.1088	373.1135	3.27
Acetylsalicin-B	327.1088	373.1135	4.40
Salicin-7-sulfate	365.0543	N/A	2.68
Salirepin-7-sulfate-A	381.0493	N/A	1.68
Salirepin-7-sulfate-B	381.0501	N/A	2.59
Tremuloidin-A	389.1249	435.1295	6.26
Tremuloidin-B	389.1249	435.1295	6.97
Tremuloidin-C	389.1249	435.1295	7.64
Tremuloidin-D	389.1249	435.1295	7.75
Diglucoside-salicin-A	401.1460	447.1515	3.75
Diglucoside-salicin-B	401.1460	447.1515	3.89
Diglucoside-salicin-C	401.1460	447.1516	3.97
Nigracin-A	405.1186	451.1239	6.02
Deltoidin-B	405.1186	451.1239	6.27
Deltoidin-C	405.1186	451.1239	6.50
Salicyloylsalicin-A	405.1200	451.1239	8.18
Salicyloylsalicin-B	405.1200	451.1239	8.24
Cinnamoylsalicin-A	415.1403	461.1461	7.50
Cinnamoylsalicin-C	415.1403	461.1461	7.77
Cinnamoylsalicin-B	415.1403	461.1461	7.99
Cinnamoylsalicin-D	415.1403	461.1461	8.19
Cinnamoylsalicin-E	415.1403	461.1461	8.71
Salicortin-A	423.1297	469.1345	5.23
Salicortin-B	423.1297	469.1345	5.28
Populoside-B-X	431.1354	477.1398	5.80
Populoside-B-G	431.1354	477.1398	6.00
Populoside-B-H	431.1354	477.1398	6.30
Populoside-B-serecia-1	431.1354	477.1398	6.48
Populoside-B-A	431.1354	477.1398	6.63
Populoside-B-B	431.1354	477.1398	6.75
Populoside-B-C	431.1354	477.1398	7.03
Populoside-B-serecia-2	431.1354	477.1398	7.15
Populoside-B-D	431.1354	477.1398	7.30
Populoside-B-E	431.1354	477.1398	7.39
Populoside-B-F	431.1354	477.1398	7.50
Idescarpin-A	439.1250	485.1320	5.56
Idescarpin-B	439.1250	485.1320	6.64

Idescarpin-C	439.1250	485.1320	8.23
Grandidentoside-A	439.1614	485.1664	5.64
Grandidentoside-B	439.1614	485.1664	5.77
Grandidentoside-C	439.1614	485.1664	6.07
Grandidentoside-D	439.1614	485.1664	6.47
Populoside-A-B	447.1302	N/A	5.66
Populoside-A-C	447.1302	N/A	5.87
Populoside-A-D	447.1302	N/A	6.06
Populoside-A-E	447.1302	N/A	6.18
Populoside-A-G	447.1302	N/A	6.75
Populoside-A-idesia-1	447.1310	N/A	6.40
Populoside-A-F	447.1310	N/A	6.61
Populoside-A-A	447.1347	N/A	5.49
Populoside-C-1	461.1453	N/A	7.53
Populoside-C-2	461.1453	N/A	7.59
Acetylsalicortin-A	465.1400	511.1455	6.50
Acetylsalicortin-B	465.1400	511.1455	6.87
Diacetylsalicyloylsalicin	489.1408	535.1467	6.90
Salicortin-7-sulfate	503.0862	N/A	4.82
Diacetylsalicortin-A	507.1508	553.1563	5.64
Diacetylsalicortin-B	507.1508	553.1563	7.96
Salicyloyltremuloidin-A	509.1446	555.1515	9.36
Salicyloyltremuloidin-B	509.1446	555.1515	11.4
Populoside-7-sulfate-A	527.0871	N/A	5.70
Tremulacin-A	527.1555	573.1608	8.55
Tremulacin-B	527.1555	573.1608	9.20
Tremulacin-C	527.1555	573.1608	9.49
Tremulacin-D	527.1555	573.1608	10.46
Tremulacinol	529.1724	575.1778	7.97
Cinnamoylsalicyloylsalicin-A	535.1637	581.1689	9.95
Cinnamoylsalicyloylsalicin-B	535.1637	581.1689	10.23
HCH-deltoidin-A	543.1503	589.1555	7.04
HCH-nigracin-B	543.1503	589.1555	7.29
HCH-nigracin-C	543.1503	589.1555	7.42
HCH-deltoidin-D	543.1503	589.1555	8.13
HCH-deltoidin-E	543.1503	589.1555	8.69
Cinnamoylsalicortin-A	553.1712	599.1773	8.85
Cinnamoylsalicortin-C	553.1712	599.1773	8.95
Cinnamoylsalicortin-B	553.1712	599.1773	9.30
Cinnamoylsalicortin-D	553.1712	599.1773	9.54
Cinnamoylsalicortin-E	553.1712	599.1773	9.85
Cinnamoylsalicortin-F	553.1712	599.1773	10.00
HCH-salicortin-A	561.1622	607.1667	7.00

HCH-salicortin-B	561.1622	607.1667	7.45
HCH-salicortin-C	561.1622	607.1667	7.59
HCH-salicortin-D	561.1622	607.1667	8.36
HCH-salicortin-E	561.1622	607.1667	8.53
HCH-salicortin-F	561.1622	607.1667	8.78
HCH-salicortin-G	561.1622	607.1667	8.99
HCH-salicortin-H	561.1622	607.1667	9.23
HCH-salicortin-I	561.1622	607.1667	9.69
HCH-salicortin-J	561.1622	607.1667	9.83
HCH-salicortin-K	561.1622	607.1667	10.11
Acetyltremulacin	569.1674	615.1727	9.83
HCH-populoside-B-A	569.1674	615.1733	7.77
HCH-populoside-B-B	569.1674	615.1733	7.90
HCH-populoside-B-C	569.1674	615.1733	8.05
HCH-populoside-B-D	569.1674	615.1733	8.14
HCH-populoside-B-E	569.1674	615.1733	8.25
HCH-populoside-B-F	569.1674	615.1733	8.48
HCH-populoside-B-G	569.1674	615.1733	8.65
HCH-populoside-B-H	569.1674	615.1733	8.76
Homaloside-D-1	579.1731	625.1782	5.77
Homaloside-D-2	579.1731	625.1786	6.02
HCH-acetylsalicyloylsalicin-A	585.1622	631.1683	6.73
HCH-acetylsalicyloylsalicin-B	585.1622	631.1683	7.40
HCH-acetylsalicyloylsalicin-C	585.1622	631.1683	7.53
HCH-acetylsalicyloylsalicin-D	585.1622	631.1683	7.73
HCH-acetylsalicyloylsalicin-E	585.1622	631.1683	7.96
HCH-acetylsalicyloylsalicin-F	585.1622	631.1683	8.13
HCH-acetylsalicyloylsalicin-G	585.1622	631.1683	8.23
HCH-acetylsalicyloylsalicin-H	585.1622	631.1683	8.38
Acetylcinnamoylsalicortin-A	595.1823	641.1896	10.55
Acetylcinnamoylsalicortin-B	595.1823	641.1896	10.78
Lasiandrin-A	603.1740	649.1768	8.02
Lasiandrin-B	603.1740	649.1768	8.86
Lasiandrin-C	603.1740	649.1768	9.68
HCH-tremulacin	665.1877	711.1939	9.81
HCH-cinnamoylsalicortin-A	691.2033	737.2099	10.5
HCH-cinnamoylsalicortin-B	691.2033	737.2099	10.7

Table 5. (Pages 176-187) Mean percent relative abundance of salicinoids detected in *Populus* and *Salix* species along with *Idesia polycarpa*. Salicinoids with a value of 100 were the most abundant in all samples of that species, while salicinoids with a value of 95 were on average 95 percent as abundant as the most abundant salicinoid in the samples of that species. Species are listed in alphabetical order, and include *Populus simaroa*, which was not used in the analyses. Salicinoids are listed in order of increasing mass as they are in Table 4.

Species	Salicin	Salirepin	Acetylsalicin-A	Acetylsalicin-B	Salicin-7-sulfate	Salirepin-7-sulfate-A	Salirepin-7-sulfate-B	Tremuloidin-A	Tremuloidin-B	Tremuloidin-C	Tremuloidin-D	Diglucoside-salicin-A
Idesia polycarpa	1.591	9.181	1.077	0.002	1.544	0.003	54.906	0.018	0.390	0.022	0.000	0.033
Populus afghanica	26.777	0.077	0.586	0.025	0.016	0.001	0.000	0.198	0.024	0.283	0.367	0.255
Populus alba	57.507	0.396	1.140	0.005	8.006	0.693	0.038	0.119	15.787	0.897	0.078	0.053
Populus angustifolia	17.586	0.000	65.409	0.332	2.253	0.010	0.002	76.081	10.459	0.620	0.028	1.987
Populus balsamifera	34.863	0.298	0.845	0.010	1.898	0.000	0.031	0.080	4.347	0.322	0.058	0.115
Populus deltoides	40.311	0.338	1.928	0.043	41.457	0.055	0.660	0.027	0.009	0.147	0.001	0.124
Populus fremontii	3.132	0.022	0.200	0.001	90.996	0.004	0.304	0.002	0.001	0.024	0.006	0.000
Populus grandidentata	51.675	0.373	1.661	0.086	1.188	0.005	0.004	0.506	26.841	0.393	0.031	0.139
Populus guzmanantlensis	13.152	0.034	0.117	0.002	6.972	0.000	0.052	0.046	10.586	3.415	0.020	0.030
Populus heterophylla	10.664	0.064	10.216	0.813	11.391	14.350	0.070	0.400	0.229	0.094	0.038	7.647
Populus koreana	14.409	0.100	0.270	0.003	0.002	0.000	0.000	0.064	2.025	0.309	0.275	0.100
Populus luziarum	6.085	0.024	0.193	0.000	7.191	0.001	0.025	0.016	3.014	1.289	0.009	0.026
Populus maximowiczii	23.949	0.111	0.490	0.200	16.867	0.038	0.092	0.053	0.016	0.081	0.025	0.334
Populus mexicana	44.763	0.195	1.722	0.003	2.875	0.017	0.016	0.206	21.088	0.308	0.086	0.059
Populus monticola	1.500	0.003	0.462	0.000	10.822	0.008	0.028	0.072	3.788	0.293	0.000	0.015
Populus nigra	19.100	0.077	0.388	0.000	0.002	0.001	0.000	0.059	0.008	1.700	1.124	0.059
Populus primaveralepensis	6.305	0.029	0.213	0.000	11.358	0.001	0.040	0.033	3.557	1.236	0.009	0.025
Populus purdomii	12.237	0.066	0.378	0.041	0.835	0.000	0.007	0.036	0.001	0.025	0.002	0.594
Populus simaroa	5.396	0.016	0.079	0.001	7.469	0.005	0.023	0.007	4.209	0.297	0.008	0.009
Populus szechuanica	10.276	0.049	0.157	0.725	6.203	0.000	0.023	0.004	1.527	0.058	0.177	0.036
Populus tremula	16.305	0.080	0.150	3.265	8.262	0.001	0.016	0.355	7.255	0.321	0.024	0.032
Populus tremuloides	35.574	0.179	2.952	0.011	0.014	0.002	0.001	0.262	23.188	0.183	0.069	0.425
Populus trichocarpa	77.794	0.639	5.412	0.005	0.471	0.009	0.001	1.454	24.607	0.466	0.038	0.865
Populus yunnanensis	17.126	0.062	0.599	0.002	1.085	0.000	0.008	0.068	4.477	0.260	0.041	0.041
Salix acutifolia	5.667	0.000	11.432	1.507	12.063	5.539	0.148	8.760	0.193	0.114	0.004	1.205
Salix alba	17.424	0.000	1.769	1.022	87.144	0.135	0.491	0.373	1.026	0.022	0.089	0.193
Salix amygdaloides	15.409	0.024	1.678	0.007	22.519	0.104	0.064	3.196	7.045	0.085	0.017	0.068
Salix appendiculata	66.545	0.000	37.697	0.000	100.000	0.038	0.092	27.671	0.735	19.415	0.009	0.620
Salix bebbiana	43.276	0.000	13.427	0.134	25.030	0.016	0.015	3.312	0.067	0.097	0.001	1.070
Salix candida	2.285	0.000	100.000	0.000	0.428	0.007	0.000	40.679	0.256	0.820	0.000	3.882
Salix caprea	67.114	0.000	5.224	0.086	2.558	0.005	0.033	2.479	6.035	1.006	0.001	0.298
Salix cinerea	3.524	0.000	11.965	0.041	0.746	0.012	0.005	16.984	0.082	0.153	0.000	3.046
Salix discolor	79.000	0.260	0.963	0.000	1.601	0.008	0.010	0.234	5.665	0.084	0.000	0.200
Salix eleagnos	16.265	0.135	0.135	0.004	0.551	0.000	0.002	0.111	4.840	0.020	0.004	0.143
Salix eriocephala	55.752	0.048	11.529	0.261	11.083	0.010	0.011	1.816	1.858	0.135	0.000	13.710
Salix gracilistyla	54.889	0.000	6.458	0.000	42.353	0.057	0.071	1.733	0.104	0.689	0.005	3.696
Salix hastata	26.581	0.000	0.762	0.768	100.000	0.019	0.376	0.029	9.894	0.041	0.021	0.106
Salix humilis	36.540	0.206	0.208	0.013	0.473	0.002	0.004	0.170	24.945	0.162	0.046	0.120
Salix integra	55.107	0.000	4.302	0.030	81.983	0.003	0.010	0.766	0.067	0.158	0.000	24.345
Salix interior	100.000	0.000	5.284	10.708	39.778	0.039	0.380	8.992	0.082	0.044	0.002	38.994
Salix irrorata	19.609	0.244	0.514	0.002	0.139	0.000	0.001	0.224	16.540	0.326	0.058	0.051
Salix jessoensis	70.769	0.000	4.565	0.000	13.297	0.072	0.042	17.507	1.407	0.191	0.000	0.712
Salix matsudana	8.219	0.000	0.455	0.134	43.879	0.041	0.774	0.039	0.005	0.002	0.000	0.047
Salix miyabeana	89.731	0.862	0.186	0.046	4.485	0.006	0.005	0.031	0.380	0.015	0.025	1.274
Salix myricoides	15.487	0.116	0.131	0.061	14.001	0.000	0.042	0.020	7.159	0.097	0.001	1.696
Salix nigra	22.471	0.097	0.762	0.061	8.716	0.106	0.071	1.033	7.666	0.205	0.013	0.164
Salix pentandra	6.016	0.010	0.308	16.953	7.979	0.003	0.067	0.084	0.978	0.089	0.001	0.068
Salix purpurea	34.703	0.186	0.208	0.004	0.233	0.000	0.000	0.387	10.853	0.121	0.002	1.205
Salix repens	45.291	0.745	0.000	0.000	0.857	0.001	0.000	0.014	5.264	0.035	0.004	0.490
Salix sericea	25.988	0.281	0.078	2.645	4.430	0.000	0.004	0.011	3.776	0.173	0.086	0.018
Salix serissima	18.276	0.077	0.230	14.506	17.527	0.000	0.041	0.029	0.094	0.026	0.001	0.016
Salix triandra	6.676	0.000	20.268	0.000	0.462	0.103	0.000	1.390	0.279	0.106	0.036	1.984
Salix udensis	22.918	0.000	36.289	0.057	0.394	0.011	0.000	56.027	0.283	1.853	0.009	5.088

Species	Diglucoside-salicin-B	Diglucoside-salicin-C	Nigracin-A	Deltoidin-B	Deltoidin-C	Salicyloylsalicin-A	Salicyloylsalicin-B	Cinnamoylsalicin-A	Cinnamoylsalicin-C	Cinnamoylsalicin-B	Cinnamoylsalicin-D
Idesia polycarpa	1.625	0.822	0.296	1.801	0.288	0.017	0.006	9.911	0.039	0.006	0.079
Populus afghanica	0.168	1.270	2.029	0.057	0.344	0.016	0.631	1.194	0.722	0.236	0.684
Populus alba	0.118	1.940	0.389	0.175	0.087	0.131	0.144	0.128	0.004	0.026	0.003
Populus angustifolia	2.471	10.999	1.301	3.048	4.571	0.349	0.101	21.371	0.004	2.434	0.022
Populus balsamifera	0.087	1.313	5.179	27.125	0.329	0.076	0.080	2.145	0.004	0.419	0.001
Populus deltoides	0.087	2.596	1.284	1.640	0.376	0.107	0.040	2.772	0.001	0.235	0.002
Populus fremontii	0.007	0.004	0.005	0.049	0.176	0.022	0.177	0.041	0.011	0.000	0.004
Populus grandidentata	0.097	2.190	0.254	0.941	0.654	0.114	0.177	0.745	3.417	0.218	0.762
Populus guzmanantlensis	0.061	0.679	2.542	0.271	0.316	0.010	0.043	1.514	0.004	0.410	0.003
Populus heterophylla	0.972	4.377	83.377	2.521	0.417	0.058	0.025	3.287	0.125	0.133	0.023
Populus koreana	0.056	0.489	3.882	0.188	0.033	0.000	0.060	2.078	0.008	0.697	0.007
Populus luziarum	0.031	0.366	2.664	0.030	0.088	0.071	0.077	0.001	0.002	0.000	0.001
Populus maximowiczii	0.516	0.843	54.672	1.566	0.388	0.012	0.195	0.822	0.012	0.123	0.009
Populus mexicana	0.083	1.174	1.048	0.434	0.252	0.568	0.074	3.815	0.006	0.697	0.004
Populus monticola	0.023	0.395	0.457	0.047	0.066	0.090	0.125	0.212	0.001	0.034	0.001
Populus nigra	0.055	1.008	9.212	0.037	0.167	0.016	0.081	1.592	0.016	0.514	0.004
Populus primaveralepensis	0.046	0.404	2.424	0.045	0.152	0.092	0.093	0.045	0.002	0.000	0.002
Populus purdomii	0.113	0.340	1.312	0.150	0.063	0.008	0.027	0.027	0.002	0.000	0.002
Populus simaroa	0.004	0.123	0.213	0.516	0.059	0.179	0.164	0.682	0.000	0.135	0.002
Populus szechuanica	0.025	0.972	6.353	0.132	0.051	0.007	0.065	0.000	0.027	0.000	0.016
Populus tremula	0.022	0.359	0.118	0.054	0.073	0.054	0.194	0.015	0.618	0.005	0.648
Populus tremuloides	0.235	7.758	0.558	0.883	0.605	0.234	0.198	0.467	0.009	0.099	0.005
Populus trichocarpa	0.279	5.153	16.022	54.946	0.294	0.090	0.076	8.339	0.020	2.307	0.012
Populus yunnanensis	0.218	0.246	9.182	16.717	0.093	0.038	0.061	2.630	0.006	0.722	0.000
Salix acutifolia	62.544	100.000	4.254	7.793	1.796	0.022	0.029	0.112	0.007	0.010	0.000
Salix alba	1.999	11.389	0.172	0.202	0.765	0.006	0.041	0.157	0.026	0.002	0.024
Salix amygdaloides	0.622	4.135	0.110	0.427	3.934	0.236	0.384	3.351	0.009	0.973	0.005
Salix appendiculata	1.107	1.213	2.145	2.670	8.883	0.230	0.093	0.054	0.000	0.000	0.009
Salix bebbiana	1.186	70.272	0.818	0.735	4.854	0.025	0.025	0.003	0.000	0.001	0.001
Salix candida	3.830	24.503	1.177	0.824	0.086	0.000	0.000	0.011	0.000	0.000	0.000
Salix caprea	0.420	19.836	1.195	0.988	0.495	0.071	0.058	0.012	0.000	0.000	0.002
Salix cinerea	4.120	100.000	2.143	1.279	0.363	0.002	0.000	0.019	0.005	0.000	0.010
Salix discolor	0.710	5.229	2.601	0.306	1.118	0.092	0.460	0.053	0.029	0.006	0.016
Salix eleagnos	0.042	2.106	0.023	0.118	1.350	0.043	0.297	0.003	0.005	0.000	0.014
Salix eriocephala	3.229	34.428	13.237	2.782	4.741	0.183	0.164	0.436	0.037	0.140	0.027
Salix gracilistyla	6.249	100.000	2.014	1.029	0.643	0.000	0.014	0.011	0.000	0.000	0.003
Salix hastata	1.165	0.568	0.250	0.196	0.436	0.009	0.076	0.206	0.120	0.007	0.072
Salix humilis	0.095	3.394	0.285	0.234	0.631	0.024	0.951	0.254	0.057	0.047	0.061
Salix integra	2.709	13.250	2.600	1.122	1.152	0.034	0.065	0.003	0.000	0.000	0.010
Salix interior	31.602	71.956	0.492	2.778	15.144	0.077	0.054	0.042	0.003	0.008	0.002
Salix irrorata	0.053	0.950	0.305	0.048	1.247	0.053	1.117	0.059	0.037	0.004	0.018
Salix jessoensis	20.892	42.646	1.063	6.300	16.324	0.214	0.137	61.964	0.024	6.146	0.009
Salix matsudana	1.059	2.788	0.399	0.027	0.305	0.003	0.132	2.695	0.012	0.476	0.009
Salix miyabeana	0.607	1.425	4.254	0.236	0.489	0.000	2.323	0.001	0.001	0.001	0.001
Salix myricoides	0.303	1.500	0.268	0.089	0.211	0.007	0.478	0.000	0.207	0.000	0.231
Salix nigra	3.334	5.648	0.069	0.440	2.723	0.087	0.311	6.171	0.031	1.070	0.045
Salix pentandra	0.536	1.125	0.137	0.071	0.315	0.004	0.112	0.113	0.004	0.016	0.005
Salix purpurea	0.583	5.452	1.271	0.246	0.631	0.008	0.453	0.012	0.005	0.000	0.002
Salix repens	0.312	10.002	1.197	0.156	1.330	0.008	0.167	0.043	0.000	0.000	0.001
Salix sericea	0.253	0.532	0.062	0.052	0.641	0.036	0.223	1.922	0.330	0.360	0.547
Salix serissima	0.360	0.280	0.106	0.048	0.259	0.000	0.251	0.263	0.005	0.001	0.004
Salix triandra	2.373	100.000	4.457	1.047	5.564	0.149	0.018	0.243	0.000	0.018	0.008
Salix udensis	13.015	100.000	2.724	12.932	34.040	1.464	0.173	0.995	2.186	0.154	1.318

Species	Cinnamoylsalicin-E	Salicortin-A	Salicortin-B	Populoside-B-X	Populoside-B-G	Populoside-B-H	Populoside-B-serecia-1	Populoside-B-A	Populoside-B-B	Populoside-B-C	Populoside-B-serecia-2	Populoside-B-D
Idesia polycarpa	0.000	0.000	3.671	0.018	5.641	0.080	2.414	0.072	13.386	1.154	0.039	0.003
Populus afghanica	0.057	65.333	100.000	0.087	0.012	12.630	0.042	13.488	1.311	0.063	0.830	0.026
Populus alba	0.015	17.120	74.609	0.035	0.010	2.779	0.079	2.490	0.293	0.006	0.086	0.114
Populus angustifolia	0.002	0.000	100.000	0.605	0.493	0.226	0.111	0.349	5.727	0.000	0.077	0.000
Populus balsamifera	0.005	26.510	100.000	0.183	0.026	4.844	0.422	4.857	8.079	0.135	0.189	0.511
Populus deltoides	0.001	58.606	56.412	1.053	0.031	6.810	1.427	2.969	14.380	0.076	0.348	2.610
Populus fremontii	0.008	23.659	38.849	0.060	0.052	0.061	0.011	0.008	1.091	0.814	0.000	2.376
Populus grandidentata	0.008	0.000	72.896	0.060	0.017	1.321	0.044	1.472	0.716	0.003	0.311	0.011
Populus guzmanantlensis	0.000	0.000	100.000	0.089	0.006	0.525	0.059	0.569	0.859	0.003	0.011	0.060
Populus heterophylla	0.006	26.905	38.465	0.044	0.150	0.440	0.507	0.586	1.403	0.068	0.043	0.002
Populus koreana	0.003	0.000	100.000	0.024	0.005	0.164	0.060	0.198	4.055	0.405	0.190	0.850
Populus luziarum	0.000	0.000	100.000	0.059	0.003	0.007	0.011	0.001	0.027	0.003	0.006	0.083
Populus maximowiczii	0.003	57.141	76.066	0.259	0.048	7.484	0.967	9.541	3.997	0.568	0.748	0.781
Populus mexicana	0.168	2.190	73.866	0.003	0.003	1.604	0.165	1.575	1.112	0.000	0.438	0.004
Populus monticola	0.000	0.000	100.000	0.004	0.002	0.061	0.002	0.033	0.008	0.000	0.001	0.037
Populus nigra	0.014	0.000	100.000	0.066	0.005	2.151	0.021	2.677	0.904	0.000	0.670	0.031
Populus primaveralepensis	0.000	0.000	100.000	0.045	0.003	0.010	0.008	0.001	0.054	0.004	0.008	0.070
Populus purdomii	0.003	0.000	100.000	0.043	0.008	0.019	0.207	0.167	1.961	0.241	0.295	0.115
Populus simaroa	0.000	0.000	100.000	0.003	0.001	0.080	0.023	0.053	0.352	0.001	0.001	0.001
Populus szechuanica	0.005	0.000	100.000	0.013	0.002	0.006	0.049	0.011	0.342	0.435	0.333	0.001
Populus tremula	0.044	0.000	100.000	0.004	0.002	0.003	0.000	0.001	0.118	0.014	0.139	0.008
Populus tremuloides	0.003	0.000	83.619	0.045	0.012	0.060	0.849	0.549	0.592	0.010	0.404	0.066
Populus trichocarpa	0.006	21.671	73.002	0.053	0.044	0.538	0.055	0.488	4.242	0.149	0.161	0.320
Populus yunnanensis	0.008	0.000	100.000	0.020	0.037	10.918	0.180	11.584	3.858	0.036	0.243	0.040
Salix acutifolia	0.000	4.723	10.257	0.798	0.411	1.462	0.000	0.000	0.338	0.000	0.000	0.401
Salix alba	0.036	16.698	12.521	0.360	0.121	0.640	0.009	0.005	0.616	0.205	0.175	2.244
Salix amygdaloides	0.137	0.000	89.858	0.043	0.283	0.815	0.046	1.347	0.737	0.010	0.287	0.019
Salix appendiculata	0.000	4.335	15.478	0.196	0.679	0.289	1.765	0.395	0.148	0.000	0.047	0.023
Salix bebbiana	0.000	0.000	6.053	0.000	0.008	0.006	0.021	0.048	0.049	0.000	0.000	0.000
Salix candida	0.000	0.000	1.580	0.000	0.000	0.000	0.000	0.000	0.000	0.000	0.000	0.000
Salix caprea	0.000	0.000	100.000	0.000	0.000	0.441	0.309	0.104	0.051	0.000	0.000	5.240
Salix cinerea	0.000	0.289	1.149	0.264	0.126	0.386	0.035	0.023	0.043	0.046	0.006	0.023
Salix discolor	0.009	0.000	100.000	0.224	0.352	0.159	0.000	0.033	1.222	0.012	0.528	0.016
Salix eleagnos	0.004	0.000	100.000	0.063	0.849	0.006	0.002	0.001	0.144	0.002	0.142	0.001
Salix eriocephala	0.008	0.000	80.519	0.159	1.468	0.230	0.004	0.135	0.497	0.387	0.182	0.002
Salix gracilistyla	0.000	0.989	3.180	0.000	0.000	0.045	0.000	0.000	0.000	0.000	0.000	0.000
Salix hastata	0.429	29.625	21.461	0.129	0.027	0.162	0.146	0.012	3.215	0.229	1.774	4.811
Salix humilis	0.029	0.000	83.622	0.124	0.127	0.633	0.043	0.795	0.815	0.008	0.555	0.011
Salix integra	0.000	0.207	6.879	0.000	0.000	0.099	0.018	0.031	0.000	0.001	0.001	0.007
Salix interior	0.000	38.578	31.668	0.092	0.044	0.180	0.007	0.007	0.100	0.010	0.017	0.036
Salix irrorata	1.075	0.000	70.077	0.000	0.011	0.007	0.018	0.003	0.934	0.039	0.450	0.186
Salix jessoensis	0.000	0.000	100.000	0.000	0.107	7.615	0.478	3.797	16.309	0.088	0.035	0.194
Salix matsudana	0.038	37.869	21.418	0.031	0.039	12.838	0.611	13.869	1.775	0.062	0.287	0.060
Salix miyabeana	0.011	0.000	100.000	0.003	0.010	0.050	0.000	0.000	0.373	0.012	0.249	0.010
Salix myricoides	0.001	0.000	100.000	0.001	0.697	0.197	0.085	0.051	0.014	0.001	0.008	0.001
Salix nigra	1.380	41.934	83.569	0.015	0.031	17.995	0.141	17.454	3.960	0.027	2.222	0.052
Salix pentandra	0.109	2.288	3.769	0.033	0.006	0.063	0.016	0.037	0.398	0.016	0.114	0.512
Salix purpurea	0.003	0.000	100.000	0.002	0.129	0.038	0.019	0.009	0.085	0.006	0.037	0.000
Salix repens	0.001	0.000	100.000	0.019	0.003	0.041	0.000	0.002	0.143	0.004	0.141	0.282
Salix sericea	0.408	0.000	100.000	0.008	3.144	0.495	1.691	0.857	1.204	0.028	0.944	0.010
Salix serissima	0.023	6.622	9.475	0.004	0.015	0.009	0.137	0.117	0.103	0.015	0.057	4.409
Salix triandra	0.000	2.587	8.631	0.081	0.370	3.444	0.000	0.390	0.303	0.049	0.000	0.010
Salix udensis	0.150	0.869	3.063	1.205	0.348	6.860	0.000	0.967	1.984	0.539	0.234	0.274

Species	Populoside-B-E	Populoside-B-F	Idescarpin-A	Idescarpin-B	Idescarpin-C	Grandidentoside-A	Grandidentoside-B	Grandidentoside-C	Grandidentoside-D	Populoside-A-B	Populoside-A-C	Populoside-A-D
Idesia polycarpa	0.149	0.027	100.000	0.632	0.564	0.256	1.795	0.178	0.011	0.041	0.228	0.186
Populus afghanica	0.050	0.012	0.899	0.000	0.000	1.057	4.045	1.309	0.399	3.493	0.000	3.583
Populus alba	0.113	0.001	0.822	0.006	0.000	1.385	0.227	0.112	0.214	0.218	0.743	3.189
Populus angustifolia	0.113	0.048	0.753	0.002	0.002	2.071	1.433	1.205	0.423	0.169	0.000	1.652
Populus balsamifera	0.617	0.038	1.450	0.003	0.000	10.105	11.513	5.323	1.998	1.750	4.618	2.343
Populus deltoides	1.769	0.289	1.365	0.000	0.000	19.080	8.145	2.944	3.852	6.559	4.416	0.994
Populus fremontii	1.607	0.125	1.444	0.002	0.000	5.346	7.151	0.091	0.013	0.056	0.219	0.069
Populus grandidentata	0.058	0.001	0.725	0.005	0.000	1.133	0.160	0.077	0.276	0.110	0.092	0.171
Populus guzmanantlensis	0.186	0.001	0.537	0.006	0.000	1.785	0.160	0.054	0.361	0.061	0.380	0.039
Populus heterophylla	0.071	0.002	1.137	0.001	0.000	2.548	2.125	0.082	0.148	0.038	0.028	0.159
Populus koreana	0.080	0.023	1.249	0.000	0.000	2.348	3.345	1.173	0.784	0.133	0.737	1.531
Populus luziarum	0.037	0.000	0.730	0.000	0.000	0.078	0.067	0.069	0.001	0.004	0.179	0.023
Populus maximowiczii	0.953	0.057	2.007	0.004	0.000	8.598	4.536	1.719	0.869	3.129	4.126	1.993
Populus mexicana	0.113	0.000	0.337	0.005	0.000	1.146	0.461	0.096	0.194	0.116	0.018	0.062
Populus monticola	0.026	0.000	0.647	0.000	0.000	0.079	0.005	0.007	0.014	0.003	0.003	0.002
Populus nigra	0.000	0.004	0.757	0.011	0.000	0.728	0.104	0.076	0.186	0.300	0.018	0.428
Populus primaveralepensis	0.029	0.000	0.771	0.000	0.000	0.091	0.085	0.077	0.007	0.005	0.283	0.027
Populus purdomii	0.230	0.001	1.233	0.019	0.000	7.293	4.067	1.297	0.240	0.035	2.594	1.436
Populus simaroa	0.056	0.002	0.629	0.000	0.002	0.730	0.064	0.017	0.144	0.010	0.186	0.012
Populus szechuanica	0.063	0.061	0.989	0.001	0.000	0.972	4.372	1.352	0.262	0.008	0.722	1.959
Populus tremula	0.009	0.001	0.545	0.002	0.000	0.003	0.198	0.087	0.045	0.001	0.004	0.024
Populus tremuloides	0.023	0.006	0.836	0.004	0.000	0.341	0.230	0.087	0.045	0.025	0.086	0.252
Populus trichocarpa	0.044	0.015	0.676	0.007	0.000	1.611	4.349	3.898	1.228	0.155	0.238	0.725
Populus yunnanensis	0.000	0.000	0.874	0.007	0.000	6.000	2.344	1.075	0.984	2.134	1.372	0.660
Salix acutifolia	0.289	0.000	0.000	0.000	0.011	4.177	2.530	1.534	0.596	0.817	0.365	3.163
Salix alba	1.180	0.000	0.187	0.000	0.000	4.098	3.875	3.003	0.960	0.418	0.538	1.983
Salix amygdaloides	0.108	0.021	1.305	0.000	0.000	0.398	0.252	0.151	0.167	0.075	0.006	0.062
Salix appendiculata	0.074	0.008	0.000	0.000	0.016	0.156	0.150	2.312	0.136	0.172	0.101	0.308
Salix bebbiana	0.014	0.000	0.022	0.004	0.004	0.304	0.052	0.388	0.566	0.046	0.015	0.223
Salix candida	0.000	0.000	0.000	0.031	0.013	0.081	0.239	3.128	1.174	0.035	0.016	0.408
Salix caprea	3.179	0.000	0.678	0.000	0.000	0.114	0.072	0.187	0.098	0.223	0.025	0.074
Salix cinerea	0.025	0.002	0.000	0.000	0.018	0.212	0.142	1.080	0.436	0.160	0.264	1.580
Salix discolor	0.000	0.000	0.883	0.001	0.000	0.011	0.407	0.685	0.076	0.084	0.008	0.785
Salix eleagnos	0.001	0.001	1.501	0.010	0.000	0.001	0.024	0.020	0.007	0.006	0.001	0.025
Salix eriocephala	0.004	0.001	1.288	0.000	0.000	0.190	0.238	0.270	0.102	0.234	0.011	1.481
Salix gracilistyla	0.000	0.000	0.000	0.000	0.002	0.140	0.063	0.153	0.068	0.050	0.013	0.085
Salix hastata	3.073	0.069	0.129	0.001	0.001	1.518	2.471	1.687	0.670	0.134	0.127	2.249
Salix humilis	0.004	0.003	0.569	0.000	0.000	0.050	0.166	0.187	0.051	0.028	0.004	0.188
Salix integra	0.012	0.003	0.032	0.003	0.003	0.039	0.017	0.043	0.038	0.030	0.006	0.006
Salix interior	0.031	0.289	0.256	0.000	0.000	0.112	0.146	0.283	0.087	0.118	0.143	0.478
Salix irrorata	0.020	0.034	1.106	0.000	0.000	0.000	0.007	0.156	0.074	0.200	0.010	0.150
Salix jessoensis	1.415	0.054	0.532	0.000	0.000	8.151	1.372	0.957	1.287	1.098	0.022	1.487
Salix matsudana	0.096	0.015	0.608	0.000	0.000	2.295	5.415	2.609	1.002	0.737	0.115	0.700
Salix miyabeana	0.004	0.000	1.434	0.000	0.001	0.001	0.104	0.231	0.046	0.006	0.006	0.395
Salix myricoides	0.001	0.001	1.192	0.007	0.000	0.036	0.091	0.034	0.007	0.007	0.003	0.014
Salix nigra	0.156	0.009	1.987	0.005	0.000	1.128	0.318	0.310	0.335	0.805	0.004	0.693
Salix pentandra	0.510	0.010	0.045	0.000	0.000	1.406	0.871	0.614	0.461	0.298	0.078	0.255
Salix purpurea	0.001	0.000	1.124	0.005	0.000	0.015	0.053	0.065	0.006	0.020	0.002	0.105
Salix repens	0.348	0.000	1.647	0.047	0.000	0.025	0.442	0.346	0.069	0.002	0.001	0.148
Salix sericea	0.007	0.001	1.534	0.009	0.000	0.170	0.110	0.057	0.045	0.012	0.132	0.177
Salix serissima	4.293	0.000	0.057	0.000	0.000	0.003	0.292	0.207	0.069	0.010	0.003	0.103
Salix triandra	0.030	0.000	0.000	0.266	0.000	0.297	0.362	0.835	0.527	4.461	5.365	5.269
Salix udensis	0.146	0.668	0.000	0.008	0.004	0.196	0.703	1.399	0.669	1.061	28.595	22.847

Species	Populoside-A-E	Populoside-A-G	Populoside-A-idesia-1	Populoside-A-F	Populoside-A-A	Populoside-C-1	Populoside-C-2	Acetylsalicortin-A	Acetylsalicortin-B	Diacetylsalicyloylsalicin	Salicortin-7-sulfate
Idesia polycarpa	0.023	0.027	2.041	1.020	0.078	0.463	0.556	0.049	0.000	0.002	0.001
Populus afghanica	0.706	0.019	0.029	0.027	3.550	0.000	0.000	0.124	0.010	0.004	0.003
Populus alba	0.142	0.175	0.009	0.836	0.016	0.028	0.014	0.014	0.000	0.001	0.164
Populus angustifolia	0.512	0.000	0.147	4.455	0.155	0.074	0.000	0.153	1.239	0.034	0.166
Populus balsamifera	0.614	1.470	0.054	12.131	0.161	0.099	0.010	0.133	0.002	0.347	0.082
Populus deltoides	1.868	5.803	0.132	31.405	3.783	0.515	0.110	0.087	0.023	4.542	26.813
Populus fremontii	0.048	6.634	0.119	19.883	0.100	0.722	0.604	0.001	0.001	0.000	22.313
Populus grandidentata	0.078	0.028	0.006	0.080	0.061	0.007	0.004	0.065	0.006	0.003	0.001
Populus guzmanantlensis	0.083	0.142	0.004	0.601	0.112	0.027	0.014	0.014	0.001	0.000	0.025
Populus heterophylla	0.009	0.247	0.006	0.191	0.015	0.011	0.050	5.861	0.009	0.002	0.304
Populus koreana	0.146	0.034	0.074	0.092	0.009	0.023	0.000	0.066	0.045	0.060	0.000
Populus luziarum	0.202	0.057	0.001	0.239	0.004	0.241	0.108	0.025	0.000	0.000	0.065
Populus maximowiczii	2.013	3.098	0.238	10.029	0.996	0.366	0.173	0.089	0.038	17.170	5.045
Populus mexicana	0.027	0.007	0.010	0.004	0.000	0.000	0.000	0.009	0.001	0.000	0.008
Populus monticola	0.010	0.009	0.002	0.040	0.003	0.010	0.004	0.009	0.000	0.000	0.159
Populus nigra	0.097	0.062	0.004	0.248	0.376	0.020	0.006	0.031	0.013	0.000	0.000
Populus primaveralepensis	0.240	0.048	0.002	0.218	0.005	0.141	0.058	0.029	0.001	0.000	0.080
Populus purdomii	0.337	0.603	0.083	2.989	0.118	0.034	0.012	0.363	0.003	0.003	0.011
Populus simaroa	0.023	0.006	0.002	0.031	0.001	0.000	0.000	0.021	0.001	0.000	0.018
Populus szechuanica	0.084	0.095	0.016	0.502	0.028	0.000	0.002	1.613	0.013	1.584	0.023
Populus tremula	0.002	0.028	0.000	0.058	0.000	0.009	0.002	16.343	0.404	0.000	0.042
Populus tremuloides	0.095	0.037	0.003	0.182	0.022	0.021	0.015	0.040	0.001	0.013	0.001
Populus trichocarpa	0.116	0.060	0.036	0.156	0.038	0.037	0.001	0.088	0.000	0.005	0.020
Populus yunnanensis	0.687	0.123	0.020	0.566	0.015	0.015	0.000	0.019	0.000	0.001	0.099
Salix acutifolia	0.139	0.105	0.029	0.699	0.063	0.006	0.000	8.535	0.021	0.014	0.132
Salix alba	0.037	0.868	0.061	5.039	0.028	0.161	0.050	13.106	0.121	0.045	13.979
Salix amygdaloides	0.043	0.077	0.002	0.021	0.071	0.042	0.000	0.017	0.002	0.001	0.007
Salix appendiculata	0.065	0.183	0.007	0.150	0.009	0.000	0.000	0.211	2.564	0.020	0.000
Salix bebbiana	0.005	0.011	0.037	0.088	0.002	0.000	0.000	0.451	0.024	0.143	0.064
Salix candida	0.142	0.142	0.014	0.028	0.010	0.000	0.000	0.107	0.047	0.000	0.100
Salix caprea	0.059	0.148	0.000	0.766	0.004	0.014	0.013	0.671	6.381	0.032	0.007
Salix cinerea	0.347	0.081	0.028	0.102	0.079	0.005	0.002	0.126	0.018	0.025	0.041
Salix discolor	0.039	0.028	0.000	0.028	0.008	0.006	0.003	0.021	0.083	0.006	0.010
Salix eleagnos	0.006	0.002	0.001	0.002	0.001	0.000	0.000	0.275	7.241	0.001	0.000
Salix eriocephala	0.028	0.050	0.011	0.247	0.007	0.000	0.000	0.064	0.040	0.015	0.068
Salix gracilistyla	0.008	0.023	0.003	0.060	0.005	0.000	0.003	0.340	0.096	0.005	0.016
Salix hastata	0.035	1.372	0.032	8.055	0.026	0.253	0.090	8.721	0.204	0.212	13.029
Salix humilis	0.006	0.019	0.002	0.004	0.283	0.003	0.003	0.054	0.000	0.006	0.003
Salix integra	0.006	0.003	0.002	0.047	0.007	0.001	0.000	0.209	0.065	0.004	0.028
Salix interior	0.177	0.111	0.007	0.118	0.014	0.042	0.002	75.639	0.000	0.002	0.403
Salix irrorata	0.022	0.002	0.011	0.005	0.000	0.002	0.002	0.039	0.094	0.004	0.000
Salix jessoensis	0.146	0.061	0.007	0.159	0.034	0.128	0.025	0.038	0.023	0.000	0.046
Salix matsudana	0.153	0.010	0.027	0.051	0.005	0.003	0.003	1.006	0.316	0.009	24.889
Salix miyabeana	0.002	0.002	0.024	0.007	0.006	0.016	0.016	0.003	0.008	0.001	0.004
Salix myricoides	0.002	0.003	0.000	0.001	0.000	0.003	0.002	0.659	0.004	0.000	0.004
Salix nigra	0.174	0.088	0.069	0.005	0.012	0.000	0.000	0.028	0.002	0.002	0.053
Salix pentandra	0.059	0.047	0.036	0.250	0.054	0.004	0.116	100.000	0.991	0.003	1.011
Salix purpurea	0.005	0.004	0.002	0.007	0.009	0.003	0.004	0.005	0.001	0.002	0.100
Salix repens	0.015	0.044	0.001	0.231	0.003	0.055	0.032	0.007	0.006	0.002	0.002
Salix sericea	0.009	0.048	0.004	0.001	0.006	0.086	0.086	3.755	0.001	0.001	0.003
Salix serissima	0.000	0.128	0.023	0.664	0.000	0.345	0.161	100.000	0.128	0.003	1.106
Salix triandra	0.290	0.010	0.010	0.082	0.036	0.094	0.094	0.452	0.030	0.088	0.291
Salix udensis	1.843	1.687	0.608	0.162	1.084	0.005	0.010	0.443	0.026	0.343	0.040

Species	Diacetylsalicortin-A	Diacetylsalicortin-B	Salicyloyltremuloidin-A	Salicyloyltremuloidin-B	Populoside-7-sulfate-A	Tremulacin-A	Tremulacin-B	Tremulacin-C	Tremulacin-D	Tremulacinol
Idesia polycarpa	0.012	0.000	0.007	0.003	0.002	2.957	0.000	0.000	0.004	0.092
Populus afghanica	0.150	0.005	0.102	0.000	0.025	0.035	0.166	0.002	0.003	0.000
Populus alba	0.176	0.002	0.002	0.017	0.091	75.566	0.088	0.000	0.313	2.221
Populus angustifolia	0.269	0.078	0.034	0.014	0.169	0.732	0.023	0.000	0.000	0.030
Populus balsamifera	1.246	0.001	0.042	0.013	0.040	36.336	0.149	0.008	0.242	4.822
Populus deltoides	2.228	0.001	0.000	0.000	3.726	0.037	0.000	0.000	0.000	0.012
Populus fremontii	0.227	0.000	0.000	0.000	1.579	0.052	0.000	0.005	0.000	0.000
Populus grandidentata	0.144	0.003	0.001	0.040	0.001	89.538	0.095	0.000	0.358	4.077
Populus guzmanantlensis	0.047	0.002	0.143	0.030	0.029	80.697	0.196	0.002	0.697	5.265
Populus heterophylla	0.316	0.001	0.354	0.018	0.000	6.401	0.019	0.129	0.000	0.120
Populus koreana	0.313	0.015	0.124	0.007	0.002	21.552	0.195	0.000	0.073	2.630
Populus luziarum	0.003	0.000	0.013	0.046	0.148	67.189	0.002	0.000	0.106	0.840
Populus maximowiczii	1.111	0.002	0.015	0.000	0.537	0.024	0.001	0.078	0.001	0.006
Populus mexicana	0.082	0.001	0.000	0.077	0.000	98.557	0.063	0.000	0.425	4.335
Populus monticola	0.001	0.000	0.000	0.067	0.003	85.999	0.049	0.000	0.126	1.441
Populus nigra	0.099	0.013	0.271	0.000	0.014	0.000	0.276	0.001	0.043	0.000
Populus primaveralepensis	0.003	0.000	0.015	0.057	0.255	68.922	0.002	0.000	0.146	1.113
Populus purdomii	0.765	0.000	0.001	0.000	0.011	0.002	0.000	0.000	0.000	0.000
Populus simaroa	0.008	0.000	0.000	0.064	0.044	64.463	0.017	0.000	0.208	1.139
Populus szechuanica	0.130	0.000	0.158	0.015	0.020	20.856	0.109	0.008	0.008	0.593
Populus tremula	0.000	0.005	0.000	0.030	0.002	51.246	0.009	0.000	0.082	0.243
Populus tremuloides	0.056	0.001	0.000	0.066	0.001	82.552	0.178	0.001	0.520	8.009
Populus trichocarpa	0.204	0.010	0.017	0.048	0.013	78.033	0.102	0.000	0.114	10.369
Populus yunnanensis	0.760	0.006	0.006	0.009	0.050	48.612	0.074	0.016	0.157	4.194
Salix acutifolia	0.581	0.155	0.000	0.000	0.017	1.862	0.000	0.000	0.000	0.276
Salix alba	0.513	0.474	0.000	0.001	0.011	8.898	0.076	0.000	0.000	0.681
Salix amygdaloides	0.059	0.005	0.002	0.064	0.002	88.826	0.169	0.000	0.490	3.868
Salix appendiculata	0.092	0.000	0.000	0.000	1.379	3.784	0.000	0.000	0.000	0.434
Salix bebbiana	1.001	0.040	0.000	0.000	0.027	0.262	0.000	0.000	0.000	0.013
Salix candida	0.798	0.000	0.000	0.000	3.190	0.963	0.000	0.000	0.000	0.021
Salix caprea	0.020	0.043	0.000	0.004	0.134	44.488	0.002	0.029	0.125	5.642
Salix cinerea	0.081	0.100	0.000	0.000	0.009	0.438	0.000	0.000	0.000	0.043
Salix discolor	0.136	0.001	0.000	0.004	0.036	32.989	0.000	0.000	0.047	15.763
Salix eleagnos	0.000	0.007	0.000	0.016	0.004	50.318	0.049	0.010	0.223	6.102
Salix eriocephala	0.015	0.010	0.000	0.016	0.034	24.044	0.007	0.000	0.025	2.456
Salix gracilistyla	0.004	0.037	0.000	0.000	0.257	0.514	0.000	0.000	0.000	0.076
Salix hastata	0.188	0.783	0.000	0.011	0.005	59.041	0.173	0.000	0.066	3.053
Salix humilis	0.008	0.001	0.000	0.098	0.000	100.000	0.024	0.000	0.756	14.918
Salix integra	0.004	0.112	0.000	0.000	0.009	0.323	0.000	0.000	0.000	0.028
Salix interior	0.068	0.012	0.000	0.000	0.000	0.316	0.000	0.000	0.000	0.046
Salix irrorata	0.000	0.001	0.036	0.079	0.002	100.000	0.031	0.000	0.818	13.751
Salix jessoensis	1.058	0.099	0.000	0.000	0.137	27.124	0.000	0.000	0.043	0.730
Salix matsudana	0.306	0.058	0.001	0.000	0.010	0.045	0.000	0.004	0.000	0.011
Salix miyabeana	0.005	0.001	0.002	0.000	0.003	2.667	0.002	0.000	0.005	0.090
Salix myricoides	0.004	0.000	0.000	0.029	0.000	41.720	0.018	0.000	0.178	9.046
Salix nigra	0.150	0.006	0.000	0.095	0.002	100.000	0.081	0.020	0.240	1.775
Salix pentandra	0.179	18.514	0.000	0.002	0.001	7.370	0.005	0.001	0.007	2.987
Salix purpurea	0.002	0.001	0.001	0.018	0.002	65.260	0.051	0.000	0.187	3.476
Salix repens	0.006	0.000	0.000	0.003	0.027	26.872	0.014	0.000	0.057	8.650
Salix sericea	0.022	0.001	0.001	0.066	0.001	27.794	0.012	0.000	0.023	1.062
Salix serissima	0.000	6.401	0.000	0.000	0.006	0.946	0.000	0.000	0.000	0.033
Salix triandra	3.132	0.172	0.000	0.000	0.000	2.147	0.000	0.000	0.000	0.111
Salix udensis	0.116	0.048	0.192	0.001	0.057	1.730	0.006	0.000	0.001	0.158

Species	Cinnamoylsalicyloylsalicin-A	Cinnamoylsalicyloylsalicin-B	HCH-deltoidin-A	HCH-nigracin-B	HCH-nigracin-C	HCH-deltoidin-D	HCH-deltoidin-E	Cinnamoylsalicortin-A	Cinnamoylsalicortin-C
Idesia polycarpa	0.000	0.002	0.002	0.009	0.000	0.006	0.001	0.000	0.001
Populus afghanica	0.002	0.036	0.000	12.713	0.055	0.000	0.000	0.000	0.000
Populus alba	0.001	0.000	0.051	0.007	0.018	0.632	0.414	0.001	0.001
Populus angustifolia	0.003	0.000	0.083	4.209	0.000	0.002	0.005	0.000	0.000
Populus balsamifera	0.001	0.005	0.073	0.130	0.114	0.229	0.040	0.002	0.001
Populus deltoides	0.000	0.000	0.005	0.020	0.018	0.000	0.001	0.267	0.086
Populus fremontii	0.000	0.000	0.005	0.000	0.000	0.000	0.000	0.179	0.105
Populus grandidentata	0.000	0.003	0.160	0.011	0.020	0.485	0.304	0.000	0.001
Populus guzmanantlensis	0.000	0.003	0.554	0.011	0.040	0.655	0.230	0.000	0.001
Populus heterophylla	0.020	0.143	0.023	5.845	0.661	0.045	0.024	0.000	0.002
Populus koreana	0.000	0.002	0.000	14.040	0.121	0.133	0.016	0.000	0.000
Populus luziarum	0.000	0.001	1.150	0.024	0.020	0.451	0.085	0.001	0.001
Populus maximowiczii	0.004	0.007	0.008	0.000	0.217	0.000	0.000	0.066	0.024
Populus mexicana	0.002	0.007	0.104	0.079	0.320	0.656	0.155	0.000	0.001
Populus monticola	0.000	0.000	0.124	0.005	0.018	0.760	0.187	0.001	0.001
Populus nigra	0.005	0.027	0.000	33.555	0.038	0.000	0.000	0.000	0.000
Populus primaveralepensis	0.000	0.001	1.073	0.024	0.024	0.462	0.097	0.001	0.001
Populus purdomii	0.000	0.005	0.001	0.010	0.052	0.000	0.001	0.001	0.001
Populus simaroa	0.000	0.000	0.231	0.000	0.011	0.488	0.160	0.000	0.000
Populus szechuanica	0.000	0.001	0.000	37.462	0.005	0.196	0.069	0.000	0.000
Populus tremula	0.000	0.001	0.022	0.004	0.008	0.430	0.126	0.082	0.000
Populus tremuloides	0.000	0.001	0.173	0.002	0.016	0.548	0.205	0.000	0.000
Populus trichocarpa	0.000	0.005	0.175	0.452	0.017	0.400	0.214	0.000	0.000
Populus yunnanensis	0.004	0.010	0.044	0.073	0.034	0.352	0.128	0.000	0.000
Salix acutifolia	0.000	0.000	0.000	0.054	0.006	0.012	0.000	0.000	0.000
Salix alba	0.004	0.001	0.023	0.068	0.068	0.130	0.019	0.100	0.051
Salix amygdaloides	0.001	0.002	0.044	0.005	0.186	1.239	0.179	0.000	0.000
Salix appendiculata	0.000	0.000	0.000	0.000	0.000	0.006	0.000	0.000	0.000
Salix bebbiana	0.000	0.000	0.006	0.050	0.001	0.001	0.000	0.001	0.020
Salix candida	0.000	0.000	0.000	0.049	0.000	0.012	0.000	0.000	0.000
Salix caprea	0.000	0.000	0.094	0.002	0.002	0.239	0.159	0.000	0.000
Salix cinerea	0.000	0.000	0.009	0.020	0.000	0.000	0.000	0.000	0.000
Salix discolor	0.000	0.000	0.073	0.047	0.025	0.152	0.030	0.014	0.624
Salix eleagnos	0.000	0.000	0.060	0.007	0.011	0.350	0.114	0.000	0.000
Salix eriocephala	0.000	0.001	0.033	0.025	0.036	0.302	0.052	0.000	0.001
Salix gracilistyla	0.000	0.000	0.004	0.002	0.000	0.006	0.000	0.000	0.000
Salix hastata	0.085	0.007	0.119	0.053	0.109	0.654	0.091	0.049	0.000
Salix humilis	0.001	0.005	0.316	0.016	0.026	1.027	0.155	0.002	0.000
Salix integra	0.000	0.000	0.098	0.006	1.475	0.011	0.000	0.000	0.000
Salix interior	0.000	0.000	0.023	0.000	0.018	0.158	0.003	0.000	0.000
Salix irrorata	0.001	0.001	0.237	0.007	0.006	0.566	0.161	0.002	0.000
Salix jessoensis	0.000	0.000	0.007	0.057	0.012	0.080	0.095	0.000	0.000
Salix matsudana	0.000	0.001	0.000	0.038	0.029	0.021	0.000	0.002	0.000
Salix miyabeana	0.000	0.001	0.002	0.046	0.005	0.008	0.004	0.000	0.000
Salix myricoides	0.000	0.001	0.053	0.009	0.003	0.534	0.098	0.010	0.000
Salix nigra	0.003	0.006	0.086	0.017	0.266	2.301	0.395	0.000	0.000
Salix pentandra	0.006	0.003	0.012	0.015	0.007	0.119	0.017	0.001	0.001
Salix purpurea	0.000	0.001	0.096	0.026	0.012	0.303	0.142	0.000	0.000
Salix repens	0.000	0.000	0.015	0.035	0.011	0.338	0.103	0.000	0.000
Salix sericea	0.003	0.025	0.043	0.006	0.018	0.306	0.117	0.026	0.000
Salix serissima	0.001	0.000	0.000	0.019	0.011	0.013	0.004	0.030	0.023
Salix triandra	0.000	0.000	19.858	1.480	0.000	0.000	0.000	0.000	0.000
Salix udensis	0.006	0.026	0.000	0.006	0.034	0.067	0.045	0.005	0.000

Species	Cinnamoylsalicortin-B	Cinnamoylsalicortin-D	Cinnamoylsalicortin-E	Cinnamoylsalicortin-F	HCH-salicortin-A	HCH-salicortin-B	HCH-salicortin-C	HCH-salicortin-D	HCH-salicortin-E	HCH-salicortin-F
Idesia polycarpa	0.023	0.001	0.000	0.000	0.145	0.003	0.002	0.001	0.000	0.001
Populus afghanica	0.003	0.004	0.162	0.434	37.078	0.254	0.231	0.110	0.032	0.061
Populus alba	0.014	0.018	0.002	0.009	16.091	0.172	0.216	0.119	0.000	0.101
Populus angustifolia	0.000	0.000	0.000	0.018	0.350	0.000	0.000	0.000	0.000	0.000
Populus balsamifera	0.016	0.018	0.001	0.002	15.587	0.230	0.234	0.116	0.007	0.190
Populus deltoides	0.002	0.001	0.002	0.001	98.506	0.655	0.647	1.760	0.497	0.427
Populus fremontii	0.000	0.000	0.000	0.004	97.458	0.265	0.362	0.671	0.248	0.034
Populus grandidentata	3.218	4.615	0.005	0.001	0.516	0.016	0.025	0.001	0.000	0.001
Populus guzmanantlensis	0.041	0.042	0.000	0.000	1.999	0.040	0.045	0.000	0.000	0.019
Populus heterophylla	0.001	0.004	0.000	0.005	88.553	0.347	0.274	0.699	0.257	0.089
Populus koreana	0.009	0.009	0.005	0.008	1.173	0.038	0.030	0.002	0.003	0.004
Populus luziarum	0.004	0.077	0.000	0.000	3.423	0.031	0.035	0.000	0.000	0.006
Populus maximowiczii	0.003	0.005	0.001	0.003	94.358	2.527	2.273	3.195	1.047	1.727
Populus mexicana	0.037	0.078	0.559	2.653	1.504	0.037	0.046	0.000	0.000	0.006
Populus monticola	0.026	0.039	0.000	0.001	4.432	0.036	0.035	0.000	0.000	0.004
Populus nigra	0.001	0.001	0.025	0.058	3.504	0.076	0.068	0.000	0.012	0.022
Populus primaveralepensis	0.004	0.088	0.000	0.000	3.926	0.045	0.050	0.003	0.000	0.006
Populus purdomii	0.000	0.001	0.000	0.002	8.664	0.352	0.283	0.065	0.012	0.254
Populus simaroa	0.009	0.052	0.000	0.000	0.795	0.015	0.020	0.000	0.000	0.001
Populus szechuanica	0.005	0.014	0.006	0.037	7.572	0.036	0.035	0.004	0.013	0.007
Populus tremula	7.434	15.460	0.010	0.035	2.972	0.035	0.038	0.000	0.000	0.021
Populus tremuloides	0.048	0.049	0.000	0.000	0.381	0.016	0.018	0.000	0.000	0.001
Populus trichocarpa	0.026	0.030	0.000	0.000	5.727	0.074	0.072	0.014	0.001	0.024
Populus yunnanensis	0.023	0.031	0.000	0.008	17.984	0.422	0.378	0.140	0.000	0.191
Salix acutifolia	0.004	0.000	0.000	0.000	3.505	0.000	0.015	0.055	0.000	0.004
Salix alba	0.000	0.004	0.015	0.205	66.719	0.012	0.012	0.879	0.183	0.000
Salix amygdaloides	0.031	0.085	1.604	1.539	0.276	0.016	0.022	0.002	0.000	0.000
Salix appendiculata	0.010	0.120	0.000	0.000	0.691	0.009	0.000	0.000	0.000	0.000
Salix bebbiana	0.178	0.004	0.000	0.000	0.234	0.011	0.011	0.000	0.000	0.000
Salix candida	0.000	0.000	0.000	0.000	0.452	0.000	0.000	0.000	0.000	0.000
Salix caprea	0.004	0.038	0.000	0.000	1.396	0.019	0.050	0.004	0.000	0.015
Salix cinerea	0.002	0.021	0.000	0.000	0.000	0.006	0.009	0.003	0.000	0.000
Salix discolor	1.745	0.214	0.000	0.021	0.115	0.000	0.003	0.002	0.000	0.000
Salix eleagnos	0.006	0.009	0.005	0.022	0.183	0.000	0.023	0.000	0.000	0.002
Salix eriocephala	0.037	0.175	0.010	0.032	0.027	0.000	0.012	0.000	0.000	0.000
Salix gracilistyla	0.000	0.000	0.000	0.000	0.522	0.003	0.007	0.000	0.000	0.000
Salix hastata	0.000	0.011	0.028	0.279	32.763	0.044	0.053	0.233	0.028	0.000
Salix humilis	0.350	0.784	0.047	0.123	0.125	0.000	0.000	0.000	0.000	0.000
Salix integra	0.000	0.005	0.000	0.000	0.000	0.000	0.000	0.000	0.000	0.000
Salix interior	0.002	0.000	0.000	0.000	56.582	0.000	0.000	0.694	0.000	0.000
Salix irrorata	0.016	0.058	0.011	0.119	0.088	0.006	0.006	0.000	0.000	0.000
Salix jessoensis	0.000	0.000	0.000	0.000	2.089	0.017	0.011	0.016	0.000	0.016
Salix matsudana	0.002	0.004	0.035	0.128	100.000	0.193	0.220	2.434	0.495	0.000
Salix miyabeana	0.000	0.002	0.001	0.003	0.137	0.003	0.004	0.001	0.001	0.000
Salix myricoides	1.674	3.239	0.000	0.003	0.279	0.012	0.017	0.000	0.000	0.001
Salix nigra	0.047	0.233	1.874	7.949	34.682	0.248	0.245	0.130	0.000	0.073
Salix pentandra	0.003	0.010	0.001	0.011	1.991	0.001	0.000	0.018	0.000	0.000
Salix purpurea	0.004	0.006	0.000	0.004	0.206	0.012	0.011	0.000	0.000	0.000
Salix repens	0.001	0.001	0.000	0.001	0.454	0.013	0.032	0.000	0.000	0.007
Salix sericea	4.213	10.530	0.177	0.863	0.198	0.007	0.009	0.000	0.000	0.001
Salix serissima	0.000	0.000	0.000	0.005	3.643	0.000	0.000	0.030	0.000	0.004
Salix triandra	0.000	0.000	0.000	0.000	1.313	0.000	0.000	0.000	0.000	0.000
Salix udensis	0.002	0.013	0.001	0.000	1.100	0.002	0.014	0.000	0.000	0.000

Species	HCH-salicortin-G	HCH-salicortin-H	HCH-salicortin-I	HCH-salicortin-J	HCH-salicortin-K	Acetyltremulacin	HCH-populoside-B-A	HCH-populoside-B-B	HCH-populoside-B-C	HCH-populoside-B-D
Idesia polycarpa	0.001	0.000	0.000	0.000	0.000	0.022	0.159	0.240	0.440	7.420
Populus afghanica	0.063	0.024	0.012	0.021	0.004	0.000	0.179	0.138	0.267	0.000
Populus alba	0.102	0.034	0.014	0.025	0.009	0.000	0.056	0.038	0.019	0.001
Populus angustifolia	0.011	0.000	0.000	0.000	0.000	0.000	0.015	0.125	3.207	0.696
Populus balsamifera	0.180	0.066	0.022	0.031	0.007	0.001	0.041	0.029	0.323	0.374
Populus deltoides	0.321	0.070	0.508	0.626	0.239	0.003	0.433	0.290	0.569	2.751
Populus fremontii	0.042	0.007	0.086	0.110	0.034	0.000	0.001	0.004	0.012	0.093
Populus grandidentata	0.003	0.001	0.001	0.003	0.000	0.001	0.000	0.012	0.033	0.002
Populus guzmanantlensis	0.018	0.006	0.000	0.010	0.000	0.000	0.000	0.001	0.004	0.016
Populus heterophylla	0.135	0.026	0.134	0.138	0.067	0.000	0.092	0.067	0.204	0.786
Populus koreana	0.012	0.003	0.000	0.002	0.000	0.005	0.000	0.115	0.299	0.048
Populus luziarum	0.006	0.000	0.000	0.002	0.000	0.000	0.000	0.000	0.009	0.006
Populus maximowiczii	1.519	0.539	1.287	1.722	0.558	0.005	0.369	0.319	0.479	0.230
Populus mexicana	0.006	0.000	0.000	0.006	0.000	0.000	0.103	0.000	1.899	0.000
Populus monticola	0.004	0.000	0.001	0.002	0.000	0.000	0.000	0.000	0.003	0.002
Populus nigra	0.030	0.009	0.006	0.007	0.000	0.004	0.037	0.261	0.456	0.000
Populus primaveralepensis	0.008	0.003	0.001	0.002	0.000	0.000	0.001	0.000	0.012	0.005
Populus purdomii	0.110	0.039	0.009	0.012	0.005	0.003	0.015	0.000	0.000	0.228
Populus simaroa	0.001	0.000	0.000	0.004	0.000	0.000	0.000	0.000	0.002	0.000
Populus szechuanica	0.012	0.003	0.004	0.005	0.000	0.000	0.000	0.000	0.033	0.086
Populus tremula	0.018	0.007	0.000	0.003	0.001	0.919	0.015	0.001	0.034	0.000
Populus tremuloides	0.004	0.001	0.001	0.004	0.000	0.000	0.001	0.002	0.040	0.019
Populus trichocarpa	0.027	0.009	0.000	0.001	0.001	0.000	0.006	0.004	0.026	0.002
Populus yunnanensis	0.168	0.067	0.019	0.031	0.008	0.000	0.141	0.147	0.325	0.199
Salix acutifolia	0.000	0.000	0.006	0.000	0.000	0.005	0.011	0.263	0.006	0.016
Salix alba	0.230	0.000	0.298	0.094	0.159	0.191	0.023	0.080	0.887	0.030
Salix amygdaloides	0.005	0.000	0.000	0.002	0.000	0.000	0.034	2.541	1.403	0.006
Salix appendiculata	0.000	0.000	0.000	0.000	0.000	0.000	0.000	0.000	1.031	1.031
Salix bebbiana	0.000	0.000	0.003	0.001	0.001	0.001	0.003	0.000	0.002	0.024
Salix candida	0.000	0.000	0.000	0.000	0.000	0.000	0.000	0.000	0.000	0.000
Salix caprea	0.022	0.000	0.000	0.000	0.000	0.069	0.015	0.047	0.000	0.445
Salix cinerea	0.000	0.000	0.000	0.000	0.002	0.000	0.103	0.063	0.000	0.025
Salix discolor	0.000	0.000	0.000	0.001	0.000	0.000	0.042	0.013	0.244	0.012
Salix eleagnos	0.009	0.000	0.001	0.005	0.000	7.078	0.000	5.967	0.045	0.199
Salix eriocephala	0.000	0.000	0.000	0.000	0.000	0.000	0.045	10.061	0.054	0.226
Salix gracilistyla	0.000	0.000	0.000	0.000	0.000	0.000	0.000	0.009	0.000	0.000
Salix hastata	0.036	0.013	0.000	0.059	0.214	0.602	0.000	0.159	2.379	0.148
Salix humilis	0.000	0.000	0.007	0.003	0.000	0.000	0.000	0.000	0.000	0.000
Salix integra	0.000	0.001	0.003	0.002	0.000	0.004	0.000	0.011	0.000	0.040
Salix interior	0.324	0.000	0.020	0.100	0.037	0.000	0.016	0.003	0.000	0.000
Salix irrorata	0.000	0.000	0.000	0.003	0.000	0.097	0.001	0.002	0.046	0.004
Salix jessoensis	0.006	0.000	0.000	0.000	0.000	0.000	0.172	0.006	0.031	0.000
Salix matsudana	0.116	0.000	0.880	0.680	0.250	0.000	21.702	18.160	1.304	1.359
Salix miyabeana	0.001	0.000	0.000	0.000	0.000	0.002	0.001	0.017	0.015	0.001
Salix myricoides	0.003	0.001	0.000	0.003	0.000	0.000	0.000	2.342	0.000	0.111
Salix nigra	0.077	0.031	0.010	0.025	0.024	0.000	3.039	1.961	5.081	0.000
Salix pentandra	0.008	0.002	0.001	0.000	0.001	2.795	0.003	0.002	0.023	0.002
Salix purpurea	0.002	0.000	0.000	0.002	0.000	0.000	0.001	0.527	0.040	0.015
Salix repens	0.010	0.002	0.000	0.003	0.000	0.000	0.005	0.001	0.024	0.000
Salix sericea	0.000	0.000	0.000	0.000	0.000	0.014	0.000	17.080	1.031	5.645
Salix serissima	0.012	0.000	0.001	0.002	0.001	0.030	0.011	0.009	0.033	0.088
Salix triandra	0.000	0.000	0.000	0.000	0.000	0.074	0.074	0.007	0.006	0.000
Salix udensis	0.000	0.000	0.000	0.000	0.000	0.000	0.014	0.020	0.031	0.004

Species	HCH-populoside-B-E	HCH-populoside-B-F	HCH-populoside-B-G	HCH-populoside-B-H	Homaloside-D-1	Homaloside-D-2	HCH-acetylsalicyloylsalicin-A	HCH-acetylsalicyloylsalicin-B
Idesia polycarpa	4.045	0.142	0.006	0.002	37.756	24.965	0.084	0.052
Populus afghanica	1.439	0.204	0.003	0.001	0.000	0.000	0.010	0.607
Populus alba	0.002	0.023	0.007	0.004	0.000	0.003	0.074	15.857
Populus angustifolia	0.197	0.825	0.003	0.000	0.015	0.004	0.875	12.738
Populus balsamifera	0.045	0.095	0.019	0.002	0.009	0.000	0.034	1.034
Populus deltoides	0.957	0.198	0.793	0.306	0.000	0.000	0.785	1.160
Populus fremontii	0.066	0.056	0.625	0.491	0.002	0.000	0.000	0.187
Populus grandidentata	0.004	0.051	0.000	0.000	0.000	0.001	0.005	0.027
Populus guzmanantlensis	0.014	0.067	0.000	0.001	0.000	0.005	0.004	0.334
Populus heterophylla	0.283	0.015	0.000	0.001	0.234	0.246	0.004	0.012
Populus koreana	0.136	0.239	0.000	0.000	0.000	0.000	0.000	2.774
Populus luziarum	0.005	0.005	0.001	0.000	0.000	0.000	0.002	0.198
Populus maximowiczii	0.268	0.356	0.161	0.120	0.004	0.000	0.000	1.757
Populus mexicana	1.268	2.214	0.031	0.001	0.000	0.000	0.076	0.312
Populus monticola	0.003	0.065	0.003	0.002	0.000	0.000	0.000	0.010
Populus nigra	0.475	0.463	0.000	0.000	0.000	0.000	0.119	0.235
Populus primaveralepensis	0.003	0.049	0.000	0.000	0.000	0.000	0.002	0.277
Populus purdomii	0.144	0.219	0.000	0.002	0.000	0.000	0.000	1.567
Populus simaroa	0.002	0.051	0.001	0.001	0.000	0.000	0.002	0.266
Populus szechuanica	0.602	0.010	0.000	0.000	0.000	0.000	0.000	0.792
Populus tremula	0.006	0.045	0.000	0.014	0.000	0.001	0.000	0.016
Populus tremuloides	0.014	0.047	0.001	0.002	0.034	0.049	0.002	0.006
Populus trichocarpa	0.010	0.031	0.001	0.001	0.006	0.007	0.009	0.088
Populus yunnanensis	0.046	0.192	0.000	0.000	0.000	0.018	0.000	1.278
Salix acutifolia	0.000	0.013	0.402	0.196	0.000	0.008	0.041	0.015
Salix alba	0.037	0.610	2.800	1.358	0.000	0.000	0.009	1.003
Salix amygdaloides	0.087	2.303	0.053	0.004	0.000	0.001	0.002	0.208
Salix appendiculata	0.176	0.000	0.000	0.000	0.000	0.000	0.217	0.000
Salix bebbiana	0.005	0.000	0.000	0.002	0.110	0.045	0.069	0.003
Salix candida	0.000	0.000	0.000	0.000	0.000	0.039	0.000	0.000
Salix caprea	0.176	0.006	0.000	0.004	0.016	0.013	0.000	0.000
Salix cinerea	0.003	0.000	0.000	0.000	0.000	0.036	0.178	0.021
Salix discolor	0.008	0.116	0.000	0.009	0.000	0.010	0.004	0.014
Salix eleagnos	0.004	0.049	0.000	0.000	0.000	0.000	0.000	0.008
Salix eriocephala	0.005	0.045	0.064	0.018	0.131	0.017	0.000	0.022
Salix gracilistyla	0.000	0.000	0.000	0.000	0.000	0.011	0.069	0.005
Salix hastata	0.145	1.579	2.398	1.431	0.000	0.013	0.016	1.328
Salix humilis	0.036	0.290	0.000	0.000	0.000	0.011	0.002	0.027
Salix integra	0.001	0.000	0.000	0.000	0.013	0.028	0.002	0.000
Salix interior	0.000	0.053	0.000	0.000	0.000	0.000	0.109	0.000
Salix irrorata	0.005	0.038	0.001	0.001	0.005	0.000	0.000	0.005
Salix jessoensis	0.000	0.013	0.000	0.000	0.000	0.025	0.000	0.048
Salix matsudana	0.855	0.646	0.077	0.072	0.000	0.097	0.000	0.323
Salix miyabeana	0.000	0.006	0.000	0.000	0.000	0.000	0.003	0.018
Salix myricoides	0.017	0.024	0.000	0.000	0.005	0.004	0.000	0.003
Salix nigra	0.234	4.607	0.047	0.000	0.000	0.004	0.007	1.244
Salix pentandra	0.001	0.017	0.029	0.026	0.000	0.000	0.000	0.016
Salix purpurea	0.004	0.022	0.001	0.000	0.001	0.000	0.000	0.008
Salix repens	0.001	0.022	0.001	0.000	0.000	0.000	0.000	0.020
Salix sericea	4.347	0.364	0.000	0.000	0.008	0.007	0.002	0.025
Salix serissima	0.069	0.076	0.822	0.695	0.000	0.000	0.000	0.016
Salix triandra	0.007	0.000	0.000	0.000	2.859	0.284	0.000	0.136
Salix udensis	0.022	0.003	0.011	0.000	0.292	0.000	0.045	0.000

Species	HCH-acetylsalicyloylsalicin-C	HCH-acetylsalicyloylsalicin-D	HCH-acetylsalicyloylsalicin-E	HCH-acetylsalicyloylsalicin-F	HCH-acetylsalicyloylsalicin-G	HCH-acetylsalicyloylsalicin-H
Idesia polycarpa	0.603	0.107	0.174	0.000	3.074	1.879
Populus afghanica	0.096	0.020	0.010	0.000	0.000	0.001
Populus alba	1.810	0.366	0.104	0.023	0.000	0.000
Populus angustifolia	0.250	0.212	0.050	0.000	0.000	0.008
Populus balsamifera	2.725	0.453	0.724	0.061	0.000	0.000
Populus deltoides	6.989	1.242	20.382	2.770	0.002	0.000
Populus fremontii	1.630	0.663	11.517	2.627	0.000	0.000
Populus grandidentata	0.139	0.038	0.002	0.000	0.000	0.000
Populus guzmanantlensis	1.639	0.259	0.036	0.006	0.001	0.000
Populus heterophylla	0.019	0.002	0.002	0.002	0.005	0.002
Populus koreana	3.299	0.826	0.125	0.007	0.000	0.000
Populus luziarum	1.906	0.207	0.020	0.002	0.000	0.000
Populus maximowiczii	5.006	1.276	3.388	0.649	0.009	0.000
Populus mexicana	0.003	0.001	0.014	0.000	0.000	0.003
Populus monticola	0.070	0.009	0.006	0.002	0.000	0.000
Populus nigra	0.133	0.038	0.006	0.000	0.000	0.000
Populus primaveralepensis	2.877	0.302	0.035	0.005	0.000	0.000
Populus purdomii	2.314	0.359	0.210	0.033	0.000	0.000
Populus simaroa	1.345	0.212	0.026	0.004	0.001	0.000
Populus szechuanica	2.784	0.438	0.017	0.000	0.000	0.000
Populus tremula	0.044	0.008	0.003	0.008	0.001	0.000
Populus tremuloides	0.006	0.003	0.002	0.000	0.000	0.001
Populus trichocarpa	0.061	0.007	0.015	0.005	0.000	0.001
Populus yunnanensis	5.116	0.911	0.136	0.024	0.000	0.000
Salix acutifolia	0.007	0.000	0.716	0.083	0.000	0.000
Salix alba	0.131	0.271	6.162	1.128	0.000	0.000
Salix amygdaloides	0.004	0.009	0.003	0.002	0.000	0.001
Salix appendiculata	0.068	0.000	0.054	0.000	0.000	0.000
Salix bebbiana	0.131	0.008	0.026	0.007	0.011	0.008
Salix candida	0.000	0.000	0.045	0.000	0.000	0.000
Salix caprea	0.021	0.000	0.014	0.000	0.000	0.000
Salix cinerea	0.015	0.000	0.061	0.007	0.000	0.000
Salix discolor	0.001	0.005	0.002	0.000	0.000	0.001
Salix eleagnos	0.004	0.004	0.001	0.002	0.000	0.001
Salix eriocephala	0.033	0.006	0.082	0.004	0.000	0.006
Salix gracilistyla	0.000	0.000	0.005	0.000	0.000	0.007
Salix hastata	0.189	0.182	4.542	0.744	0.000	0.000
Salix humilis	0.004	0.010	0.001	0.000	0.000	0.001
Salix integra	0.008	0.001	0.016	0.000	0.000	0.000
Salix interior	0.009	0.000	0.023	0.000	0.000	0.000
Salix irrorata	0.001	0.001	0.002	0.000	0.000	0.001
Salix jessoensis	0.015	0.000	0.036	0.000	0.000	0.000
Salix matsudana	0.275	0.074	0.061	0.008	0.060	0.067
Salix miyabeana	0.000	0.000	0.001	0.000	0.000	0.001
Salix myricoides	0.002	0.003	0.001	0.000	0.000	0.000
Salix nigra	0.006	0.025	0.010	0.001	0.000	0.007
Salix pentandra	0.001	0.002	0.015	0.002	0.000	0.000
Salix purpurea	0.002	0.016	0.001	0.000	0.000	0.000
Salix repens	0.008	0.002	0.001	0.000	0.000	0.000
Salix sericea	0.059	0.012	0.009	0.007	0.002	0.005
Salix serissima	0.005	0.005	0.125	0.026	0.000	0.000
Salix triandra	0.241	0.007	0.011	0.000	0.000	0.000
Salix udensis	0.020	0.000	0.013	0.002	0.000	0.004

Species	Acetylcinnamoylsalicortin-A	Acetylcinnamoylsalicortin-B	Lasiandrin-A	Lasiandrin-B	Lasiandrin-C	HCH-tremulacin	HCH-cinnamoylsalicortin-A	HCH-cinnamoylsalicortin-B
Idesia polycarpa	0.000	0.000	0.002	0.000	0.000	0.005	0.000	0.000
Populus afghanica	0.000	0.000	0.000	0.000	0.000	0.000	0.000	0.000
Populus alba	0.000	0.000	0.000	0.001	0.000	7.556	0.000	0.000
Populus angustifolia	0.002	0.000	0.000	0.000	0.000	0.000	0.000	0.000
Populus balsamifera	0.001	0.000	0.000	0.000	0.000	0.379	0.000	0.000
Populus deltoides	0.001	0.000	0.035	0.000	0.000	0.000	0.000	0.000
Populus fremontii	0.000	0.000	0.019	0.000	0.000	0.000	0.000	0.000
Populus grandidentata	0.001	0.000	0.001	0.000	0.000	0.183	0.005	0.006
Populus guzmanantlensis	0.000	0.000	0.000	0.000	0.000	0.252	0.000	0.000
Populus heterophylla	0.000	0.000	8.828	0.015	0.024	3.299	0.000	0.000
Populus koreana	0.000	0.000	0.000	0.000	0.000	0.057	0.000	0.000
Populus luziarum	0.000	0.000	0.000	0.000	0.000	0.097	0.000	0.000
Populus maximowiczii	0.000	0.000	0.038	0.000	0.001	0.001	0.000	0.001
Populus mexicana	0.000	0.000	0.000	0.000	0.000	0.615	0.000	0.000
Populus monticola	0.000	0.000	0.000	0.000	0.000	0.118	0.000	0.000
Populus nigra	0.000	0.000	0.001	0.000	0.000	0.000	0.000	0.000
Populus primaveralepensis	0.000	0.000	0.000	0.000	0.000	0.113	0.000	0.000
Populus purdomii	0.000	0.000	0.049	0.000	0.000	0.000	0.000	0.000
Populus simaroa	0.000	0.000	0.000	0.000	0.000	0.097	0.000	0.000
Populus szechuanica	0.000	0.000	0.169	0.000	0.000	0.035	0.000	0.000
Populus tremula	0.081	0.466	0.731	0.001	0.000	0.808	0.023	0.061
Populus tremuloides	0.000	0.000	0.001	0.000	0.000	0.158	0.000	0.000
Populus trichocarpa	0.000	0.000	0.001	0.000	0.000	0.279	0.000	0.000
Populus yunnanensis	0.000	0.000	0.000	0.000	0.000	0.797	0.000	0.000
Salix acutifolia	0.000	0.000	8.799	0.006	0.074	0.000	0.000	0.000
Salix alba	0.000	0.000	32.960	0.000	0.369	17.924	0.001	0.001
Salix amygdaloides	0.001	0.000	0.001	0.000	0.000	0.219	0.000	0.000
Salix appendiculata	0.000	0.000	0.111	0.000	0.000	0.008	0.000	0.000
Salix bebbiana	0.002	0.037	0.340	0.000	0.000	0.000	0.000	0.000
Salix candida	0.000	0.000	0.036	0.000	0.000	0.000	0.000	0.000
Salix caprea	0.000	0.000	0.013	0.000	0.000	0.060	0.000	0.000
Salix cinerea	0.000	0.000	0.048	0.000	0.000	0.000	0.000	0.000
Salix discolor	0.014	0.001	0.001	0.000	0.000	0.021	0.000	0.000
Salix eleagnos	0.000	0.000	0.000	0.000	0.000	0.126	0.000	0.000
Salix eriocephala	0.001	0.000	0.101	0.000	0.000	0.013	0.000	0.000
Salix gracilistyla	0.000	0.000	0.020	0.000	0.000	0.123	0.000	0.000
Salix hastata	0.000	0.000	6.373	0.022	0.022	53.960	0.002	0.007
Salix humilis	0.002	0.000	0.000	0.000	0.000	0.173	0.000	0.000
Salix integra	0.001	0.000	0.077	0.000	0.000	0.013	0.000	0.000
Salix interior	0.000	0.000	95.287	0.218	0.697	0.000	0.000	0.000
Salix irrorata	0.000	0.000	0.000	0.000	0.000	0.131	0.000	0.000
Salix jessoensis	0.000	0.000	0.004	0.000	0.000	0.112	0.000	0.000
Salix matsudana	0.000	0.000	0.691	0.001	0.001	0.000	0.000	0.001
Salix miyabeana	0.000	0.000	0.003	0.000	0.000	0.001	0.000	0.000
Salix myricoides	0.000	0.000	0.000	0.000	0.000	0.098	0.001	0.002
Salix nigra	0.004	0.000	0.020	0.000	0.000	26.762	0.001	0.002
Salix pentandra	0.001	0.007	37.520	0.572	0.168	1.665	0.000	0.001
Salix purpurea	0.000	0.000	0.002	0.000	0.000	0.057	0.000	0.000
Salix repens	0.000	0.000	0.005	0.000	0.000	0.068	0.000	0.000
Salix sericea	0.003	0.000	0.003	0.000	0.000	0.019	0.001	0.003
Salix serissima	0.000	0.001	51.074	1.022	0.458	0.228	0.000	0.000
Salix triandra	0.000	0.000	0.241	0.000	0.000	0.000	0.000	0.000
Salix udensis	0.000	0.000	0.081	0.000	0.000	0.018	0.001	0.000

References

Agrawal, A. A., & Fishbein, M. (2008). Phylogenetic escalation and decline of plant defense strategies. *Proceedings of the National Academy of Sciences*, *105*(29), 10057–10060. https://doi.org/10.1073/pnas.0802368105

Agrawal, A. A., Petschenka, G., Bingham, R. A., Weber, M. G., & Rasmann, S. (2012). Toxic cardenolides: Chemical ecology and coevolution of specialized plant–herbivore interactions. *New Phytologist*, *194*(1), 28–45. https://doi.org/10.1111/j.1469-8137.2011.04049.x

Babst, B. A., Harding, S. A., & Tsai, C.-J. (2010). Biosynthesis of phenolic glycosides from phenylpropanoid and benzenoid precursors in Populus. *Journal of Chemical Ecology*, *36*(3), 286–297. https://doi.org/10.1007/s10886-010-9757-7

Barco, B., & Clay, N. K. (2019). Evolution of glucosinolate diversity via whole-genome duplications, gene rearrangements, and substrate promiscuity. *Annual Review of Plant Biology*, *70*(1), 585–604. https://doi.org/10.1146/annurev-arplant-050718-100152

Bastide, P., Solís-Lemus, C., Kriebel, R., William Sparks, K., & Ané, C. (2018). Phylogenetic comparative methods on phylogenetic networks with reticulations. *Systematic Biology*, *67*(5), 800–820. https://doi.org/10.1093/sysbio/syy033

Berenbaum, M. R., & Zangerl, A. R. (1996). Phytochemical Diversity. In J. T. Romeo, J. A. Saunders, & P. Barbosa (Eds.), *Phytochemical Diversity and Redundancy in Ecological Interactions* (pp. 1–24). Springer US. https://doi.org/10.1007/978-1-4899-1754-6_1

Bezanson, J., Edelman, A., Karpinski, S., & Shah, V. B. (2017). Julia: A fresh approach to numerical computing. *SIAM Review*, *59*(1), 65–98. https://doi.org/10.1137/141000671

Boeckler, G. A., Gershenzon, J., & Unsicker, S. B. (2011). Phenolic glycosides of the Salicaceae and their role as anti-herbivore defenses. *Phytochemistry*, *72*(13), 1497–1509. https://doi.org/10.1016/j.phytochem.2011.01.038

Bray, J. R., & Curtis, J. T. (1957). An ordination of the upland forest communities of Southern Wisconsin. *Ecological Monographs*, *27*(4), 325–349. https://doi.org/10.2307/1942268

Cacho, N. I., Kliebenstein, D. J., & Strauss, S. Y. (2015). Macroevolutionary patterns of glucosinolate defense and tests of defense-escalation and resource availability hypotheses. *New Phytologist*, *208*(3), 915–927. https://doi.org/10.1111/nph.13561

Carmona, D., Lajeunesse, M. J., & Johnson, M. T. J. (2011). Plant traits that predict resistance to herbivores. *Functional Ecology*, *25*(2), 358–367. https://doi.org/10.1111/j.1365-2435.2010.01794.x

Chao, A., Chiu, C.-H., & Jost, L. (2014). Unifying species diversity, phylogenetic diversity, functional diversity, and related similarity and differentiation measures through hill numbers. *Annual Review of Ecology, Evolution, and Systematics*, *45*(1), 297–324. https://doi.org/10.1146/annurev-ecolsys-120213-091540

Chedgy, R. J., Köllner, T. G., & Constabel, C. P. (2015). Functional characterization of two acyltransferases from *Populus trichocarpa* capable of synthesizing benzyl benzoate and

salicyl benzoate, potential intermediates in salicinoid phenolic glycoside biosynthesis. *Phytochemistry*, *113*, 149–159. https://doi.org/10.1016/j.phytochem.2014.10.018

Clarke, K. R. (1993). Non-parametric multivariate analyses of changes in community structure. *Australian Journal of Ecology*, *18*(1), 117–143. https://doi.org/10.1111/j.1442-9993.1993.tb00438.x

Cole, C. T., Morrow, C. J., Barker, H. L., Rubert-Nason, K. F., Riehl, J. F. L., Köllner, T. G., Lackus, N. D., & Lindroth, R. L. (2021). Growing up aspen: Ontogeny and trade-offs shape growth, defence and reproduction in a foundation species. *Annals of Botany*, *127*(4), 505–517. https://doi.org/10.1093/aob/mcaa070

Cope, O. L., Keefover-Ring, K., Kruger, E. L., & Lindroth, R. L. (2021). Growth–defense trade-offs shape population genetic composition in an iconic forest tree species. *Proceedings of the National Academy of Sciences*, *118*(37), e2103162118. https://doi.org/10.1073/pnas.2103162118

Dickmann, D. I., & Kuzovkina, J. (2014). Poplars and willows of the world, with emphasis on silviculturally important species. In *Poplars and willows: Trees for society and the environment* (pp. 8–91). CABI.

Diner, B., Berteaux, D., Fyles, J., & Lindroth, R. L. (2009). Behavioral archives link the chemistry and clonal structure of trembling aspen to the food choice of North American porcupine. *Oecologia*, *160*(4), 687–695. https://doi.org/10.1007/s00442-009-1340-y

Donaldson, J. R., Stevens, M. T., Barnhill, H. R., & Lindroth, R. L. (2006). Age-related shifts in leaf chemistry of clonal aspen (*Populus tremuloides*). *Journal of Chemical Ecology*, *32*(7), 1415–1429. https://doi.org/10.1007/s10886-006-9059-2

Edgar, R. C. (2004). MUSCLE: Multiple sequence alignment with high accuracy and high throughput. *Nucleic Acids Research*, *32*(5), 1792–1797. https://doi.org/10.1093/nar/gkh340

Ehrlich, P. R., & Raven, P. H. (1964). Butterflies and plants: A study in coevolution. *Evolution*, *18*(4), 586–608. https://doi.org/10.2307/2406212

Feeny, P. (1976). Plant apparency and chemical defense. In J. W. Wallace & R. L. Mansell (Eds.), *Biochemical Interaction Between Plants and Insects* (pp. 1–40). Springer US. https://doi.org/10.1007/978-1-4684-2646-5_1

Feistel, F., Paetz, C., Lorenz, S., Beran, F., Kunert, G., & Schneider, B. (2017). *Idesia polycarpa* (Salicaceae) leaf constituents and their toxic effect on *Cerura vinula* and *Lymantria dispar* (Lepidoptera) larvae. *Phytochemistry*, *143*, 170–179. https://doi.org/10.1016/j.phytochem.2017.08.008

Fellenberg, C., Corea, O., Yan, L.-H., Archinuk, F., Piirtola, E.-M., Gordon, H., Reichelt, M., Brandt, W., Wulff, J., Ehlting, J., & Peter Constabel, C. (2020). Discovery of salicyl benzoate UDP-glycosyltransferase, a central enzyme in poplar salicinoid phenolic glycoside biosynthesis. *The Plant Journal*, *102*(1), 99–115. https://doi.org/10.1111/tpj.14615

Forrister, D. L., Endara, M.-J., Soule, A. J., Younkin, G. C., Mills, A. G., Lokvam, J., Dexter, K. G., Pennington, R. T., Kidner, C. A., Nicholls, J. A., Loiseau, O., Kursar, T. A., & Coley,

P. D. (2023). Diversity and divergence: Evolution of secondary metabolism in the tropical tree genus *Inga*. *New Phytologist*, *237*(2), 631–642. https://doi.org/10.1111/nph.18554

Fraenkel, G. S. (1959). The Raison d'Être of Secondary Plant Substances. *Science*, *129*(3361), 1466–1470.

Fussi, B., Lexer, C., & Heinze, B. (2010). Phylogeography of *Populus alba* (L.) and *Populus tremula* (L.) in Central Europe: Secondary contact and hybridisation during recolonisation from disconnected refugia. *Tree Genetics & Genomes*, *6*(3), 439–450. https://doi.org/10.1007/s11295-009-0262-5

Godschalx, A. L., Stady, L., Watzig, B., & Ballhorn, D. J. (2016). Is protection against florivory consistent with the optimal defense hypothesis? *BMC Plant Biology*, *16*(1), 32. https://doi.org/10.1186/s12870-016-0719-2

Gordon, H., Fellenberg, C., Lackus, N. D., Archinuk, F., Sproule, A., Nakamura, Y., Köllner, T. G., Gershenzon, J., Overy, D. P., & Constabel, C. P. (2022). CRISPR/Cas9 disruption of UGT71L1 in poplar connects salicinoid and salicylic acid metabolism and alters growth and morphology. *The Plant Cell*, *34*(8), 2925–2947. https://doi.org/10.1093/plcell/koac135

Holmes, K. D., Fine, P. V. A., Mesones, I., Alvarez-Manjarrez, J., Venturini, A. M., Peay, K. G., & Salazar, D. (2025). Evolutionary trajectories of shoots vs. roots: plant volatile metabolomes are richer but less structurally diverse belowground in the tropical tree genus *Protium*. *Plants*, *14*(2), Article 2. https://doi.org/10.3390/plants14020225

Huber, F., Ridder, L., Verhoeven, S., Spaaks, J. H., Diblen, F., Rogers, S., & Hooft, J. J. J. van der. (2021). Spec2Vec: Improved mass spectral similarity scoring through learning of structural relationships. *PLOS Computational Biology*, *17*(2), e1008724. https://doi.org/10.1371/journal.pcbi.1008724

Hunziker, P., Lambertz, S. K., Weber, K., Crocoll, C., Halkier, B. A., & Schulz, A. (2021). Herbivore feeding preference corroborates optimal defense theory for specialized metabolites within plants. *Proceedings of the National Academy of Sciences of the United States of America*, *118*(47), 1–6.

Jones, C. G., & Firn, R. D. (1991). On the evolution of plant secondary chemical diversity. *Philosophical Transactions of the Royal Society of London. Series B: Biological Sciences*, *333*(1267), 273–280. https://doi.org/10.1098/rstb.1991.0077

Keefover-Ring, K. (2022). The chemical biogeography of a widespread aromatic plant species shows both spatial and temporal variation. *Ecology and Evolution*, *12*(9). https://doi.org/10.1002/ece3.9265

Keefover-Ring, K., Ahnlund, M., Abreu, I. N., Jansson, S., Moritz, T., & Albrectsen, B. R. (2014). No evidence of geographical structure of salicinoid chemotypes within *Populus tremula*. *PLOS ONE*, *9*(10), e107189. https://doi.org/10.1371/journal.pone.0107189

Keefover-Ring, K., Carlsson, M., & Albrectsen, B. R. (2014). 2′-(Z)-Cinnamoylsalicortin: A novel salicinoid isolated from *Populus tremula*. *Phytochemistry Letters*, *7*, 212–216. https://doi.org/10.1016/j.phytol.2013.11.012

Kessler, A., & Kalske, A. (2018). Plant secondary metabolite diversity and species interactions. *Annual Review of Ecology, Evolution, and Systematics*, *49*(Volume 49, 2018), 115–138. https://doi.org/10.1146/annurev-ecolsys-110617-062406

Khabbazian, M., Kriebel, R., Rohe, K., & Ané, C. (2016). Fast and accurate detection of evolutionary shifts in Ornstein–Uhlenbeck models. *Methods in Ecology and Evolution*, *7*(7), 811–824. https://doi.org/10.1111/2041-210X.12534

Kruger, E. L., Keefover-Ring, K., Holeski, L. M., & Lindroth, R. L. (2020). To compete or defend: Linking functional trait variation with life-history tradeoffs in a foundation tree species. *Oecologia*, *192*(4), 893–907. https://doi.org/10.1007/s00442-020-04622-y

Kulasekaran, S., Cerezo-Medina, S., Harflett, C., Lomax, C., De Jong, F., Rendour, A., Ruvo, G., Hanley, S. J., Beale, M. H., & Ward, J. L. (2021). A willow UDP-glycosyltransferase involved in salicinoid biosynthesis. *Journal of Experimental Botany*, *72*(5), 1634–1648. https://doi.org/10.1093/jxb/eraa562

Kunert, M., Langley, C., Lucier, R., Ploss, K., Rodríguez López, C. E., Serna Guerrero, D. A., Rothe, E., O'Connor, S. E., & Sonawane, P. D. (2023). Promiscuous CYP87A enzyme activity initiates cardenolide biosynthesis in plants. *Nature Plants*, *9*(10), 1607–1617. https://doi.org/10.1038/s41477-023-01515-9

Lackus, N. D., Müller, A., Kröber, T. D. U., Reichelt, M., Schmidt, A., Nakamura, Y., Paetz, C., Luck, K., Lindroth, R. L., Constabel, C. P., Unsicker, S. B., Gershenzon, J., & Köllner, T. G. (2020). The occurrence of sulfated salicinoids in poplar and their formation by sulfotransferase11 [OPEN]. *Plant Physiology*, *183*(1), 137–151. https://doi.org/10.1104/pp.19.01447

Lauron-Moreau, A., Pitre, F. E., Argus, G. W., Labrecque, M., & Brouillet, L. (2015). Phylogenetic relationships of American willows (*Salix* L., Salicaceae). *PLOS ONE*, *10*(4), e0121965. https://doi.org/10.1371/journal.pone.0121965

Lencioni, S. J., Massatti, R., Keefover-Ring, K., & Holeski, L. M. (2024). The cost of self-defense: Browsing effects in the rare plant species *Salix arizonica*. *Ecology and Evolution*, *14*(11), e70582. https://doi.org/10.1002/ece3.70582

Lexer, C., Fay, M. F., Joseph, J. A., Nica, M.-S., & Heinze, B. (2005). Barrier to gene flow between two ecologically divergent *Populus* species, *P. alba* (white poplar) and *P. tremul*a (European aspen): The role of ecology and life history in gene introgression. *Molecular Ecology*, *14*(4), 1045–1057. https://doi.org/10.1111/j.1365-294X.2005.02469.x

Lindroth, R. L., & Hemming, J. D. C. (1990). Responses of the gypsy moth (Lepidoptera: Lymantriidae) to tremulacin, an aspen phenolic glycoside. *Environmental Entomology*, *19*(4), 842–847. https://doi.org/10.1093/ee/19.4.842

Lindroth, R. L., Hsia, M. T. S., & Scriber, J. M. (1987). Characterization of phenolic glycosides from quaking aspen. *Biochemical Systematics and Ecology*, *15*(6), 677–680. https://doi.org/10.1016/0305-1978(87)90045-7

Lindroth, R. L., & Pajutee, M. S. (1987). Chemical analysis of phenolic glycosides: Art, facts, and artifacts. *Oecologia*, *74*(1), 144–148. https://doi.org/10.1007/BF00377359

Lindroth, R. L., Scriber, J. M., & Hsia, M. T. S. (1988). Chemical ecology of the tiger swallowtail: mediation of host use by phenolic glycosides. *Ecology*, *69*(3), 814–822. https://doi.org/10.2307/1941031

Lopez-Nieves, S., Yang, Y., Timoneda, A., Wang, M., Feng, T., Smith, S. A., Brockington, S. F., & Maeda, H. A. (2018). Relaxation of tyrosine pathway regulation underlies the evolution of betalain pigmentation in Caryophyllales. *New Phytologist*, *217*(2), 896–908. https://doi.org/10.1111/nph.14822

Marinček, P., Léveillé-Bourret, É., Heiduk, F., Leong, J., Bailleul, S. M., Volf, M., & Wagner, N. D. (2024). Challenge accepted: Evolutionary lineages versus taxonomic classification of North American shrub willows (*Salix*). *American Journal of Botany*, *111*(7), e16361. https://doi.org/10.1002/ajb2.16361

Maron, J. L., Agrawal, A. A., & Schemske, D. W. (2019). Plant–herbivore coevolution and plant speciation. *Ecology*, *100*(7), e02704. https://doi.org/10.1002/ecy.2704

Marquis, R. J., Salazar, D., Baer, C., Reinhardt, J., Priest, G., & Barnett, K. (2016). Ode to Ehrlich and Raven or how herbivorous insects might drive plant speciation. *Ecology*, *97*(11), 2939–2951. https://doi.org/10.1002/ecy.1534

Martinsen, G. D., Driebe, E. M., & Whitham, T. G. (1998). Indirect interactions mediated by changing plant chemistry: Beaver browsing benefits beetles. *Ecology*, *79*(1), 192–200. https://doi.org/10.1890/0012-9658(1998)079[0192:IIMBCP]2.0.CO;2

Mason, C. J., Rubert-Nason, K., Lindroth, R. L., Shi, J., & Hoover, K. (2021). Salicinoid phenolics reduce adult *Anoplophora glabripennis* (Cerambicidae: Lamiinae) feeding and egg production. *Arthropod-Plant Interactions*, *15*(1), 127–136. https://doi.org/10.1007/s11829-020-09802-4

Monson, R. K., Trowbridge, A. M., Lindroth, R. L., & Lerdau, M. T. (2022). Coordinated resource allocation to plant growth–defense tradeoffs. *New Phytologist*, *233*(3), 1051–1066. https://doi.org/10.1111/nph.17773

Moore, B. D., Andrew, R. L., Külheim, C., & Foley, W. J. (2014). Explaining intraspecific diversity in plant secondary metabolites in an ecological context. *New Phytologist*, *201*(3), 733–750. https://doi.org/10.1111/nph.12526

Murtagh, F., & Legendre, P. (2014). Ward's hierarchical agglomerative clustering method: Which algorithms implement ward's criterion? *Journal of Classification*, *31*(3), 274–295. https://doi.org/10.1007/s00357-014-9161-z

Neilson, E. H., Goodger, J. Q. D., Woodrow, I. E., & Møller, B. L. (2013). Plant chemical defense: At what cost? *Trends in Plant Science*, *18*(5), 250–258. https://doi.org/10.1016/j.tplants.2013.01.001

Núñez-Farfán, J., & Kariñho-Betancourt, E. (2015). Is escalation of plant defence a common macroevolutionary outcome of plant–herbivore interactions? *The New Phytologist*, *208*(3), 635–637.

Ogutcen, E., de Lima Ferreira, P., Wagner, N. D., Marinček, P., Vir Leong, J., Aubona, G., Cavender-Bares, J., Michálek, J., Schroeder, L., Sedio, B. E., Vašut, R. J., & Volf, M. (2024). Phylogenetic insights into the Salicaceae: The evolution of willows and beyond.

Molecular Phylogenetics and Evolution, *199*, 108161. https://doi.org/10.1016/j.ympev.2024.108161

Pearl, I. A., & Darling, S. F. (1977). Studies on the leaves of the family Salicaceae. 17. Hot-water extractives of the leaves of *Populus heterophylla* L. *Journal of Agricultural and Food Chemistry*, *25*(4), 730–734. https://doi.org/10.1021/jf60212a035

Pentzold, S., Zagrobelny, M., Rook, F., & Bak, S. (2014). How insects overcome two-component plant chemical defence: Plant β-glucosidases as the main target for herbivore adaptation. *Biological Reviews*, *89*(3), 531–551. https://doi.org/10.1111/brv.12066

Petrén, H., Anaia, R. A., Aragam, K. S., Bräutigam, A., Eckert, S., Heinen, R., Jakobs, R., Ojeda-Prieto, L., Popp, M., Sasidharan, R., Schnitzler, J.-P., Steppuhn, A., Thon, F. M., Unsicker, S. B., van Dam, N. M., Weisser, W. W., Wittmann, M. J., Yepes, S., Ziaja, D., … Junker, R. R. (2024). Understanding the chemodiversity of plants: Quantification, variation and ecological function. *Ecological Monographs*, *94*(4), e1635. https://doi.org/10.1002/ecm.1635

Petrén, H., Köllner, T. G., & Junker, R. R. (2023). Quantifying chemodiversity considering biochemical and structural properties of compounds with the R package chemodiv. *New Phytologist*, *237*(6), 2478–2492. https://doi.org/10.1111/nph.18685

Prudic, K. L., Khera, S., Sólyom, A., & Timmermann, B. N. (2007). Isolation, identification, and quantification of potential defensive compounds in the viceroy butterfly and its larval host–plant, carolina willow. *Journal of Chemical Ecology*, *33*(6), 1149–1159. https://doi.org/10.1007/s10886-007-9282-5

Rhoades, D. F., & Cates, R. G. (1976). Toward a general theory of plant antiherbivore chemistry. In J. W. Wallace & R. L. Mansell (Eds.), *Biochemical Interaction Between Plants and Insects* (pp. 168–213). Springer US. https://doi.org/10.1007/978-1-4684-2646-5_4

Richards, L. A., Glassmire, A. E., Ochsenrider, K. M., Smilanich, A. M., Dodson, C. D., Jeffrey, C. S., & Dyer, L. A. (2016). Phytochemical diversity and synergistic effects on herbivores. *Phytochemistry Reviews*, *15*(6), 1153–1166. https://doi.org/10.1007/s11101-016-9479-8

Rubert-Nason, K. F., Hedman, C. J., Holeski, L. M., & Lindroth, R. L. (2014). Determination of salicinoids by micro-high-performance liquid chromatography and photodiode array detection. *Phytochemical Analysis*, *25*(3), 185–191. https://doi.org/10.1002/pca.2485

Rubert-Nason, K. F., & Lindroth, R. L. (2021). Causes and consequences of condensed tannin variation in *Populus*. In *Recent Advances in Polyphenol Research* (pp. 69–112). John Wiley & Sons, Ltd. https://doi.org/10.1002/9781119545958.ch4

Rubert-Nason, K., Keefover-Ring, K., & Lindroth, R. L. (2018). Purification and analysis of salicinoids. *Current Analytical Chemistry*, *14*(4), 423–429. https://doi.org/10.2174/1573411014666171221131933

Ruuhola, T., & Julkunen-Tiitto, R. (2003). Trade-off between synthesis of salicylates and growth of micropropagated *Salix pentandra*. *Journal of Chemical Ecology*, *29*(7), 1565–1588.

Rzedowski, J. (1975). Tres dicotiledóneas mexicanas nuevas de posible interés ornamental. *Botanical Sciences*, *35*, Article 35. https://doi.org/10.17129/botsci.1151

Sanderson, B. J., Gambhir, D., Feng, G., Hu, N., Cronk, Q. C., Percy, D. M., Freaner, F. M., Johnson, M. G., Smart, L. B., Keefover-Ring, K., Yin, T., Ma, T., DiFazio, S. P., Liu, J., & Olson, M. S. (2023). Phylogenomics reveals patterns of ancient hybridization and differential diversification that contribute to phylogenetic conflict in willows, poplars, and close relatives. *Systematic Biology*, *72*(6), 1220–1232. https://doi.org/10.1093/sysbio/syad042

Sayers, E. W., Beck, J., Bolton, E. E., Brister, J. R., Chan, J., Connor, R., Feldgarden, M., Fine, A. M., Funk, K., Hoffman, J., Kannan, S., Kelly, C., Klimke, W., Kim, S., Lathrop, S., Marchler-Bauer, A., Murphy, T. D., O'Sullivan, C., Schmieder, E., … Pruitt, K. D. (2025). Database resources of the National Center for Biotechnology Information in 2025. *Nucleic Acids Research*, *53*(D1), D20–D29. https://doi.org/10.1093/nar/gkae979

Schmid, R., Heuckeroth, S., Korf, A., Smirnov, A., Myers, O., Dyrlund, T. S., Bushuiev, R., Murray, K. J., Hoffmann, N., Lu, M., Sarvepalli, A., Zhang, Z., Fleischauer, M., Dührkop, K., Wesner, M., Hoogstra, S. J., Rudt, E., Mokshyna, O., Brungs, C., … Pluskal, T. (2023). Integrative analysis of multimodal mass spectrometry data in MZmine 3. *Nature Biotechnology*, *41*(4), 447–449. https://doi.org/10.1038/s41587-023-01690-2

Schnurrer, F., Nakamura, Y., & Paetz, C. (2024). A mechanism to transform complex salicinoids with caffeoylquinic acids in lepidopteran specialist herbivores (Notodontidae). *Journal of Chemical Ecology*, *50*(1), 71–83. https://doi.org/10.1007/s10886-023-01464-9

Schnurrer, F., & Paetz, C. (2023). Reductive conversion leads to detoxification of salicortin-like chemical defenses (salicortinoids) in Lepidopteran specialist herbivores (Notodontidae). *Journal of Chemical Ecology*, *49*(5), 251–261. https://doi.org/10.1007/s10886-023-01423-4

Sedio, B. E., Rojas Echeverri, J. C., Boya P., C. A., & Wright, S. J. (2017). Sources of variation in foliar secondary chemistry in a tropical forest tree community. *Ecology*, *98*(3), 616–623. https://doi.org/10.1002/ecy.1689

Sherman, D. H. (2005). The Lego-ization of polyketide biosynthesis. *Nature Biotechnology*, *23*(9), 1083–1084. https://doi.org/10.1038/nbt0905-1083

Smilanich, A. M., Fincher, R. M., & Dyer, L. A. (2016). Does plant apparency matter? Thirty years of data provide limited support but reveal clear patterns of the effects of plant chemistry on herbivores. *New Phytologist*, *210*(3), 1044–1057. https://doi.org/10.1111/nph.13875

Solís-Lemus, C., Bastide, P., & Ané, C. (2017). PhyloNetworks: A package for phylogenetic networks. *Molecular Biology and Evolution*, *34*(12), 3292–3298. https://doi.org/10.1093/molbev/msx235

Stamatakis, A. (2014). RAxML version 8: A tool for phylogenetic analysis and post-analysis of large phylogenies. *Bioinformatics*, *30*(9), 1312–1313. https://doi.org/10.1093/bioinformatics/btu033

Stamp, N. (2003). Out of the quagmire of plant defense hypotheses. *The Quarterly Review of Biology*, *78*(1), 23–55. https://doi.org/10.1086/367580

Sweetlove, L. J., Ratcliffe, R. G., & Fernie, A. R. (2025). Non-canonical plant metabolism. *Nature Plants*, *11*(4), 696–708. https://doi.org/10.1038/s41477-025-01965-3

Tibshirani, R. (1996). Regression shrinkage and selection via the lasso. *Journal of the Royal Statistical Society. Series B (Methodological)*, *58*(1), 267–288.

Tsai, C.-J., Harding, S. A., Tschaplinski, T. J., Lindroth, R. L., & Yuan, Y. (2006). Genome-wide analysis of the structural genes regulating defense phenylpropanoid metabolism in Populus. *New Phytologist*, *172*(1), 47–62. https://doi.org/10.1111/j.1469-8137.2006.01798.x

Volf, M., Hrcek, J., Julkunen-Tiitto, R., & Novotny, V. (2015). To each its own: Differential response of specialist and generalist herbivores to plant defence in willows. *Journal of Animal Ecology*, *84*(4), 1123–1132. https://doi.org/10.1111/1365-2656.12349

Volf, M., Leong, J. V., de Lima Ferreira, P., Volfová, T., Kozel, P., Matos-Maraví, P., Hörandl, E., Wagner, N. D., Luntamo, N., Salminen, J.-P., Segar, S. T., & Sedio, B. E. (2023). Contrasting levels of β-diversity and underlying phylogenetic trends indicate different paths to chemical diversity in highland and lowland willow species. *Ecology Letters*, *26*(9), 1559–1571. https://doi.org/10.1111/ele.14273

Vorel, A., Válková, L., Hamšíková, L., Maloň, J., & Korbelová, J. (2015). Beaver foraging behaviour: Seasonal foraging specialization by a choosy generalist herbivore. *Behavioral Ecology and Sociobiology*, *69*(7), 1221–1235. https://doi.org/10.1007/s00265-015-1936-7

Wang, S., Alseekh, S., Fernie, A. R., & Luo, J. (2019). The structure and function of major plant metabolite modifications. *Molecular Plant*, *12*(7), 899–919. https://doi.org/10.1016/j.molp.2019.06.001

Ward, J. H. (1963). Hierarchical grouping to optimize an objective function. *Journal of the American Statistical Association*, *58*(301), 236–244. https://doi.org/10.2307/2282967

Wetzel, W. C., & Whitehead, S. R. (2020). The many dimensions of phytochemical diversity: Linking theory to practice. *Ecology Letters*, *23*(1), 16–32. https://doi.org/10.1111/ele.13422

Whitehead, S. R., Bass, E., Corrigan, A., Kessler, A., & Poveda, K. (2021). Interaction diversity explains the maintenance of phytochemical diversity. *Ecology Letters*, *24*(6), 1205–1214. https://doi.org/10.1111/ele.13736

Woolbright, S. A., Rehill, B. J., Lindroth, R. L., DiFazio, S. P., Martinsen, G. D., Zinkgraf, M. S., Allan, G. J., Keim, P., & Whitham, T. G. (2018). Large effect quantitative trait loci for salicinoid phenolic glycosides in *Populus*: Implications for gene discovery. *Ecology and Evolution*, *8*(7), 3726–3737. https://doi.org/10.1002/ece3.3932

Yánez-Segovia, S., Ramírez, C. C., Lindroth, R. L., & Fuentes-Contreras, E. (2023). Resistance against *Leucoptera sinuella* (Lepidoptera: Lyonetiidae) among hybrid clones of *Populus* spp. in central Chile. *Journal of Economic Entomology*, *116*(5), 1662–1670. https://doi.org/10.1093/jee/toad129

Zhang, C., Rabiee, M., Sayyari, E., & Mirarab, S. (2018). ASTRAL-III: Polynomial time species tree reconstruction from partially resolved gene trees. *BMC Bioinformatics*, *19*(6), 153. https://doi.org/10.1186/s12859-018-2129-y

Conclusions

How plants defend themselves from antagonists is a crucial component of understanding how our natural world functions, as those defenses are the gatekeepers of stored, biologically-relevant energy from the sun. Plant defensive chemistry can be dynamic, changing depending on the physical and temporal scale at which it is being examined, but reflects the evolutionary processes of the past that have formed the plants we see around us today. In these three chapters, I examined patterns of salicinoid diversity across space, ontogeny, and evolutionary timescales. In the first two chapters, I highlighted the diversity and complexity of salicinoid diversity in *Populus heterophylla*, finding multiple chemotypes throughout its range, reminiscent of the chemotypes of *Populus tremula* found by Keefover-Ring et al. (2014). The frequency of occurrence of these chemotypes differed by region, with *P. heterophylla* populations west of the Appalachian Mountains tending to have lower chemotypic – and thus lower salicinoid – diversity than populations east of the mountains. Interestingly, populations in the northeast portion of the species range had lower chemotypic diversity, and in the south populations had high chemotypic diversity. This distribution mirrors the population structure and estimated range expansion of the species, as populations on either side of the mountains have restricted gene flow between them, and ancestral area prediction models show that the extant lineage of *P. heterophylla* originated in the south or southeastern United States. Likely, following a period or periods of warming during the Pleistocene, *P. heterophylla* proceeded to disperse northward on either side of the Appalachian Mountains, expanding its range in a stepwise manner until it reached its current distribution. Founder effects during this range expansion could be a reason for the lower chemotype diversity of the western and northeastern populations of *P. heterophylla*, but more work is needed to determine if this is the case.

My second chapter explored the patterns of salicinoid diversity in leaves of different age classes in *P. heterophylla*, finding that immature carbon-sink leaves are defended at greater quantities of salicinoids than mature carbon-source leaves, despite the limited value those immature carbon-sink leaves have to the plant from a resource-acquisition perspective. My findings, in the context of the Optimal Defense Hypothesis and other work on the value of a leaf, highlight the investment strategy that *P. heterophylla* utilizes in protecting its future carbon-sources. Interestingly, the composition of salicinoids is not consistent across the two age classes, and individual salicinoids can be a greater or lower percentage of total salicinoids by mass in each age class, depending on the whole-plant chemotype and particular salicinoid. This discrepancy suggests either a given age class produces a more effective defensive composition for that development stage, or that there are unknown biosynthetic pathways and molecular dynamics at work in the production of this diverse suite of salicinoids. Given the efficacy of *P. heterophylla*'s quantitative salicinoid defense against *Popillia japonica*, a generalist insect herbivore, I suspect the reasons for different compositions of salicinoids are more likely the result of relaxed selective pressure on the production of any specific compound, but maintained selective pressure via generalists on total quantity of salicinoids and thus flux through biosynthetic pathways. However, selection pressure by specialist herbivores on the production of novel compounds and suites of compounds can not be ruled out as a reason for these differences between age classes.

In my third chapter, I expanded my investigation of salicinoid diversity to encompass 52 *Populus* and *Salix* species, in addition to *Idesia polycarpa*, to determine the pattern of salicinoid evolution in the two genera, utilizing phylogenetic comparative methods. I found that the ancestral salicinoid arsenal was likely very similar to that of extant *Populus tremuloides* and

Salix amygdaloides, mainly consisting of salicin, tremuloidin, salicortin, and tremulacin. While many extant *Populus* and *Salix* still produce this combination of salicinoids, there have also been numerous changes in salicinoid diversity across the phylogeny, with many lineages leading to single taxa and clades, such as *Populus* subgenus *Eupopulus* and of *Salix pentandra*, *Salix alba*, and *Salix serissima*, shifting from the ancestral suite to new combinations of salicinoids with iterations on the same salicin core. While I discuss possible reasons for these changes, more experimentation is needed to determine the true mechanisms leading to and maintaining novel salicinoids. For example, by considering the patterns of salicinoid diversity in *P. heterophylla* from the first two chapters, in the context of the genus-level results I present in the third chapter, molecular experiments can be designed utilizing leaves of specific chemotypes from specific regions to determine potential biosynthetic mechanisms producing specific salicinoids. Researchers could also intentionally select species with different salicinoid arsenals and utilize bioassays to determine if there are ecological reasons supporting the diversification of salicinoids from the ancestral arsenal. Hopefully, researchers can utilize the atlas of salicinoids in the species I present here to design such experiments.

In all, the work I present in this dissertation highlights the importance of exploring chemical diversity at different scales to understand the scope of what is possible in different levels of taxonomic organization. Without good prior knowledge of species-specific chemistry and its degree of variation, researchers might design suboptimal experiments or not think to measure certain traits because they are thought to not exist. While the species I use in the third chapter are not as extensively sampled as *P. heterophylla* in the first two chapters, those results still give researchers a minimum number of salicinoids they should consider when working with those species. Finally, for nearly 50 years, *P. heterophylla* had been thought to not have many

salicinoids due to a single study that looked at a single tree (Pearl & Darling 1977), and yet I have demonstrated that it is one of the most complex salicinoid-producing species in existence today. I hope that my work inspires others to work with *P. heterophylla* and other species in the Salicaceae containing this class of defensive secondary compounds, and to be mindful of sources of potential intraspecific variation when examining plant chemistry and other traits.